Title
Interrogating the Mechanistic Basis for Cytokine-Mediated Glucocorticoid Resistance in Lymphoid-Driven Diseases

Permalink
https://escholarship.org/uc/item/0m1036vv

Author
Meyer, Lauren Kimberly

Publication Date
2019

Supplemental Material
https://escholarship.org/uc/item/0m1036vv#supplemental

Peer reviewed|Thesis/dissertation

Interrogating the Mechanistic Basis for Cytokine-Mediated Glucocorticoid Resistance
in Lymphoid-Driven Diseases

by
Lauren Kimberly Meyer

DISSERTATION
Submitted in partial satisfaction of the requirements for degree of
DOCTOR OF PHILOSOPHY

in

Biomedical Sciences

in the

GRADUATE DIVISION
of the
UNIVERSITY OF CALIFORNIA, SAN FRANCISCO

Approved:

Jeroen Roose   Jeroen Roose
                                                                                    Chair

Michelle Hermiston   Michelle Hermiston
Kevin Shannon   Kevin Shannon
Keith Yamamoto   Keith Yamamoto
_____   Catherine Smith
                                                                    Committee Members

Acknowledgements

The chapters in this dissertation reflect the support and guidance of many people. I would like to thank my thesis advisors, Michelle Hermiston and Kevin Shannon, for giving me the opportunity to guide the course of my thesis work and to pursue the questions I found most compelling, all while providing the support and input I needed at each stage of the process. This challenging, at times frustrating, frequently exciting, and ultimately rewarding experience has only deepened my commitment to pursuing a career as a physician scientist, and I am grateful for the ways in which their mentorship over the past few years will continue to define my pursuit of these goals. I also wish to thank my thesis committee members, Jeroen Roose, Catherine Smith, Keith Yamamoto, and Luke Gilbert for their consistent encouragement and insightful scientific input. Much of the work in these chapters arose from collaborative efforts, and I have been fortunate to work with and learn from some exceptional scientists during this process. In particular, I would like to thank Ben Huang, David Teachey, Adam Olshen, Ritu Roy, Jack Taunton, Christopher Kirk, Kim Nichols, and Katherine Verbist for helping to make much of this work possible. I would also like to thank the UCSF Medical Scientist Training Program, including Mark Anderson, our director, and Geri Ehle, our program manager. Geri has been a constant source of support and encouragement and has worked tirelessly to ensure that we have access to the guidance and resources we need to be successful. I am deeply grateful to Anica Wandler and Cristina Delgado-Martin for their invaluable friendship and unconditional support. Their understanding of the highs and lows that come with pursuing a PhD and their endless willingness to provide guidance, both personally and scientifically, were indispensable to me reaching this point. Finally, I would like to thank my family for always being there for me no matter what, for believing in my ability to achieve my goals, and for reminding me to find balance and perspective during this process.

To Betty Jean Meyer

Contributions

Chapter 2

This chapter contains previously published material from: Meyer, L.K. and Hermiston, M.L. (2019). Mechanisms of glucocorticoid response and resistance in lymphoid malignancies. In Xavier, A.C. and Cairo, M.S. (Eds.), *Resistance to Targeted Therapies in Lymphomas* (pp 1-26). Springer Publishing.

Author contributions: L.K.M. and M.L.H. co-wrote this book chapter.

Chapter 3

This chapter contains previously published material from: Meyer, L.K. and Hermiston, M.L. (2019). The bone marrow microenvironment as a mediator of chemoresistance in acute lymphoblastic leukemia. *Cancer Drug Resistance.*

Author contributions: L.K.M. and M.L.H. co-wrote this review article.

Chapter 4

This chapter contains previously published material from: Meyer, L.K., Delgado-Martin, C., Maude, S.L., Shannon, K.M., Teachey, D.T., Hermiston, M.L. (2019). *CRLF2* rearrangement in Ph-like acute lymphoblastic leukemia predicts relative glucocorticoid resistance that is overcome with MEK or Akt inhibition. *PLOS One* 14(7).

Author contributions: L.K.M., C.D.-M., S.L.M., D.T.T., and M.L.H. designed the experiments and L.K.M and C.D.-M. performed the experiments. L.K.M., K.M.S., and M.L.H. discussed results and wrote the manuscript. S.L.M. and D.T.T. established the xenograft model, provided cells for the experiments, discussed results, and edited the manuscript.

Chapter 5

This chapter contains previously published material from: Meyer, L.K., Huang, B.J., Delgado-Martin, C., Roy, R.P., Hechmer, A., Wandler, A.M., Vincent, T.L., Fortina, P., Olshen, A.B., Wood, B.L., Horton, T.M., Shannon, K.M., Teachey, D.T., Hermiston, M.L. (2019). Glucocorticoids paradoxically facilitate steroid resistance in T-cell acute lymphoblastic leukemias and thymocytes. *Journal of Clinical Investigation*.

Author contributions: L.K.M., B.J.H., C.D.-M., K.M.S., D.T.T., and M.L.H. designed the experiments and analyzed the data. L.K.M., C.D.-M., B.J.H., A.M.W., and T.L.V. performed the experiments. B.L.W. performed immunophenotyping of patient samples. P.F. performed the RNA-sequencing of the primary patient samples. B.J.H., R.P.R., A.H., and A.B.O. performed bioinformatics analysis. L.K.M. and M.L.H. wrote the manuscript. B.J.H., C.D.-M., R.P.R., A.H., A.M.W., T.L.V., P.F., A.B.O., B.L.W., T.M.H., K.M.S., and D.T.T. reviewed and edited the manuscript.

Chapter 6

The work described in this chapter constitutes part of an ongoing collaboration. Michelle Hermiston and I conceived of the project goals, designed the research questions, and analyzed and interpreted the data. Cristina Delgado-Martin generated the *in vitro* viability data. Tiffaney Vincent prepared RNA samples for RNA-seq and David Teachey designed and oversaw the execution of the RNA-seq experiment. Ritu Roy performed all of the bioinformatics analyses and Adam Olshen supervised these analyses.

Chapter 7

This chapter is adapted from a manuscript that is currently in preparation: Meyer, L.K., Delgado-Martin, C., Sharp, P.P., Huang, B.J., McMinn, D., Vincent, T.L., Horton, T.M., Wood, B.L.,

Teachey, D.T., Kirk, C.J., Taunton, J., Hermiston, M.L. KZR-508445 is a novel inhibitor of the Sec61 translocon that overcomes cytokine-induced glucocorticoid resistance in T-cell acute lymphoblastic leukemia. *In preparation.*

Author contributions: L.K.M., C.D.-M., C.J.K., J.T., and M.L.H. designed the experiments and analyzed the data. L.K.M. and C.D.-M. performed the experiments. P.P.S. designed and synthesized KZR-508445. B.J.H. analyzed RNA-seq data. D.M. provided KZR-508445 for experimental use. T.L.V. generated patient-derived xenografts and provided cells for *ex vivo* analysis. L.K.M. and M.L.H. wrote the manuscript. C.D.-M., P.P.S., B.J.H., D.M., T.L.V., T.M.H., B.L.W., D.T.T., C.J.K., and J.T. reviewed and edited the manuscript.

Chapter 8

This chapter is adapted from a manuscript that is currently in preparation: Meyer, L.K.*, Verbist, K.C.*, Albeituni, S., Scull, B., Bassett, R.C., Stroh, A.N., Tillman, H., Allen, C.E., Nichols, K.E.[†], Hermiston, M.L.[†]. Ruxolitinib sensitizes CD8 T-cells to dexamethasone-induced apoptosis in a preclinical model of hemophagocytic lymphohistiocytosis. *In preparation*. *[†]Indicates equal contributions.

Author contributions: L.K.M. and K.C.V. designed and conducted most experiments, analyzed and interpreted data, and assembled figures and wrote the manuscript. S.A., R.C.B., and A.N.S. provided technical assistance on all *in vivo* experiments, and S.A. performed luminex assays. H.T. performed and analyzed all IHC experiments. B.S. and C.E.A. collected plasma samples from patients and controls. C.E.A., K.E.N., and M.L.H. procured funding for studies, directed experimental approaches, and assisted with data interpretation. S.A., B.S., R.C.B., A.N.S., H.T., C.E.A., K.E.N., and M.L.H. reviewed and edited the manuscript.

Interrogating the Mechanistic Basis for Cytokine-Mediated Glucocorticoid Resistance in Lymphoid-Driven Diseases

Lauren Kimberly Meyer

Abstract

Glucocorticoids (GCs) are potently immunosuppressive due to their pro-apoptotic effects on lymphoid cells, leading to their utility in a wide range of clinical contexts including autoimmune diseases, hyperinflammatory conditions, and lymphoid malignancies. In addition, GCs are endogenously produced hormones that mediate a wide range of physiologic functions that are essential for life. As a result, cells of the immune system face constant exposure to GCs and therefore require intrinsic mechanisms by which to resist their pro-apoptotic effects under certain developmental and environmental conditions. The retention of these resistance mechanisms in lymphoid-driven diseases thereby poses a challenge to the clinical use of GCs in these contexts. Common γ-chain cytokines, through activation of the JAK/STAT signal transduction pathway, play essential roles in the differentiation, survival, and function of lymphoid cells. Here, we assess the interplay between GC activity and cytokine-mediated pro-survival signaling in two lymphoid-driven diseases, acute lymphoblastic leukemia and hemophagocytic lymphohistiocytosis, and demonstrate that cytokines are potent mediators of GC resistance. Mechanistically, we show that activation of STAT5 downstream of cytokine receptor signaling is necessary for cytokine-induced GC resistance. STAT5 functions as a transcription factor to upregulate expression of anti-apoptotic mediators, thereby reducing the apoptotic potential and promoting the survival of lymphoid cells. Through both genetic and pharmacologic approaches, we demonstrate that targeted inhibition of cytokine receptor signaling effectively restores GC sensitivity, and we establish the feasibility of this therapeutic approach in two *in vivo* models of disease.

Table of Contents

List of Figures

CHAPTER 5:

CHAPTER 6:

CHAPTER 7:

CHAPTER 8:

List of Tables

Chapter 1: Introduction

Chapter 1: Introduction

1.1: Glucocorticoids

Glucocorticoids (GCs) are one of the most commonly used classes of drugs in clinical medicine. Owing to their potent immunosuppressive properties, GCs are central to the treatment of many acute and chronic inflammatory conditions, autoimmune diseases, and lymphoid malignancies. GCs are small lipophilic molecules capable of diffusing through plasma membranes into cytoplasm, where they encounter the cytoplasmic GC receptor (GR). In its inactive state, GR is maintained in the cytoplasm via its association with cytoplasmic chaperone proteins. Upon ligand binding, GR undergoes a conformational change that facilitates its translocation into the nucleus, where it associates with DNA sequences known as GC response elements (GREs). GC/GR binding to these GREs facilitates their function as transcriptional enhancers, regulating the expression of a wide range of GR target genes (1) (Figure 1-1). While the GR-induced transcriptome varies widely by cell type, in cells of the lymphoid lineage this transcriptional activity is pro-apoptotic, thereby underlying the lymphotoxic effects of GCs (2).

Unlike many other drug classes used in clinical medicine, GCs are unique in that, in addition to being used therapeutically, they are endogenously produced hormones that exert a multitude of critical physiologic functions. Cortisol, an endogenous GC, is produced by the adrenal glands under regulation by the hypothalamic-pituitary-adrenal axis (HPA axis), and mediates essential homeostatic functions and physiologic stress responses (3). Of relevance to their therapeutic use as immunosuppressive agents, endogenous GCs are also crucial for shaping the development of the immune cell repertoire.

In particular, GCs have been implicated as important regulators of normal thymopoiesis. Thymopoiesis begins with the migration of bone marrow-derived stem cells to the thymus. Differentiation of these T-cell precursors progresses from a CD4/CD8 double negative (DN) stage through a CD4/CD8 double positive (DP) stage prior to differentiation into either CD4 or

CD8 single positive (SP) T-cells (4) (Figure 1-2). During the early stages of this process, developing T-cells undergo RAG-mediated recombination of T-cell receptor (TCR) loci, leading to the expression of a fully-rearranged TCR by the DP stage. Given the extraordinary number of possible TCR rearrangements, of which only a small number are both productive and non-autoreactive, these DP thymocytes are subjected to a selection checkpoint prior to further differentiation. At this checkpoint, thymocytes are exposed to self-peptides expressed by thymic epithelial cells. These early thymocytes then undergo cell death unless they are rescued by a low-affinity interaction with these peptides in a process called positive selection, which leads to a pro-survival signal downstream of the activated TCR. At the opposite extreme, those thymocytes expressing TCRs engaging in high affinity interactions with self-peptides are deleted through a process known as negative selection, which functions as a safeguard against the development of autoreactive T-cells (4).

Early evidence for the importance of endogenous GCs in the regulation of thymopoiesis stemmed from the observation that adrenalectomized mice develop thymic hyperplasia (5,6), suggesting that GCs may play a role in the modulation of the selection checkpoint. Intriguingly, studies in T-cell hybridoma systems revealed that both TCR engagement and exposure to GCs independently induced cell death, however simultaneous exposure to both stimuli was protective (7). This seemingly paradoxical finding is reconciled through a model known as mutual antagonism. Though the molecular details of this model remain to be elucidated, it implies the existence of cross-talk between the TCR and GR signaling pathways and suggests that endogenous GC activity plays a role in establishing the window of acceptable TCR signal strength between the positive and negative selection thresholds (8).

One important corollary to the fact that GCs are endogenous hormones with lymphotoxic potential is that lymphoid cells, either by virtue of their differentiation state or by exposure to cell extrinsic stimuli, such as the cytokines described below, resist these lymphotoxic effects under certain developmental or environmental conditions. This poses a challenge for the therapeutic

application of GCs, as it suggests that lymphoid cell populations possess innate and physiologic mechanisms of resisting cell death in response to GC exposure, whether endogenous or pharmacologic. The following chapters describe novel insights into the ways in which lymphoid cells in two disease contexts, acute lymphoblastic leukemia (ALL) and hemophagocytic lymphohistiocytosis (HLH), exploit these innate processes to resist the pro-apoptotic effects of therapeutic GCs.

1.2: Apoptosis

Cell death is a critical cell biologic process that is required for normal tissue development and homeostasis. Dysregulation of cell death pathways underlies a number of disease states, including cancer, where the rate of cellular proliferation outpaces the rate of cell death, and neurologic diseases such as Alzheimer's disease, which is characterized by excessive activation of cell death pathways (9). In cancer and other conditions associated with aberrant cellular proliferation, including hyperinflammation, activation of cell death pathways is a common goal of therapy. Specifically, many therapeutic agents promote cell death via activation of apoptosis, a tightly regulated program of controlled cell death that spares surrounding tissues from the damage associated with necrosis, an alternative and poorly controlled process of cell death arising following tissue injury (9).

In apoptosis, cell death is carried out by the activity of a family of cysteine-aspartic proteases known as caspases, which cleave cellular macromolecules and promote the recruitment of phagocytic cells. Depending on the initiating trigger, apoptosis may proceed via the extrinsic or intrinsic pathway. Extrinsic apoptosis is initiated in response to activation of cell surface death receptors, and is most well-characterized in the context of immune cell interactions. Intrinsic, or mitochondrial, apoptosis is instead triggered by a complex network of

intracellular processes that converge upon the regulation of the BCL-2 family of proteins localized in the outer mitochondrial membrane (9).

The BCL-2 family constitutes a complex class of proteins that can be broadly subdivided into pro- and anti-apoptotic proteins on the basis of their respective roles in regulating the permeabilization of the mitochondrial membrane. Specifically, two pro-apoptotic family members, BAX and BAK, oligomerize to form pores in the mitochondria, allowing for the release of cytochrome c, a protein that then functions in the cytoplasm to trigger caspase activation and the subsequent progression of apoptosis. The pore-forming capacity of BAX and BAK is in turn regulated by the relative balance between pro- and anti-apoptotic BCL-2 family members. For example, the proteins BID and BIM, which consist only of a BCL-2 homology 3 (BH3) protein domain, function as activator proteins, directly engaging with BAX and BAK to promote pore formation. The multi-domain anti-apoptotic family members, including BCL-2, BCL-XL, and MCL-1, function to antagonize both BAX and BAK as well as BID and BIM, and are themselves inhibited by the sensitizer class of BH3-only pro-apoptotic proteins, which includes BAD, PUMA, and NOXA (10).

The complexity and redundancy of this protein network poses significant challenges with respect to experimental interrogation of the intrinsic apoptotic pathway. Specifically, measuring expression levels of individual proteins is insufficient to appreciate the overall apoptotic potential of a cell in a given state, as that apoptotic potential is dictated both by the relative balance between the expression of pro- and anti-apoptotic family members and the nature of their respective protein-protein interactions. As an additional layer of complexity, many of these proteins also undergo a multitude of post-translational modifications that further affect their function (11). Taken together, this necessitates the use of functional assays to facilitate an integrated understanding of cellular apoptotic potential.

BH3 profiling is one such functional assay that was developed in the laboratory of Dr. Anthony Letai at the Dana Farber Cancer Institute. Likened to "poking cells with a stick" (12),

BH3 profiling relies on exposing cells to synthetic BH3 domains corresponding to endogenous BH3-only proteins or to synthetic small molecule BH3 mimetics and measuring the subsequent release of cytochrome c. A cell with increased apoptotic potential, read as one that releases more cytochrome c in response to exposure to BH3 domains, is said to be more "primed" for apoptosis (13). Taking advantage of the differing affinities of the BH3-only sensitizer proteins for the multi-domain anti-apoptotic proteins, this technique is also powered to interrogate the relative anti-apoptotic dependencies of a given cell on the basis of the response patterns produced by exposure to different BH3 domains. As these dependencies have been shown to change as a function of factors such as developmental stage (14), this has particular therapeutic relevance in light of the increasing number of BH3 mimetics currently in preclinical development or clinical use (15).

By performing BH3 profiling on cells in their basal state and in response to pro-apoptotic stimuli, including therapeutic agents, it is possible to understand at a molecular level how these stimuli promote cell death. Of particular relevance to the following chapters, mounting evidence suggests that activation of the intrinsic apoptotic pathway is required for GC-induced lymphoid cell death, with GR acting either directly or indirectly to promote the upregulation of *BIM* and the downregulation of *BCL2,* thereby promoting a pro-apoptotic state (16–18). As described in the following chapters, the BH3 profiling technique can be further extended to understand how cell extrinsic factors that promote drug resistance modulate the apoptotic potential of a cell to interfere with drug-induced cell death.

1.3: Common γ-Chain Cytokines

The vague definition of cytokines as "proteins that exert effects on cells" reflects the considerable diversity of cytokines and their ubiquitous roles in nearly all cellular processes. Most cytokines are soluble factors, produced by a cell to act in an autocrine, paracrine, or

endocrine manner to influence cellular function. The importance of cytokines is best understood in the field of immunology, where they have well-described effects to modulate immune cell differentiation, survival, and proliferation and to regulate inflammatory responses (19).

In particular, the common γ-chain family of cytokines, united by their shared use of the cytokine receptor γ-chain as a component of their heterodimeric or -trimeric receptor complexes, play an essential role in the differentiation, function, and survival of lymphoid cells. As evidence of their essentiality, inherited mutations in *IL2RG*, the gene encoding the γ-chain, underlie X-linked severe combined immunodeficiency (SCID), characterized by loss of T-cell, NK cell, and B-cell function (20). The receptors for the common γ-chain cytokines lack intrinsic kinase activity, and instead signal via their intracellular associations with the Janus kinases (JAKs). Specifically, JAK1 associates with the cytokine-specific receptor chains, while JAK3 associates with the γ-chain. Following ligand binding and subsequent receptor activation, these JAK proteins mediate phosphorylation of the intracellular domains of the cytokine receptor chains, which in turn creates phosphotyrosine binding sites for the SH2 domains of downstream effector proteins known as signal transducer and activator of transcription (STAT) proteins. Upon binding to these phosphotyrosine sites, the STAT proteins themselves become phosphorylated, facilitating their dimerization and translocation to the nucleus where they function as transcription factors to modulate target gene expression (21) (Figure 1-3).

Despite the multitude of cytokine ligands that activate JAK/STAT signaling, the remarkable diversity of the resulting downstream effector functions is carried out by only seven mammalian STAT proteins, namely STAT1-4, STAT5a, STAT5b, and STAT6. While all cytokine receptors contain tyrosine residues capable of serving as docking sites for STAT proteins, the amino acid sequence surrounding these docking sites on individual receptor chains dictates the specific STAT proteins activated in response to receptor engagement (22). However, this alone is insufficient to explain the diverse and sometimes opposing functions of cytokine receptors

that activate shared STAT proteins, necessitating additional mechanisms of specificity. Some of this specificity may arise from the fact that individual cytokine receptors retain the capacity to activate multiple STAT proteins, and the relative degree of activation may differ between STATs, creating a receptor-specific constellation of activated STAT proteins that cooperate to execute a cytokine-specific transcriptional program (23). Additionally, there have been measured differences in the relative duration of STAT protein responses elicited downstream of cytokine receptor activation, suggesting that qualitative features of this response may similarly contribute to specificity (24).

STAT protein activation downstream of the γ-chain cytokine receptors mediates a diversity of immune cell functions, summarized in Table 1-1. The following chapters describe the mechanisms by which γ-chain cytokines function as mediators of GC resistance in lymphoid-driven diseases, with particular emphasis on interleukin-2 (IL-2) and IL-7. Importantly, the receptors for both of these cytokines have been shown to predominantly activate STAT5 (25). Consistent with these findings, we demonstrate through a series of genetic and biochemical approaches that STAT5 is a key effector of GC resistance via its effect to activate an anti-apoptotic transcriptional program in T-cells.

1.4: Acute Lymphoblastic Leukemia

Acute lymphoblastic leukemia (ALL) is a malignancy arising from immature cells of the lymphoid lineage, and as such can be broadly subdivided into B-cell ALL (B-ALL) and T-cell ALL (T-ALL). ALL is the most common malignancy of childhood, and remains the leading cause of cancer-related mortality in children (26). However, owing to large-scale clinical trials conducted through national and international consortia, survival rates for children diagnosed with ALL have improved considerably over the last half-century, with aggregate survival rates now up to 90% on many trials (27). The rapid development of "-omics" technologies in recent years has led to

increasing appreciation of the molecular heterogeneity of ALL, facilitating the identification of distinct molecular subtypes of disease. This in turn has prompted efforts to improve risk stratification tools and to more effectively tailor therapy to the unique molecular features of these subtypes (28).

First recognized for their utility in the treatment of lymphoid malignancies in the 1950s (29), GCs remain central to all therapeutic regimens for ALL. In particular, the intrinsic sensitivity of ALL cells to GCs at diagnosis is one of the strongest known predictors of future relapse. On European treatment protocols, patients receive a one week prophase of GC monotherapy following diagnosis. Patients who respond poorly to GCs during this upfront window have significantly inferior long-term outcomes (30). Analogously, the induction phase of therapy in the United States, which comprises the first month of therapy, consists primarily of GCs. Patients who are minimal residual disease (MRD) positive at the end of induction, largely reflecting intrinsic GC resistance (31), face significantly higher rates of relapse (32). Despite decades of clinical use of GCs and the known prognostic significance of the GC response, there are currently no rationally designed therapeutic strategies aimed at enhancing GC sensitivity in patients who are at risk for a poor GC response.

Despite their profound efficacy however, GCs are associated with significant acute and chronic adverse effects, which can be particularly detrimental given the young average age of children diagnosed with ALL and the lengthy treatment duration, resulting in considerable cumulative GC exposure (33). These data, combined with the outstanding survival rates for many of the molecular subtypes of ALL, warrant studies focused on improving our understanding of the mechanisms of GC response and resistance in order to better inform the use of GCs in ALL therapy and to suggest cooperative therapeutic approaches to optimize their efficacy. The following chapters will describe studies in two subtypes of ALL, Philadelphia chromosome-like B-cell ALL and T-cell ALL, that seek to understand mechanisms of intrinsic GC resistance and to identify therapeutic strategies to overcome them.

1.5: Hemophagocytic Lymphohistiocytosis

A key feature of a healthy immune response is that it is self-limiting. In response to an initiating stimulus, the immune system triggers the activation of immune cells, the release of inflammatory cytokines, and the engagement of cytolytic processes that collectively result in destruction of the stimulus. Following clearance of this stimulus, the immune system re-establishes homeostasis, with associated reductions in the number of activated immune cells and in the production of inflammatory cytokines (Figure 1-4). In contrast, hemophagocytic lymphohistiocytosis (HLH) is a rare hyperinflammatory condition in which, due to inherited or acquired defects in immune cell function, immune responses are initiated but fail to be appropriately terminated. In response to an immune trigger, including infection, autoimmunity, or malignancy, this results in excessive activation of immune cells and release of inflammatory cytokines that mediate severe and often life-threatening tissue injury (34) (Figure 1-5).

As opposed to secondary HLH, which arises in the absence of an apparent causal mutation, primary HLH occurs due to inherited loss-of-function mutations in genes required for the cytolytic functions of CD8 T-cells or NK cells, most commonly in *PRF1*, the gene encoding perforin. Perforin is a key protein component of the cytotoxic granules released from CD8 T-cells and NK cells and is required for the entry of cytolytic proteins into target cells, which ultimately mediates target cell destruction (34). As evidence for the central role of perforin in this process, it was found that *Prf1$^{-/-}$* mice fail to effectively clear infections with lymphocytic choriomeningitis virus (LCMV) (35). As a result, following exposure to LCMV these mice develop an HLH-like syndrome that recapitulates many of the key features of human disease, including fever, splenomegaly, pancytopenia, hypercytokinemia, and hemophagocytosis (36). These features have made the *Prf1$^{-/-}$* mouse one the best-studied and most accurate murine models of HLH, and this model was employed for the studies described in Chapter 8.

While HLH is defined by the occurrence of excessive immune activation and failed immune resolution, the considerable diversity with respect both to causal mutations and

underlying etiologies poses a number of diagnostic and therapeutic challenges (37). For the past decades, most patients meeting the diagnostic criteria for HLH were treated according to the protocols established by the HLH-94 and HLH-2004 trials, which consist primarily of the GC dexamethasone and the chemotherapeutic agent etoposide. Even with these protocols, clinical outcomes for HLH remain poor, with a 5-year survival of only 62% on HLH-2004 (38). Encouragingly however, continued improvements in the understanding of disease pathophysiology are beginning to drive the emergence of rationally-designed therapeutic strategies. In particular, the hypercytokinemia of HLH is increasingly being recognized both as a driver of disease, necessary for stimulating the persistent activation of CD8 T-cells and innate immune cells, as well as a contributor to the clinical manifestations of disease, with these cytokines known to directly mediate much of the end-organ damage (39). Consistent with this central role for cytokines in the disease process, it was first recognized that selective neutralization of the inflammatory cytokine interferon-γ (IFN-γ) was protective against disease in the $Prf1^{-/-}$ model (36), thereby establishing proof-of-concept for a therapeutic strategy involving direct targeting of inflammatory cytokines. These preclinical studies stimulated clinical development of a human antibody against IFN-γ, known as emapalumab, which in 2018 received accelerated approval for the treatment of refractory, recurrent, or progressive HLH in both pediatric and adult patient populations (40).

The importance of IFN-γ is well-established in murine models and early trials have demonstrated the efficacy of emapalumab in a subset of patients (41), thereby clinically validating the results of those preclinical studies. Biochemically however, consideration of the signal transduction pathways activated by IFN-γ as well as a multitude of other disease-associated cytokines suggests additional candidate therapeutic targets. Specifically, the vast majority of these cytokines, including IFN-γ, activate signaling via the JAK/STAT pathway (Figure 1-3), suggesting that JAK is a central signaling node shared by these cytokines, and that

inhibition of JAK has the potential to mitigate the downstream consequences of both excessive

IFN-γ signaling as well as signaling induced by many other cytokines. Consistent with this idea,

it was recently demonstrated in both the *Prf1*$^{-/-}$ model as well as a murine model of secondary

HLH that inhibition of JAK signaling with the JAK1/2 inhibitor ruxolitinib is superior to IFN-γ

blockade with respect to attenuation of many disease parameters (42). The work described in

Chapter 8 extends these studies of ruxolitinib to examine the cooperative potential of combining

ruxolitinib with the GC dexamethasone, a key component of the current standard of care for the

treatment of HLH.
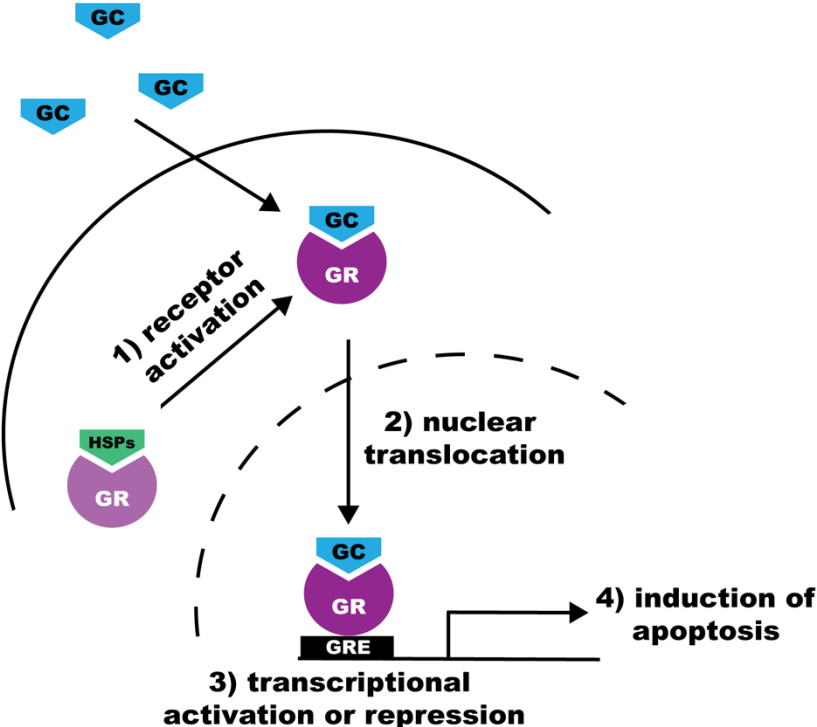
Figure 1-1: Mechanisms of GC action. GCs bind to a cytoplasmic GR (1), which induces translocation of the GC/GR complex to the nucleus (2). This complex binds to GREs to induce or repress transcription (3). In cells of the lymphoid lineage, this transcriptional activity alters the expression of components of the intrinsic apoptotic pathway, resulting in apoptosis (4).
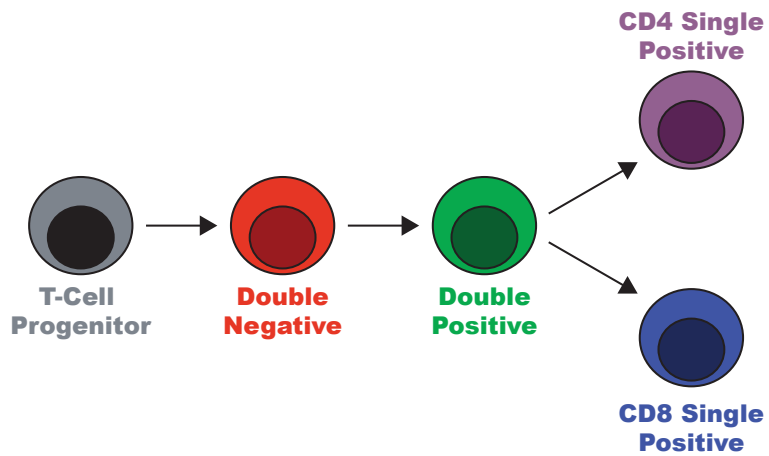
Figure 1-2: Schematic of early T-cell differentiation. T-cells progenitors in the thymus progress through a CD4/CD8 double negative (DN) stage, followed by a CD4/CD8 double positive (DP) stage, prior to differentiation into CD4 or CD8 single positive (SP) thymocytes.
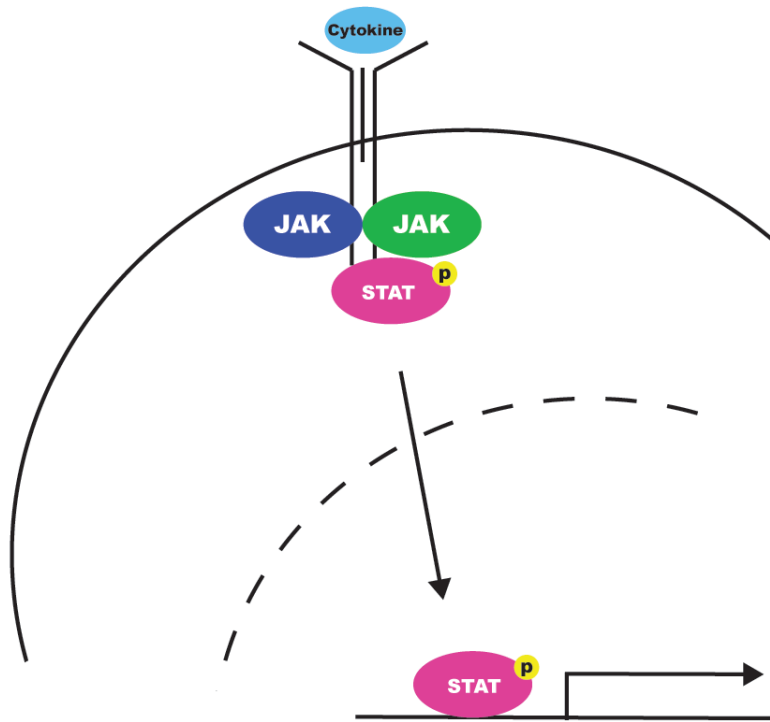
Figure 1-3: Schematic of cytokine receptor signaling. The common γ-chain family of cytokine receptors lack intrinsic kinase activity, and instead signal via intracellular associations with JAK proteins. Specifically, the cytokine-specific receptor chain associates with JAK1, and the common γ-chain associates with JAK3. JAKs catalyze the phosphorylation of tyrosine residues on the intracellular domains of the cytokine receptors, creating docking sites for STAT proteins, of which STAT5 is most essential to common γ-chain cytokine receptor signaling. These STAT proteins then become phosphorylated, promoting their dimerization and translocation to the nucleus, where they function as transcription factors to modulate target gene expression.
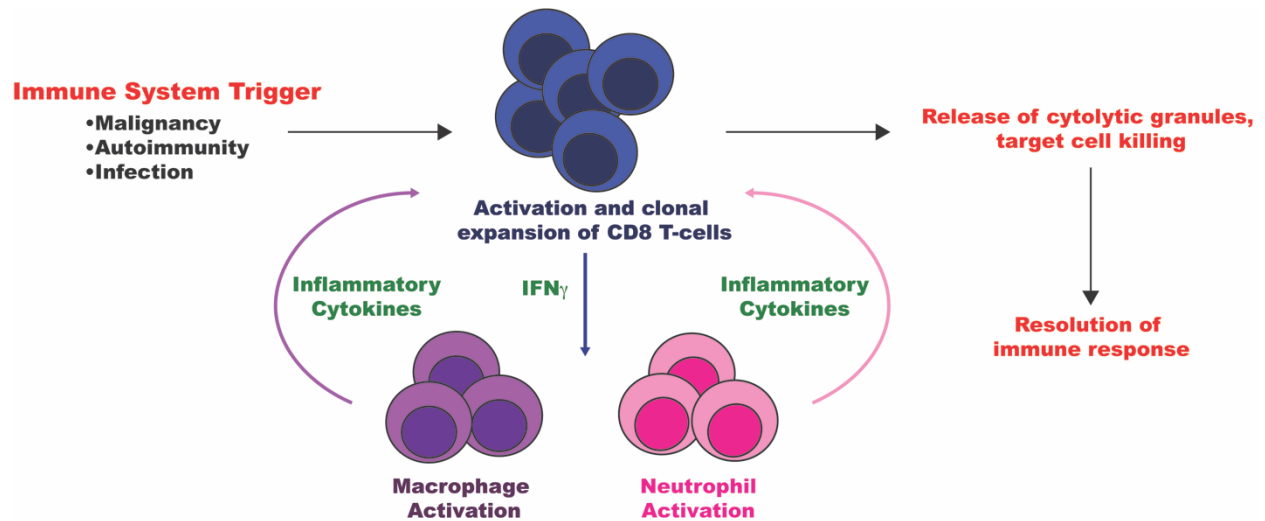
Figure 1-4: Schematic of a healthy immune response. In a healthy immune response, the immune system becomes activated in response to a trigger such as malignancy, autoimmunity, or infection. This results in activation and expansion of immune cells that secrete inflammatory cytokines to promote further immune cell activation. Due to the cytotoxic activity of immune cells, the initiating stimulus is then cleared, ultimately leading to resolution of the immune response and the return to a homeostatic state.
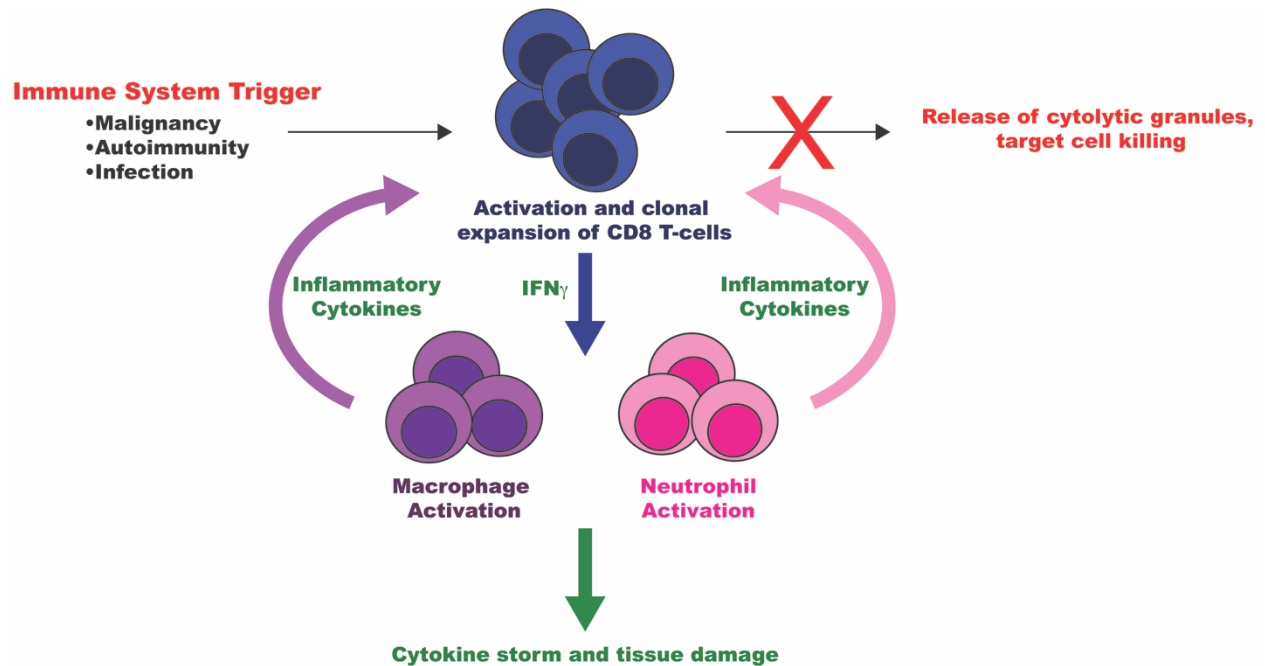
Figure 1-5: Schematic of HLH pathogenesis. Due to the impaired cytotoxic function of CD8 T-cells or NK cells in HLH, the immune system becomes appropriately activated in response to a stimulus, but is unable to effectively clear that stimulus. This results in persistent activation of immune cells, which continue to proliferate and release large amounts of inflammatory cytokines that mediate devastating tissue damage.

1.7: Table

Table 1-1: Cellular sources and functions of γ-chain cytokines (43)

Cytokine	Cellular Source(s)	Major Function(s)
IL2	Primarily CD4 T-cells, with some production by CD8 T-cells, NK cells, and NKT cells	T-cell growth, T helper cell differentiation, B-cell growth and differentiation, and NK cell proliferation
IL4	T-cells	B-cell differentiation, M2 macrophage production, and Th2 responses
IL7	Stroma	T-cell development and survival, pre-B-cell growth
IL9	T-cells	Mast cell growth, IgE and IgG production, innate lymphoid-cell survival
IL15	Dendritic cells and monocytes	T-cell growth, maintenance of memory CD8 T-cells
IL21	T helper cells and NKT cells	B cell differentiation and immunoglobulin production

Chapter 2: Mechanisms of Glucocorticoid Response and Resistance in

Lymphoid Malignancies

2.1: Abstract

Glucocorticoids are an integral component of multi-agent therapy regimens for a wide variety of lymphoid malignancies due to their potent effects to induce apoptosis in cells of the lymphoid lineage. Despite their clinical utility, *de novo* and acquired resistance to GCs is a significant clinical problem that contributes to inferior outcomes for many of these diseases. This review summarizes what is currently known about mechanisms of GC resistance in lymphoid malignancies, with a particular focus on novel therapeutic strategies currently in preclinical or clinical development that are rationally-designed to overcome GC resistance and improve clinical outcomes.

2.2: Introduction

For decades, glucocorticoids (GCs) have been a key component of therapy for the treatment of lymphoid malignancies and are widely used in both frontline and salvage therapy regimens (44)(45). In many of these cancers, the response to GC therapy is a strong prognostic indicator that is related to both overall and event-free survival (EFS) rates (44)(46)(47). In particular, patients with acute lymphoblastic leukemia (ALL) treated on Berlin-Frankfurt-Münster (BFM) protocols can be classified as having a prednisone good response (PGR) or a prednisone poor response (PPR), defined based on the response to an upfront one-week window of monotherapy consisting of the GC prednisone. In early ALL-BFM protocols, patients with a PPR had significantly inferior outcomes relative to patients with a PGR (44). These data indicate that therapeutic strategies to overcome GC resistance may significantly improve patient outcomes. The objective of this review is to highlight key concepts regarding GC resistance in lymphoid malignancies, with a specific focus on therapeutic strategies designed to overcome GC resistance.

2.3: Mechanisms of Glucocorticoid Action

GCs are a class of steroid hormones that bind to the GC receptor (GR). In the absence of endogenous or exogenous GC ligand, GR is largely retained in the cytoplasm through its association with a variety of molecular chaperone proteins, including HSP70 and HSP90 (48). Upon ligand binding, GR undergoes a conformational change that promotes translocation of the GC-GR complex to the nucleus, where it associates with DNA sequences known as GC response elements (GREs). These GREs function as enhancer elements to modulate the activity of associated gene promoters, which in turn mediate the activation or repression of target gene expression (1). The effects of GCs are highly tissue-specific due to differences in GRE binding patterns and transcriptional activities in different cell types. Importantly, while GCs exert pro-survival effects in many tissues, they potently induce cell death in cells of the lymphoid lineage (49), underlying their importance in the treatment of lymphoid malignancies.

While there is little overall consensus regarding the specific components of the GR-associated transcriptome that mediate the effects of GCs on lymphoid cells, many groups have demonstrated that activation of the intrinsic apoptotic pathway is required for GC-induced cell death (49). Consistent with this idea, the concept of a "BCL2 rheostat" has been proposed, whereby modulation of both the pro- and anti-apoptotic components of the intrinsic apoptotic pathway results in an altered apoptotic threshold that leads to cell death. Through an analysis of both basal and GC-induced expression of components of the intrinsic apoptotic pathway in primary ALL cells, Ploner *et al.* identified key expression patterns that are associated with GC-induced apoptosis. Specifically, they noted potent induction of the pro-apoptotic family members *BIM* and *BMF*, and demonstrated that loss of expression of either of these proteins is sufficient to decrease GC sensitivity. Conversely, they demonstrated that overexpression of anti-apoptotic family members, including *BCL2*, *BCL-XL*, and *MCL1*, impairs GC-induced apoptosis, an effect that is reversed upon experimental silencing of these genes (50). Taken together, these data suggest that coordinate modulation of both pro- and anti-apoptotic family members contributes

to GC-induced apoptosis. Jing *et al.* further elucidated the importance of such a BCL2 rheostat through an analysis of ALL patient derived xenografts (PDXs). Using chromatin immunoprecipitation with sequencing (ChIP-seq), this group identified a novel GR binding site within an intronic region of the *BIM* gene. When this region was mutated to abolish GR binding, GC-induced upregulation of *BIM* expression was lost and GC sensitivity was significantly decreased, providing further evidence that GR-mediated upregulation of *BIM* is required for GC sensitivity. Furthermore, this study elucidated a series of GR-mediated transcriptional events that lead to downregulation of *BCL2* expression, and found that these events were also required for effective GC-induced apoptosis (18). Given the importance of the intrinsic apoptotic pathway in mediating GC sensitivity in lymphoid cells, it is not surprising that while diverse mechanisms of GC resistance have been elucidated in lymphoid malignancies, these mechanisms largely converge on a failure to appropriately modulate the intrinsic apoptotic pathway.

2.4: Mechanisms of Glucocorticoid Resistance

2.4.1: GR Intrinsic Mechanisms of GC Resistance

<u>*NR3C1* Mutations</u>

The GR protein, which is encoded by the *NR3C1* gene*,* is comprised of three major functional domains: the ligand binding domain (LBD), the DNA binding domain (DBD), and the N-terminal transactivation domain (NTD), which interacts with the transcriptional machinery and with transcriptional coregulators to mediate the effects of GR on gene expression (48). Mutations in each of these domains have been identified in the context of familial and sporadic generalized GC resistance, where they lead to complete or partial insensitivity of target tissues to both endogenous and exogenous GCs (51). In addition to generalized GC resistance, localized GC resistance that is attributable to *NR3C1* mutations has been reported in a number of disease contexts, including asthma and autoimmune diseases (52). Given this precedent for

GC resistance mediated by GR mutations, many groups have hypothesized that pre-existing

mutations in the GR gene, or mutations acquired over the course of GC therapy, may contribute

to *de novo* or acquired GC resistance in lymphoid malignancies. Much of this work has focused

on CCRF-CEM cells, a cell line model of human T-cell ALL (T-ALL) that has been studied

extensively in the context of GC sensitivity and resistance. Early studies involving CCRF-CEM

cells identified considerable heterogeneity in the clonal composition of the cell line, leading to

the subsequent isolation and characterization of a number of subclonal cell lines with varying

degrees of GC sensitivity (53). In an analysis of the parental CCRF-CEM cell line, a

heterozygous point mutation was identified in the LBD, and functional studies demonstrated

impaired functionality of this mutant allele (54)(55)(56)(57). However, this same heterozygous

mutation has since been identified in both GC sensitive and GC resistant subclones derived

from the parental CCRF-CEM cell line, suggesting that additional events are required to confer

GC resistance. Consistent with this idea, it has been shown that the GC resistant subclones

derived from the GC sensitive parental cell line express this mutant allele in the absence of a

wild-type allele, resulting in complete impairment of GR activity (54). Interestingly, this LBD point

mutation was identified in biopsy tissue taken after the initiation of treatment from the patient

from whom CCRF-CEM cells were derived, suggesting that it was acquired *in vivo* and was

likely selected for over the course of GC treatment (58). Similar to CCRF-CEM cells, Jurkat

cells, another human T-ALL cell line, are heterozygous for a mutation that impairs GR

transcriptional activity. Unlike CCRF-CEM cells however, Jurkat cells also express low basal

levels of GR and fail to induce expression of GR upon GC exposure, resulting in profound GC

resistance (59).

Based on this evidence supporting a role for *NR3C1* mutations as a cause of GC

resistance in cultured cell lines, multiple groups have conducted studies to determine whether

such mutations cause clinically relevant GC resistance in patients receiving GC therapy for the

treatment of lymphoid malignancies. In an analysis of a panel of cell lines derived from paired

diagnostic and relapse samples taken from pediatric patients with ALL, Beesley *et al.* identified

significant variability in GC sensitivity. Upon sequencing the *NR3C1* gene in these cell lines, this

group identified a number of polymorphisms, all of which had previously been shown to have a

negligible effect on GC sensitivity (52), but no deleterious mutations. This finding led them to

conclude that *NR3C1* mutations are not a common mechanism of naturally-acquired GC

resistance (60). Consistent with these findings, sequencing of *NR3C1* in a larger cohort of

diagnostic pediatric ALL samples revealed a similar distribution of polymorphisms, but these

polymorphisms failed to correlate with the clinical response to prednisone therapy and did not

occur at a significantly higher rate than previously reported in the general population (61),

supporting the conclusion that *NR3C1* mutations are not a common cause of *de novo* GC

resistance. However, there have been a number of reports demonstrating the presence of

deleterious *NR3C1* mutations that are undetectable at diagnosis but are significantly enriched at

the time of disease relapse, suggesting that the acquisition of such mutations may confer

acquired GC resistance (62)(63)(64). Taken together, the existing data suggest that *NR3C1*

mutations are a relatively minor cause of GC resistance in human lymphoid malignancies,

particularly at the time of diagnosis, but may be more important in the context of relapsed

disease following the selective pressure of exposure to GC therapy.

Modulation of GR Expression and Function

In addition to GR mutations, expression levels of GR have been evaluated as a potential

biomarker for GC sensitivity and resistance. Using large cohorts of diagnostic ALL samples,

early clinical data suggested that the absolute number of GRs in lymphoblasts is positively

correlated with the clinical response to GC monotherapy (65), the likelihood of disease

remission (66), and with five-year EFS rates (67). More recently, GR expression has been

shown to carry prognostic significance specifically in the context of pediatric B-cell ALL (B-ALL)

harboring the *ETV6/RUNX1* fusion oncogene. In these patients, deletions of *NR3C1* resulting in

loss of GR protein expression are associated with increased minimal residual disease (MRD) and with risk of relapse (68). Despite these findings, other studies have failed to identify a clinically meaningful relationship between basal GR expression at diagnosis and the clinical response to GC therapy. In an analysis of GR protein expression in diagnostic samples taken from patients treated on ALL-BFM protocols, there was no significant difference in GR expression between PPR and PGR patient groups (69), suggesting that basal GR expression may be an unsuitable biomarker for predicting GC sensitivity. However, it has been shown that in lymphoid cells, exposure to GCs results in autoinduction of GR expression mediated by a direct transcriptional effect of GR (70), and multiple studies have demonstrated that expression levels of GR after autoinduction, rather than basal expression levels, are required for a GC response and may be a better predictor of GC sensitivity. Using a titratable expression system in a human T-ALL cell line, Ramdas *et al.* demonstrated that basal levels of GR may be insufficient to confer GC sensitivity, but that levels comparable to those achieved following GC exposure and subsequent autoinduction of GR expression are sufficient to mediate GC-induced apoptosis (71). Consistent with these data, a failure to autoinduce GR expression upon GC exposure has been implicated in GC resistance in Jurkat T-ALL cells (59) and in multiple myeloma cell lines (72).

Several studies have also identified other genetic and epigenetic events that lead to altered GR expression levels, and may therefore contribute to GC resistance. For example, loss-of-function mutations in the E3 ubiquitin ligase *FBXW7* have been associated with a favorable prognosis and an early response to GC therapy in ALL (73)(74). A later study demonstrated that FBXW7 mediates the ubiquitination and subsequent proteasomal degradation of GR, leading to insufficient GR levels to mediate GC-induced apoptosis. This same study found that inactivation of FBXW7 in an *in vitro* system was sufficient to restore GR expression and consequently, GC sensitivity (75). The NALP3 inflammasome has also been implicated as a modulator of cellular GR levels. In an analysis of GC resistant primary ALL

samples, it was found that decreased promoter methylation of *CASP1* and *NLRP3* resulted in

increased expression of the NALP3 inflammasome, and that the associated increase in caspase

1 activity caused increased cleavage of GR protein, leading to an attenuated GC response

mediated by a loss of GR protein expression (76). Therefore, while basal GR expression has

not proven to be a tractable biomarker with clinical utility for predicting GC sensitivity, altered

levels of GR expression may nonetheless contribute to a poor GC response.

       In addition to GR expression levels, post-transcriptional processing of the GR mRNA

results in multiple GR isoforms, which may also play a role in dictating GC sensitivity. GRα is

the most abundant GR isoform and has been shown to mediate the pro-apoptotic effects of GCs

in lymphocytes. Exon 9 of *NR3C1* encodes a portion of the LBD, and alternative splicing of this

exon distinguishes the GRα isoform from the GRβ isoform (48). The GRβ isoform does not bind

GCs, does not have transcriptional activity, and has been shown to exert a dominant negative

effect on the GRα protein, thereby impeding its pro-apoptotic activity (77). Additionally,

alternative splicing involving the intron between exons 3 and 4 gives rise to the GRγ isoform,

which has an altered DBD. Therefore, GRγ retains ligand binding capacity but has limited

transcriptional activity (48). Finally, alternative splicing involving the LBD results in the

production of the GR-A and GR-P isoforms, both of which fail to bind ligand (48). As a result of

the impaired activity of multiple GR isoforms, many groups have studied the relationship

between GC sensitivity and the relative expression and distribution of these isoforms in a variety

of lymphoid malignancies. One of the earliest such studies focused on a patient with chronic

lymphocytic leukemia (CLL) who was found to have generalized GC resistance. An analysis of

the expression pattern of GR isoforms in cells taken from this patient demonstrated decreased

GRα expression and increased GRβ expression, resulting in an altered ratio between the two

isoforms (78). Given the dominant negative effect of GRβ on GRα, this group concluded that the

altered ratio may contribute to the generalized GC resistance observed in this patient.

Consistent with these findings, an analysis of 23 diagnostic ALL samples revealed an inverse correlation between the GRβ/GRα ratio and the number of apoptotic cells following *in vitro* exposure to prednisolone, further indicating that high expression of GRβ impairs GC sensitivity (79). Relative to diagnostic samples, relapsed ALL samples have also been shown to have a decreased mRNA to protein ratio of GRα (80). Similarly, GRγ expression has been shown to be increased in PPR patients relative to PGR patients, which is consistent with the idea that GRγ expression might impair the transcriptional activity of GRα, leading to an inferior GC response (81).

Further regulation of GR activity is mediated by the chaperone protein systems that interact with GR, the two most important of which are the HSP70 and HSP90 systems. These chaperones assist with maintaining GR in a conformation in which it is competent for ligand binding and they facilitate the subsequent nuclear translocation of ligand-bound GR (82). Given the central role of chaperone proteins in modifying GR activity, several groups have hypothesized that aberrant expression or activity of these chaperone systems could contribute to GC resistance in lymphoid malignancies. However, in an analysis of PPR and PGR patients treated on ALL-BFM trials, there was no correlation between *in vivo* GC sensitivity and HSP90 expression (83). In a more in-depth analysis looking at mRNA expression of key chaperone proteins in GC sensitive versus GC resistant ALL cells, there were also no meaningful differences in transcript expression (84). While this finding does not exclude the possibility that differences in protein expression of these chaperones may underlie differences in GC sensitivity, these studies suggest that chaperone proteins likely do not play a significant role in clinical GC resistance in lymphoid malignancies.

2.4.2: GR Extrinsic Mechanisms of GC Resistance

Epigenetic Regulation of GR Activity

Changes in GR target gene expression require the association of ligand-bound GR with a GRE (1). Some of the cell- and tissue-specificity of GCs may be mediated by differences in chromatin accessibility, as GR binding has been shown to occur predominantly at accessible chromatin sites (85). Given this requirement for pre-existing chromatin accessibility, a number of groups have assessed the role for an altered epigenetic landscape as a mediator of GC resistance. Chromatin accessibility is maintained in part through the activity of the SWI/SNF complex (85), and decreased expression of core components of this complex correlate with the occurrence of GC resistance in ALL cells (86). In an analysis of gene expression and DNA methylation patterns in matched pairs of pediatric B-ALL samples obtained at the time of diagnosis and at relapse, Hogan *et al.* identified a distinct pattern of gene expression associated with relapse and found that this gene expression pattern co-occurred with increased promoter methylation (87). With the addition of the DNA methyltransferase inhibitor decitabine, this relapse-specific gene expression pattern could be reverted, allowing for re-expression of hypermethylated genes. Exposure to decitabine, along with the histone deacetylase (HDAC) inhibitor vorinostat, resulted in significant potentiation of GC-induced apoptosis (88), suggesting that modification of the epigenetic landscape may facilitate GR-mediated changes in gene expression that lead to apoptosis. Similarly, it was shown that elevated expression of a number of HDAC genes is common in patients who have a PPR (89). Consistent with these findings, Jones *et al.* reported a high frequency of deletions of *TBL1XR1,* a component of the nuclear receptor corepressor (NCoR) complex, in patients with B-ALL. These deletions stabilize NCoR, which represses GR activity by decreasing its recruitment to target gene loci and by recruiting HDAC3 to further promote inhibition of target gene expression. Treating these cells with an HDAC inhibitor was sufficient to restore GC sensitivity (90). Collectively, these data suggest that GC sensitivity is mediated in part by a permissive epigenetic landscape, and that the use of

epigenetic modulators may represent a therapeutic strategy to enhance GC sensitivity in lymphoid malignancies that are associated with an altered epigenetic landscape.

<u>Signal Transduction</u>

Dysregulated signal transduction is a hallmark feature of many lymphoid malignancies including T-ALL (91), B-ALL (92), and non-Hodgkin lymphoma (NHL) (93). Importantly, the downstream effectors of these signal transduction pathways exhibit known cross-talk with GR signaling and transcriptional activity (94). As a result of these interactions, aberrant regulation of these signal transduction pathways is an important cause of GC resistance in lymphoid malignancies and significant attention has been devoted to the use of targeted signal transduction inhibitors as a strategy to overcome GC resistance.

Cyclic Adenosine Monophosphate (cAMP) Signaling. cAMP is a second messenger molecule that initiates signaling cascades responsible for mediating a variety of immune cell functions. cAMP is generated through the catalytic activity of adenylate cyclases and is degraded by a family of enzymes called phosphodiesterases (PDEs) (95). It has long been known that in addition to GCs, activation of cAMP decreases lymphoid cell proliferation and induces apoptosis (96). Furthermore, it has been shown in T-cell lines that stimulation of cAMP signaling has a synergistic effect to induce cell death when combined with the GC dexamethasone (DEX) (97), and that cAMP and GCs likely converge to promote the upregulation of BIM expression (98)(99), thereby facilitating the induction of apoptosis. Given the pro-apoptotic effects of cAMP and the effects of PDEs to decrease the cellular pool of cAMP, significant attention has been devoted to the development of PDE inhibitors (100), and a number of groups have evaluated the efficacy of PDE inhibitors as a means of overcoming GC resistance in lymphoid malignancies. In the CCRF-CEM cell line, both a non-specific PDE inhibitor and rolipram, a PDE4-specific inhibitor, significantly potentiated DEX-induced apoptosis (101). In primary CLL cells, rolipram synergized with GCs to induce apoptosis, and this effect

was associated with increased GR-mediated transcriptional activity (102). Furthermore, in these same cells, it was found that rolipram exposure resulted in an increase in both transcript and protein expression of GRα (103). In patients, PDE4 overexpression has been observed in a cohort of primary diffuse large B-cell lymphoma (DLBCL) samples. Consistent with the data in leukemia cell lines, inhibition of PDE4 in DLBCL cells was sufficient to restore GC sensitivity (104). Finally, in a large-scale gene expression analysis of primary DLBCL samples obtained from patients who received treatment with cyclophosphamide, adriamycin, vincristine, and prednisone (CHOP), elevation of PDE4 expression was enriched in patients with fatal or refractory disease relative to patients who were cured with CHOP therapy (105). Taken together, these data suggest that alterations in cAMP pathway signaling may contribute to GC resistance in lymphoid malignancies and that therapeutic targeting of this pathway may have clinical utility.

Mitogen Activated Protein Kinase (MAPK) Signaling. The three best studied MAPKs are p38, ERK, and JNK, all of which become activated downstream of a signaling cascade induced by cellular exposure to mitogenic stimuli (106). Each of these MAPKs has been shown to modulate GC sensitivity, resulting in a considerable number of studies devoted to investigating the therapeutic potential of MAPK pathway signaling modulators as a means of enhancing GC sensitivity. In GC resistant clones derived from the parental CCRF-CEM cells, inhibition of p38 MAPK decreased DEX sensitivity, while inhibition of ERK activity increased sensitivity. These data implicate p38 as a positive regulator of GC activity and ERK as a negative regulator of GC activity (107), suggesting that distinct arms of the MAPK signaling cascade interact differently with the GR pathway. Consistent with these findings, it has been shown that exposing CCRF-CEM cells to DEX results in increased phosphorylation and activation of p38, one substrate of which is GR itself. Specifically, this study demonstrated that p38 mediates Ser-211 phosphorylation of GR (108), which has been shown to increase the transcriptional activity of GR (48), thereby providing a mechanistic explanation for the positive effect of p38 activity on

GC sensitivity. Another study demonstrated that inhibition of p38 in CCRF-CEM cells resulted in decreased induction of BIM expression upon DEX exposure, leading to an attenuated apoptotic response and suggesting that p38 might further contribute to GC sensitivity by enabling the upregulation of BIM expression (109).

Other studies have focused on elucidating the molecular basis for the inhibitory effect of ERK signaling on GC sensitivity. Importantly, ERK has been shown to phosphorylate BIM, preventing it from interacting with other members of the intrinsic apoptotic pathway to induce apoptosis (110). To determine whether this mechanism contributes to ERK-mediated GC resistance, Rambal *et al.* demonstrated in ALL cell lines and primary patient samples a synergistic interaction between a MEK inhibitor and DEX, with simultaneous exposure to both agents resulting in increased BIM expression due to a reduction in ERK-mediated BIM phosphorylation (111). In addition to ERK, JNK activation has previously been implicated as a negative regulator of GC sensitivity. In contrast to p38, JNK is known to catalyze an inhibitory phosphorylation of GR, resulting in decreased transcriptional activity (112). Jones *et al.* further established the role of ERK and JNK as negative regulators of GC sensitivity through an shRNA screen designed to identify genes that modify prednisolone sensitivity in B-ALL cell lines. Interestingly, this screen identified *MEK2*, which activates ERK, and *MEK4*, which activates JNK, as important candidate GC resistance genes. Through a variety of functional studies, the authors demonstrated that loss of MEK2 expression induced generalized chemosensitivity, including to GCs, through a p53-dependent mechanism and that loss of MEK4 increased expression of GR, leading to improved GC sensitivity. Furthermore, they demonstrated the clinical relevance of these findings by assessing ERK activity in paired diagnostic and relapse samples from patients with B-ALL and found increased levels of phosphorylated ERK in the relapsed samples (113), consistent with the idea that aberrant activation of ERK signaling may contribute to GC resistance. Given the large number of past and current clinical trials conducted in a wide variety of malignancies (114), the addition of small molecules that modulate MAPK

pathway activity may be a feasible strategy for overcoming GC resistance in some lymphoid malignancies.

PI3K/AKT/mTOR Signaling. The PI3K/AKT/mTOR pathway is another signal transduction pathway that is commonly dysregulated in lymphoid malignancies and represents a potential therapeutic target for strategies aimed at overcoming GC resistance. In a recent study involving a large cohort of pediatric T-ALL samples, *AKT1* and *PTEN* mutations were two of only several genetic lesions that had a univariable association with relapse (91), suggesting that mutational activation of this pathway may play a role in therapy resistance, including to GCs. In another analysis of primary B-ALL samples, patients with increased phosphorylated AKT at diagnosis had a significantly inferior response to steroid-containing induction therapy and had decreased overall and relapse-free survival (115). These studies provide correlative evidence for the role of aberrant PI3K/AKT/mTOR pathway activity in GC resistance. To more directly assess a mechanistic basis for this relationship, Piovan *et al.* demonstrated using co-immunoprecipitation that AKT1 binds to and phosphorylates GR on Ser-134, a phosphorylation event that impairs nuclear translocation of ligand-activated GR. Using the *PTEN*-null CCRF-CEM cell line, the authors demonstrated through both *in vitro* and *in vivo* studies that combined treatment with GCs and the AKT inhibitor MK2206 is sufficient to reverse GC resistance (116). One class of proteins that has been found to cooperate with AKT to modulate GC activity is the 14-3-3 class of phospho-serine/threonine binding proteins, which regulate the subcellular localization of proteins with phosphorylated serine or threonine residues, including phosphorylated GR (117). Consistent with this function, the 14-3-3σ protein interacts with GR upon AKT1-mediated Ser-134 phosphorylation, resulting in impaired nuclear translocation of ligand-bound GR and leading to reduced transcriptional activity in the presence of GCs (117)(118). Similarly, it has been shown that more proximal inhibition of this pathway with a PI3K inhibitor results in synergy when combined with GCs, both *in vitro* and in an *in vivo* xenograft model (119). In B-ALL cell lines and primary diagnostic patient samples, PI3K

inhibition augmented nuclear translocation of ligand-activated GR through a reduction in Ser-134 phosphorylation (120), further confirming the effect of aberrant PI3K/AKT pathway inhibition to promote cytoplasmic retention of GR and prevent transcriptional activation.

One important downstream effector of PI3K/AKT pathway activation is mTOR (121), and many groups have studied the role of aberrant mTOR activation as a mediator of GC resistance in lymphoid malignancies. Using a chemical genomics approach, Wei *et al.* compared a large number of drug-associated gene expression profiles with the gene expression signature of GC sensitive and resistant ALL cells. Through this analysis, they determined that the changes in gene expression associated with exposure to the mTOR inhibitor rapamycin matched that associated with GC sensitive cells, suggesting that rapamycin may show efficacy by altering the gene expression pattern in GC resistant cells to better mimic that of GC sensitive cells. They further demonstrated that exposure to rapamycin sensitized cells to GCs through a mechanism involving downregulation of expression of the anti-apoptotic protein MCL1 (122). Similarly, Gu *et al.* demonstrated a synergistic relationship between rapamycin and DEX in a panel of T-ALL cells, and further elucidated the mechanistic basis for this interaction by identifying a synergistic induction of expression of the pro-apoptotic BAX and BIM proteins in conjunction with downregulation of MCL1 (123). In addition, it has been shown that simultaneous exposure to an mTOR inhibitor and GCs results in a synergistic induction of the cyclin-dependent kinase (CDK) inhibitor proteins p21 and p27 (123)(124), suggesting that mTOR inhibitors and GCs converge both to induce cell cycle arrest and activation of the intrinsic apoptotic pathway. This effect was further demonstrated *in vivo* using PDXs derived from primary patient T- and B-ALL samples, and the combinatorial effect of mTOR inhibition and GCs was found to be particularly effective in T-ALL samples with loss of *PTEN* expression (125), providing further evidence that aberrant regulation of upstream PI3K/AKT pathway activity results in altered mTOR activity that can be targeted therapeutically to augment the GC response. Finally, given the direct effects of both AKT and mTOR on GC sensitivity, several groups have investigated the efficacy of the dual

PI3K and mTOR inhibitor BEZ235, reasoning that dual inhibition at two critical points in this pathway may have a more profound effect to induce GC sensitivity. Indeed, in ALL cell lines and primary patient samples both *in vitro* and *in vivo*, synergy has been demonstrated between BEZ235 and DEX (126)(127), suggesting that multiple nodes within this pathway are viable therapeutic targets for augmenting GC sensitivity.

JAK/STAT Signaling. The JAK/STAT signaling pathway is the critical effector pathway of cytokine receptor signaling, which plays a crucial role in mediating survival, proliferation, and differentiation of lymphoid cells (128). Not surprisingly, aberrant activation of this pathway is common in lymphoid malignancies (91)(129), and significant attention has been devoted to assessing the role of JAK/STAT pathway inhibition as a novel treatment modality. Activation of cytokine receptors recruits JAK proteins to intracellular domains of cytokine receptors, and these activated JAK proteins recruit and phosphorylate STAT proteins, which translocate to the nucleus and function as transcription factors (128). Interestingly, GR and one of these STAT proteins, STAT5, have been shown to physically interact at certain genomic loci. Specifically, STAT5 is known to inhibit the action of GR on GR target genes (130). Consistent with this inhibitory role of JAK/STAT signaling on GR activity, inhibition of this pathway has been shown to overcome GC resistance in a number of lymphoid malignancies. In Philadelphia chromosome-like B-ALL, which is associated with aberrant JAK/STAT pathway activation, the combination of a JAK2 specific inhibitor and DEX demonstrated *in vitro* synergy and showed improved survival in an *in vivo* xenograft model (131). Similarly, in primary diagnostic T-ALL samples, exposure to the cytokine interleukin-7 resulted in increased JAK/STAT pathway activity that induced GC resistance and could be overcome with the addition of the JAK1/2 inhibitor ruxolitinib (132). Finally, in CLL cells, GC resistance was found to be associated with autocrine activation of another STAT protein, STAT3, and inhibition of STAT3 activation with ruxolitinib resulted in increased sensitivity to DEX *in vitro* (133).

NOTCH Signaling. NOTCH receptors are transmembrane receptors that, upon ligand binding, undergo a series of cleavage events to release the activated intracellular component of NOTCH from the membrane, allowing it to translocate to the nucleus and function as a transcription factor. The γ-secretase complex mediates the final step in this processing (134). Due to the important role of NOTCH signaling in the pathogenesis of T-cell malignancies, inhibitors of this γ-secretase complex have been evaluated as potential therapeutic agents for the treatment of these diseases in combination with GCs. Specifically, in T-ALL cell lines, γ-secretase inhibitors have been shown to sensitize cells to the cytotoxic effects of DEX (135). Several groups have demonstrated that the combination of γ-secretase inhibitors and GCs facilitates autoinduction of GR and potentiates the induction of BIM expression, leading to increased cell death in both *in vitro* and *in vivo* model systems (136)(137). Despite these promising preclinical findings, the clinical utility of γ-secretase inhibitors has been limited by severe gastrointestinal toxicity (138). However, in an elegant study conducted in a T-ALL xenograft model, it was shown that simultaneous exposure to a γ-secretase inhibitor and DEX not only overcame GC resistance, but also attenuated the toxicities associated with the γ-secretase inhibitor (136), suggesting that the combination of γ-secretase inhibitors and GCs may be a viable therapeutic strategy to enhance GC sensitivity. Finally, at least one study has evaluated the efficacy of an anti-NOTCH1 monoclonal antibody in a T-ALL PDX model and demonstrated potentiation of GC activity when given in combination (139).

Src Family Kinase Signaling. In T-cells, the Src family kinases Lck and Fyn mediate critical signal transduction events downstream of the T-cell receptor (TCR) (140). Through the use of reverse-phase protein arrays applied to PPR and PGR T-ALL samples, Lck was found to be aberrantly activated in PPR patients relative to PGR patients (141). Consistent with these findings, inhibition of Lck with the Src family kinase inhibitor dasatinib has demonstrated *in vitro*

efficacy to enhance GC sensitivity (142) and has been shown to impair the engraftment of T-ALL cells *in vivo* relative to treatment with either agent alone (141).

Metabolism

In addition to studies demonstrating the importance of GR expression levels as a mediator of GC sensitivity, many groups have demonstrated that metabolic processes that limit the availability of GC ligand can similarly contribute to GC resistance. In normal physiology, the 11β-hydroxysteroid dehydrogenase (HSD) class of enzymes mediates the conversion between cortisol, the active endogenous hormone, and cortisone, the inert form of the hormone. Specifically, 11β-HSD1 regenerates cortisol from cortisone while 11β-HSD2 inactivates cortisol (143). In an analysis of primary patient ALL samples, basal 11β-HSD1 expression was found to be higher in GC sensitive samples relative to GC resistant samples. Furthermore, 11β-HSD1 expression was upregulated in response to DEX exposure specifically in the GC sensitive samples but not in the GC resistant samples, suggesting that 11β-HSD1 may participate in a GC-regulated feedback loop to maintain the availability of ligand for GR binding (144). The same group similarly analyzed 11β-HSD2 expression in the GC resistant T-ALL cell line MOLT4F and the GC sensitive CCRF-CEM cell line and demonstrated that 11β-HSD2 expression was higher in the setting of GC resistance. They further demonstrated that pharmacologic inhibition of 11β-HSD2 was sufficient to potentiate GC-induced apoptosis (145). Consistent with these findings, 11β-HSD2 expression was compared between GC resistant T-ALL cell lines, GC sensitive NHL cell lines, and normal peripheral T-cells. In the GC resistant cell lines, 11β-HSD2 expression was found to be significantly elevated relative to the GC sensitive cell lines or normal T-cells (146). To determine how 11β-HSD2 is dynamically regulated in the presence of GCs, transcript and protein expression as well as enzymatic activity were assessed in the GC sensitive CEM-C7 cell line after exposure to DEX. This analysis

demonstrated a reduction in expression and enzymatic activity upon DEX exposure, suggesting that, in contrast to 11β-HSD1, GC-induced downregulation of 11β-HSD2 may be important for maintaining GC sensitivity (147).

In addition to HSDs, glutathione *S*-transferases (GSTs) are a class of enzymes involved in the metabolism of a wide variety of drugs, including steroids (148). In an analysis of PGR and PPR patient samples from children treated on an ALL-BFM protocol, deletion of the GST family member *GSTT1* was enriched in the PPR patient group and was associated with an increased risk of relapse (149). These data suggest that genetic lesions involving GST genes might contribute to differences in clinical GC response, though further studies are needed to determine whether aberrant GST activity plays a significant role in altering the availability of GC ligand and whether this contributes to GC resistance.

While metabolism of GCs themselves may play a role in modulating GC sensitivity, GC resistance has also been attributed to the aberrant activity of key bioenergetic metabolic pathways. Specifically, it has been shown in both ALL cell lines and in primary patient ALL samples that GC resistance is associated with increased rates of glycolysis, oxidative phosphorylation, and cholesterol biosynthesis. In a gene expression profiling study using ALL cell lines, pathways involved in these metabolic processes emerged as the top biological pathways associated with GC resistance. Furthermore, when these gene sets were studied in the context of primary patient samples, enrichment for these gene sets was a strong predictor of relapse (150), suggesting that activation of these bioenergetic pathways may promote chemoresistance. The same group went on to demonstrate that inhibition of glycolysis, oxidative phosphorylation, or cholesterol biosynthesis was sufficient to sensitize GC resistant T-ALL cells to GCs (151), further supporting the idea that aberrant activation of cellular metabolic processes may confer GC resistance.

Based on these findings, significant attention has been devoted to studying the role of glucose metabolism as a modulator of GC sensitivity. In an analysis of a large cohort of primary

B-ALL samples with varying degrees of *in vitro* prednisolone sensitivity, genes associated with carbohydrate metabolism were found to be differentially expressed between GC sensitive and GC resistant samples (152). Furthermore, in ALL cell lines and primary patient samples, prednisolone resistance was found to correlate with increased glucose consumption, and inhibition of glycolysis with the metabolite 2-deoxy-D-glucose (2-DG) sensitized cells to GCs, supporting the idea that excessive metabolic activity may impair GC-induced apoptosis (153). To further assess the relationship between glucose consumption and GC sensitivity, GC sensitive ALL cell lines and primary patient samples were exposed to DEX, which was found to inhibit glycolysis, leading to decreased glucose consumption that was mediated by a reduction in the expression of the glucose transporter GLUT1. This group went on to demonstrate that culturing cells in low glucose conditions resulted in increased DEX-induced apoptosis (154). Taken together, these data suggest that a reduction in glucose metabolism may be required for optimal GC-induced apoptosis. Consistent with this idea, it was shown that in prednisolone sensitive primary B-ALL samples, MCL1 expression decreased upon exposure to prednisolone, while it did not decrease in prednisolone resistant samples. Genetic silencing of MCL1 was found to be associated with an increase in glucose consumption, and simultaneous inhibition of glycolysis and silencing of MCL1 resulted in further sensitization to prednisolone (155). The importance of excessive glucose metabolism as a mediator of GC resistance has also been studied in the context of NHL cell lines and primary patient samples. In these cells, inhibition of glycolysis was found to synergize with methylprednisolone to induce cell cycle arrest and apoptosis (156). Providing a genetic explanation for the relationship between altered glucose metabolism and GC sensitivity, Chan *et al.* recently performed ChIP-seq to assess the binding pattern of transcription factors that are commonly inactivated in B-ALL, including PAX5 and IKZF1. They demonstrated that in B-ALL, these transcription factors are recruited to genetic loci that encode positive and negative regulators of glucose uptake. Re-expression of PAX5 and IKZF1 in B-ALL cells resulted in decreased glucose uptake and was sufficient to overcome

prednisolone resistance (157). The authors speculated that the hypermetabolic state associated with the deletion of these transcription factors facilitates leukemogenesis and simultaneously facilitates resistance to GC therapy.

In addition to glucose metabolism, aberrant lipid metabolism has also been shown to contribute to GC resistance. Specifically, lymphoid cells have been shown to have a unique dependency on exogenously synthesized cholesterol, and similar to glycolysis, GCs may exert their pro-apoptotic effects in part through inhibiting this cholesterol synthesis pathway. Indeed, in GC sensitive CEM-C7 cells, DEX was found to inhibit cholesterol synthesis, while this did not occur effectively in GC resistant CEM-C1 cells. Furthermore, exposure of CEM-C7 cells to exogenous cholesterol decreased DEX sensitivity, suggesting that DEX resistance may be mediated in part by increased cholesterol metabolism (158). Further supporting these data, T-ALL PDXs treated with a GC-containing four-drug induction regimen that acquired *in vivo* drug resistance were found to have altered cholesterol metabolism. In these samples, exposure to DEX and simvastatin, an inhibitor of cholesterol biosynthesis, demonstrated *ex vivo* synergy (159). These data suggest that additional preclinical studies may be warranted to evaluate the use of drugs that modulate bioenergetic pathways as a means of overcoming GC resistance.

MicroRNAs

MicroRNAs (miRNAs) are short non-coding RNAs that are most commonly contained within introns. Once transcribed, they bind to complementary sequences within the 3' untranslated region (3'UTR) of target gene mRNAs. Through this activity, miRNAs function primarily as negative regulators of translation, though they may have other repressive and activating roles (160). Dysfunctional expression of miRNAs is a common feature of many cancers, including hematologic malignancies. In ALL samples, a miRNA microarray analysis of paired diagnostic and relapse samples identified a distinct miRNA profile in the relapse samples relative to the diagnostic samples (161). Similarly, in a study involving miRNA sequencing of

samples from patients with Burkitt lymphoma, DLBCL, and follicular lymphoma, many miRNAs were found to be aberrantly expressed in lymphoma cells relative to normal lymphoid cells. Functionally, these miRNAs were found to be associated with altered regulation of key signal transduction pathways, including the Ras/MAPK and PI3K/AKT signaling pathways, suggesting that these miRNAs may play a role both in lymphomagenesis and in chemoresistance, including GC resistance (162).

MiR-17. In B-ALL cell lines, DEX exposure downregulated expression of miR-17 in GC sensitive but not in GC resistant cells. ChIP-seq analysis demonstrated that this is mediated by direct GR binding to the miR-17 locus specifically in GC sensitive cells. Functionally, miR-17 was found to target the BIM transcript for silencing, and pharmacologic inhibition of miR-17 increased DEX sensitivity with an associated increase in BIM expression (163).

MiR-100/99a. The miRNA species miR-100/99a has also been implicated in GC resistance and is known to be downregulated in samples from ALL patients with clinically high risk features. Specifically, low expression has been associated with inferior leukemia-free and overall survival (164). In cell lines, ectopic expression of miR-100/99a promoted DEX-induced apoptosis through a reduction in expression of the miR-100/99a target FKBP51. The reduction in FKBP51 expression was associated with increased nuclear localization of ligand-bound GR and decreased expression of mTOR, subsequently leading to a reduction in MCL1 expression which further potentiated apoptosis (164).

MiR-124. The role of MiR-124 as a mediator of GC resistance was first appreciated in the context of sepsis, where it was found that miR-24 represses the GRα transcript (165), suggesting that its overexpression might mediate GC resistance by decreasing the availability of GR protein for ligand binding. Indeed, miR-124 expression was found to be increased in prednisolone resistant ALL cell lines and in PPR patient samples and overexpression of miR-124 in ALL cells was associated with a reduction in GR protein expression (166). However, at least one study has suggested the opposite effect of miR-124 in GC sensitivity. In DLBCL cells,

miR-124 expression was found to decrease expression of PDE4B, thereby relieving the inhibitory effect on cAMP signaling and increasing GC sensitivity (167). Further studies are therefore needed to elucidate the role of miR-124 in modulating GC sensitivity in distinct lymphoid malignancies.

MiR-128b and miR-221. In MLL-AF4 ALL, miR-128b and miR-221 were found to be downregulated relative to other types of ALL. Overexpression of these miRNAs in MLL-AF4 ALL cell lines resulted in increased sensitivity to GCs, which was accompanied by downregulation of MLL, AF4, and their associated fusion genes (168). Further implicating low miR-128b as a mediator of GC resistance in MLL-AF4 ALL, miR-128b mutations found in both cell lines and primary patient samples were shown to impair the appropriate processing of miR-128b. This resulted in GC resistance mediated by a failure to downregulate the expression of fusion oncogenes involving MLL and AF4, though the mechanisms by which MLL and AF4 themselves contribute to GC resistance are currently unknown (169).

MiR-142-3p. MiR-142-3p was initially shown in T-regulatory cells to target adenylyl cyclase 9 mRNA for silencing, resulting in a reduction in the cellular pool of cAMP due to the loss of adenylyl cyclase enzymatic activity (170). Elevated expression of miR-142-3p in primary T-ALL samples was found to be associated with an increased risk of relapse and decreased leukemia-free survival relative to patients with lower miR-142-3p expression. Consistent with its known effects on the adenylyl cyclase 9 transcript, high miR-142-3p expression was associated with increased cAMP pathway activity. Furthermore, miR-142-3p was found to target the GRα transcript for repression via direct binding to the 3'UTR. In this context, inhibition of miR-142-3p overcame GC resistance both by facilitating an increase in cAMP pathway activity and an increase in GRα expression (171).

MiR-182. In an analysis of variety of murine and human malignant lymphoid cell lines, miR-182 expression was higher in GC resistant cells relative to GC sensitive cells, and high

expression was associated with decreased FOXO3A expression. One important downstream target of FOXO3A is BIM, and high expression of miR-182 was also associated with a reduction in BIM expression. Consistent with this activity, overexpression of miR-182 restored BIM expression, thereby overcoming GC resistance (172).

MiR-185-5p. Finally, miR-185-5p was found to be overexpressed in GC sensitive ALL cell lines. One target of miR-185-5p is the mTORC2 mRNA. Forced overexpression of miR-185-5p in GC resistant ALL cells restored GC sensitivity with a concomitant reduction in mTORC2 activity (173).

2.5: Conclusion

Given the pleiotropic effects of GCs and the innumerable interactions between GR and a wide variety of cellular processes, it is not surprising that the mechanisms of GC resistance are complex and that our understanding of these mechanisms is constantly evolving (Figure 2-1). However, despite a well-justified concern for GC resistance and its associated clinical implications, GCs are profoundly efficacious in the treatment of lymphoid malignancies and will undoubtedly remain an integral component of therapy. Therefore, there is an urgent need to translate the findings from the numerous preclinical and clinical studies highlighted in this review into standard clinical practice for the treatment of these diseases. With the application of large-scale sequencing and epigenetic profiling technologies, the development of small molecule and biologic therapeutics, and increasing access to patient-derived tissue samples, there is significant potential for the elucidation of additional causes of GC resistance and the identification and implementation of novel therapeutic strategies to overcome them.

2.6: Acknowledgements

2.7: Figures
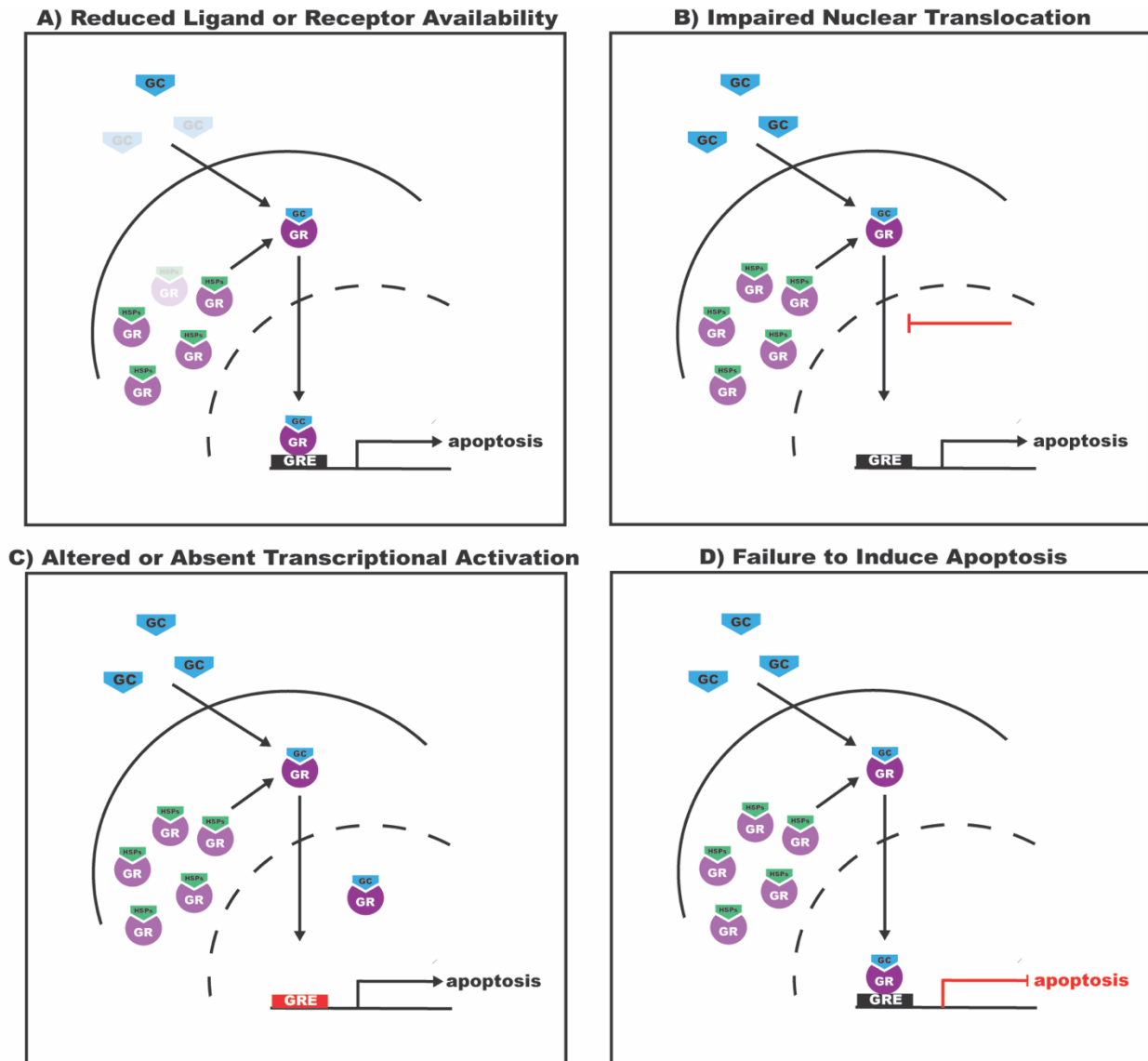
Figure 2-1: Mechanisms of GC Resistance. GC resistance may arise due to processes that impact any component of normal GR signaling, including the availability of GC ligand or GR (A), nuclear translocation of the activated GC/GR complex (B), transcriptional activity of ligand-bound GR (C), or the induction of apoptosis (D).

Chapter 3: The Bone Marrow Microenvironment as a Mediator of Chemoresistance in Acute Lymphoblastic Leukemia

3.1: Abstract

Acute lymphoblastic leukemia (ALL) is a malignancy of immature lymphoid cells that arises due to clonal expansion of cells that undergo developmental arrest and acquisition of pathogenic mutations. With the introduction of intensive multi-agent chemotherapeutic regimens, survival rates for ALL have improved dramatically over the past several decades, though survival rates for adult ALL continue to lag behind those of pediatric ALL. Resistance to chemotherapy remains a significant obstacle in the treatment of ALL, and chemoresistance due to molecular alterations within ALL cells have been described. In addition to these cell-intrinsic factors, the bone marrow microenvironment has more recently been appreciated as a cell-extrinsic mediator of chemoresistance, and it is now known that stromal cells within the bone marrow microenvironment, through direct cell-cell interactions and through the release of lymphoid-acting soluble factors, contribute to ALL pathogenesis and chemoresistance. This review discusses mechanisms of chemoresistance mediated by factors within the bone marrow microenvironment and highlights novel therapeutic strategies that have been investigated to overcome chemoresistance in this context.

3.2: Introduction

Acute lymphoblastic leukemia (ALL) is a malignancy of immature lymphoid cells of either the B-cell (B-ALL) or T-cell (T-ALL) lineage. ALL is the most common malignancy of childhood, and survival rates for children with ALL now approach 90% on modern treatment protocols, with even better survival rates for some molecular subtypes (174). In contrast, survival rates for adult ALL remain lower at 30-40% (175). In both contexts, improvements in survival were achieved in recent decades due in large part to the continued optimization of intensive multi-agent chemotherapy. The agents most commonly utilized in the treatment of ALL and their mechanisms of action are outlined in Table 3-1. Despite these improvements, patients with relapsed or refractory ALL continue to face inferior outcomes, underscoring the importance of

studies aimed at understanding the drivers of chemoresistance and identifying novel therapeutic strategies to restore chemosensitivity.

The genomic landscapes of both pediatric and adult ALL have been extensively characterized (176–178), and in many cases the presence of specific molecular or cytogenetic alterations can be correlated with prognosis or with resistance to a particular chemotherapeutic agent (116,179–182). These genetic factors therefore represent cell-intrinsic drivers of chemoresistance, and there have been considerable efforts to target these resistance mechanisms through the use of biologic and small molecule therapeutic agents. Equally important however are the complex and diverse cell-extrinsic factors that similarly modulate response to chemotherapy and clinical outcomes in ALL.

Specifically, both normal hematopoietic progenitor cells and ALL cells residing in the bone marrow receive key survival, proliferative, and homing signals from the bone marrow microenvironment. This microenvironment is classically subdivided into two distinct niches comprised of the endosteal niche and the vascular niche. In the endosteal niche, hematopoietic cells maintain direct cell-cell interactions with osteoblasts, which support hematopoietic cell survival and proliferation. The vascular niche consists of small sinusoidal blood vessels within the marrow cavity, which ensure the movement of oxygen, nutrients, and cellular homing factors in and out of the bone marrow, thereby supporting hematopoietic cell function and maintaining communication with other tissue types (183). Given these abundant interactions between the bone marrow microenvironment and ALL cells, there is significant interest in elucidating the microenvironmental drivers of chemoresistance in ALL and in identifying novel therapeutic strategies to overcome these cell-extrinsic mechanisms of chemoresistance (184–186).

3.3: Cell-Cell Interactions in the Bone Marrow Microenvironment

A number of model systems of have been investigated for their ability to facilitate the *ex vivo* analysis of primary patient ALL cells, which demonstrate a high rate of spontaneous

apoptosis under standard cell culture conditions. In particular, it has been shown that co-culture with bone marrow stromal cells (BMSCs) significantly enhances the survival of leukemic blasts *ex vivo* (187). Specifically, this survival effect is often dependent upon direct contact with BMSCs, as BMSC conditioned media is insufficient to mediate the same improvement in cell survival (188). These studies highlight the importance of cell-cell interactions with BMSCs for the survival and proliferation of ALL cells, and a number of studies, many of which are described below, have demonstrated that these cell-cell interactions mediate chemoresistance.

3.3.1: Integrins

Integrins are a class of transmembrane cell adhesion receptors that make up a critical component of the extracellular matrix (ECM). Integrins are comprised of heterodimers of a number of distinct α and β subunits and each have specific ligand-binding capabilities, determined predominantly by the identity of the α subunit. Upon engagement by extracellular stimuli, activated integrins mediate a variety of signal transduction events leading to modulation of a wide range of cellular processes, including cell survival, gene expression, and cell motility (189).

Despite the ubiquitous expression of this class of cell adhesion receptors throughout all tissue types, distinct integrin heterodimers demonstrate tissue-specific expression patterns. The β1-containing integrins, collectively known as very-late activation antigens (VLAs), heterodimerize with α4 subunits (CD49b) to form VLA-4. VLA-4 is highly expressed on hematopoietic progenitors and more mature blood cells, including healthy leukocytes and leukemic blasts, and functions to mediate trafficking of these cells within and out of the bone marrow (189). Importantly, aberrant expression of VLA-4 in leukemic blasts has been associated with chemoresistance and poor clinical outcomes. For example, amongst patients enrolled on the Children's Oncology Group (COG) B-ALL trial P9906 who were minimal residual

disease (MRD) positive following one month of induction chemotherapy, those with low α4

integrin expression had significantly improved overall survival (OS) relative to those with high α4

integrin expression (190). Another analysis of samples from children with relapsed B-ALL

enrolled on the ALL-REZ BFM 2002 trial from the Berlin-Frankfurt-Münster (BFM) study group

demonstrated that patients with increased *VLA4* expression at the time of first relapse had a

significantly impaired response to chemotherapy and inferior event-free survival (EFS) and OS

(191). The authors of this study went on to demonstrate that VLA-4 blocking antibodies

attenuated the adhesion of B-ALL cells to BMSCs *in vitro*, and that this was sufficient to

decrease cellular proliferation and overcome the cytarabine resistance conferred by co-culture

with BMSCs (191).

In healthy hematopoietic cells, VLA-4 demonstrates high affinity for vascular cell

adhesion molecule-1 (VCAM-1), a cell surface protein that is highly expressed on the vascular

endothelium, as well as the ECM glycoproteins fibronectin and osteopontin (192). In particular, it

is this affinity for VCAM-1 that is thought to play the predominant role in hematopoietic cell

trafficking, as antibodies against VCAM-1 are sufficient to reduce progenitor cell adhesion to

BMSCs both *in vitro* (193) and *in vivo* (194), while anti-fibronectin antibodies are not (195). In

the context of leukemia, the VLA-4/VCAM-1 interaction is similarly thought to be the primary

mediator of chemoresistance. Co-culture of ALL cell lines with BMSCs, but not with BMSC

conditioned media, significantly reduced sensitivity to cytarabine and etoposide, an effect that

was abrogated in the presence of VCAM-1 blocking antibodies (196).

Mechanistically, engagement of the VLA-4/VCAM-1 axis has been shown to activate

pro-survival signaling pathways in ALL cells that in turn mediate chemoresistance. For example,

in vitro stimulation of VLA-4 was shown to activate the PI3K/Akt signaling pathway in a B-ALL

cell line, concomitant with the induction of adriamycin resistance, and inhibition of PI3K was

sufficient to restore adriamycin sensitivity (197). Furthermore, Astier *et al*. analyzed global gene

expression changes in ALL cells following *in vitro* engagement of VLA-4 and found that a number of apoptotic regulators, including members of the caspase family, are significantly downregulated following VLA-4 activation while pro-survival factors, such as XIAP and survivin, are upregulated, together contributing to a chemoresistant state (198). Interestingly, there is also evidence to suggest that chemoresistance is mediated by reciprocal signaling through the VLA-4/VCAM-1 axis. Jacamo *et al.* demonstrated that co-culture of BMSCs with leukemic blasts resulted in an upregulation of NFκB signaling in the BMSCs themselves, and that this was attenuated in the presence of a VLA-4 blocking antibody. Furthermore, genetic or chemical inhibition of NFκB signaling in BMSCs restored sensitivity to vincristine in ALL cells both *in vitro* and *in vivo*. The authors speculate that the paracrine effects of many NFκB target genes, including cytokines, that are induced in the presence of ALL cells may in turn facilitate the protective microenvironment provided by the BMSCs (199). Finally, VLA-4 may promote chemoresistance via its interactions with ion channels present at the leukemic cell surface. In particular, the potassium channel $K_V11.1$ has been shown to be overexpressed in ALL cell lines and patient samples (200). Intriguingly, VLA-4 can form cell surface signaling complexes involving $K_V11.1$, that in turn lead to activation of ERK and PI3K/Akt signaling with the concomitant induction of chemoresistance (201).

Given the well-established role of VLA-4 as a mediator of chemoresistance in ALL cells, there has been increasing interest in augmenting chemosensitivity through the use of anti-VLA-4 therapeutics, many of which have been used successfully in a number of autoimmune and inflammatory conditions due to their ability to modulate leukocyte activity. Natalizumab is a humanized monoclonal antibody that targets the $\alpha4$ integrin subunit, thereby inhibiting VLA-4 and the closely related $\alpha4\beta7$ integrin, which similarly binds VCAM-1 (202). Hsieh *et al.* demonstrated that natalizumab significantly prolonged survival in a xenograft model of B-ALL when combined with multi-agent chemotherapy consisting of vincristine, dexamethasone, and *L-*

asparaginase relative to chemotherapy alone (190). Other therapeutic approaches involve peptide or non-peptide ligands that compete with VCAM-1 for VLA-4 binding. One such small molecule, TBC3486, has significantly increased affinity for VLA-4 relative to $\alpha 4\beta 7$ and has been shown to enhance chemosensitivity *in vitro* in B-ALL cells co-cultured with BMSCs and *in vivo* in a xenograft model of B-ALL (203).

In addition to VLA-4, several other integrins have been implicated in chemoresistance in ALL. For example, CD11b is an α integrin that is typically expressed on myeloid cells and plays an important role in cellular migration and extravasation during an immune response (204). While expression in lymphoid cells is usually restricted to memory B-cells, Rhein *et al*. investigated the significance of aberrant CD11b expression on pre-B-ALL blasts. In this analysis, the authors demonstrated that high CD11b expression at diagnosis was an independent poor prognostic factor, with the CD11b-high patients demonstrating significantly higher rates of post-induction MRD relative to the CD11b-low patients. Furthermore, they demonstrated that the blasts remaining at the end of induction therapy had significantly higher CD11b expression relative to the cells analyzed prior to the initiation of therapy (205). Further studies are needed to assess the functional significance of increased CD11b expression on B-ALL cells. Finally, in T-ALL cell lines and patient samples, the collagen-binding $\alpha 2\beta 1$ integrin has been shown to confer resistance to doxorubicin. Engagement of the $\alpha 2\beta 1$ integrin with collagen resulted in increased activity of the MAPK signaling pathway and sustained expression of the anti-apoptotic protein Mcl-1. Consistent with these findings, doxorubicin sensitivity could be restored with MEK inhibition (206).

3.3.2: Cadherins

First described for their role in regulating epithelial-to-mesenchymal transitions during normal embryonic development, cadherins have since been recognized as a structurally and

functionally diverse superfamily of transmembrane proteins that play important roles in normal cellular processes and in the development and progression of cancer (207). The intracellular domains of cadherin proteins interact with a multitude of signal transduction effectors to carry out a variety of cellular processes. One crucial class of intracellular effectors is the catenin family of proteins, which provide a physical link between the intracellular domains of cadherin proteins and the actin cytoskeleton, thereby facilitating the role of cadherins in maintaining cell adhesion. In immune cells, the β-catenin protein, through its involvement in canonical Wnt pathway signaling, plays a critical role in the regulation of immune processes (208).

Canonical Wnt signaling involves the binding of Wnt1 ligands to their receptor, known as Frizzled (Frz). In the absence of ligand binding, the intracellular β-catenin destruction complex is stabilized, resulting in low levels of intracellular β-catenin. Upon ligand binding, this complex becomes destabilized, allowing for an increase in levels of β-catenin protein in the cytoplasm. This β-catenin protein then translocates to the nucleus and associates with the TCF/LEF transcription factor complex, converting it from a repressive complex to an activating complex, which in turn activates a transcriptional program that mediates processes such as cell proliferation and differentiation (209).

Of the cadherin subfamilies, the Fat cadherins are the most commonly mutated in ALL, and many reports have demonstrated their tumor suppressive activity. In an analysis of primary T-ALL samples from adult patients, Neumann *et al.* determined that 12% of the samples in their cohort had missense or nonsense mutations in *FAT1*, leading to loss of expression (210). Similar *FAT1* mutations have subsequently been reported in pediatric T-ALL (177). Interestingly, loss of function mutations in *FAT1* have been associated with augmented Wnt pathway signaling. Specifically, Morris *et al.* demonstrated that the tumor suppressive effects of wild-type FAT1 protein derive from its ability to bind β-catenin at the periphery of the cell, thereby sequestering it in the cytoplasm and preventing its localization to the nucleus and activation of

TCF/LEF complex (211). This aberrant activation of Wnt/β-catenin signaling has been implicated as a mediator of chemoresistance in ALL. Upon exposure of ALL cell lines and primary patient samples to BMSCs, Yang *et al*. found that the resulting cytarabine resistance was associated with inactivation of the β-catenin destruction complex and upregulation of members of the Wnt signaling pathway. Inhibition of β-catenin was sufficient to restore chemosensitivity both *in vitro* and *in vivo* (212). An integrated analysis of pairs of diagnostic and relapsed pediatric ALL samples incorporating gene expression, copy number alterations, and DNA methylation analyses revealed that dysregulation of this pathway was enriched at the time of disease relapse (213), providing correlative evidence that altered Wnt/β-catenin signaling may be a clinically relevant mediator of resistance to chemotherapy. This same group went on to functionally test this interaction by demonstrating that, in contrast to their corresponding diagnostic samples, relapsed samples had significant overactivation of Wnt/β-catenin signaling and were highly refractory to the glucocorticoid prednisolone. In this context, the Wnt inhibitor iCRT14 synergized with prednisolone to induce apoptosis in relapsed patient samples (214).

Intriguingly, other reports suggest that Fat cadherins may instead function as oncogenes, where they contribute to disease progression and chemoresistance. For example, de Bock, *et al*. demonstrated that ALL cell lines express higher levels of Fat1 relative to healthy blood or bone marrow cells. The authors also demonstrated in two cohorts of pediatric patients with B-ALL that high *FAT1* expression was associated with inferior relapse-free and overall survival (215). The same authors subsequently found that some T-ALL cell lines and patient samples express a truncated version of the *FAT1* transcript, which in turn results in expression of a truncated protein that lacks the extracellular domain. Furthermore, this protein was found to cooperate with the Notch signaling pathway, described below, thereby serving an oncogenic function (216).

3.3.3: Galectins

The lectin family of cell surface proteins recognizes and binds to carbohydrates, leading to downstream signal transduction events that play crucial roles in normal physiology and in a variety of disease states (217). The galectins represent a subclass of lectins with binding specificity for β-galactoside epitopes, commonly found in association with proteins that undergo glycosylation during their trafficking through the secretory pathway. As a result of their distinct affinities for specific glycoproteins, galectins provide a means of interpreting the information contained within these glycosylation events and converting that information into intracellular signal transduction processes. The ability of galectins to bind their glycoprotein ligands is facilitated in part by their ability to form higher order multimeric structures, thereby increasing their binding capacity (218). In particular, galectin-3, which is commonly overexpressed in cancer, has extensive oligomerization capabilities, allowing it to form dynamic lattice structures at the cell surface that modulate the movement and activity of its glycoprotein binding partners (219).

Galectin-3 was first identified as a potential mediator of chemoresistance in ALL cells through an analysis of gene expression changes following co-culture of ALL cells with BMSCs. Jurkat T-ALL cells were rendered resistant to doxorubicin upon co-culture with BMSCs, concomitant with upregulation of galectin-3. Forced overexpression of galectin-3 in these cells was sufficient to confer chemoresistance in the absence of BMSCs (220). Consistent with these findings, Fei *et al*. found that *in vitro*, patient-derived B-ALL cells harvested from underneath a BMSC feeder cell layer, where they maintained direct cell-cell contact with feeder cells, had more galectin-3 on their cell surface relative to cells found in suspension above the cell layer or cells cultured in the absence of BMSCs (221). These same authors went on to assess secreted galectin-3 levels in the growth medium from BMSCs cultured in the absence or presence of ALL cells, and found that BMSCs secreted more galectin-3 in the context of ALL cell co-culture relative to culture of BMSCs alone, while ALL cells alone did not secrete galectin-3 under any

conditions. These results suggested that the elevated galectin-3 found on the cell surface of ALL cells had a stromal origin. The authors further confirmed this by demonstrating that exosomes derived from BMSCs, but not from ALL cells, contained galectin-3 and that these exosomes were secreted by BMSCs and subsequently taken up by ALL cells (222). Hu *et al*. similarly demonstrated that co-culture of ALL cells with BMSCs resulted in increased cell surface galectin-3 and chemoresistance, and extended this finding to demonstrate that transcriptional targets of the Wnt/β-catenin signaling pathway, previously implicated in chemoresistance (212,214), were upregulated in wild-type ALL cells co-cultured with BMSCs but not in galectin-3 knockout cells, suggesting that activation of this pathway is galectin-3-dependent (223). Interestingly, galectin-3 inhibitors have demonstrated efficacy in acute myeloid leukemia (224), diffuse large B-cell lymphoma (225), and multiple myeloma (226,227). Additional studies are necessary to determine whether such inhibitors may similarly augment chemosensitivity in the context of ALL.

3.3.4: Notch Signaling

The Notch signal transduction pathway is unique in several ways. First, its activation is dependent upon direct cell-cell contact between a ligand-expressing cell, such as a T-cell, and a receptor-expressing cell, such as a BMSC. Second, unlike other non-enzymatic transmembrane receptors, upon engagement of the Notch receptor by its ligands Delta-like or Jagged, the receptor itself undergoes proteolytic cleavage. Specifically, the extracellular domain of the receptor is shed first, followed by cleavage within the transmembrane domain by the γ-secretase complex. This allows the intracellular domain of the receptor (NICD) to translocate to the nucleus and function as a transcriptional regulator (228).

In normal physiology, Notch signaling plays a critical role in T- and B-cell development. In T-cells, Notch activity is required for cell survival and proliferation during the double negative

(DN) stages of thymocyte development, and is important for β selection during the production of a fully rearranged αβ T-cell receptor (TCR) (229). Further highlighting the importance of Notch signaling for thymocyte development, ectopic expression of Delta-like 1 in the OP9 stromal cell line is sufficient to support early T-cell differentiation *ex vivo* (230). Importantly, aberrant Notch signaling is a common feature of T-ALL. In pediatric T-ALL, activating mutations in components of the Notch signaling pathway, including in *NOTCH1* itself, are found in nearly 80% of diagnostic samples (177). Though not found to be mutationally activated in B-ALL, Notch signaling does also play an important role in B-cell development where it promotes the differentiation of marginal zone and follicular zone B-cells (231).

Interestingly, within the bone marrow microenvironment, Notch signaling has been shown to mediate chemoresistance in the setting of hypoxia. Specifically, the bone marrow is a highly hypoxic environment, with a reported oxygen saturation of only 87.5% in healthy subjects, compared to 99% in peripheral blood (232). Upon exposure to a hypoxic environment, cells upregulate expression of the transcription factor hypoxia-inducible factor-1α (HIF-1α), which mediates a variety of tissue-specific transcriptional programs (233). In solid tumor cells, it has been shown that Notch signaling is induced in response to hypoxia and functions to promote cellular motility and invasiveness (234). Zou *et al.* similarly demonstrated that in the setting of hypoxia, T-ALL cells undergo HIF-1α-dependent Notch activation. In T-ALL cell lines, exposure to hypoxia was sufficient to confer chemoresistance, and this could be overcome with Notch silencing (235).

Due to the role for Notch signaling as a mediator of chemoresistance, there is interest in pharmacologically targeting the Notch signaling pathway. In addition to monoclonal antibodies targeting Notch receptors or ligands (236), significant attention has been devoted to the preclinical and clinical development of γ secretase inhibitors (GSIs). Interestingly, numerous preclinical studies have demonstrated the ability of GSIs to augment chemosensitivity (237–

239). Unfortunately, early single agent clinical trials involving GSIs were limited by severe gastrointestinal toxicity (240). However, Real *et al*. demonstrated through a series of elegant *in vivo* experiments that GSIs effectively overcome glucocorticoid resistance in T-ALL, and that concomitant exposure to glucocorticoids and GSIs abrogates the gastrointestinal toxicity associated with GSIs, thereby restoring the potential for the use of GSIs to modulate response to chemotherapy in T-ALL (241). This strategy was employed in a clinical trial involving relapsed or refractory pediatric solid tumors and T-cell leukemia (NCT01088763).

3.4: Soluble Factors

In addition to direct cell-cell interactions, a number of secretory products made by cells within the bone marrow microenvironment engage with receptors on lymphoid cells to mediate functions such as cell proliferation and survival. Like the factors described above, many of these soluble products have similarly been shown to mediate chemoresistance.

3.4.1: TNFα

TNFα is a pro-inflammatory cytokine that is responsible for normal immune system homeostasis and plays numerous well-established roles in the development and maintenance of malignancy (242). Produced by macrophages, natural killer cells, and T-cells, TNFα normally functions as a regulator of hematopoiesis when present in conjunction with other growth factors that similarly act to maintain the appropriate size and function of the hematopoietic compartment (243). Interestingly, a polymorphism in the *TNF* gene itself, which results in higher plasma levels of TNFα, has been shown to corelate with poor outcomes in a number of hematologic malignancies, including Hodgkin's (244) and non-Hodgkin's lymphoma (245). Consistent with these findings, Lauten *et al.* demonstrated in a cohort of children treated on BFM protocols that amongst patients with a prednisone poor response, those with *TNF* gene polymorphisms had a

higher rate of relapse (246). Mechanistically, TNFRII signaling has been shown to activate the PI3K/Akt signal transduction pathway, leading to downstream pro-survival signaling. Activation of this pathway has been associated with the induction of doxorubicin resistance in ALL cell lines (247), though further studies are needed to fully elucidate the relationship between altered TNFα expression and signaling and clinical outcomes for patients with ALL.

3.4.2: γ Chain Cytokines

Consisting of interleukin (IL)-2, 4, 7, 9, 15, and 21, the common γ chain family of cytokines exert their effects on immune cells via a receptor that contains one or more cytokine-specific receptor chains as well as the common cytokine receptor γ chain. These multimeric receptor complexes lack intrinsic enzymatic activity and instead recruit downstream effectors via their cytoplasmic domains. Specifically, the cytokine-specific receptor chains most commonly recruit the kinase JAK1, while the γ chain recruits JAK3. Activation of these JAK proteins results in phosphorylation of the cytoplasmic domains of the receptor subunits, which in turn creates docking sites for the STAT family of transcription factors, with STAT protein binding specificity determined by the identity of the specific receptor docking sites. Upon recruitment to activated cytokine receptors, these STAT proteins undergo JAK-mediated phosphorylation, leading to their translocation to the nucleus where they function as transcription factors to mediate target gene expression (43). Due to their central roles in regulating the differentiation, survival, and proliferation of healthy lymphoid cells, it is not surprising that γ chain cytokine receptors play an important role in mediating chemoresistance in ALL.

Produced by T-cells, IL-4 acts on a multitude of immune cell subtypes leading to a wide range of downstream effects. For example, IL-4 is a signature cytokine in the differentiation of naïve CD4+ T-cells into the Th2 subtype of T helper cells. In the B-cell lineage, IL-4 functions as a B-cell differentiation factor, promoting immunoglobulin isotype switching, and in the myeloid

lineage, IL-4 is important for the development of M2 macrophages (43). Importantly, IL-4 has been implicated in glucocorticoid resistance in both non-malignant (248,249) and malignant T-cells. Serafin *et al.* discovered that in T-ALL patients with a poor initial response to the glucocorticoid prednisone, the *IL4* gene was upregulated downstream of aberrant activation of LCK, a Src family non-receptor tyrosine kinase that is important for lymphocyte development and activation. The authors demonstrated that culturing glucocorticoid sensitive T-ALL cell lines in the presence of IL-4 was sufficient to confer glucocorticoid resistance (250). Interestingly, in conjunction with TNFα, IL-4 is also a potent inducer of VCAM-1 expression (251), with TNFα and IL-4 exposure promoting the adhesion of ALL cells to bone marrow fibroblasts in culture (193,252). As described above, the VLA-4/VCAM-1 axis has been implicated in chemoresistance in a variety of model systems.

IL-7 is produced by the stromal cells of the bone marrow and thymus and plays a crucial nonredundant role in lymphoid cell development and survival. Activation of the IL-7 receptor (IL-7R) primarily recruits the STAT5 transcription factors, which induce expression of antiapoptotic proteins such as BCL-2. Interestingly, many studies of early thymocyte development have demonstrated an interaction between IL-7R signaling, T-cell receptor (TCR) signaling, and endogenous glucocorticoid exposure that is critical for the appropriate development of the T-cell repertoire. Specifically, in normal T-cell development, IL-7R is expressed at high levels in the early DN thymocyte population, thereby maintaining cell survival prior to rearrangement of the T-cell receptor (TCR) (43). Upon induction of TCR rearrangement during the late DN and early double positive (DP) stage of development, IL-7R is transiently downregulated, thereby abrogating its strong pro-survival signal (253). At this stage, exposure to endogenous glucocorticoids is sufficient to induce cell death unless the cell is rescued by pro-survival signaling following successful TCR rearrangement (8). In this model, loss of IL-7R-mediated pro-survival signaling is required to enable an apoptotic response to endogenous glucocorticoids in the absence of an appropriately rearranged TCR. In the context of T-ALL,

signaling through the IL-7R/JAK/STAT5 pathway has been shown to confer resistance to pharmacologic concentrations of glucocorticoids, suggesting that this normal developmental process is co-opted in this malignant state to promote chemotherapy resistance.

Specifically, gain-of-function mutations in the IL-7R/JAK/STAT5 pathway occur in 25% of pediatric and young adult T-ALLs (177), underscoring the strong selective pressure for activation of this pathway as a mediator of T-cell survival. Both mutational and non-mutational activation of this pathway have been implicated in glucocorticoid resistance in T-ALL. For example, Li *et al.* demonstrated in diagnostic samples from children with T-ALL that mutations in the IL-7R/JAK/STAT5 pathway were associated with decreased *ex vivo* prednisolone sensitivity and with inferior relapse free survival. The authors went on to express mutant alleles of IL-7R pathway genes in glucocorticoid sensitive T-ALL cell lines and found that many of these mutations were sufficient to confer resistance to glucocorticoids, but not to other chemotherapies (182). Consistent with this idea, we previously demonstrated that IL-7-induced glucocorticoid resistance most commonly occurs in T-ALLs that lack activating mutations in the IL-7R/JAK/STAT5 pathway, and that this resistance phenotype is enriched in T-ALLs of the early T-cell precursor (ETP) subset, which correspond to the early DN stages of thymocyte development. Like Li *et al.*, we similarly found that IL-7-mediated effects on chemoresistance are specific to glucocorticoids (132). We later showed that glucocorticoid resistance is mediated specifically by induction of the anti-apoptotic protein BCL-2 downstream of STAT5, and can be overcome with inhibition of JAK. Interestingly, we further demonstrated that this mechanism of IL-7-induced glucocorticoid resistance occurs in distinct subpopulations of healthy developing thymocytes both *in vivo* and *ex vivo*, and that T-ALLs with gene expression signatures resembling early stages of thymocyte development are enriched for this resistance phenotype (254). Taken together, these data provide strong evidence for a developmentally-retained mechanism by which T-ALLs, arising from stages of thymocyte development that rely on IL-7R

signaling, can utilize this pathway to resist apoptosis in response to glucocorticoid therapy even in the absence of activating pathway mutations.

While not a γ chain cytokine receptor, the thymic stromal lymphopoietin (TSLP) receptor (TSLP-R) consists of a heterodimer of the IL-7Rα chain and cytokine receptor-like factor 2 (CRLF2), and plays a role in normal B-cell development (255). Aberrant signaling through TSLP-R, most commonly mediated by chromosomal rearrangements of *CRLF2* and/or mutational activation of its downstream effector, *JAK2*, is a hallmark feature of Philadelphia chromosome-like (Ph-like) B-ALL. These leukemias demonstrate a gene expression signature that is similar to that of Ph-positive B-ALL but lack the *BCR-ABL1* translocation (129). Importantly, *CRLF2* rearrangements and *JAK2* mutations, collectively leading to increased TSLP-R signaling capacity, have been associated with poor outcomes in patients with Ph-like ALL (256). Similar to T-ALL, we previously demonstrated that *CRLF2*-rearranged Ph-like B-ALL samples uniformly demonstrate *in vitro* glucocorticoid resistance (257).

Given the role of cytokine-mediated JAK/STAT signaling in the pathogenesis and chemoresistance of ALL cells, there has been considerable interest in targeting this pathway as a means of improving clinical outcomes. While several approaches have been studied, including the use of reducing agents to disrupt disulfide bond formation within IL-7R, blocking antibodies against IL-7R, and IL-7R-directed chimeric antigen receptor (CAR) T-cells (258), small molecule inhibitors of JAK are currently furthest along in clinical development. Ruxolitinib is a JAK1/2 inhibitor that has shown efficacy as a single agent in xenograft models of ETP T-ALL (259) and Ph-like ALL (260), and has been shown to sensitize ALL cells to glucocorticoids *in vitro* (132,254,257). Consistent with these promising results, clinical trials have been initiated to investigate the efficacy of ruxolitinib in ALL (NCT03571321 and NCT02723994).

3.4.3: Chemokines

Chemokines are a subclass of cytokines that are specifically responsible for the export of immune cells from the bone marrow and for the homing of these cells to sites of infection and inflammation. Chemokine ligands characteristically contain one or more cysteine residues, enabling their division into the XC, CC, CXC, CX3C subgroups on the basis of the location of their cysteine residues within their amino acid sequences. Upon secretion, chemokines bind to G-protein-coupled receptors (GPCRs), with some receptors showing specificity for a single ligand and others capable of binding multiple distinct ligands (261). In particular, CXCR4 signaling has been implicated in the initiation and progression of ALL, and has further been shown to mediate chemoresistance.

CXCL12, also called stromal derived factor 1 (SDF-1) is the chemokine ligand for the CXCR4 receptor and is expressed ubiquitously at all stages of development, where it plays an important role in tissue homeostatic functions, including within the hematopoietic compartment (262). Importantly, aberrant CXCL12/CXCR4 signaling has been functionally implicated in leukemogenesis and associated with poor clinical outcomes. For example, it has been shown that the protein phosphatase calcineurin is aberrantly activated in T-ALL and is required for the activity of leukemia initiating cells (263). Passaro *et al*. further demonstrated that cell surface expression of CXCR4 is regulated by calcineurin activity, and the presence of CXCR4 at the cell surface is required for the migratory capability of T-ALL cells. The authors further showed that silencing of CXCR4 was associated with the induction of apoptosis in a T-ALL cell line and in a patient-derived xenograft model of T-ALL (264). In pediatric B-ALL, high CXCR4 expression was associated with inferior relapse free survival (265), and in adult B-ALL, phosphorylated CXCR4, corresponding to an active form of the receptor, was associated with reduced OS (266).

To assess the relationship between CXCR4 expression and chemosensitivity in ALL, Sison *et al*. utilized primary samples from infants with mixed lineage leukemia (*MLL*)-rearranged

ALL, a high-risk molecular subtype of B-ALL that is associated with poor outcomes. Consistent with other reports, the authors found that exposure to BMSCs conferred chemoresistance and that co-treatment with the CXCR4 antagonist plerixafor was sufficient to restore chemosensitivity (267). The same group went on to demonstrate that in response to chemotherapy, ALL cells upregulate expression of CXCR4, priming them to respond to BMSC-secreted CXCL12. In light of these findings, the authors demonstrated the efficacy of a combinatorial therapeutic strategy involving plerixafor in an *in vivo* xenograft model and found that co-treatment with plerixafor abrogated the protective effect of the bone marrow microenvironment on the response to chemotherapy (268). As a result of these promising results in preclinical models, the Pediatric Oncology Experimental Therapeutics Investigators' Consortium conducted a phase 1 study to evaluate the potential for combining plerixafor with the chemotherapies cytarabine and etoposide in children with relapsed or refractory acute leukemia (NCT01319864). While the only clinical responses observed in this cohort occurred in children with AML, the number of patients with ALL was small (269). Based on these results, the role of plerixafor in augmenting chemosensitivity remains to be studied in additional patient cohorts in conjunction with other chemotherapy backbones.

3.4.4: Asparagine

The introduction of *L*-asparaginase into modern treatment regimens has dramatically improved outcomes for patients with ALL (270). The efficacy of *L*-asparaginase relies upon the unique requirement for asparagine in leukemia cells. In healthy cells, asparagine is a non-essential amino acid, synthesized intracellularly through the activity of asparagine synthetase. In contrast, ALL cells lack sufficient expression of asparagine synthetase to meet their requirement for asparagine, thereby relying instead on exogenous sources. The use of *L*-asparaginase exploits this dependency by hydrolyzing asparagine, thus depriving ALL cells of this exogenous supply (271). BMSCs have been shown to contribute to *L*-asparaginase resistance through

upregulation of asparagine synthetase. Specifically, Iwamoto *et al.* demonstrated that expression of the gene encoding asparagine synthetase, *ASNS*, was significantly higher in BMSCs than in ALL cells themselves, and that co-culture of ALL cells with BMSCs conferred resistance to *L*-asparaginase, suggesting that BMSCs function as an exogenous source of asparagine for ALL cells (272).

3.5: Conclusion

Comprehensive analyses of the genomic and transcriptomic landscape of ALL have revealed many factors that contribute to chemoresistance and poor clinical outcomes for patients with ALL. In contrast to these cell-intrinsic drivers of chemoresistance, cell-extrinsic factors are less well-appreciated for their role in modulating clinical outcomes. As described here, the bone marrow microenvironment, through direct cell-cell interactions and the production of soluble factors, plays a complex and multifactorial role in determining the response of ALL cells to chemotherapy. This review highlights a number of efforts to target the microenvironment as a means of augmenting the efficacy of chemotherapy. While many of the preclinical studies described here present promising results, further studies are needed to validate these therapeutic strategies in other preclinical model systems and to facilitate their eventual clinical implementation.

3.6: Acknowledgements

3.7: Table

Table 3-1: Mechanisms of action of chemotherapeutic agents used in the treatment of acute lymphoblastic leukemia.

Drug	Mechanism of Action
Asparaginase	• Cleaves exogenous asparagine to deprive ALL cells of this amino acid
Clofarabine	• Purine nucleoside analog that inhibits synthesis and repair of DNA
Corticosteroids (prednisone or dexamethasone)	• Glucocorticoid receptor agonists that induce pro-apoptotic effects in lymphoid cells
Daunorubicin and Doxorubicin	• Anthracyclines that inhibit topoisomerases
Etoposide	• Topoisomerase II inhibitor
Methotrexate	• Antimetabolite that inhibits dihydrofolate reductase to inhibit synthesis of purine nucleotides
Vincristine	• Microtubule-destabilizing agent

Chapter 4: *CRLF2* Rearrangement in Ph-Like Acute Lymphoblastic Leukemia Predicts

Glucocorticoid Resistance that is Overcome with MEK or Akt Inhibition

4.1: Abstract

Philadelphia chromosome-like (Ph-like) acute lymphoblastic leukemia (ALL) is a genetically heterogeneous subtype of B-cell ALL characterized by chromosomal rearrangements and mutations that result in aberrant cytokine receptor and kinase signaling. In particular, chromosomal rearrangements resulting in the overexpression of cytokine receptor-like factor 2 (*CRLF2*) occur in 50% of Ph-like ALL cases. *CRLF2* overexpression is associated with particularly poor clinical outcomes, though the molecular basis for this is currently unknown. Glucocorticoids (GCs) are integral to the treatment of ALL and GC resistance at diagnosis is an important negative prognostic factor. Given the importance of GCs in ALL therapy and the poor outcomes for patients with *CRLF2* overexpression, we hypothesized that the aberrant signal transduction associated with *CRLF2* overexpression might mediate intrinsic GC insensitivity. To test this hypothesis, we exposed Ph-like ALL cells from patient-derived xenografts to GCs and found that *CRLF2* rearranged (*CRLF2$_R$*) leukemias uniformly demonstrated reduced GC sensitivity *in vitro*. Furthermore, targeted inhibition of signal transduction with the MEK inhibitor trametinib and the Akt inhibitor MK2206, but not the JAK inhibitor ruxolitinib, was sufficient to augment GC sensitivity. These data suggest that suboptimal GC responses may in part underlie the poor clinical outcomes for patients with *CRLF2* overexpression and provide rationale for combination therapy involving GCs and signal transduction inhibitors as a means of enhancing GC efficacy.

4.2: Introduction

Philadelphia chromosome-like (Ph-like) acute lymphoblastic leukemia (ALL) is a subtype of B-cell ALL that displays a gene expression profile resembling that of *BCR-ABL1*-positive ALL but lacks the *BCR-ABL1* translocation. Instead, Ph-like ALL is characterized by genetic alterations that result in aberrant cytokine receptor and kinase signaling (273). In particular, 50%

of Ph-like ALL cases harbor chromosomal rearrangements that result in overexpression of cytokine receptor-like factor 2 (*CRLF2*), which heterodimerizes with the interleukin-7 receptor alpha chain to form the thymic stromal lymphopoietin receptor (TSLPR) (256). Upon activation by TSLP ligand, TSLPR signals through the JAK/STAT, Ras/MAPK, and PI3K/Akt/mTOR pathways (274). Importantly, overexpression of *CRLF2* is associated with a particularly poor prognosis, with these patients demonstrating significantly worse relapse-free survival relative to patients without *CRLF2* overexpression (256,275). While the molecular basis for this clinical observation is currently unknown, this suggests that these patients may have intrinsic resistance to conventional chemotherapy.

Glucocorticoids (GCs) are an integral component of therapy for patients with ALL (30). GCs act by binding to a cytoplasmic GC receptor (GR), which promotes translocation of the GC/GR complex to the nucleus and induction of a transcriptional program that results in apoptosis in lymphoid cells (1). Downstream effectors of signal transduction pathways have been shown to inhibit several of these processes, including nuclear translocation of ligand-activated GR (116,276) and induction of the GR transcriptional program (113). Furthermore, cytokines present in the microenvironment have been shown to promote GC resistance in lymphoblasts by activating these signal transduction pathways (132,249,277).

Given the importance of GC resistance in ALL and the comparatively poor clinical outcomes for patients with *CRLF2* overexpression, we hypothesized that the aberrant signal transduction associated with *CRLF2* overexpression might contribute to suboptimal responses to GC therapy. We tested this hypothesis by assessing *in vitro* drug responses in $CRLF2$-rearranged ($CRLF2_R$) and -non-rearranged ($CRLF2_{NR}$) cells from patient-derived xenografts of Ph-like ALL, and found that $CRLF2_R$ samples were uniformly less sensitive to GCs relative to many $CRLF2_{NR}$ samples. Furthermore, we demonstrated that GC sensitivity could be significantly enhanced with concomitant signal transduction inhibition, providing rationale for

further evaluation of a combination therapy strategy as a means of augmenting GC sensitivity in patients with *CRLF2* overexpression.

4.3: Results

Eleven of the 19 Ph-like leukemias were positive for *CRLF2* rearrangements. Of these, nine expressed transcripts corresponding to the *IGH@-CRLF2* rearrangement and two were positive for the *P2RY8-CRLF2* rearrangement. Seven of these $CRLF2_R$ leukemias had concomitant activating mutations in *JAK2*. All eight $CRLF2_{NR}$ Ph-like leukemias had point mutations or rearrangements involving other kinases previously implicated in Ph-like ALL (278) (Supplemental Table 4-1).

Both *IGH@-CRLF2* and *P2RY8-CRLF2* translocations have been reported to result in *CRLF2* overexpression (279). Consistent with these data, the $CRLF2_R$ leukemias analyzed in the current study exhibited higher cell surface TSLPR protein expression relative to $CRLF2_{NR}$ leukemias (p=0.0003; Figure 4-1A). We next assessed the induction of phosphorylated (p) STAT5, ERK, and Akt in response to short-term TSLP stimulation in $CRLF2_R$ and $CRLF2_{NR}$ leukemias. Four of 10 $CRLF2_R$ leukemias, including two that lacked a concomitant *JAK2* mutation, markedly induced pSTAT5 in response to short-term TSLP stimulation, while $CRLF2_{NR}$ leukemias did not (Figure 4-1B). $CRLF2_R$ leukemias also induced pERK and pAkt in response to TSLP, with no induction in the $CRLF2_{NR}$ leukemias (p=0.001 and p=0.002 versus $CRLF2_{NR}$ leukemias, respectively; Figures 4-1C-D). There were no differences in basal levels of pSTAT5, pERK, or pAkt between $CRLF2_R$ and $CRLF2_{NR}$ leukemias (Supplemental Figure 4-1).

To test the hypothesis that aberrant signal transduction might impair GC sensitivity in $CRLF2_R$ leukemias, we assessed the response to DEX *in vitro*. In the presence of DEX, all 11 $CRLF2_R$ leukemias retained greater than 50% survival at 48 hours, in contrast to only four $CRLF2_{NR}$ leukemias (p=0.006 versus $CRLF2_{NR}$ leukemias; Figure 4-2A). Importantly, this

difference in DEX sensitivity was not explained by differences in GR expression (Supplemental Figure 4-2A). Given the uniform DEX insensitivity in the $CRLF2_R$ leukemias, we asked whether inhibition of one or more signal transduction pathways downstream of TSLPR might augment DEX-induced cell death in these samples. We treated these leukemias with the combination of DEX and inhibitors of JAK1/2 (ruxolitinib), MEK (trametinib), or Akt (MK2206) at concentrations that attenuated TSLP-induced signaling in the $CRLF2_R$ Ph-like ALL cell line Mutz-5 (Supplemental Figures 4-2B-D) and that did not demonstrate toxicity in healthy PBMCs (Supplemental Figure 4-2E). In the $CRLF2_R$ samples, ruxolitinib had no significant single agent effect when assessed across the entire cohort, but it showed increased efficacy in samples with a $JAK2$ mutation relative to those without (p=0.03; Supplemental Figure 4-3A). Furthermore, the combination of DEX and ruxolitinib was not more effective than either agent alone (Figure 4-2B). In contrast, trametinib and MK2206, which showed moderate single-agent activity (p=0.005 and p=0.04 versus vehicle, respectively), were significantly more effective in combination with DEX relative to either single agent alone (p=0.005 and p<0.0001 versus DEX alone, respectively; Figures 4-2C-D). Bliss independence analysis confirmed these findings, demonstrating no interaction between DEX and RUX but cooperativity between DEX and trametinib and DEX and MK2206 (Figures 4-2E-G). In the $CRLF2_{NR}$ samples, these signal transduction inhibitors demonstrated variable effects, with some modulation of DEX sensitivity in several samples that demonstrated relative insensitivity to DEX as a single agent (Supplemental Figures 4-3B-D).

4.4: Discussion

Taken together, these data demonstrate that Ph-like ALL samples with $CRLF2$ rearrangements uniformly demonstrate limited GC sensitivity *in vitro*. Furthermore, these data suggest a model whereby dysregulated signal transduction in the context of $CRLF2$ overexpression contributes to relative GC resistance. This provides rationale for a clinical strategy involving combination therapy with GCs and signal transduction inhibitors as a means

of enhancing GC efficacy. A precedent for this type of combination therapy approach includes the addition of ABL kinase inhibitors to standard chemotherapy regimens for children with Ph-positive ALL, which has dramatically improved clinical outcomes for these patients (280). Together with the known prognostic value of GC sensitivity, our findings suggest that the inferior survival rates for patients with *CRLF2* overexpression may be driven at least in part by suboptimal responses to GC therapy. These data support further evaluation of *CRLF2* rearrangement status as a clinical biomarker for relatively poor sensitivity to GCs, thereby enabling the identification of patients who may benefit from the addition of molecularly targeted therapy to conventional anti-leukemia chemotherapy.

4.5: Methods

To assess GC sensitivity in Ph-like ALL cells, cryopreserved splenocytes were obtained from 19 patient-derived xenografts of high-risk Ph-like ALL established from treatment-naïve diagnostic samples banked in the Children's Hospital of Philadelphia leukemia biorepositories. Written informed consent for the use of diagnostic specimens for future research was obtained from patients or their guardians at the time of sample collection, according to the Declaration of Helsinki and the National Cancer Institute and the institutional review board of Children's Hospital of Philadelphia, which approved this study. As a control to assess for *in vitro* drug toxicity, peripheral blood mononuclear cells (PBMCs) from healthy donors were obtained from Vitalant. Rearrangements involving the *CRLF2* locus were detected as previously described (256). Cells were thawed, allowed to rest for 1 hour at 37˚C, then cultured at 37˚C in media supplemented with 25 ng/mL recombinant human TSLP (Peprotech, Rocky Hill, NJ, USA). Ruxolitinib (Selleckchem, Houston, TX, USA), a JAK1/2 inhibitor, was used at 500nM while dexamethasone (DEX; Sigma-Aldrich, St. Louis, MO, USA), a synthetic GC, trametinib (Selleckchem), a MEK1/2 inhibitor, and MK2206 (Selleckchem), a pan-Akt inhibitor, were used

at 1μM. Cells were harvested at 48 hours and flow cytometry was performed as previously described using a FACSVerse flow cytometer (BD Biosciences, San Jose, CA, USA) (259). Antisera included anti-human CD45, anti-cleaved caspase-3, anti-TSLPR, anti-STAT5 (pY694), anti-ERK1/2 (pT202/pY204), anti-Akt (pS473) (BD Biosciences), and anti-GR (Cell Signaling, Danvers, MA, USA). Signal strength was quantified as the median fluorescence intensity (MFI) of cells negative for cleaved caspase-3 within the human CD45-positive gate. Viability assays were performed via calculation of the frequency of Hoechst (ThermoFisher, Waltham, MA, USA) negative cells in the human CD45-positive gate. All viability data are presented as the percentage of viable cells in the drug-treated condition relative to the percentage of viable cells in the corresponding vehicle control condition for each individual sample. The average viability across all samples in the vehicle control condition at 48 hours was 39% +/- 23%. Statistical analyses were performed using Prism 8 (GraphPad, San Diego, CA, USA). All tests were two-sided and the threshold for significance was p≤0.05. Specifically, comparisons between groups were made using t-tests, with one-way ANOVA and Tukey's method for multiple comparisons adjustment used for comparisons of three or more groups. Drug-drug interactions were assessed using the Bliss independence model of synergy (281).

4.6: Acknowledgements

4.7: Figures
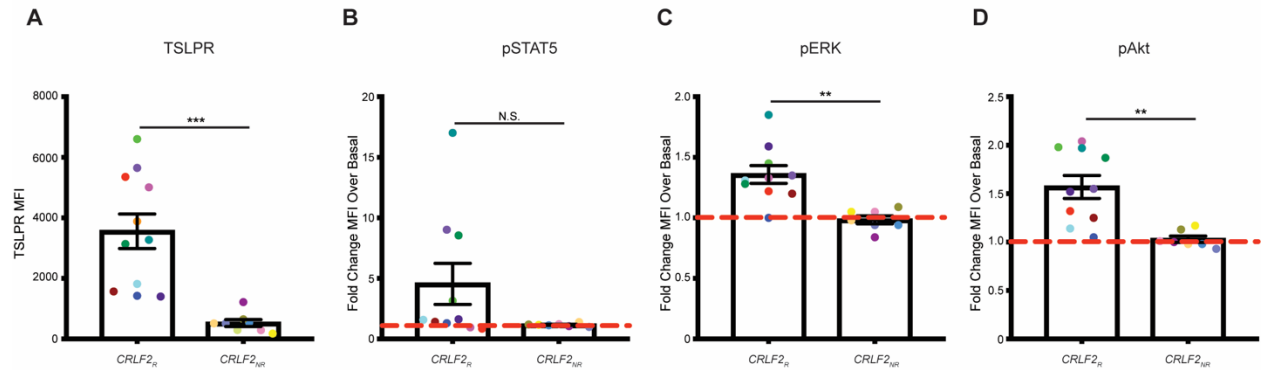
Figure 4-1: *CRLF2_R* leukemias demonstrate TSLPR overexpression and increased signal transduction activity relative to *CRLF2_NR* leukemias. (**A**) MFI of TSLPR cell surface protein expression as determined by antibody staining and flow cytometry in cells from *CRLF2_R* and *CRLF2_NR* samples. Individual patient samples are shown in the same color in all figures and in Supplemental Table 4-1. (**B-D**) Induction of (**B**) pSTAT5, (**C**) pERK, and (**D**) pAkt in *CRLF2_R* and *CRLF2_NR* samples in response to a 30-minute stimulation with 25ng/mL TSLP, presented as the fold change in MFI following TSLP stimulation relative to the basal condition. Samples JH721 and NL432 were not included in this analysis due to limitations in cell number. Error bars represent the standard error of the mean. Statistical significance was assessed using a two-sample t-test. ****p<0.0001, ***p<0.001, **p<0.01, *p<0.05.
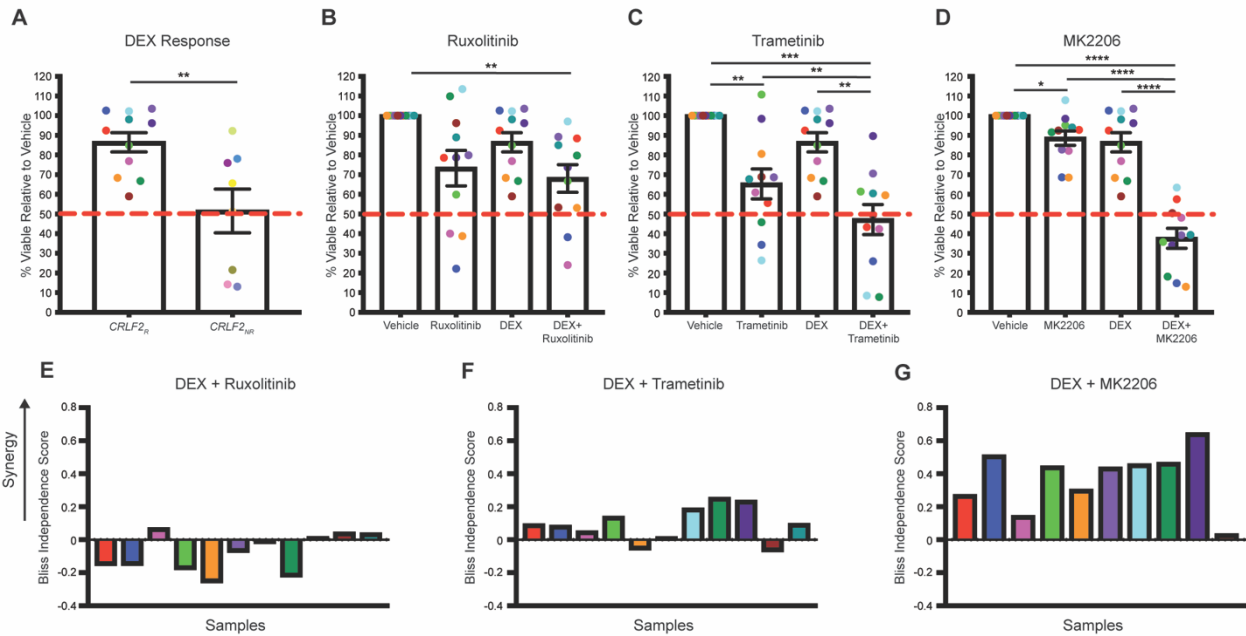
Figure 4-2: *CRLF2ᵣ* leukemias are uniformly DEX resistant and can be sensitized to DEX with targeted inhibition of MEK or Akt. (**A**) Cell viability in response to 1µM DEX, presented as the percentage of viable cells in the DEX treated condition relative to the vehicle control condition in *CRLF2ᵣ* and *CRLF2ₙᵣ* samples. (**B-D**) Cell viability of *CRLF2ᵣ* samples following exposure to 1µM DEX, (**B**) 500nM ruxolitinib, (**C**) 1µM trametinib, (**D**) 1µM MK2206, or a combination of DEX and a targeted inhibitor presented as the percentage of viable cells in the drug treated conditions relative to the vehicle control condition. (**E-G**) Bliss independence scores for the combination of DEX and ruxolitinib (**E**), trametinib (**F**), or MK2206 (**G**) in *CRLF2ᵣ* samples, in which positive values indicate a synergistic interaction between the two agents. Error bars represent the standard error of the mean. Statistical significance was assessed using a two-sample t-test (A) or one-way ANOVA with Tukey's method for multiple comparisons adjustment (B-D). ****p<0.0001, ***p<0.001, **p<0.01, *p<0.05.
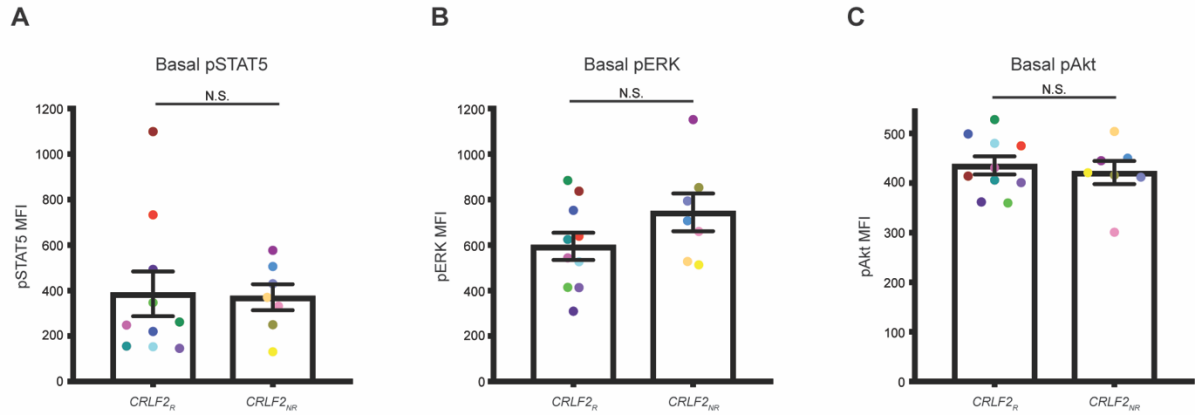
Supplemental Figure 4-1: Basal pathway activity is not different between *CRFL2~R~* and *CRLF2~NR~* samples. MFI of basal (**A**) pSTAT5, (**B**) pERK, and (**C**) pAkt in *CRLF2~R~* and *CRLF2~NR~* leukemias. Error bars represent the standard error of the mean. Statistical significance was assessed using a two-sample t-test.
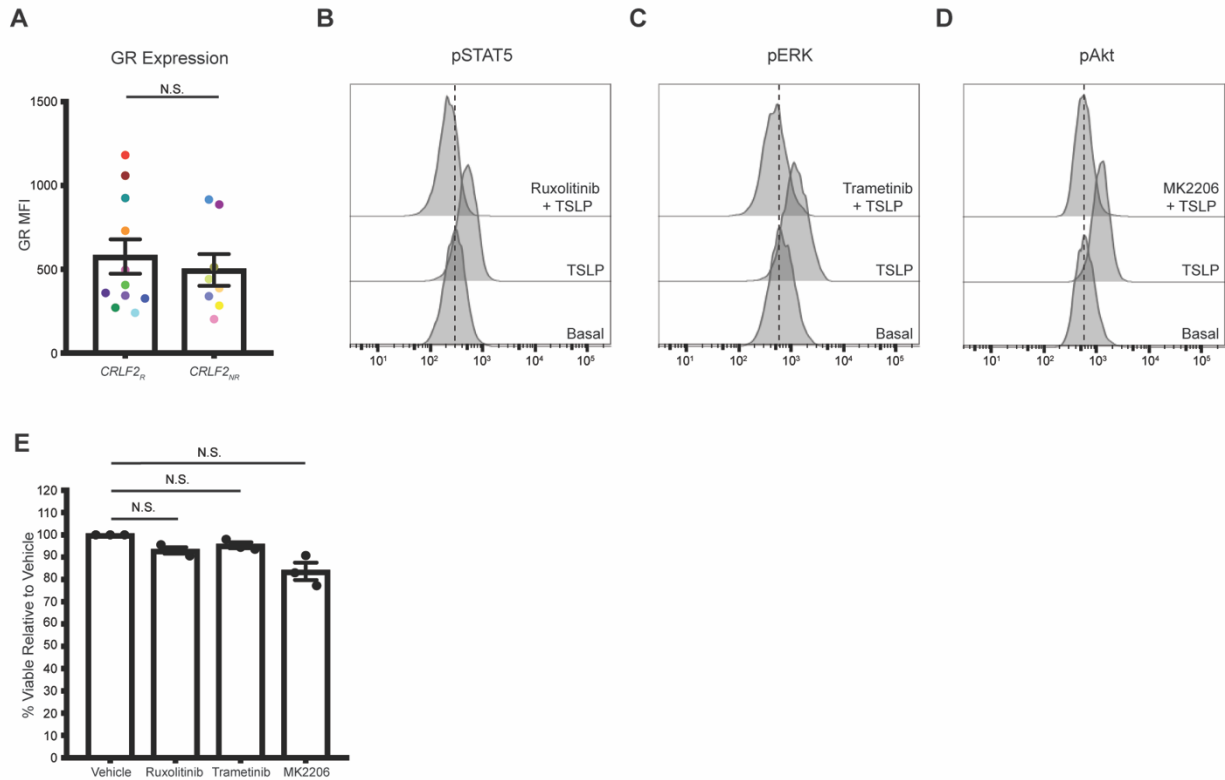
Supplemental Figure 4-2: Signal transduction inhibitors effectively inhibit pathway activity and are not toxic to PBMCs. (**A**) MFI of intracellular GR protein expression as determined by flow cytometry in $CRLF2_R$ and $CRLF2_{NR}$ samples. (**B-D**) Histograms indicating levels of (**B**) pSTAT5, (**C**) pERK, or (**D**) pAkt following TSLP stimulation with or without one hour pre-treatment with 500nM ruxolitinib, 1μM trametinib, or 1μM MK2206, respectively, in the $CRLF2_R$ Ph-like ALL cell line Mutz-5. (**E**) Viability of PBMCs from three healthy donors following exposure to 500nM ruxolitinib, 1μM trametinib, or 1μM MK2206. Error bars represent the standard error of the mean. Statistical significance was assessed using a two-sample t-test (A) or one-way ANOVA with Tukey's method for multiple comparisons adjustment (E).
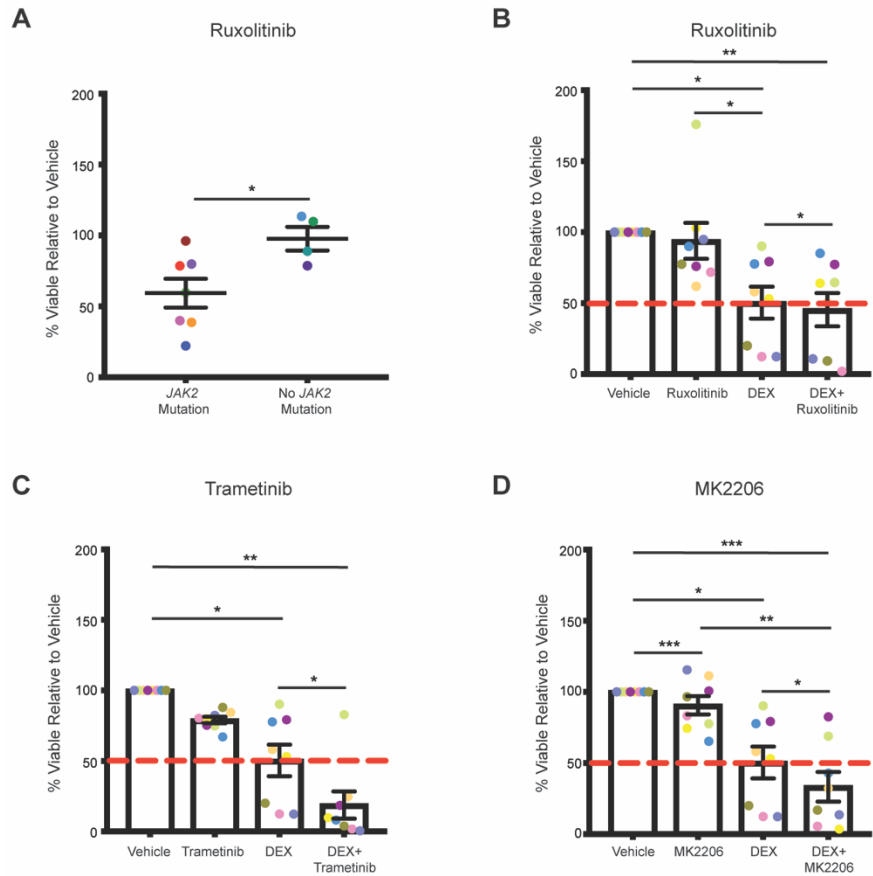
Supplemental Figure 4-3: Effects of signal transduction inhibitors on *CRLF2_{NR}* samples.
(A) Cell viability of *CRLF2_R* samples with *JAK2* mutations versus those without *JAK2* mutations following exposure to 500nM ruxolitinib. **(B-D)** Cell viability of *CRLF2_{NR}* samples following exposure to 1µM DEX, (**B**) 500nM ruxolitinib, (**C**) 1µM trametinib, (**D**) 1µM MK2206, or a combination of DEX and a targeted inhibitor presented as the percentage of viable cells in the drug treated conditions relative to the vehicle control condition. Error bars represent the standard error of the mean. Statistical significance was assessed using a paired t-test (A) or one-way ANOVA with Tukey's method for multiple comparisons adjustment (B-D). ****$p<0.0001$, ***$p<0.001$, **$p<0.01$, *$p<0.05$.

4.8: Table

Supplemental Table 4-1: Characteristics of Ph-like ALL Samples

Cytokine Receptor and Kinase Mutations				
Sample ID	*CRLF2 $_R$*	*JAK1/2* Mutation	Other Kinase Mutations	Color Code
NH612	*IGH@*	*JAK2* GPinsR683		
JH331	*IGH@*	*JAK2* R683G		
JH652	*IGH@*	*JAK2* R683G		
JH561	*IGH@*	*JAK2* R683G		
JH721	*IGH@*	*JAK2* I682F		
JH732	*IGH@*	*JAK2* P933R		
JH021	*IGH@*	*JAK1* V658F		
NH362	*IGH@*			
NH441	*IGH@*		*FLT3* N609ins23aa	
JH581	*P2RY8*	*JAK2* QGinsR683		
JH352	*P2RY8*	*JAK1* L624_R629>W		
JL491		*JAK1* S646F		
NL482A			*BCR-JAK2*	
NL482B			*IL7R, SH2B3*	
NL432			*EBF1-PDGFRB*	
NH011			*NUP214-ABL1*	
NL112			*STRN3-JAK2*	
PHL3			*ETV6-ABL1*	
PHL4			*SSBP2-CSF1R*	

Chapter 5: Glucocorticoids Paradoxically Facilitate Steroid Resistance in T-Cell Acute Lymphoblastic Leukemias and Thymocytes

5.1: Abstract

Glucocorticoids (GCs) are a central component of therapy for patients with T-cell acute lymphoblastic leukemia (T-ALL) and while resistance to GCs is a strong negative prognostic indicator in T-ALL, mechanisms of GC resistance remain poorly understood. Using diagnostic samples from patients enrolled on the frontline Children's Oncology Group (COG) T-ALL clinical trial AALL1231, we demonstrated that one-third of primary T-ALLs were resistant to GCs when cultured in the presence of interleukin-7 (IL7), a cytokine that is critical for normal T-cell function and that plays a well-established role in leukemogenesis. We demonstrated that in these T-ALLs and in distinct populations of normal developing thymocytes, GCs paradoxically induced their own resistance by promoting upregulation of IL7 receptor (IL7R) expression. In the presence of IL7, this augmented downstream signal transduction resulting in increased STAT5 transcriptional output and upregulation of the pro-survival protein BCL-2. Taken together, we demonstrated that IL7 mediates an intrinsic and physiologic mechanism of GC resistance in normal thymocyte development that is retained during leukemogenesis in a subset of T-ALLs and is reversible with targeted inhibition of the IL7R/JAK/STAT5/BCL-2 axis.

5.2: Introduction

T-cell acute lymphoblastic leukemia (T-ALL) is a genetically heterogeneous disease characterized by a range of alterations involving transcription factors, cell cycle regulators, and signal transduction effectors (282). Unlike B-cell ALL (B-ALL), where genetic factors are widely used to inform risk stratification and subsequent intensification of therapy (283), few genetic lesions in T-ALL have independent prognostic significance (282). As a result, efforts to implement risk-adapted therapeutic strategies have been limited by a lack of genetic biomarkers, highlighting the need for functional studies aimed instead at elucidating recurrent patterns of drug response and resistance across the spectrum of T-ALL.

While outcomes for children with T-ALL have improved dramatically over the past several decades, children with relapsed T-ALL continue to face poor survival rates (284), suggesting that novel strategies are needed to improve the upfront efficacy of therapy in order to induce deeper remissions and decrease the likelihood of disease relapse. Glucocorticoids (GCs) are a central component of T-ALL therapy, and the initial response to GC therapy is an important predictor of long-term outcomes (285). For example, on the ALL-BFM 95 trial, patients were stratified into those who had a prednisone good response (PGR) and those who had a prednisone poor response (PPR) following seven days of prednisone monotherapy. Patients with a PGR had an eight-year event free survival rate of 81.3%, as opposed to only 55.1% for patients with a PPR (30). These data demonstrate that intrinsic differences in GC sensitivity exist at the time of disease diagnosis and that these differences can have long-term prognostic significance. Despite decades of clinical use, a comprehensive understanding of the mechanistic basis for differential intrinsic GC sensitivity is lacking. GCs act by binding to a cytoplasmic GC receptor (GR), which promotes translocation of GR to the nucleus where it binds to target gene loci and induces a transcriptional program that results in apoptosis in lymphoid cells (49). Unlike other agents used in the treatment of T-ALL, GCs are unique in that they also exist as endogenous hormones that play critical roles in normal T-cell physiology. For example, endogenous GC activity has been shown to interact with T-cell receptor (TCR) signaling to shape the developing T-cell repertoire (286,287) and to promote T-cell homeostasis in the periphery following an immune response (288). Given these frequent encounters with GCs in normal physiology and the fact that GCs are potent inducers of apoptosis in both normal and transformed lymphoid cells, we reasoned that T-cells must possess intrinsic mechanisms that allow them to resist GC-induced apoptosis under certain developmental and environmental conditions. Furthermore, we hypothesized that these mechanisms may be retained during leukemogenesis and exploited to confer resistance to GC therapy in T-ALL.

One critical endogenous factor in the T-ALL microenvironment is the cytokine interleukin-7 (IL7). In addition to promoting the survival and differentiation of developing thymocytes (4), the IL7 receptor (IL7R)/JAK/STAT5 signaling pathway contributes to T-ALL pathogenesis and disease maintenance (289–291). We previously demonstrated that over half of primary treatment-naïve T-ALL patient samples are intrinsically resistant to the glucocorticoid dexamethasone (DEX) when cultured in the presence of IL7. Of these DEX resistant samples, half could be sensitized to DEX with inhibition of JAK signaling (132). Interestingly, the majority of samples with JAK/STAT5-mediated DEX resistance lacked activating mutations in components of the IL7R/JAK/STAT5 pathway. In the present study, we analyzed a larger cohort of fresh diagnostic samples obtained from pediatric patients enrolled on the COG frontline T-ALL clinical trial AALL1231, with the goal of establishing the mechanistic basis for this DEX resistance phenotype. In this cohort, we demonstrated that one-third of primary diagnostic samples are resistant to DEX specifically when cultured in the presence of IL7. Furthermore, we found that subsets of normal developing thymocytes similarly demonstrate this IL7-induced DEX resistance phenotype. Through functional analyses, we elucidated a mechanism by which GCs paradoxically induce their own resistance by augmenting the pro-survival activity of the IL7R/JAK/STAT5 pathway in distinct subsets of developing thymocytes and T-ALLs. Taken together, these data suggest that IL7 facilitates GC resistance in developing thymocyte populations, and that subsets of T-ALL cells retain this capacity to utilize IL7 as a means of resisting GC-induced apoptosis. These findings have significant therapeutic implications, as they suggest that inhibiting the IL7R/JAK/STAT5 pathway or its transcriptional targets may enhance GC efficacy in patients who exhibit a poor initial response to GC therapy.

5.3: Results

JAK signaling mediates dexamethasone resistance in a subset of T-ALLs

In a large independent cohort consisting of 73 samples from patients enrolled on COG AALL1231, we validated our previous finding that in vitro DEX sensitivity is highly variable across T-ALL (Figure 5-1A) (132). Importantly, these differences in DEX sensitivity are not dose-dependent, but persist at saturating concentrations of DEX (Supplemental Figure 5-1A). Defining "DEX resistant" as samples that retain greater than 50% cell viability following DEX exposure, we found that 63% of primary diagnostic samples are intrinsically DEX resistant when cultured in the presence of IL7 (Figure 5-1A). Binding of IL7 to IL7R results in the recruitment of JAK1 and JAK3, which subsequently become phosphorylated to create docking sites for STAT5 (253). Consistent with our previous findings (132), inhibition of JAK signaling with the JAK1/2 inhibitor ruxolitinib (RUX) was sufficient to overcome DEX resistance in 54% of these DEX resistant samples (p<0.0001 for DEX versus DEX+RUX and for RUX versus DEX+RUX; Figure 5-1B).

To facilitate further studies aimed at investigating the mechanistic basis for DEX resistance mediated by JAK signaling, we next evaluated the human T-ALL cell line CCRF-CEM for its utility as a model system in which to study the DEX resistance phenotype observed in these primary patient T-ALL samples. This analysis revealed a dose-dependent reduction in DEX sensitivity with increasing concentrations of IL7 (Figure 5-1C and Supplemental Figure 5-1B). Consistent with the primary patient samples, RUX was sufficient to completely restore DEX sensitivity in CCRF-CEM cells in the presence of IL7 (Figure 5-1D). Furthermore, Bliss independence analysis indicated a synergistic interaction between DEX and RUX (Figure 5-1E). To ensure that this sensitization effect was due specifically to JAK1 inhibition by RUX and not to off-target effects, we also utilized the JAK3 inhibitor tofacitinib, which should similarly inhibit IL7R signaling, and the JAK2 inhibitor CHZ868, which should not inhibit IL7R signaling. In this analysis, tofacitinib phenocopied the effects of RUX to overcome IL7-induced DEX resistance

while CHZ868 had no effect on cell viability (Supplemental Figure 5-1C), suggesting that on-target inhibition of JAK1 or JAK3 is sufficient to abrogate IL7-induced DEX resistance.

Dexamethasone exposure augments IL7R/JAK/STAT5 pathway activity

To confirm that IL7 induces DEX resistance in CCRF-CEM cells via signaling through IL7R, we first used CRISPR/Cas9 genome editing to generate clonal populations of scramble control and IL7Rα knockout (KO) CCRF-CEM cells (Supplemental Figure 5-2A). In the KO clones, loss of IL7Rα expression was sufficient to restore DEX sensitivity in the presence of IL7 (Figure 5-2A). We next asked whether IL7R signaling interferes with the activation and/or function of GR. First, to determine whether exposure to IL7 alters the availability of GR for DEX binding, we assessed GR protein expression in CCRF-CEM cells treated with DEX with or without IL7. Under these conditions, DEX exposure effectively induced GR expression to comparable levels regardless of the presence of IL7 (Supplemental Figure 5-2B). Furthermore, upon exposure to DEX both in the absence and presence of IL7, GR effectively translocated to the nucleus and became phosphorylated on Ser211 (Supplemental Figure 5-2C), a modification that has been shown to correlate with the capacity to activate or repress transcription (292). Finally, to determine whether IL7 interferes with induction of the GR transcriptional program, we performed RNA sequencing (RNA-seq) on four scramble control CCRF-CEM cell clones exposed to vehicle control or DEX with or without IL7 for four hours to elucidate primary GR target genes. Under these conditions, IL7 did not interfere with GR-mediated transcript induction or repression (Supplemental Figure 5-2D and Supplemental Table 5-1). Taken together, these data suggest that GR activity remains intact in the presence of IL7.

In some mature T-cell populations, GCs have been shown to induce expression of IL7Rα (293–296). Specifically, chromatin immunoprecipitation (ChIP) studies in both murine (297) and human (298) lymphocytes have demonstrated that GR is recruited to a GR binding

motif in a noncoding sequence upstream of the IL7Rα promoter, and deletion of this region is sufficient to abrogate GR-induced upregulation of IL7Rα (293), suggesting that IL7Rα upregulation occurs as a direct transcriptional effect of activated GR. To determine if DEX modulates IL7Rα expression in CCRF-CEM cells, we measured *IL7RA* transcript before and after DEX exposure and found a time-dependent increase in *IL7RA* transcript expression (Figure 5-2B) that occurred both in the absence and presence of IL7 (Supplemental Figure 5-2E). DEX exposure also increased IL7Rα protein expression at the cell surface relative to untreated cells (p<0.0001). This increase was inhibited in the presence of the translation inhibitor cycloheximide (CHX), suggesting that the increase in cell surface IL7Rα reflects *de novo* protein synthesis rather than re-localization of existing protein (Figure 5-2C). Given our finding that inhibition of JAK signaling is sufficient to sensitize cells to DEX in the presence of IL7, we next asked whether the increase in cell surface IL7Rα expression is associated with an increased capacity for JAK signaling downstream of IL7R. We first exposed CCRF-CEM cells to DEX for 24 hours, then stimulated them with IL7 and measured the induction of phosphorylated STAT5 (pSTAT5) as a downstream effector of JAK signaling (Supplemental Figure 5-2F). Under these conditions, DEX exposure resulted in significantly more robust pSTAT5 induction in response to IL7 stimulation relative to untreated cells (p=0.0002). Furthermore, pre-treating these cells with RUX for one hour prior to IL7 stimulation was sufficient to abrogate the increased JAK/STAT5 signaling following DEX exposure (Figure 5-2D and Supplemental Figure 5-2G). Importantly, IL7 stimulation, either with or without DEX pre-treatment, did not induce phosphorylation of other STAT proteins that are activated downstream of other γ chain cytokine receptors (Supplemental Figure 5-2H). Given this specific increase in STAT5 activation upon IL7 stimulation following DEX exposure, we then asked whether the increase in IL7Rα expression is associated with a sustained increase in STAT5 transcriptional activity. To test this, we transiently transfected CCRF-CEM cells with a STAT5-luciferase reporter construct and

assessed STAT5-induced luciferase activity in cells exposed to DEX in the presence or absence of IL7 for 36 hours. This analysis revealed a significant induction of STAT5 transcriptional activity in cells exposed to the combination of DEX and IL7 relative to either DEX or IL7 alone (p<0.0001 versus both DEX alone and IL7 alone). Furthermore, the addition of RUX was sufficient to overcome this increase in transcriptional activity (Figure 5-2E). To further confirm this increase in STAT5 transcriptional output, we performed RNA-seq on scramble control CCRF-CEM cell clones treated with DEX with or without IL7 for four hours. Using gene set enrichment analysis (GSEA) with gene sets derived from published STAT5 ChIP with sequencing (ChIP-seq) data in human CD4+ T-cells (299), we found enrichment for transcriptional targets of STAT5A and STAT5B (p<0.0001; FDR<0.0001), STAT5A alone (p=0.002; false discovery rate (FDR)=0.001), and STAT5B alone (p<0.0001; FDR=0.001) in cells exposed to DEX plus IL7 relative to IL7 alone (Figure 5-2F and Supplemental Table 5-2), further supporting the finding that, in the presence of IL7, DEX exposure augments activation of the STAT5 transcriptional program.

BCL-2 is a critical mediator of IL7-induced dexamethasone resistance

Based on these findings, we hypothesized that STAT5 may be an important downstream mediator of DEX resistance in the presence of IL7. To directly interrogate the role of STAT5 in this context, we used CRISPR/Cas9 genome editing to generate clonal populations of STAT5A KO, STAT5B KO, and STAT5A/B double KO CCRF-CEM cells (Figure 5-3A). Importantly, deletion of one or both STAT5 isoforms did not affect expression of GR relative to scramble control clones (Supplemental Figure 5-3A). Exposure of STAT5 KO cells to DEX in the presence or absence of IL7 revealed that deletion of STAT5B, but not of STAT5A, was sufficient to significantly attenuate DEX resistance in the presence of IL7 (Figure 5-3B and Supplemental Figure 5-3B). These data suggest that transcriptional targets of STAT5B represent candidate DEX resistance genes. To identify these candidate genes, we performed RNA-seq on scramble

control and STAT5A/B KO CCRF-CEM cell clones treated with DEX with or without IL7 for sixteen hours. Using these data, we found that deletion of STAT5A/B did not affect the capacity for DEX-induced upregulation of *IL7RA* (Supplemental Figure 5-3C), further confirming that IL7R upregulation is a GR-dependent but STAT5-independent transcriptional event. Using differential expression analysis, we identified the top differentially expressed genes between scramble control cells treated with DEX alone or with the combination of DEX and IL7 (Supplemental Table 5-3). We then compared this gene list to the core enrichment genes from the STAT5B gene set (Figure 5-2F and Supplemental Table 5-2) to identify STAT5B target genes that are differentially expressed in cells exposed to DEX relative to the combination of DEX and IL7. This analysis identified the anti-apoptotic family member *BCL2* (log fold change = 1.48 for DEX+IL7 relative to DEX alone) and the Rho guanine nucleotide exchange factor *ARHGEF3* (log fold change = 1.64) as two candidate mediators of DEX resistance in the presence of IL7 (Figure 5-3C). Consistent with their presence on both of these gene lists, targeted analysis of the RNA-seq data revealed that these genes were induced by the combination of DEX and IL7 relative to DEX or IL7 alone only in the scramble control clones and not in the STAT5A/B KO clones (Figures 5-3D-E).

Given the anti-apoptotic function of BCL-2 and the importance of downregulation of BCL-2 for DEX-induced apoptosis in T-ALL cells (18), we focused subsequent analyses on BCL-2 expression and function. Interestingly, other anti-apoptotic BCL-2 family members were not regulated in a similar manner in response to DEX and IL7 (Supplemental Figure 5-3D), suggesting a BCL-2-specific effect. To determine whether the induction of BCL-2 expression upon exposure to DEX and IL7 is mediated specifically by STAT5B, we assessed BCL-2 protein expression in scramble control and STAT5 single and double KO CCRF-CEM cell clones. This analysis revealed upregulation of BCL-2 with the combination of DEX and IL7 in scramble control and STAT5A single KO clones, but not in either the STAT5B single KO or STAT5A/B

double KO clones, consistent with a central role for STAT5B in the regulation of BCL-2 expression (Figure 5-3F and Supplemental Figure 5-3E).

Given that this increased STAT5 transcriptional activity depends first on the upregulation of IL7Rα as a primary transcriptional target of GR, we reasoned that STAT5-mediated upregulation of BCL-2 must occur as a secondary transcriptional effect following exposure to DEX and IL7. To test this, we performed qPCR to measure the changes in expression over time of *BCL2* and of primary GR target genes in CCRF-CEM cells cultured in the presence of DEX and IL7. This analysis revealed that while primary GR transcriptional targets are upregulated as early as two hours following DEX treatment, *BCL2* is not significantly upregulated until the eight-hour time point (Supplemental Figure 5-3F). To further confirm that *BCL2* is upregulated as a secondary transcriptional target, we exposed CCRF-CEM cells to DEX with or without IL7 in the presence or absence of CHX and measured transcript and protein expression of *BCL2* and of the primary GR transcriptional target *BCL2L11* (BIM) (18). CHX was sufficient to inhibit the upregulation of BIM and BCL-2 protein expression, suggesting effective inhibition of translation and *de novo* protein synthesis (Supplemental Figure 5-3G). *BCL2L11* transcript expression was induced by DEX both in the absence and presence of CHX, consistent with this being a primary transcriptional target of GR, the upregulation of which is not dependent on intermediary *de novo* protein synthesis. In contrast, *BCL2* transcript expression was upregulated only in the absence of CHX, suggesting a dependence on *de novo* protein synthesis, consistent with this being a secondary transcriptional event (Figure 5-3G).

To establish the functional significance of BCL-2 upregulation, we first performed BH3 profiling with the BCL-2 inhibitor ABT-199 in CCRF-CEM cells treated with DEX with or without IL7. Under these conditions, DEX alone produced a significant increase in apoptotic priming (p=0.0007). This effect was attenuated in the presence of IL7 (p=0.64), suggesting that the increase in BCL-2 expression with the combination of DEX and IL7 is sufficient to oppose the induction of the apoptotic program (Figure 5-4A). To determine whether ABT-199 may have a

therapeutic role to enhance DEX sensitivity in the presence of IL7, we exposed CCRF-CEM cells to DEX in the presence of IL7 and increasing concentrations of ABT-199. This analysis demonstrated that ABT-199 potently sensitizes cells to DEX in the presence of IL7 in a synergistic manner (Figures 5-4B-C). In addition, we utilized a series of short hairpin RNAs (shRNAs) to knock down BCL-2 expression in CCRF-CEM cells and found that loss of BCL-2 expression increases sensitivity to DEX in the presence of IL7 in a manner that correlates with the degree of BCL-2 knockdown (Supplemental Figure 5-4A and Figures 5-4D-E). To assess the importance of high BCL-2 expression in a patient cohort for which clinical outcome data are available, we next analyzed published gene expression data from 265 diagnostic T-ALL samples obtained from patients enrolled on the prior COG T-ALL trial AALL0434 (282). Consistent with our in vitro findings, we found that patients who were minimal residual disease (MRD) positive at the end of induction therapy had significantly higher BCL-2 expression relative to patients who were MRD negative (p=0.0009 for patients with MRD <1% and p<0.0001 for patients with MRD >1%; Figure 5-4F), suggesting a relationship between high BCL-2 expression and relative GC resistance. In contrast, shRNA-mediated knockdown of the other candidate resistance gene, *ARHGEF3*, had no effect to overcome IL7-induced DEX resistance (Supplemental Figures 5-4B-C) and *ARHGEF3* expression did not differ according to MRD status in the AALL0434 patient cohort (Supplemental Figure 5-4D). Taken together, these data support a model (Figure 5-4G) whereby DEX (i), through upregulating IL7Rα expression (ii), paradoxically induces its own resistance by augmenting JAK/STAT5 signaling (iii) and activation of STAT5B target genes (iv), including *BCL2*. This upregulation of BCL-2 in turn is sufficient to antagonize the pro-apoptotic effects of DEX.

IL7 induces dexamethasone resistance in subsets of developing thymocytes

We next sought to determine why IL7-mediated DEX resistance occurs only in a subset of primary patient T-ALL samples. In our previous patient cohort, we demonstrated that 64% of

samples with IL7-mediated DEX resistance did not have activating mutations in the

IL7R/JAK/STAT5 pathway (132), suggesting that this phenotype is not dictated by the

mutational status of a T-ALL sample. Given these findings, an alternative hypothesis is that IL7-

mediated DEX resistance might reflect a physiologic mechanism of GC resistance that occurs in

normal populations of developing thymocytes, as both GC sensitivity and IL7R expression are

known to vary throughout development (4,300). To test this hypothesis, we evaluated normal

murine thymocytes to determine if IL7R/JAK/STAT5 signaling modulates DEX sensitivity. We

first exposed mice to DEX in vivo and assessed the relative sensitivity of the major thymocyte

subpopulations. In this analysis, DEX induced a significant reduction in overall thymic cellularity

($p=0.02$; Supplemental Figure 5-5A) and resulted in a dramatic shift in the distribution of the

major thymocyte subpopulations. Consistent with previous reports (300), we found that DEX

induced a significant reduction in the proportion of CD4/CD8 double positive (DP) thymocytes

($p<0.0001$), with a compensatory increase in the percentage of the earlier double negative (DN)

thymocytes ($p=0.005$) and later single positive (SP) thymocytes ($p<0.0001$ for both CD4 and

CD8 SP thymocytes; Figure 5-5A and Supplemental Figures 5-5B-C). Importantly, we

recapitulated the findings by other investigators (301) that GR expression is paradoxically

lowest at the DP stage of development despite these cells being highly DEX sensitive,

suggesting that GR expression is insufficient to explain this pattern of differential sensitivity

(Supplemental Figure 5-5D). To determine if this differential DEX sensitivity reflects differences

in the apoptotic potential of these thymocyte subpopulations in their basal state, we performed

BH3 profiling on freshly harvested thymocytes. We found that DP thymocytes have significantly

higher apoptotic potential relative to DN or SP thymocytes ($p=0.002$, $p=0.0004$, and $p=0.01$

versus DN, CD4 SP, and CD8 SP thymocytes, respectively; Figure 5-5B), consistent with the

pattern of DEX sensitivity observed in vivo.

We next evaluated basal IL7Rα expression and signaling capacity across the major

thymocyte subpopulations. Consistent with previous reports (4), we found a reduction in IL7Rα

expression and IL7-induced pSTAT5 in the DP thymocytes relative to the DN and SP thymocytes (Figures 5-5C-D). Based on these findings and the pattern of DEX sensitivity we observed in vivo, we hypothesized that the presence of IL7 in the in vivo microenvironment might activate JAK/STAT5 signaling in DN and SP thymocytes, which could in turn confer protection against the GC surges that occur during a physiologic stress response (302) and against pharmacologic concentrations of GCs. To test this hypothesis, we first exposed thymocytes to vehicle or DEX ex vivo in the absence or presence of increasing concentrations of IL7. DN and SP thymocytes demonstrated profound DEX resistance specifically in the presence of IL7, while DP thymocytes remained highly sensitive to DEX regardless of IL7 (Figure 5-5E), consistent with their reduced IL7Rα expression (Figure 5-5C). To determine whether the mechanism of JAK/STAT5-mediated DEX resistance that we elucidated in CCRF-CEM cells is applicable in these thymocyte subpopulations, we exposed thymocytes to DEX ex vivo and assessed cell surface IL7Rα expression and BCL-2 expression. Consistent with the observed pattern of DEX resistance in the presence of IL7, DN and SP thymocytes significantly upregulated both IL7Rα expression (p<0.0001 for DN, CD4 SP and CD8 SP thymocytes; Figure 5-5F) and BCL-2 expression (p=0.01, p=0.0005, and p=0.001 for DN, CD4 SP, and CD8 SP thymocytes, respectively; Figure 5-5G) following exposure to DEX in the presence of IL7. Finally, to determine if this mechanism is applicable in vivo under normal physiologic conditions, we treated mice with DEX and assessed BCL-2 protein expression in the major thymocyte subpopulations. DN and CD4 SP thymocytes, but not DP thymocytes, significantly upregulated BCL-2 expression in response to DEX (p=0.007 and p=0.004 for DN and CD4 SP thymocytes, respectively; Figure 5-5H). Finally, to determine whether human thymocytes demonstrate a similar pattern of IL7Rα expression and IL7-induced DEX resistance throughout development, we performed ex vivo analysis of healthy human thymocytes. Similar to the pattern observed in murine thymocytes, DN and SP thymocytes had the most significant increase in cell surface

IL7Rα expression following exposure to DEX (Supplemental Figure 5-5E) and had the most profound IL7-induced DEX resistance (Supplemental Figure 5-5F).

Developmental stage correlates with IL7-induced dexamethasone resistance in T-ALL

To further address the hypothesis that IL7R/JAK/STAT5-mediated DEX resistance may be retained from normal thymocyte development in a subset of T-ALLs, we performed RNA-seq on 76 primary diagnostic T-ALL samples from patients enrolled on COG AALL1231. Using a gene set derived from a comparison of early versus late developing thymocytes (303), we performed unbiased hierarchical clustering of these patient samples to classify samples as developmentally "early" or "late" (Figure 5-6A). We next performed detailed in vitro analysis of 15 of the early T-ALL samples and 12 of the late T-ALL samples isolated from patient derived xenografts (PDXs). Additional information about these samples is presented in Supplemental Table 5-4. There were no differences in basal GR expression between these two groups (Supplemental Figure 5-6A). Upon analysis of cell surface IL7Rα expression, we found that the early samples tended to have higher basal IL7Rα expression and a more robust induction of IL7Rα upon exposure to DEX (Figure 5-6B). This higher basal IL7Rα expression was also associated with an increased response to IL7 stimulation, as measured by pSTAT5 (Supplemental Figure 5-6B). Consistent with this finding, only the early sample group demonstrated a significant increase in DEX resistance in the presence of IL7 (p=0.0007 and p=0.69 for early and late samples, respectively; Figure 5-6C). To determine whether this resistance phenotype was associated with activating mutations in the IL7R/JAK/STAT pathway, we performed variant calling using the RNA-seq data and found no enrichment for IL7R pathway mutations in the early samples (Supplemental Figure 5-6C and Supplemental Table 5-5), consistent with our previous analysis (132). Similar to the findings in CCRF-CEM cells, these early samples demonstrated an increase in BCL-2 protein expression in the presence of IL7,

which was further augmented upon concomitant exposure to DEX and attenuated with the addition of RUX (Figure 5-6D). Moreover, both RUX and ABT-199 significantly sensitized early T-ALL samples to DEX in the presence of IL7 (p<0.0001 and p=0.0005 for the addition of RUX or ABT-199, respectively, to DEX plus IL7; Figure 5-6E). To evaluate the utility of RUX for overcoming DEX resistance in vivo in a preclinical model, we transplanted mice with early T-ALL T24 and treated them with DEX with or without RUX, using survival as the primary endpoint. As we observed in vitro (Supplemental Figure 5-6D), the combination of DEX and RUX demonstrated increased in vivo efficacy relative to either agent alone (p=0.003 for RUX versus DEX+RUX and p=0.02 for DEX versus DEX+RUX; Figure 5-6F).

5.4: Discussion

The poor survival rates observed in children with relapsed T-ALL (284) suggest a need for strategies to enhance the efficacy of upfront therapy as a means of improving cure rates by decreasing the likelihood of disease relapse. While many studies have focused on understanding mechanisms of acquired drug resistance that arise during T-ALL treatment (304), the goal of our current study was instead to elucidate mechanisms of intrinsic drug resistance that dictate the initial response to therapy. In particular, the prognostic significance of the initial GC response in T-ALL (285) suggests a need for a deeper understanding of the mechanisms governing intrinsic differences in GC sensitivity. Here we demonstrate that functional analysis of a large number of diagnostic patient samples reveals recurrent patterns of intrinsic GC resistance across this otherwise genetically heterogeneous patient population. We confirm in this validation cohort that over half of the diagnostic T-ALL samples analyzed exhibit intrinsic DEX resistance in vitro, which has in turn been shown to correlate with clinical outcomes (305). Furthermore, we show that within this subset, half of the samples are resistant to DEX specifically in the presence of IL7.

Our data support a model whereby GCs paradoxically induce their own resistance by upregulating IL7Rα expression. In the presence of IL7, this leads to increased downstream signal transduction and STAT5 transcriptional output. This ultimately results in the upregulation of BCL-2, which is sufficient to counteract the pro-apoptotic effect of DEX. Given the prevalence of this phenotype, our data suggest that a significant percentage of T-ALL patients may benefit from the upfront addition of JAK or BCL-2 inhibitors as a means of improving the efficacy of GC therapy. Furthermore, we demonstrate the synergistic potential of combining DEX with these agents, suggesting that combination therapy may allow for a reduction in DEX dosing, thereby minimizing the numerous acute and chronic toxicities associated with steroid exposure (306) while simultaneously maximizing efficacy. In addition, our data demonstrate that STAT5B is primarily responsible for the upregulation of BCL-2 expression in this context, consistent with previous reports demonstrating that knockdown of STAT5A is insufficient to modulate IL7-mediated regulation of BCL-2 expression (289). Interestingly, this is also consistent with the finding that activating mutations in *STAT5B*, but not in *STAT5A*, commonly occur in T-ALL *(282)*. These data support further investigation of the use of ABT-199 as a rational therapeutic strategy to enhance the efficacy of DEX in patients with *STAT5B*-mutated T-ALL.

In addition to mediating GC resistance in over one-third of diagnostic T-ALL samples, we demonstrate that IL7 similarly induces GC resistance in those populations of normal thymocytes in which IL7R signaling is important for survival and proliferation (4). Developing thymocytes are continuously exposed to endogenous GCs, but we and others (300) demonstrate that susceptibility to GC-induced apoptosis is variable over the course of thymocyte development. These data suggest that normal thymocyte populations must possess intrinsic mechanisms of GC resistance at distinct stages of development and/or under certain environmental conditions. In particular, we find that IL7-induced DEX resistance occurs in DN thymocytes and is enriched in T-ALL samples with an "early thymocyte" gene expression signature. Importantly, these early thymocytes undergo gene rearrangement to generate a fully rearranged TCR, which will be

94

tested for functionality and auto-reactivity in the subsequent DP stage, a key process in the generation of mature functional T-cells (4). Teleologically, susceptibility to GC-induced apoptosis would be maladaptive early in development, as it would limit the availability of cells for this selection process. Our data therefore suggest that IL7-induced GC resistance may protect these early thymocyte populations from apoptosis in the presence of endogenous GCs. Furthermore, we demonstrate that this mechanism of intrinsic resistance is retained in T-ALLs resembling early thymocytes, where it may be exploited to enable resistance to pharmacologic concentrations of GCs.

Taken together, our data provide strong rationale for the idea that differential sensitivity to GC therapy at the time of disease diagnosis reflects developmentally programmed mechanisms of intrinsic GC resistance that are retained during the process of leukemogenesis. This work supports further studies aimed at elucidating additional mechanisms of GC resistance at distinct stages of thymocyte development as a means of understanding the factors that contribute to intrinsic GC resistance in T-ALL.

5.5: Methods

Patient samples and patient derived xenografts

Diagnostic blood samples were obtained from patients enrolled on the COG trial AALL1231. Immunophenotyping was performed and reviewed by immunophenotyping experts in COG. To establish patient derived xenografts, cells were injected into NOD/SCID/*Il2rg*^{tm1wjl}/Szj (NSG) mice obtained from Jackson Laboratories. Engraftment was monitored using flow cytometric analysis of peripheral blood with antibodies against human CD45 (BD Biosciences; 560973) and CD7 (BioLegend; 343105).

CCRF-CEM cells

CCRF-CEM cells were purchased from the UCSF Cell Culture Facility (ATCC CCL-119). Cells were authenticated via short tandem repeat DNA profiling and were routinely tested for mycoplasma contamination using the PlasmoTest detection kit (InvivoGen).

Preclinical trial

Five five-week-old male NSG mice per treatment arm were randomized to receive vehicle control, DEX, RUX, or the combination of DEX and RUX once the peripheral blood blast count reached 1%. RUX was administered in chow form (Incyte) continuously over the trial duration. DEX (Fresenius Kabi and Children's Hospital of Philadelphia Pharmacy) was administered at 7.5mg/kg/day by intraperitoneal injection. Mice were euthanized when they became moribund.

In vivo dexamethasone treatment in C57BL/6x129Sv/Jae mice and isolation of human and murine thymocytes

Six to eight-week-old male F1 C57BL/6x129Sv/Jae mice were obtained from the University of California, San Francisco Laboratory Animal Resource Center (LARC) breeding core. Mice were treated with 2mg/kg dexamethasone sodium phosphate (NDC 63323-516-10; University of California, San Francisco pharmacy) or vehicle control (phosphate buffered saline) once daily for three days. Healthy human thymocytes were obtained from children undergoing cardiothoracic surgery at the University of California, San Francisco. Antibodies against murine CD4 (BioLegend; 100425) and CD8 (BioLegend; 100707) or human CD4 (Biolegend; 317420) or CD8 (BioLegend; 344706) were used to identify thymocyte subpopulations.

In vitro viability assays

In vitro viability assays were performed by exposing cells to vehicle control or dexamethasone (Sigma; D4902), ruxolitinib (Selleckchem; S1378), tofacitinib (Selleckchem; S5001), CHZ868 (MedKoo; 407137), or ABT-199 (ApexBio; A8194) for 72 hours (CCRF-CEM cells), 48 hours (PDX cells), or 24 hours (thymocytes) with or without recombinant human or murine IL7 (Peprotech; 200-07 and 217-17). Cells were then stained with Hoechst 33258 (Molecular Probes; H3569) and analyzed by flow cytometry.

CRISPR/Cas9 genome editing of CCRF/CEM cells

Cas9 protein containing a nuclear localization signal (Cas9-NLS) was purchased from the QB3 MacroLab at the University of California, Berkeley. Trans-activating CRISPR RNA (tracrRNA) and single guide RNAs (sgRNAs) were purchased from Dharmacon. sgRNA sequences targeting IL7Rα, STAT5A, and STAT5B were obtained from the Brunello sgRNA library (307) and are as follows: IL7Rα – AAAGAGCAATATATGTGTGA; STAT5A – ACATTCTGTACAATGAACAG; STAT5B – GTTCATTGTACAATATATGG. The scramble control cells were generated using a non-targeting sgRNA: GGTTCTTGACTACCGTAATT.

Ribonucleoproteins were prepared according to established methods (308). Electroporation was performed using the Amaxa Cell Line Nucleofector Kit C (Lonza, VACA-1004) and an Amaxa Nucleofector II Device with the electroporation code X-001. Editing was assessed by PCR amplification using the following primers: IL7Rα forward – 5'-TGAACATGCCTCCACTCACC-3'; IL7Rα reverse – 5'-CACACCTGGGTTTGAAGATCC-3'; STAT5A forward – 5'- TGGGGATAGTTCCTGAGGCT-3'; STAT5A reverse – 5' TGCCACCTCTTACACTTGCC-3'; STAT5B forward – 5'- TGTGCCCCTTAGGATGAAGC-3'; STAT5B reverse – 5'- AATCACAGGAGGCACTGTTCC-3'. The amplicons were Sanger

sequenced and the sequencing traces were analyzed using the TIDE analysis software (309). Clonal populations were generated using limiting dilution cell plating.

Western blotting

For analysis of protein expression in whole cell lysates, CCRF-CEM cells were resuspended in RIPA buffer. For analysis of cytoplasmic and nuclear protein, protein fractions were generated using the NE-PER kit (ThermoFisher Scientific; 78833). Immunoblotting was performed with the following antibodies: STAT5A (Abcam; ab32043), STAT5B (Abcam; ab178941), GR (Cell Signaling Technology; 12041), GR pS211 (Cell Signaling Technology; 4161), β-actin (Cell Signaling Technology; 3700), and p84 (Genetex; GTX70220). Donkey anti-rabbit IRDye800 and donkey anti-mouse IRDye680 secondary antibodies (LI-COR Biosciences) were used and imaging was performed using the Odyssey Imaging System (LI-COR Biosciences).

Quantitative PCR (qPCR)

CCRF-CEM cells were cultured in the presence or absence of 1μM DEX, 100ng/mL IL7, and/or 10μg/mL cycloheximide for 16 hours unless otherwise indicated. RNA was isolated using the RNeasy Mini Kit (Qiagen) and cDNA was generated using the Superscript III kit (ThermoFisher Scientific). Taqman quantitative PCR probes (Applied Biosystems) were used in conjunction with Taqman Master Mix (Applied Biosystems) to assess transcript levels for the following genes: *GAPDH* (Hs02786624_g1; VIC-MGB)*, IL7Rα* (Hs00902334_m1; FAM-MGB)*, BCL2L11* (Hs00708019_s1; FAM-MGB)*, BCL2* (Hs00608023_m1; FAM-MGB)*, FKBP5* (Hs01561006_m1; FAM-MGB)*, GILZ* (Hs00608272_m1; FAM-MGB)*, NR3C1* (H200353740_m1; FAM-MGB)*, MYC* (Hs00153408_m1; FAM-MGB), and *ARHGEF3* (Hs00989814_m1; FAM-MGB)*.* Experiments were performed in technical triplicate and were run

on a QuantStudio 5 Real-Time PCR Instrument (Applied Biosystems). The fold change in transcript expression was calculated relative to cells treated with vehicle control using the delta-delta Ct method, unless otherwise indicated, with the use of *GAPDH* transcript for normalization.

Measurement of cell surface IL7Rα

For analysis of cell surface IL7Rα expression, cells were treated with 1µM DEX for 24 hours. Murine thymocyte experiments were performed in the presence of 100pg/mL recombinant murine IL7. Antibodies against human (BioLegend; 351315) or murine (Tonbo Biosciences; 20-1271) IL7Rα were used in conjunction with Hoechst 33258 to allow for gating on viable cells. Data are presented as the median fluorescent intensity (MFI) of the IL7Rα signal.

Cytokine stimulation and intracellular flow cytometry

Phosphoflow cytometry for measurement of STAT protein phosphorylation following IL7 stimulation was performed as previously described (132). Briefly, CCRF-CEM cells were exposed to vehicle control or 1µM DEX for 24 hours, allowed to rest for one hour in serum free media, and stimulated with IL7 at a concentration of 100ng/mL for 15 minutes. PDX cells were similarly allowed to rest in serum free media for one hour followed by stimulation with 100ng/mL IL7 for 15 minutes. Cells were subsequently fixed with 2% paraformaldehyde and permeabilized with methanol. STAT protein phosphorylation was assessed using antibodies against pSTAT1 pY701 (BD Biosciences; BDB612564), pSTAT3 pY705 (BD Biosciences; BDB612569), pSTAT5 pY694 (BD Biosciences; BDB612599), and pSTAT6 pY641 (BD Biosciences; BDB612601). BIM and BCL-2 protein expression were assessed following cell fixation and permeabilization using antibodies against BIM (Cell Signaling Technology; 2933) and anti-human (Life Technologies; A15796) or anti-mouse (BioLegend; 633509) BCL-2. GR expression was assessed using an

anti-GR antibody. A donkey anti-rabbit secondary antibody (Jackson ImmunoResearch Laboratories) was used for flow cytometric detection of BIM and GR protein.

Luciferase reporter assay

CCRF-CEM cells were transiently transfected with the pGL4.52[*luc2P*/STAT5 RE/hygro] vector (Promega; E4651) using the Lipofectamine 3000 Transfection Reagent (Life Technologies). Eighteen hours after transfection, cells were treated in the absence or presence of 1μM DEX, 100ng/mL recombinant human IL7, and/or 500nM ruxolitinib for 36 hours. Luciferase activity was assessed with the ONE-Glo Luciferase Assay System (Promega) and a Biotek Synergy 2 instrument. Relative luminescence was calculated by normalizing values to those obtained from cells treated with vehicle control.

RNA-seq analysis

Scramble control and STAT5 knockout CCRF-CEM cell clones were cultured in vehicle control or in the presence or absence of 1μM DEX and/or 100ng/mL recombinant human IL7 for 4 or 16 hours. RNA was isolated using the RNeasy Mini Kit and cDNA was generated using the Superscript III kit and quantified using a NanoDrop spectrophotometer (ThermoFisher). RNA quality was assessed using an Agilent Bioanalyzer (Agilent Technologies). Libraries were prepared using 1ng of RNA and were sequenced on the HiSeq 2500 (Illumina) to generate 50bp single end reads.

GR regulated genes were identified using edgeR, as previously described (310), by comparing scramble control clones treated with vehicle to those treated with DEX for four hours. A gene set was created using the statistical thresholds of absolute log fold change >1 and false discovery rate (FDR) <0.05. This analysis was then applied to perform the same comparison between scramble control clones treated with vehicle versus DEX plus IL7 for four hours. For the analysis of STAT5 target genes, gene set enrichment analysis (GSEA) was performed as

previously described (311) by comparing scramble control clones treated with IL7 versus DEX plus IL7 using gene sets derived from published STAT5 ChIP-seq experiments in human CD4+ T-cells (299). The default settings were used for GSEA, including permutation based on phenotype. These data have been deposited in NCBI's Gene Expression Omnibus and are accessible through GEO Series accession number GSE137893.

For the fresh diagnostic T-ALL samples, total RNA was prepared using Trizol (ThermoFisher) based extraction. Samples were purified and concentrated using the RNeasy Mini or RNeasy MinElute Kit alone with the DNase Set (Qiagen). RNA concentration was determined using a NanoDrop spectrophotometer. RNA quality was assessed using an Agilent 2200 TapeStation (Agilent Technologies). 100ng of RNA was used to prepare libraries using the TruSeq RNA Exome RNA kit (Illumina). For RNA samples with DV_{200} below 30%, 200ng of total RNA was used to prepare libraries. Libraries were sequenced on a NextSeq 500 using 150bp paired-end chemistry.

Primary T-ALL cell transcript expression was calculated via a local software pipeline built around the Bowtie 2 Aligner (v2.3.4.1) and RSEM's (v1.2.3.0) expectation-maximization quantification that utilized the Ensembl GRCh38 release 85 reference. After demultiplexing, converting primary sequence data to fastq format, and trimming adapters, sequences were aligned against an HG38 rRNA reference using the bwa (v0.7.12) aligner in order to screen out rRNA. Only non-rRNA aligning sequences advanced into the Bowtie 2/RSEM analysis stream. These data were used to generate gene signatures associated with early versus late thymocyte development via hierarchical clustering and dendrogram analysis.

All sequencing analysis, including read alignment, quality and performance metrics, post-processing, variant calling, and variant annotation were performed as previously described (312,313) using the hg38 build of the human genome. Briefly, reads were aligned with Burrows-Wheeler Aligner (314) and processed using Picard (http://broadinstitute.github.io/picard) and the Genome Analysis Toolkit (GATK) (315) to perform base quality recalibration and multiple

sequence realignment. Single nucleotide variants and indels were detected with the MuTect (316) and BCFtools algorithms, respectively. Variants were negatively selected against based on IGSR SNP (317) and ExAC SNP (318) databases and positively selected for based on recurrently mutated sites or regions within COSMIC (Acute T Lymphoblastic Leukemia associated subset of mutations) (319) or as previously reported (282). Candidate somatic mutations were manually reviewed using Integrative Genomics Viewer (320). These data have been deposited in NCBI's Gene Expression Omnibus and are accessible through GEO Series accession number GSE137768.

BH3 profiling

BH3 profiling was performed according to established methods (321). CCRF-CEM cells were treated with or without 1µM DEX and/or 100ng/mL recombinant human IL7 for 16 hours prior to analysis. Thymocyte BH3 profiling was performed immediately after harvesting thymocytes. Cytochrome c staining was performed using an anti-cytochrome c antibody (BioLegend; 612310).

shRNA-mediated knockdown of BCL2 and ARHGEF3

The miR30-PGK-NeoR-IRES-GFP cassette from LMN-GFP (307) was cloned into a pCDH Expression Lentivector (System Biosciences) to generate the construct pCDH-LMN-GFP. Short hairpin RNA (shRNA) sequences targeting human *BCL2* are as follows: shBCL2-1 – 5'-TTTTATTCCAATTCCTTTCGGA-3'; shBCL2-2 – 5'-TAGCTGATTTGAAACTTCCCAA-3'; shBCL2-3 – 5'-TACTTCATCACTATCTCCCGGT-3'; shBCL2-4 – 5'-TTTAAGTACAGCATGATCCTCT-3'; and shBCL2-5 – 5'-TATCAGTCTACTTCCTCTGTGA-3'. shRNA sequences targeting human *ARHGEF3* are as follows: shARHGEF3-1 – 5'-TTTGATTCAACTCTTGTTCTGT-3'; shARHGEF3-2 – TATATCTTGTCACACAGCTTGA-3'; shARGHEF3-3 – TATAGCTTCTTCCAAGTGCTGC-3'. 97-mer oligonucleotides were generated

as previously described (322) and amplified using the following primers: forward – 5'-

TACAATACTCGAGAAGGTATATTGCTGTTGACAGTGAGCG-3'; reverse –

ACTTAGAAGAATTCCGAGGCAGTAGGCA-3'. A non-targeting shRNA (shControl) sequence

was used as a control: 5'-TAGATAAGCATTATAATTCCTA-3'. Oligonucleotides were cloned

into the EcoRI and XhoI sites of pCDH-LMN-GFP and lentivirus was generated via calcium

phosphate transfection of HEK293T cells using the packaging and envelope plasmids psPAX2

and pCMV-VSVG. Viral supernatants were collected 48 hours after transfection and

concentrated using Lenti-X Concentrator (Clontech). Following lentiviral transduction, GFP

positive cells were sorted using a Sony SH800 instrument and subsequently expanded.

Flow cytometry

Flow cytometry was performed using a BD FACSVerse and data were analyzed using FlowJo

software.

Statistics

Statistical analyses were performed using Prism 8 (GraphPad). All tests were two-sided

and the threshold for significance was $p \leq 0.05$. Comparisons between groups were made using

t-tests, with one-way ANOVA and Tukey's method for multiple comparisons adjustment for

comparisons of three or more groups. For in vivo survival analysis, the log-rank test was used to

perform pairwise comparisons between survival curves. Interactions between drugs were

assessed using Bliss independence analysis (281). Error bars represent the standard error of

the mean.

Study Approval

Written informed consent for the use of diagnostic specimens for research was obtained

from patients or their guardians at the time of sample collection, according to the Declaration of

Helsinki, the National Cancer Institute, and institutional review boards of participating sites. All animal experiments were conducted following protocols that were approved by the Institutional Animal Care and Use Committees and Institutional Review Boards of Children's Hospital of Philadelphia or the University of California, San Francisco.

5.6: Acknowledgements

5.7: Figures

Figure 5-1: JAK/STAT inhibition overcomes DEX resistance in a subset of primary T-ALL samples and in the T-ALL cell line CCRF-CEM. (A) Viability relative to vehicle control of cells from 73 primary diagnostic T-ALL samples exposed to 2.5μM DEX for 48 hours in the presence of 25ng/mL IL7. The red line indicates the 50% viability cutoff used to define "DEX resistant". **(B)** Viability relative to vehicle control of cells from the 46 DEX resistant primary diagnostic T-ALL samples in (A) exposed to 2.5μM DEX and/or 0.5μM RUX for 48 hours in the presence of 25ng/mL IL7. Statistical significance was assessed using one-way ANOVA with Tukey's method for multiple comparisons adjustment. **(C)** Viability of CCRF-CEM cells exposed to DEX in the absence or presence of increasing concentrations of IL7 for 72 hours in technical triplicate. **(D)** Viability of CCRF-CEM cells exposed to DEX in the presence of 25ng/mL IL7 in the absence or presence of increasing concentrations of RUX in technical triplicate. The no IL7 (black line) and the 25ng/mL IL7 (red line) conditions are re-plotted from figure 5-1C. **(E)** Heatmap of Bliss independence scores calculated as the average of technical triplicates for the combination of DEX and RUX in CCRF-CEM cells cultured in the presence of 25ng/mL IL7 for 72 hours, in which positive values, indicated in red, are indicative of a synergistic interaction. All CCRF-CEM cell data are representative of three independent experiments. ****$p<0.0001$, ***$p<0.001$, **$p<0.01$, *$p<0.05$.
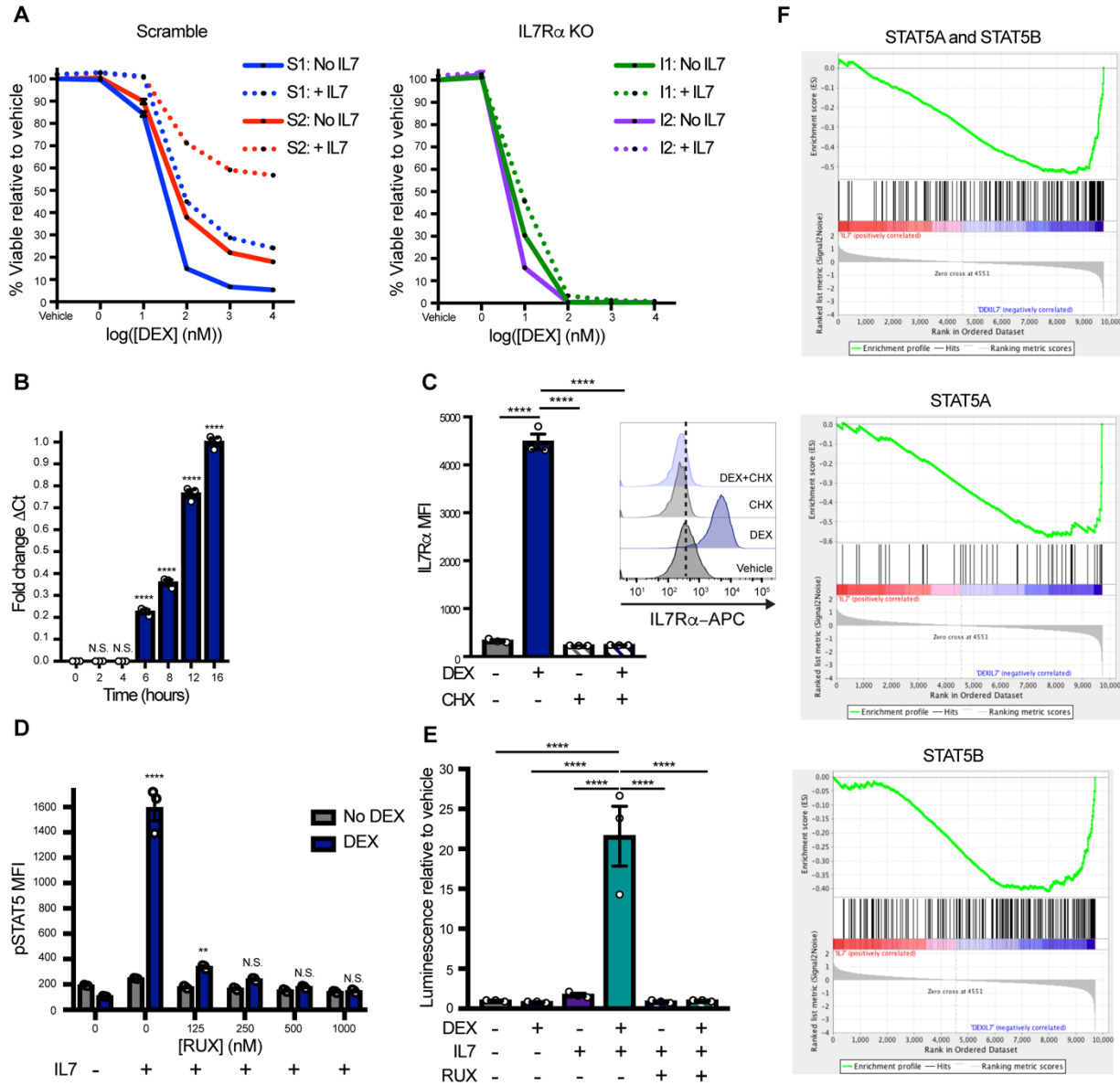
Figure 5-2: DEX exposure augments IL7R expression and downstream JAK/STAT signaling. (A) Viability of scramble control (S1 and S2; left) and IL7R KO (I1 and I2; right) CCRF-CEM cell clones exposed to DEX in the absence (solid lines) or presence (dotted lines) of 25ng/mL IL7 in technical triplicate for 72 hours. **(B)** Fold change relative to the 16 hour time point of the ΔCt of *IL7RA* transcript relative to *GAPDH* as determined by qPCR performed in technical triplicate in CCRF-CEM cells exposed to 1µM DEX and 100ng/mL IL7 for the indicated period of time. **(C)** MFI of IL7Rα in CCRF-CEM cells treated with or without 1µM DEX and/or 10µg/mL CHX in technical triplicate for 24 hours. Inset shows representative histograms of IL7Rα in CCRF-CEM cells treated with or without 1µM DEX and/or 10µg/mL CHX for 24 hours. **(D)** MFI of pSTAT5 in CCRF-CEM cells treated with or without 1µM DEX for 24 hours in the absence of IL7 followed by a one-hour exposure to vehicle control or RUX prior to a 15-minute stimulation with 100ng/mL IL7 in technical triplicate. Significance is relative to the DEX-treated condition in the absence of IL7 stimulation. **(E)** Relative luminescence of CCRF-CEM cells transfected with the STAT5 reporter construct and treated with or without 1µM DEX, 100ng/mL

IL7, and 500nM RUX in technical triplicate for 36 hours prior to lysis and measurement of luciferase activity. **(F)** GSEA plots of STAT5 gene expression signatures comparing scramble control clones (n=4) treated with 100ng/mL IL7 versus the combination of 1µM DEX and 100ng/mL IL7 for 16 hours. Statistical significance was assessed using one-way ANOVA with Tukey's method for multiple comparisons adjustment (B-E). With the exception of the RNA-seq experiment, all data are representative of three independent experiments. ****p<0.0001, ***p<0.001, **p<0.01, *p<0.05, N.S. – not significant.
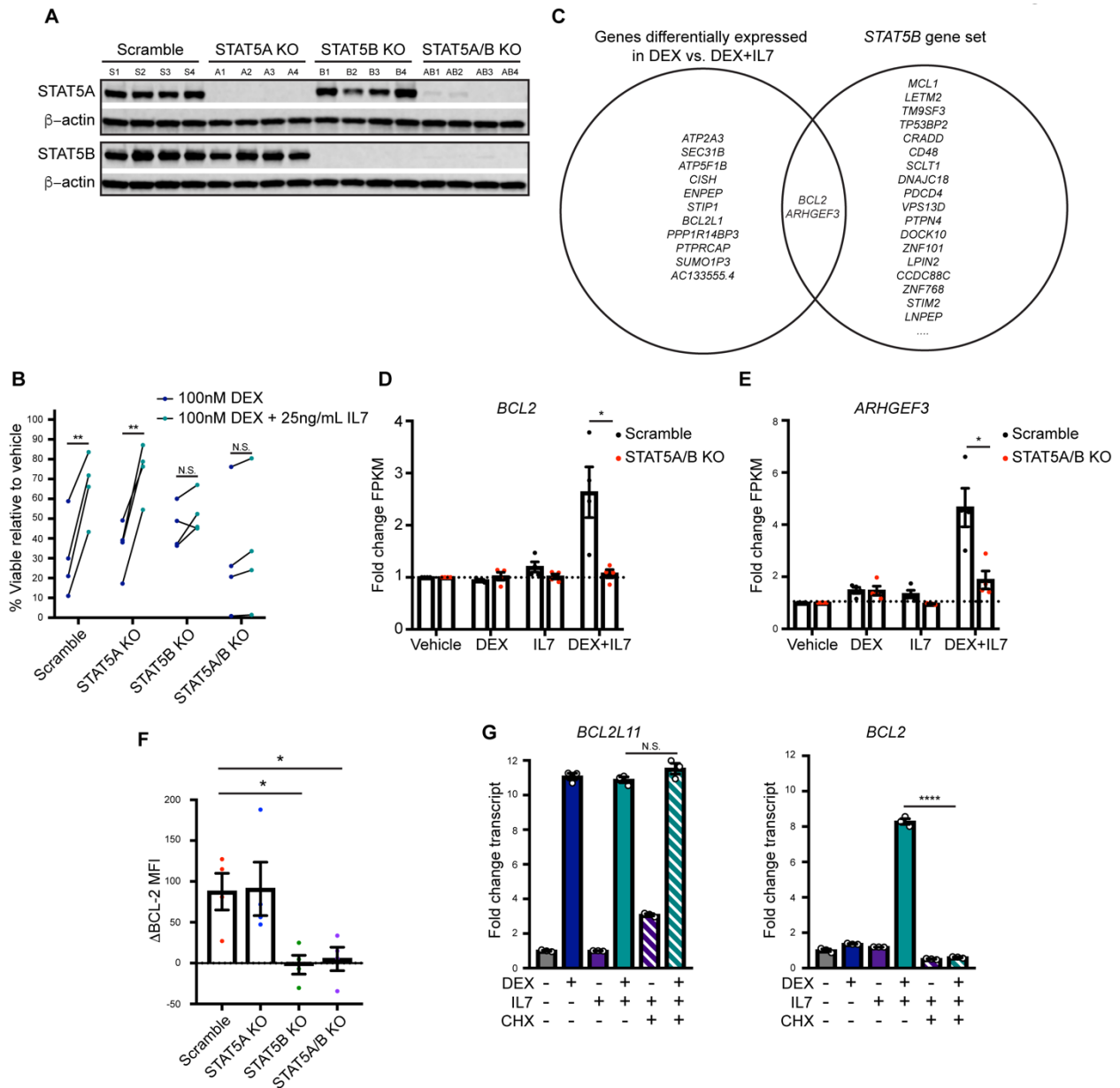
Figure 5-3: STAT5B, but not STAT5A, mediates the upregulation of BCL-2 expression in cells exposed to the combination of DEX and IL7. (A) Evaluation of STAT5A and STAT5B expression by Western blot in independent scramble control (S) and STAT5 single (A or B) and double (AB) KO CCRF-CEM cell clones (n=4 per genotype). **(B)** Viability of independent scramble control and STAT5 KO CCRF-CEM cell clones (n=4 per genotype) treated with 100nM DEX with or without 25ng/mL IL7 for 72 hours. **(C)** Venn diagram depicting the overlap between the top differentially expressed genes between scramble control CCRF-CEM cell clones (n=4) treated with DEX versus DEX+IL7 and *STAT5B* target genes. **(D-E)** Fold change in the FPKM values for **(D)** *BCL2* transcript and **(E)** *ARHGEF3* transcript as determined by RNA-seq analysis of scramble control (n=4) and STAT5A/B double KO (n=4) CCRF-CEM cell clones treated in the

absence or presence of 100ng/mL IL7 and/or 1µM DEX for 16 hours. **(F)** ∆MFI of BCL-2 protein expression in scramble control (n=4) and STAT5 KO (n=4) CCRF-CEM cell clones treated with 100ng/mL IL7 and 1µM DEX relative to 100ng/mL IL7 alone for 48 hours. **(G)** *BCL2L11* and *BCL2* transcript expression in CCRF-CEM cells cultured in the absence or presence of 1µM DEX, 100ng/mL IL7, and/or 10µg/mL CHX for 16 hours as determined by qPCR performed in technical triplicate. Statistical significance was assessed using a paired t-test (B), two-sample t-tests (D and E), or one-way ANOVA with Tukey's method for multiple comparisons adjustment (F and G). With the exception of the RNA-seq experiment, all data are representative of three independent experiments. ****$p < 0.0001$, ***$p < 0.001$, **$p < 0.01$, *$p < 0.05$, N.S. – not significant.
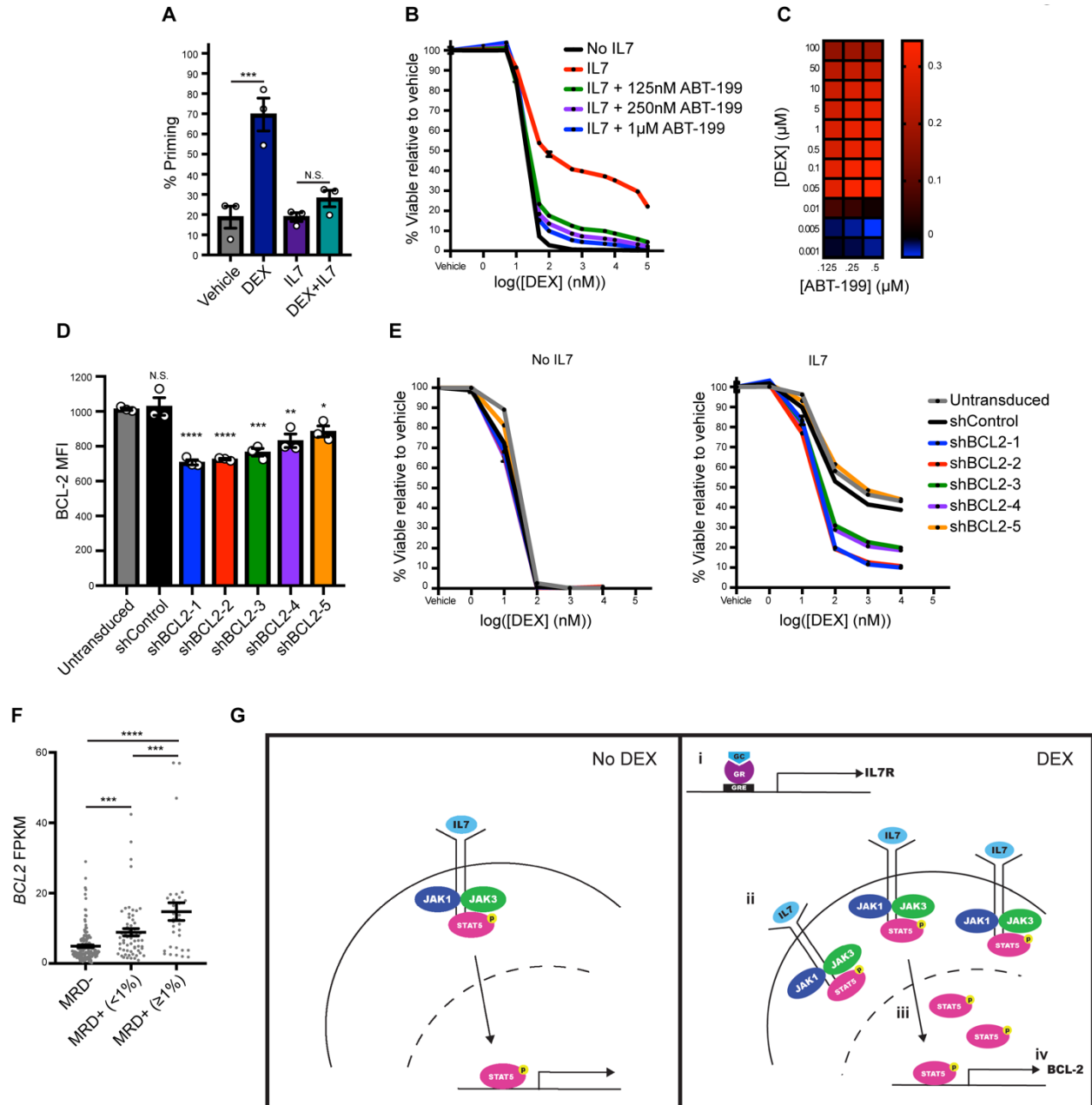
Figure 5-4: BCL-2 mediates IL7-induced DEX resistance. (A) Percent priming of CCRF-CEM cells treated in the absence or presence of 1μM DEX and/or 100ng/mL IL7 in technical triplicate for 16 hours followed by BH3 profiling with 0.5μM ABT-199 for 90 minutes. **(B)** Viability of CCRF-CEM cells treated with DEX in the absence or presence of 25ng/mL IL7 and increasing concentrations of ABT-199 for 72 hours in technical triplicate. The no IL7 (black line) and the 25ng/mL IL7 (red line) conditions are re-plotted from figure 5-1C. **(C)** Heatmap of Bliss independence scores calculated as the average of technical triplicates for the combination of DEX and ABT-199 in the presence of 25ng/mL IL7. **(D)** MFI of BCL-2 protein expression assessed in technical triplicate in untransduced CCRF-CEM cells and CCRF-CEM cells transduced with a non-targeting shRNA control (shControl) or a *BCL2*-targeting shRNA (shBCL2-1-5). Statistical significance is relative to the untransduced cells. **(E)** Viability of

untransduced or shRNA-transduced CCRF-CEM cells treated with DEX in the absence (left) or presence (right) of 25ng/mL IL7 in technical triplicate for 72 hours. **(F)** FPKM values for *BCL2* transcript obtained from published RNA-seq data from diagnostic samples from patients enrolled on COG AALL0434, stratified based on day 29 bone marrow MRD. **(G)** Schematic of the proposed model for the mechanism by which DEX paradoxically induces steroid resistance in T-ALL cells in the presence of IL7. In the presence of DEX (right), GR induces an increase in IL7R expression (i) leading to an increase in IL7R at the cell surface (ii). This in turn leads to an increase in STAT5 transcriptional activity (iii) that ultimately results in the upregulation of BCL-2 (iv). Statistical significance was assessed using one-way ANOVA with Tukey's method for multiple comparisons adjustment (A, D, and F). All CCRF-CEM cell data are representative of three independent experiments. ****$p<0.0001$, ***$p<0.001$, **$p<0.01$, *$p<0.05$, N.S. – not significant.
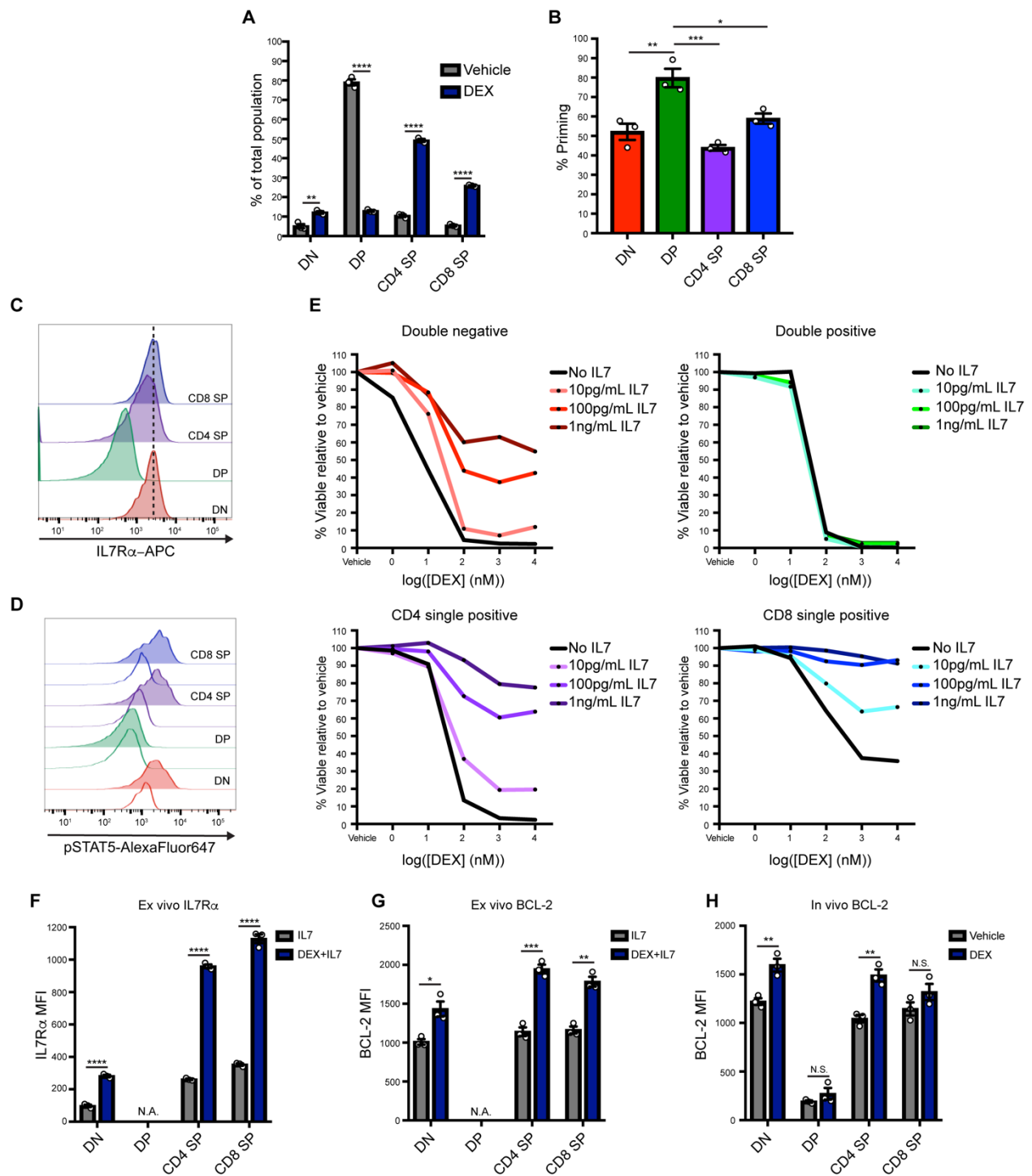
Figure 5-5: IL7 induces DEX resistance in subpopulations of normal developing thymocytes. (A) Percentage of thymocyte subpopulations in thymi isolated from mice treated with vehicle control (n=3) or DEX (n=3) at 2mg/kg/day for three days. **(B)** Percent priming of thymocytes in the basal state following BH3 profiling with 1μM synthetic BIM peptide in technical triplicate for 90 minutes. **(C)** Histograms of the basal expression of IL7Rα in the major murine

thymocyte subpopulations. **(D)** Histograms of pSTAT5 in the major murine thymocyte subpopulations in the basal state (unfilled histograms) and following a 15-minute stimulation with 100ng/mL IL7 (filled histograms). **(E)** Viability of murine thymocyte subpopulations following ex vivo treatment for 24 hours with DEX in the absence or presence of increasing concentrations of IL7. **(F)** MFI of IL7Rα in murine thymocytes treated ex vivo in the presence of 100pg/mL IL7 with or without 1µM DEX in technical triplicate for 24 hours. DP cells could not be analyzed due to lack of viable cells remaining after DEX exposure (not analyzed; N.A.). **(G)** MFI of BCL-2 in murine thymocytes treated ex vivo in the presence of 100pg/mL IL7 with or without 1µM DEX in technical triplicate for 24 hours. DP cells could not be analyzed due to lack of viable cells remaining after DEX exposure (N.A.). **(H)** MFI of BCL-2 in thymocytes isolated from mice treated with vehicle control (n=3) or DEX (n=3) at 2mg/kg/day for three days. Statistical significance was assessed using two-sample t-tests (A, F, G, and H) or one-way ANOVA with Tukey's method for multiple comparisons adjustment (B). All data are representative of three independent experiments. ****$p<0.0001$, ***$p<0.001$, **$p<0.01$, *$p<0.05$, N.S. – not significant.
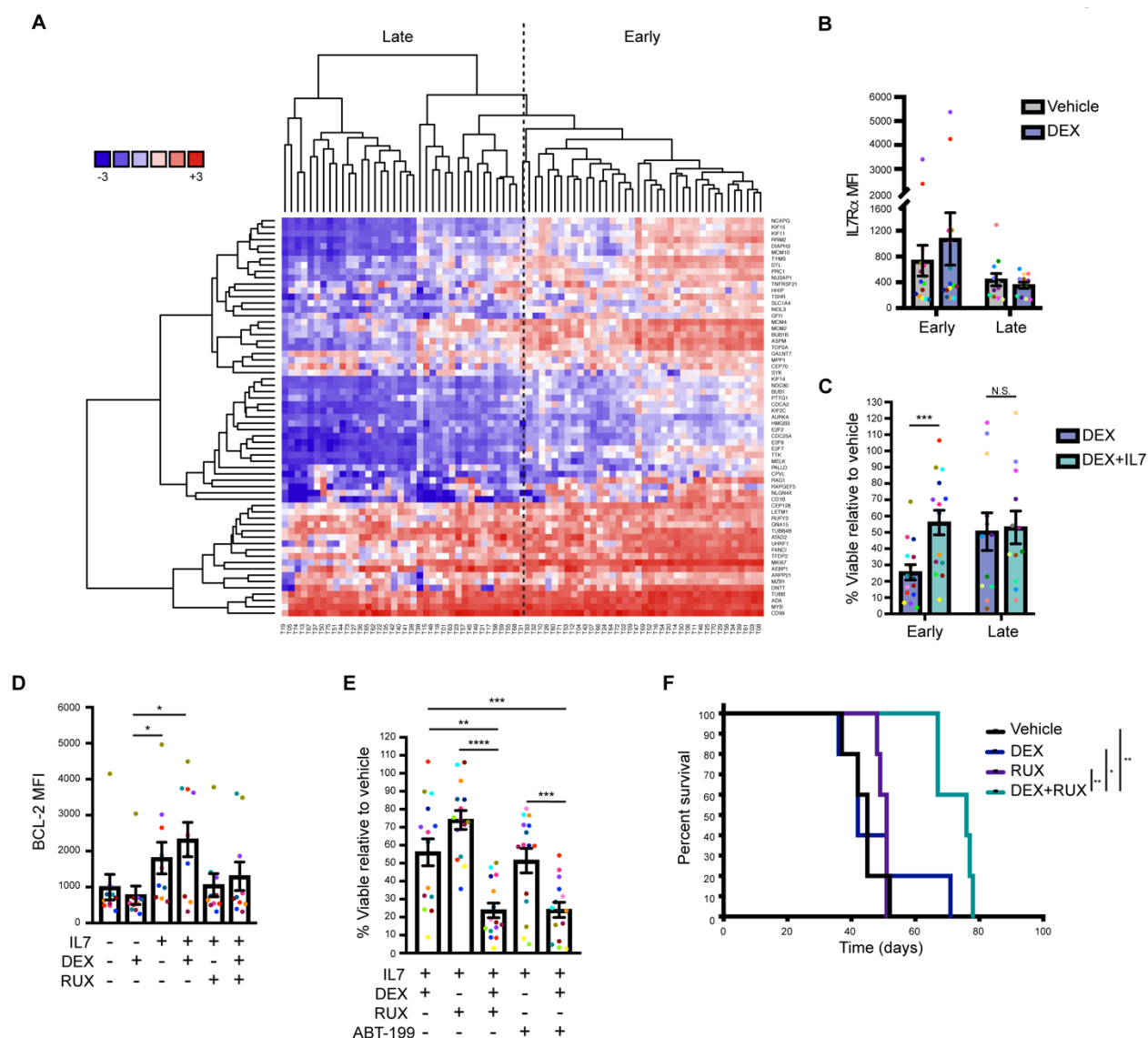
Figure 5-6: T-ALLs reflecting early stages of T-cell development demonstrate DEX resistance in the presence of IL7. (A) Heatmap depicting the clustering of 76 primary T-ALL samples by expression of genes that are upregulated in early developing thymocytes relative to later developing thymocytes. **(B)** MFI of cell surface IL7R in 15 early and 12 late T-ALL PDX samples following exposure to 1µM DEX for 24 hours in technical triplicate. **(C)** Viability relative to vehicle control of 15 early and 12 late T-ALL PDX samples treated with 1µM DEX in the absence or presence of 25ng/mL IL7 for 48 hours in technical triplicate. **(D)** MFI of BCL-2 protein expression in 10 early T-ALL PDX samples following exposure to 100ng/mL IL7 with or without 1µM DEX and 500nM RUX for 16 hours in technical triplicate. Some samples were not analyzed due to limitations in cell numbers. **(E)** Viability relative to vehicle control of 15 early T-ALL samples exposed to 25ng/mL IL7 with or without 1µM DEX and/or 500nM RUX or 1µM ABT-199 for 48 hours in technical triplicate. **(F)** Kaplan-Meier survival analysis of mice transplanted with early T-ALL T24 and treated with vehicle control (n=5), DEX (n=5), RUX (n=5), or the combination of DEX and RUX (n=5). Statistical significance was assessed using paired t-tests (B and C), one-way ANOVA with Tukey's method for multiple comparisons

114

adjustment (D and E), or a log-rank test (F). ****p<0.0001, ***p<0.001, **p<0.01, *p<0.05, N.S. – not significant.
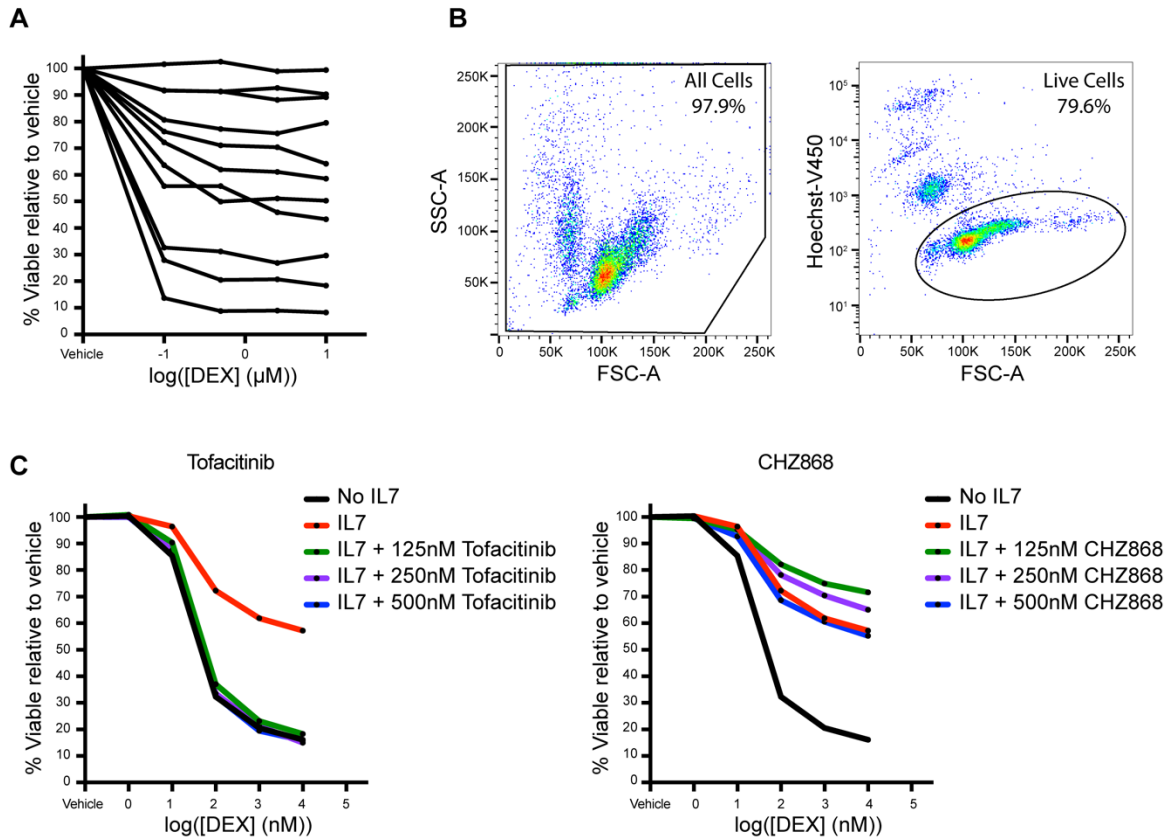
Supplemental Figure 5-1: JAK1 and JAK3 inhibition overcome IL7-induced DEX resistance in T-ALL cells. (A) Viability of 11 representative primary diagnostic T-ALL samples exposed to increasing concentrations of DEX for 48 hours in the presence of 25ng/mL IL7. **(B)** Gating strategy used to assess viability by Hoechst stain and flow cytometry in CCRF-CEM cells. **(C)** Viability of CCRF-CEM cells exposed to DEX in the presence of 25ng/mL IL7 in the absence or presence of increasing concentrations of tofacitinib (left) or CHZ868 (right) for 72 hours in technical triplicate. The data for the no IL7 (black line) and IL7 (red line) conditions on the left are re-plotted in the graph on the right. Viability data in (C) are representative of two independent experiments.

A

IL7Rα–APC

B

GR
β–actin

C

Cytoplasm   Nucleus

Vehicle DEX IL7 DEX+IL7   Vehicle DEX IL7 DEX+IL7

GR
p84
β–actin

GR pS211
p84
β–actin

D

Vehicle   DEX   DEX+IL7   Vehicle   DEX   DEX+IL7
1 2 3 4 1 2 3 4 1 2 3 4   1 2 3 4 1 2 3 4 1 2 3 4

-3   +3

E

Fold change FPKM

Vehicle   DEX   IL7   DEX+IL7

F

All Cells 89.6%

Single Cells 94.6%

Single Cells 96.6%

Cleaved Caspase 3 Negative 99.4%

G

1μM RUX+IL7
500nM RUX+IL7
250nM RUX+IL7
125nM RUX+IL7
IL7
Basal

pSTAT5-AlexaFluor647

H

Fold change MFI

N.S.   N.S.   N.S.

pSTAT1   pSTAT3   pSTAT6

☐ Basal - Unstimulated
▨ Vehicle - IL7 Stimulated
▧ DEX Treated - IL7 Stimulated

117

Supplemental Figure 5-2: The combination of IL7 and DEX augments the STAT5 transcriptional program. (A) Histograms of IL7Rα expression in scramble control (S1 and S2) and IL7Rα KO (I1 and I2) CCRF-CEM cell clones. **(B)** Evaluation of GR expression by Western blot in CCRF-CEM cells treated with or without 1μM DEX and/or 100ng/mL IL7 for 24 hours. **(C)** Evaluation of total and phosphorylated GR (pS211) expression by Western blot in cytoplasmic and nuclear protein fractions from CCRF-CEM cells treated with or without 100ng/mL IL7 for 15 minutes followed by vehicle control or 1μM DEX for one hour. An anti-β-actin antibody was used as a cytoplasmic loading control and an anti-p84 antibody was used as a nuclear loading control. **(D)** Heatmap of GR target genes as determined by RNA-seq in scramble control clones (n=4) treated with or without 1μM DEX and 100ng/mL IL7 for four hours. **(E)** Fold change in the fragments per kilobase million (FPKM) values of *IL7RA* transcript as determined by RNA-seq in four independent scramble control clones treated with or without 1μM DEX in the presence or absence of 100ng/mL IL7 for four hours. **(F)** Gating strategy used for measurement of intracellular proteins by flow cytometry in CCRF-CEM cells. **(G)** Representative histograms of pSTAT5 in CCRF-CEM cells treated with 1μM DEX in the absence of IL7 for 24 hours followed by a one-hour exposure to vehicle control or increasing concentrations of RUX prior to a 15-minute stimulation with 100ng/mL IL7. **(H)** Fold change in the MFI of pSTAT1, pSTAT3, or pSTAT6 following a 15 minute stimulation with 100ng/mL IL7 in CCRF-CEM cells cultured in vehicle control or 1μM DEX in technical triplicate for 24 hours. Statistical significance was assessed using one-way ANOVA with Tukey's method for multiple comparisons adjustment. With the exception of the RNA-seq experiment, all data are representative of three independent experiments.
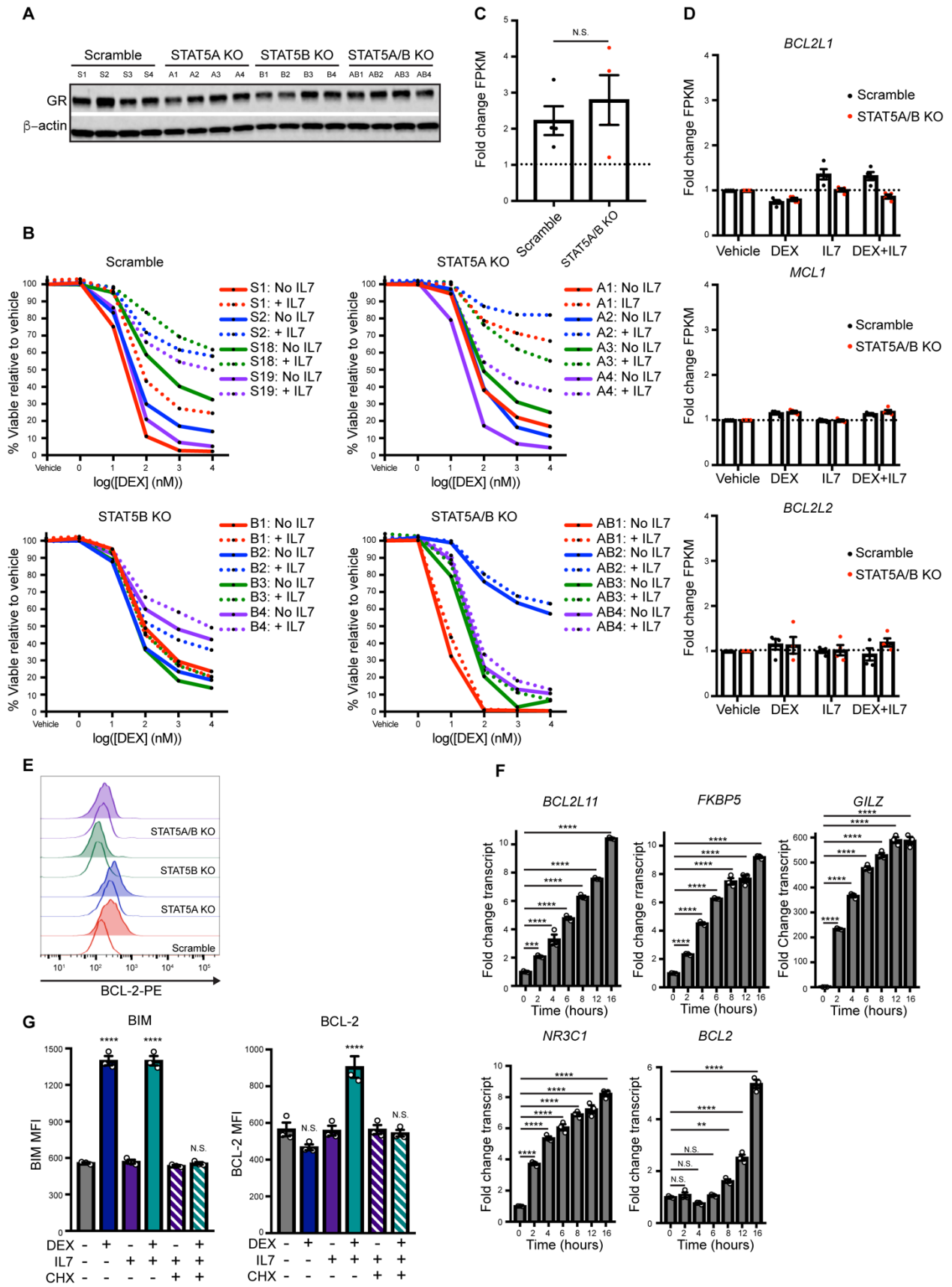
Supplemental Figure 5-3: *BCL2* is a STAT5 target gene that is enriched in cells treated with DEX and IL7 relative to IL7 alone. (A) Evaluation of GR expression by Western blot in scramble control and STAT5 KO CCRF-CEM cell clones (n=4 per genotype). **(B)** Viability of scramble control and STAT5 KO CCRF-CEM cell clones (n=4 per genotype) treated with DEX without (solid lines) or with (dotted lines) 25ng/mL IL7 for 72 hours. **(C)** Fold change in the FPKM for *IL7RA* in scramble control (n=4) and STAT5A/B KO (n=4) CCRF-CEM cell clones following exposure to 1μM DEX for four hours relative to vehicle control. **(D)** Fold change in the FPKM for *BCL2L1, MCL1,* and *BCL2L2* transcripts as determined by RNA-seq analysis of scramble control (n=4) and STAT5A/B double KO (n=4) CCRF-CEM cell clones treated in the absence or presence of 100ng/mL IL7 and/or 1μM DEX for 16 hours. **(E)** Histograms of BCL-2 protein expression in a representative clone from each group treated with 100ng/mL IL7 in the absence (unfilled histograms) versus presence (filled histograms) of 1μM DEX for 48 hours. **(F)** Fold change in transcript expression of four known primary GR target genes and *BCL2* following exposure to 1μM DEX and 100ng/mL IL7 for various time points relative to cells exposed to vehicle control as determined by qPCR performed in technical triplicate. **(G)** MFI of BIM and BCL-2 protein expression performed in technical triplicate in CCRF-CEM cells exposed to vehicle control or 1μM DEX with or without 100ng/mL IL7 in the absence or presence of 10μg/mL CHX for 24 hours. Significance is relative to the vehicle control condition. Statistical significance was assessed using a two-sample t-test (C) or one-way ANOVA with Tukey's method for multiple comparisons adjustment (F and G). With the exception of the RNA-seq experiment, all data are representative of three independent experiments. ****$p<0.0001$, ***$p<0.001$, **$p<0.01$, *$p<0.05$, N.S. – not significant.
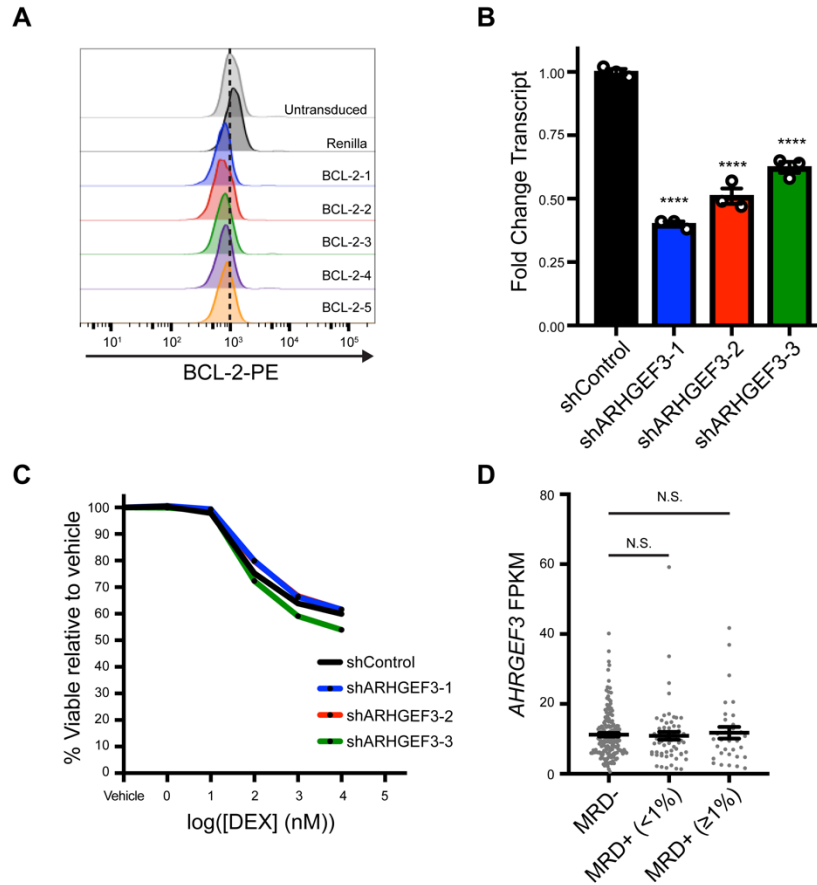
Supplemental Figure 5-4: *ARHGEF3* **is not a mediator of IL7-induced DEX resistance. (A)** Representative histograms of BCL-2 protein expression in untransduced CCRF-CEM cells and CCRF-CEM cells transduced with a non-targeting shRNA control (shControl) or a *BCL2*-targeting shRNA (shBCL2-1-5). **(B)** Fold change in the transcript expression of *ARHGEF3* in CCRF-CEM cells transduced with shControl or an *ARHGEF3*-targeting shRNA (shARHGEF3-1-3). **(C)** Viability of shRNA-transduced CCRF-CEM cells treated with DEX in the presence of 25ng/mL IL7 in technical triplicate for 72 hours. **(D)** FPKM values for *ARHGEF3* transcript obtained from published RNA-seq data from diagnostic samples from patients enrolled on COG AALL0434, stratified based on day 29 bone marrow MRD. Statistical significance was assessed using one-way ANOVA with Tukey's method for multiple comparisons adjustment (B and D). All CCRF-CEM cell data are representative of three independent experiments. ****$p<0.0001$, ***$p<0.001$, **$p<0.01$, *$p<0.05$, N.S. – not significant.
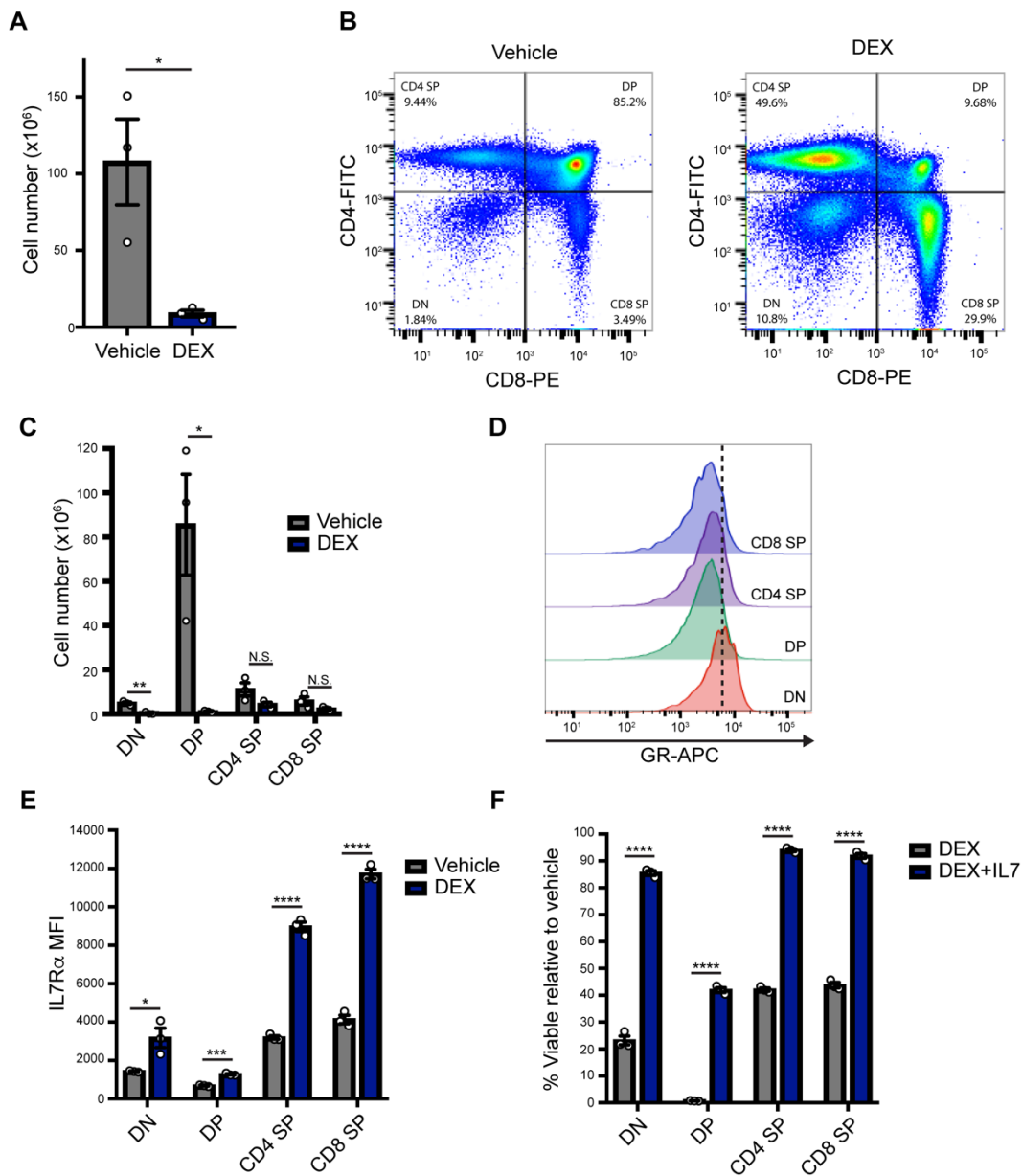
Supplemental Figure 5-5: DN and SP thymocytes demonstrate IL7-induced DEX resistance. (A) Absolute number of thymocytes in thymi isolated from mice treated with vehicle control (n=3) or DEX (n=3) at 2mg/kg/day for three days. **(B)** Representative FACS plots demonstrating the distribution of the major thymocyte subpopulations in thymi isolated from mice treated with vehicle control or DEX at 2mg/kg/day for three days. **(C)** Absolute number of thymocytes in each of the major thymocyte subpopulations in thymi isolated from mice treated with vehicle control (n=3) or DEX (n=3) at 2mg/kg/day for three days. **(D)** Histograms of the basal expression of GR in the major murine thymocyte subpopulations. **(E)** MFI of IL7R in human thymocytes treated ex vivo in the presence or absence of 1μM DEX in technical triplicate for 24 hours. **(F)** Viability of human thymocytes treated ex vivo with 1μM DEX with or without 25ng/mL IL7 in technical triplicate for 24 hours. Statistical significance was assessed using two-sample t-tests (A, C, E, and F). All murine thymocyte data are representative of three

independent experiments. All human thymocyte data are representative of two independent experiments. ****p<0.0001, ***p<0.001, **p<0.01, *p<0.05.
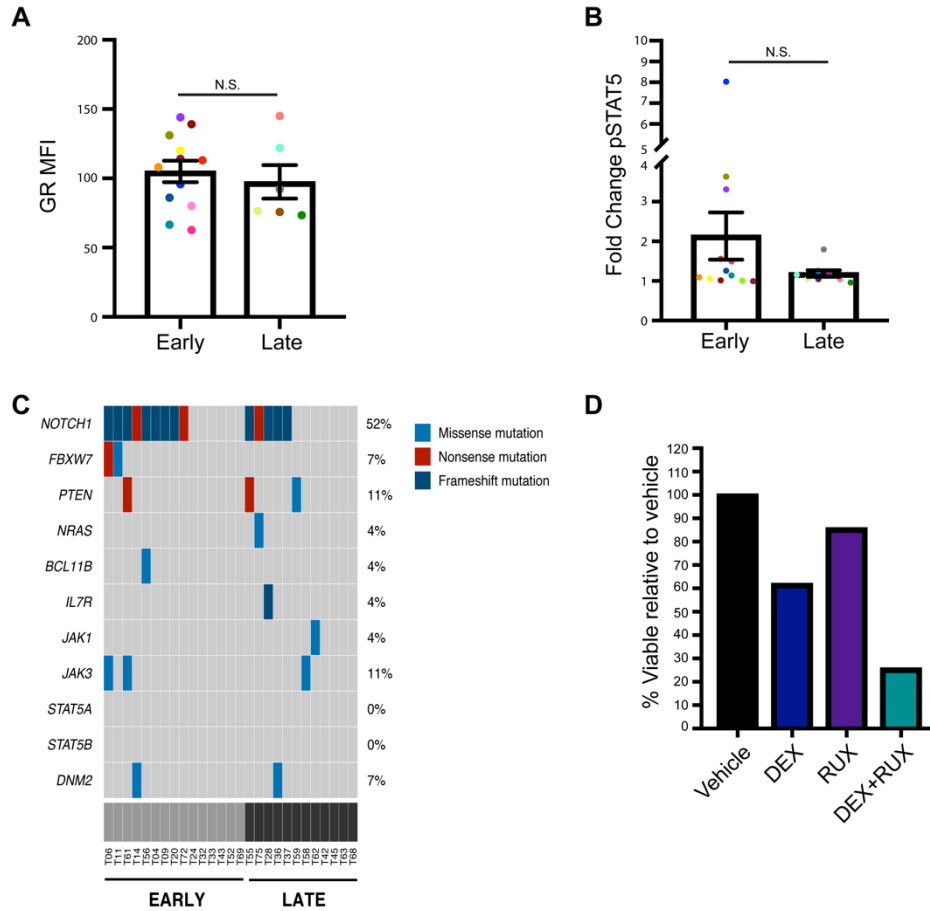
Supplemental Figure 5-6: IL7R/JAK/STAT pathway mutations are not enriched in early versus late T-ALLs. (A) MFI of GR protein in 12 early and 6 late T-ALLs. Some samples were not analyzed due to limitations in cell number. Statistical significance was analyzed using a two-sample t-test. **B)** MFI of pSTAT5 in 12 early and 9 late T-ALL PDX samples following stimulation with 100ng/mL IL7 for 15 minutes in technical triplicate. Some samples were not analyzed due to limitations in cell number. **(C)** Oncoplot depicting the occurrence of mutations in genes previously implicated in T-ALL in 15 early and 12 late T-ALL PDX samples. **(D)** Viability relative to vehicle control of cells from T-ALL T24 exposed to 25ng/mL IL7 with or without 1μM DEX and/or 500nM RUX in vitro for 48 hours. N.S. – not significant.

5.8: Bridge to Chapters 6, 7, and 8

Chapter 5 presents studies that defined the mechanistic basis for cytokine-induced DEX resistance in T-ALL. Using both genetic and pharmacologic approaches, we demonstrated that activation of STAT5 downstream of cytokine receptor signaling promotes the upregulation of anti-apoptotic proteins. These proteins alter the apoptotic potential of the cell, thereby rendering it refractory to DEX-induced apoptosis. Inhibition of JAK/STAT signaling with RUX is sufficient to restore this apoptotic potential, underscoring the synergy observed upon combined treatment with DEX and RUX in the presence of cytokine. The studies described in Chapters 6, 7, and 8 serve as logical extensions of this work and in many instances provide further validation and extended generalizability of these initial findings.

Chapter 6 describes the derivation of a novel genetic classifier with prognostic relevance in pediatric T-ALL. Specifically, it establishes the feasibility of utilizing gene expression profiling as a biomarker for response to induction chemotherapy, which relies heavily on the use of GCs. Intriguingly, through entirely orthogonal methods, this study confirmed the findings in Chapter 5 regarding the relationship between GC response and the underlying developmental origins of T-ALL. Application of this novel genetic classifier to both an experimental and validation cohort revealed that T-ALLs of the early T-cell precursor (ETP) subset, reflecting an early stage of T-cell development, have a distinct pattern of gene expression and are highly enriched for poor responses to induction chemotherapy. While most of the non-ETP samples demonstrated a gene expression pattern that was nearly the perfect inverse of the ETP gene expression pattern, a subset showed striking resemblance to the ETP samples and were highly enriched for the presence of minimal residual disease at the end of induction. These data demonstrate that developmental origins profoundly influence response to induction chemotherapy and suggest that immunophenotypic analysis of T-ALL is insufficient to appreciate this developmental heterogeneity.

A key finding of the studies in Chapter 5 relates to the requirement for DEX-induced upregulation of IL7R as a central component of this drug resistance mechanism. While this study utilized the FDA-approved JAK1/2 inhibitor RUX to establish the therapeutic feasibility of overcoming IL7-induced DEX resistance by targeting activation of the IL7R/JAK/STAT5 axis, Chapter 7 describes an entirely distinct therapeutic approach inspired specifically by this key component of the mechanism. Newly synthesized IL7R reaches the cell surface via trafficking through the cellular secretory pathway. In Chapter 7, we tested the feasibility of inhibiting the secretory pathway as a means of preventing localization of IL7R to the cell surface. A key mediator of trafficking through this pathway is the Sec61 translocon, which facilitates entry of nascent peptides corresponding to cell surface or secreted proteins into the endoplasmic reticulum. Using a novel inhibitor of the Sec61 translocon called KZR-508445, we demonstrated that Sec61 inhibition effectively attenuates the DEX-induced increase in cell surface IL7R expression and overcomes IL7-induced DEX resistance to the same degree as RUX, thereby establishing the feasibility of this alternative therapeutic approach to target this drug resistance mechanism.

Finally, Chapter 8 represents a thematic extension of these findings in T-ALL as applied to a distinct disease entity known as hemophagocytic lymphohistiocytosis (HLH). HLH shares many key features with T-ALL, including a central role for T-cells in the disease process, the prevalence of common gamma chain cytokines, including IL7, and the use of DEX as a key component of therapy. We hypothesized that, as observed in T-ALL, cytokines may mediate DEX resistance in T-cells, and that this could be mitigated upon combined exposure with RUX. Indeed, we demonstrated that cytokines potently mediate DEX resistance in CD8 T-cells, and analogous to our work in T-ALL, do so via modulation of the cellular apoptotic potential. Using both *in vivo* and *ex vivo* model systems, we provide preclinical data in favor of combining DEX and RUX as a means of improving clinical outcomes for patients with HLH.

Chapter 6: Post-Induction Minimal Residual Disease is Associated with an Early T-Cell

Precursor (ETP)-Like Gene Expression Signature in T-ALL

6.1: Abstract

T-cell acute lymphoblastic leukemia (T-ALL) is a malignancy that arises following the acquisition of mutations and developmental arrest in early developing T-cells. Due to the significant heterogeneity of this disease, there are currently no established molecular or cytogenetic biomarkers with prognostic significance, impeding efforts to implement risk-adapted therapeutic approaches. We integrated RNA-sequencing and clinical outcome data from 233 pediatric T-ALL patients who were enrolled on the Children's Oncology Group (COG) clinical trials AALL0434 and AALL1231 to evaluate the prognostic utility of gene expression profiling in pediatric T-ALL. We demonstrated that patterns of gene expression at the time of disease diagnosis are predictive of minimal residual disease (MRD) at the end of the induction phase of therapy. Using a regression-based approach, we identified a novel genetic classifier containing 119 genes that is sufficient to retain the value of gene expression profiling for MRD prediction. Consistent with previous findings, T-ALLs with the early T-cell precursor (ETP) immunophenotype were almost uniformly MRD+. Intriguingly, we found that non-ETP T-ALLs that are MRD+ have gene expression signatures that closely resemble those of ETP T-ALLs despite having distinct immunophenotypic features. Furthermore, *ex vivo* drug sensitivity profiling of non-ETP T-ALLs revealed that MRD+ samples were more resistant to the glucocorticoid dexamethasone, a central component of induction chemotherapy for T-ALL. Taken together, these data demonstrate the prognostic significance of gene expression profiling in T-ALL and establish the feasibility of using a targeted gene expression profile to predict post-induction MRD status at disease diagnosis.

6.2: Introduction

Survival rates for patients with relapsed or refractory T-cell acute lymphoblastic leukemia (T-ALL) remain at less than 10% (284) and there are currently no effective salvage therapies

available for these patients. As a result, the primary goal of T-ALL therapy is to optimize the efficacy of frontline agents in order to decrease the likelihood of future relapse. Furthermore, unlike B-cell ALL (B-ALL) where numerous molecular and cytogenetic features carry known prognostic significance and can be used for risk stratification (28), such biomarkers do not exist for T-ALL (282). These data suggest that efforts to reduce the incidence of relapsed T-ALL will depend on an improved ability to accurately risk stratify patients to enable appropriate and early interventions in patients at risk for poor treatment responses.

In the absence of molecular or cytogenetic biomarkers, minimal residual disease (MRD) at the end of induction, the first month of therapy, has historically been the most important prognostic factor. On the Children's Oncology Group (COG) trial AALL0434, patients with overt induction failure, defined as having >25% leukemic blasts in the bone marrow at the end of induction, had a disease free survival of only 54.8%, compared to 84.3% for the entire cohort (323). At the opposite extreme, on the European AIEOP-BFM-ALL 2000 trial, MRD negativity at the end of the first month of therapy was the most favorable prognostic factor (324). While these data highlight the prognostic significance of post-induction MRD, it is important to note that the use of MRD for risk stratification does not allow for risk-adapted modifications to therapy during induction, where they may effectively induce deeper remissions and decrease the likelihood of future relapse.

While there are no validated molecular or cytogenetic predictors of outcome for pediatric T-ALL, key cellular processes, such as transcriptional regulation and signal transduction, are commonly dysregulated in T-ALL despite underlying genetic diversity (177). We therefore hypothesized that genetically diverse T-ALLs may converge upon a smaller number of gene expression patterns that underlie the dysregulation of these key processes, and that these gene expression patterns may in turn have prognostic significance. Here, we demonstrate that gene expression profiling of diagnostic T-ALL samples effectively predicts post-induction MRD status. The early T-cell precursor (ETP) subset of T-ALLs, defined by distinct immunophenotypic

characteristics, is known to demonstrate poor responses to lymphoid-directed therapies, including glucocorticoids (GCs), which are prevalent during induction, resulting in high rates of post-induction MRD positivity in this subset (325). Intriguingly, we demonstrate that non-ETP T-ALLs that are MRD positive but immunophenotypically indistinct from other non-ETP T-ALLs have an ETP-like gene expression signature. These data demonstrate the feasibility of utilizing gene expression profiling for prognostic purposes at disease diagnosis and suggest that the underlying developmental features of T-ALL cells are key drivers of the response to induction chemotherapy.

6.3: Results

Unbiased hierarchical clustering distinguishes MRD+ and MRD- T-ALLs

In an initial analysis to determine whether there are recurrent gene expression patterns within pediatric T-ALL that may in turn have prognostic utility, we utilized published RNA-sequencing (RNA-seq) data obtained from diagnostic samples from 189 patients with T-ALL enrolled on COG AALL0434 (177). Unbiased hierarchical clustering of these data produced two primary clusters of samples characterized by distinct patterns of gene expression (Figure 6-1A). It has previously been shown that ETP T-ALL is associated with a gene expression pattern that is distinct from that of non-ETP T-ALL (325). Consistent with these data, our hierarchical clustering demonstrated that all of the ETP T-ALLs clustered together in cluster 1, while the near-ETP and non-ETP T-ALLs were dispersed between cluster 1 and cluster 2 (Figure 6-1A). On COG AALL0434, as with previous cohorts (326), patients with ETP T-ALL were commonly MRD+ at the end of induction (323) (Supplemental Figure 6-1). Interestingly, when we looked at the distribution of MRD+ and MRD- non-ETP T-ALLs, we found that 54% of the non-ETP T-ALLs that clustered with the ETP T-ALLs in cluster 1 were MRD+, as opposed to only 16% of the non-ETP T-ALLs in cluster 2 (Figure 6-1B).

The expression pattern of 119 genes is sufficient to retain the prognostic significance of gene expression profiling

While this hierarchical clustering analysis demonstrates the potential for utilizing gene expression profiling for prognostic purposes, there are significant barriers to the clinical implementation of diagnostic tests that rely on whole transcriptome analyses. To determine whether a smaller number of genes may be sufficient to predict post-induction MRD status, we utilized a regression-based approach with leave-one-out cross-validation to distill the T-ALL transcriptome down to 119 genes that retained the predictive value of the whole transcriptome analysis. Using the genes within this signature, we derived a sample score metric, calculated based on the weighted contribution of each of the 119 genes to the prediction of MRD status. These sample scores were scaled from 0 to 100, and each sample was subsequently assigned a sample score, with a score of 0 corresponding to the lowest risk of being MRD+ and a score of 100 corresponding to the highest risk.

We then assessed the distribution of samples scores across the samples in the AALL0434 cohort. Consistent with the finding that ETP T-ALLs were largely MRD+, we found that this subset was associated with high sample scores and a uniform pattern of expression of the 119 genes in the signature. In contrast, the majority of non-ETP T-ALLs had an inverse gene expression pattern relative to the ETP T-ALLs and tended to have lower sample scores, consistent with lower rates of MRD positivity. However, similar to the initial whole transcriptome analysis, those non-ETP T-ALLs with high sample scores had a gene expression pattern that was identical to that of the ETP T-ALLs (Figure 6-2A-B). Finally, to determine if the sample score metric derived from this 119-gene signature has prognostic value for predicting MRD status in the non-ETP T-ALL subset, we examined the frequency of MRD positivity in samples across the entire sample score distribution. This analysis revealed that increasing sample scores are associated with higher rates of MRD positivity (Figure 6-2C). Taken together, this analysis demonstrates that the expression pattern of 119 genes is sufficient to identify non-ETP

T-ALLs that appear ETP-like at a transcriptional level and that are enriched for being MRD+ at the end of induction.

BCL2 expression is associated with developmental stage and MRD status

Glucocorticoids (GCs) are a central component of induction chemotherapy for T-ALL, and a poor clinical response to GC therapy is thought to be an important driver of post-induction MRD positivity (31). We previously demonstrated that the anti-apoptotic protein BCL-2 is a key driver of intrinsic GC resistance in diagnostic T-ALL samples (254). Furthermore, we and others (327) have demonstrated that BCL-2 expression changes as a function of early T-cell development, with the earliest thymocytes expressing high levels of BCL-2, owing to cytokine-mediated pro-survival signaling. This pro-survival signal is then inhibited at later stages of development, resulting in a reduction in BCL-2 expression (4). We therefore hypothesized that *BCL2* expression may correlate with MRD status in the AALL0434 cohort. Consistent with the pattern of expression in normal thymocyte development, we found that ETP T-ALLs had significantly higher *BCL2* expression relative to the near-ETP and non-ETP samples (Figure 6-3A). Interestingly, when we separated the non-ETP T-ALL samples by MRD status, we found that the MRD+ non-ETP T-ALLs, which transcriptionally resemble ETP T-ALLs, had significantly higher *BCL2* expression (Figure 6-3B).

High sample scores and an ETP-like gene expression pattern are associated with in vitro *GC resistance.*

To further validate the prognostic utility of this 119-gene signature and associated sample score metric, we applied this model to an independent validation cohort of 44 diagnostic samples from patients enrolled on COG AALL1231 for which RNA-seq data were previously generated (254). This analysis revealed the same gene expression pattern amongst the ETP samples as was observed in the AALL0434 cohort. Similarly, we found that the ETP T-ALLs had

consistently high sample scores. Additionally, we validated the finding that a subset of non-ETP

T-ALLs have an ETP-like gene expression signature, high sample scores, and are enriched for

being MRD+ (Figure 6-4A). Given that MRD positivity is thought to primarily reflect GC

resistance, we asked whether our sample score metric correlates with *in vitro* sensitivity to the

GC dexamethasone (DEX). In an analysis of 28 samples from AALL1231, we found a

statistically significant correlation between sample score and *in vitro* DEX responses, with a high

sample score predicting relative DEX resistance (Figure 6-4B). These data are consistent with

GCs being an important driver of post-induction MRD and suggest that this 119-gene signature

may be used to identify GC resistant T-ALLs.

6.4: Discussion

The considerable molecular and cytogenetic heterogeneity of T-ALL (282) poses

significant challenges to the introduction of risk-adapted therapies, which will be necessary to

improve clinical outcomes in patients at risk for disease relapse. Historically, MRD has been one

of the most important prognostic factors for predicting long-term outcomes in T-ALL. However, a

significant limitation to the use of MRD as a biomarker is that this information is not available

until patients have completed the first month of therapy, precluding the ability to modify therapy

in a risk-adapted manner during induction.

To address this problem, we asked whether gene expression profiling performed on

diagnostic T-ALL samples may have similar prognostic utility to MRD. We demonstrated using

whole-transcriptome analysis that diagnostic samples from patients later found to be MRD+

clustered separately from those found to be MRD-. Specifically, non-ETP T-ALLs from MRD+

patients clustered more closely with ETP T-ALLs, which are highly enriched for being MRD+.

We went on to demonstrate that knowing the expression status of only 119 genes is sufficient to

retain the predictive value of gene expression profiling. By developing a sample score metric

derived from the expression of this 119-gene signature, we demonstrated that MRD+ samples

have higher sample scores than MRD- samples. While non-ETP T-ALLs on average had lower

sample scores than the ETP T-ALLs, MRD+ non-ETP T-ALLs had higher sample scores, higher

BCL2 expression, and a gene expression pattern identical to that of ETP T-ALLs. Finally, we

validated the prognostic utility of this gene expression signature in an independent cohort of

patients enrolled on COG AALL1231, where we integrated this analysis with *ex vivo* drug

sensitivity profiling to demonstrate that resistance to GCs is associated with high sample scores,

and therefore with higher rates of MRD positivity.

Taken together, these data demonstrate that gene expression profiling is a powerful tool

both for predicting the response to induction chemotherapy and for providing additional insights

into the underlying biology of T-ALL. One of the most intriguing findings from this analysis

relates to the gene expression similarities between ETP T-ALLs and MRD+ non-ETP T-ALLs,

which are immunophenotypically-defined subsets. MRD positivity has been shown to reflect

intrinsic resistance to GC therapy (31), a central component of induction regimens for T-ALL. In

addition to their therapeutic applications, GCs are unique in that they are also endogenous

hormones that play crucial roles in shaping lymphoid cell development. Consistent with this,

sensitivity to GC-induced apoptosis is known to vary as a function of normal thymocyte

development, with early thymocytes demonstrating a high degree of GC resistance owing to

strong pro-survival signals that antagonize the pro-apoptotic effects of GCs. In contrast,

thymocytes at later stages of development are exquisitely sensitive to GCs, a feature that

facilitates the appropriate deletion of thymocytes with non-functional T-cell receptor (TCR)

rearrangements, ensuring the maturation of only functional and non-autoreactive T-cells (300).

We previously demonstrated that this pattern of GC sensitivity across thymocyte development is

retained in T-ALL (254). The present study provides independent validation of these findings, as

it demonstrates that ETP T-ALLs, as well as non-ETP T-ALLs with gene expression signatures

that resemble developmentally early T-ALLs, are enriched for being MRD+, a surrogate for GC

resistance (31). This suggests that in addition to its prognostic utility, gene expression profiling and analysis of developmentally-associated gene expression patterns may identify candidate therapeutic targets for enhancing drug responses in patients who are likely to be MRD+. One such potential target is *BCL2*, which we show here to be elevated in ETP T-ALLs and MRD+ non-ETP T-ALLs. Indeed, *in vitro* analysis demonstrates that targeting *BCL2* is sufficient to overcome GC resistance in T-ALLs resembling earlier developing thymocytes (254), and the findings presented here provide rationale for further investigation of this therapeutic strategy.

Importantly, this study demonstrates that the expression pattern of a relatively small number of genes is sufficient to distinguish T-ALL samples on the basis of their developmental origins and future MRD status. This approach is therefore readily translatable to a clinically tractable targeted gene expression assay. A similar approach has demonstrated feasibility in the context of pediatric Philadelphia-chromosome like (Ph-like) ALL. Specifically, the unique Ph-like gene expression signature was used to define a genetic classifier to identify Ph-like ALL, resulting in the development of a targeted gene expression assay known as the LDA card, which was effectively incorporated into clinical practice for patients enrolled on COG AALL1131 (328). This demonstrates the feasibility of direct clinical translation of a targeted gene expression assay for pediatric T-ALL.

Taken together, this study provides strong rationale for the further development and clinical translation of a targeted gene expression-based assay as a potential alternative to post-induction MRD. We believe that such an assay has the potential to improve risk stratification and enable the implementation of a precision medicine approach to treating pediatric T-ALL.

6.5: Methods

RNA-sequencing

This analysis utilized previously published RNA-seq data from patients enrolled on COG AALL0434 (177) and COG AALL1231 (254).

Development of the 119-gene signature

The 119-gene signature was derived from the whole-transcriptome analysis of the AALL0434 cohort using a regression-based approach with leave-one-out cross validation to identify a gene signature required for optimal distinction between MRD+ and MRD- samples.

In vitro *drug sensitivity profiling*

Fresh diagnostic T-ALL samples were obtained from patients enrolled on COG AALL1231. Written informed consent for the use of diagnostic specimens for research was obtained from patients or their guardians at the time of sample collection, according to the Declaration of Helsinki, the National Cancer Institute, and institutional review boards of participating sites. Cells were cultured in the presence of 25ng/mL recombinant human interleukin-7 (Peprotech) and treated with vehicle control or 2.5μM DEX for 48 hours. Cells were then stained with Hoechst 33258 (Molecular Probes) and analyzed by flow cytometry performed using a BD FACSVerse. Data were analyzed using FlowJo software.

Statistical Analysis

Statistical analyses were performed using Prism 8 (GraphPad). All tests were two-sided and the threshold for significance was $p \leq 0.05$. Error bars represent the standard deviation.

6.6: Acknowledgements
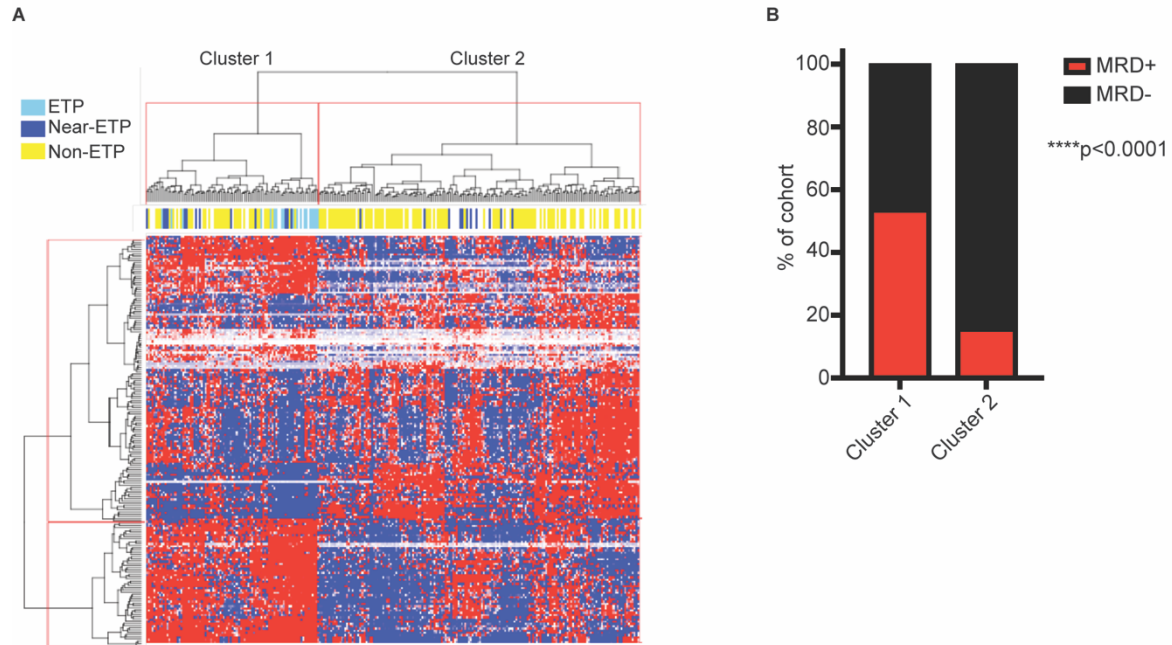
Figure 6-1: MRD+ non-ETP T-ALLs cluster with ETP T-ALLs. (A) Heatmap depicting the gene expression patterns of 189 diagnostic samples from the AALL0434 cohort following unbiased hierarchical clustering. **(B)** Distribution of MRD+ and MRD- non-ETP T-ALL samples between cluster 1 and cluster 2. Statistical significance was assessed using Fisher's exact test.
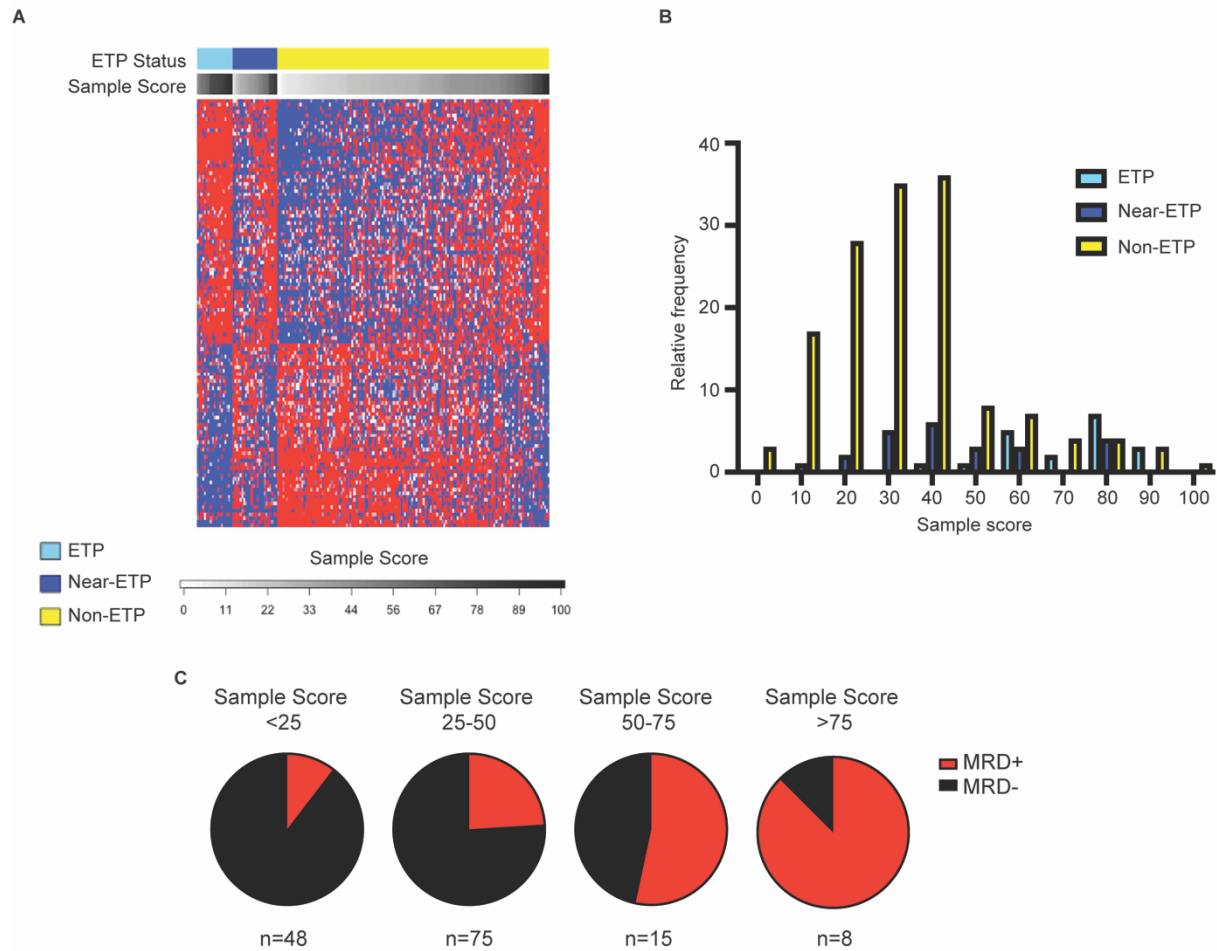
Figure 6-2: The expression pattern of 119 genes has prognostic significance. (A) Heatmap depicting the gene expression pattern of 119 genes in samples from AALL0434 organized by ETP status and sample score. **(B)** Distribution of sample scores across the ETP, near-ETP, and non-ETP samples. **(C)** Distribution of MRD status by sample score in the non-ETP T-ALL subset.
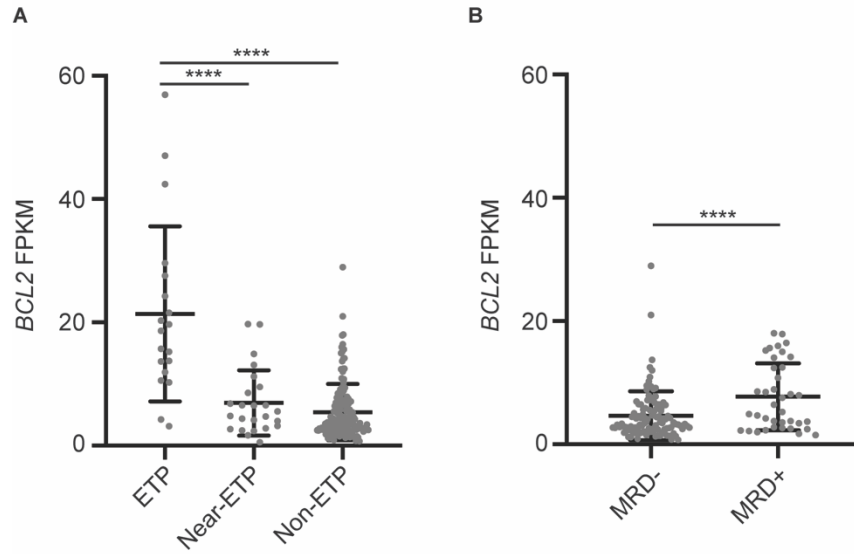
Figure 6-3: *BCL2* expression is associated with developmental stage and ETP status. (A) FPKM values for *BCL2* transcript in ETP, near-ETP, and non-ETP T-ALL samples. Statistical significance was assessed using one-way ANOVA with Tukey's method for multiple comparisons adjustment. **(B)** FPKM values for *BCL2* transcript in MRD- and MRD+ non-ETP T-ALLs. Statistical significance was assessed using two-sample t-tests. ****p<0.0001, ***p<0.001, **p<0.01, *p<0.05.
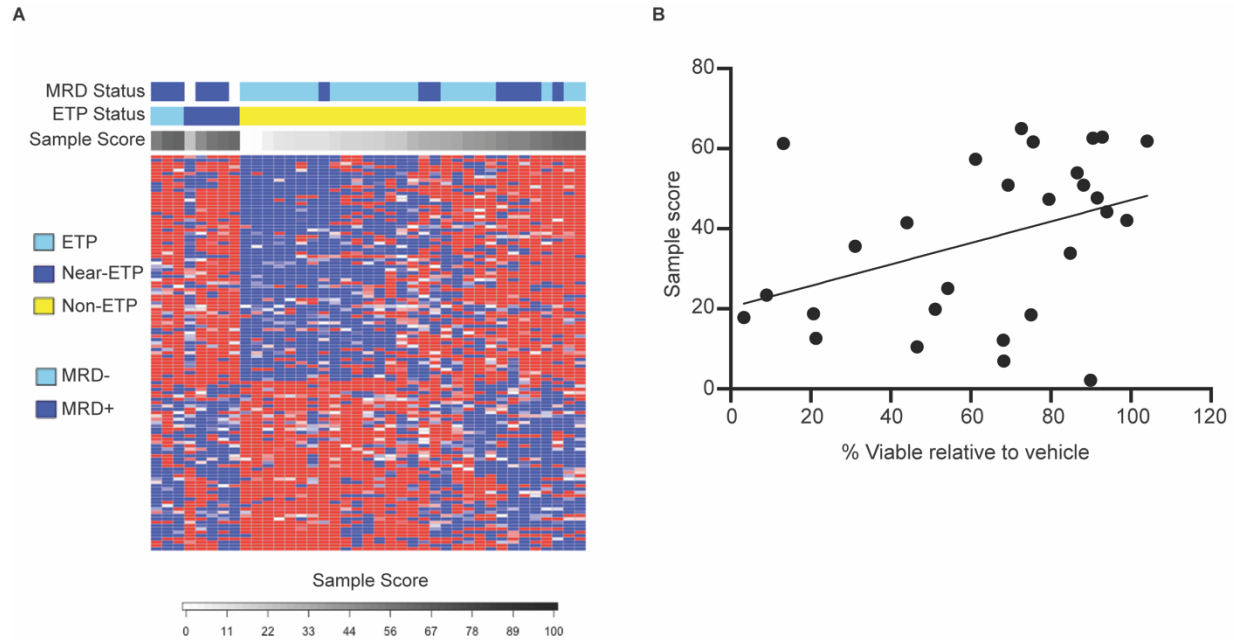
Figure 6-4: High samples scores are associated with *in vitro* GC resistance. (A) Heatmap depicting the gene expression pattern of 119 genes in samples from AALL1231 organized by ETP status and sample score, with indication of MRD status. **(B)** Viability relative to vehicle control of 28 fresh diagnostic samples from AALL1231 treated with 2.5µM DEX for 48 hours versus sample score. ****p<0.0001, ***p<0.001, **p<0.01, *p<0.05.
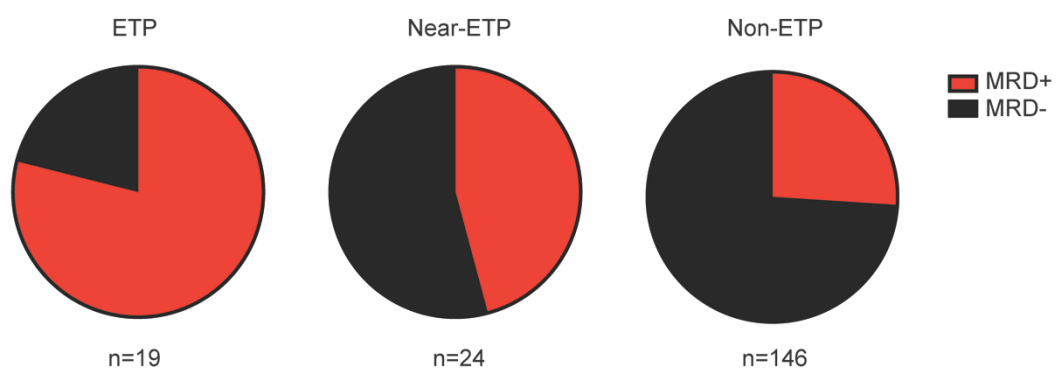
Supplemental Figure 6-1: ETP T-ALLs are commonly MRD+. Distribution of MRD status in ETP, near-ETP, and non-ETP T-ALLs from AALL0434.

Chapter 7: KZR-508445 is a Novel Inhibitor of the Sec61 Translocon that Overcomes

Cytokine-Induced Glucocorticoid Resistance in T-Cell Acute Lymphoblastic Leukemia

7.1: Abstract

Glucocorticoids (GCs) are a central component of therapy for T-cell acute lymphoblastic leukemia (T-ALL), and upfront resistance to GCs is a poor prognostic factor. We previously demonstrated that over one-third of primary patient T-ALLs are resistant to the GC dexamethasone (DEX) when cultured in the presence of interleukin-7 (IL7). Mechanistically, we demonstrated that resistance occurs following DEX-induced upregulation of IL7 receptor (IL7R) expression, leading to increased downstream pro-survival signaling. This newly synthesized IL7R reaches the cell surface via trafficking through the cellular secretory pathway, so we hypothesized that inhibiting the translocation of nascent IL7R peptide into the secretory pathway would effectively overcome IL7-induced DEX resistance. Sec61 is a protein-conducting channel in the membrane of the endoplasmic reticulum (ER) that is required for the cotranslational insertion of nascent polypeptides into the ER. Here, we demonstrate that KZR-508445, a novel inhibitor of the Sec61 translocon, potently attenuates the DEX-induced increase in cell surface IL7R in a T-ALL cell line and primary patient T-ALL cells and synergizes with DEX in the presence of IL7.

7.2: Introduction

Acute lymphoblastic leukemia (ALL) is the most common childhood malignancy, with T-cell ALL (T-ALL) accounting for approximately 15% of cases. While outcomes for children diagnosed with T-ALL have improved dramatically over the past several decades, survival rates for patients with relapsed or refractory T-ALL remain dismal, indicating a need for strategies to enhance the efficacy of frontline treatment protocols in order to induce deeper remissions and decrease the likelihood of disease relapse (32). Glucocorticoids (GCs) are a central component of T-ALL therapy and represent a particularly important target for strategies aimed at improving clinical outcomes. Specifically, the sensitivity of T-ALL cells to GCs at the time of disease

diagnosis is one of the strongest known prognostic factors for predicting future relapse, with patients who respond well to GCs during the first weeks of therapy facing significantly better outcomes relative to patients who respond poorly (285).

Through *ex vivo* analysis of primary diagnostic T-ALL samples, we have demonstrated that up to 75% of these samples are intrinsically resistant to dexamethasone (DEX), a synthetic GC used in T-ALL therapy. Furthermore, we have discovered that approximately half of these DEX resistant samples are resistant specifically when cultured in the presence of interleukin-7 (IL7) (132), a pro-survival cytokine that has previously been implicated in T-ALL pathogenesis and disease maintenance (329,330). Mechanistically, we have demonstrated that in these primary samples and in a cell line model of IL7-induced GC resistance, DEX paradoxically induces its own GC resistance by upregulating IL7 receptor (IL7R) expression. In the presence of IL7 ligand, this leads to an increase in pro-survival signaling through the IL7R/JAK/STAT5 pathway ending with the upregulation of the pro-survival protein BCL-2, which directly antagonizes GC-induced apoptosis (254). Given that upregulation of IL7R is a critical component of this resistance mechanism, we hypothesized that therapeutic strategies to inhibit the DEX-induced upregulation of IL7R would overcome IL7-induced GC resistance.

Secreted and membrane-associated proteins, including IL7R, require processing through the cellular secretory pathway to reach the cell surface. These proteins are targeted to the secretory pathway by the translation of a signal sequence on the nascent peptide, which is subsequently recognized by the Sec61 complex. This Sec61 complex is a component of the mammalian translocon, a protein-conducting channel on the membrane of the endoplasmic reticulum (ER). Upon recognition of the signal sequence, these peptides undergo productive translocation into the lumen of the ER, where post-translational processing is initiated to produce functional secreted or membrane-associated proteins (331). Small molecule inhibitors of the Sec61 translocon represent a novel therapeutic strategy to inhibit the processing of a subset of cell surface proteins, including cytokine receptors. Specifically, these compounds act

in a signal sequence-specific manner to prevent the interaction of these proteins with Sec61, thereby blocking their translocation into the ER and ultimately their secretion or expression at the cell surface (332). Sec61 modulators have demonstrated preclinical efficacy both as antimicrobial and anticancer agents (333,334). In the present study, we demonstrate that a novel inhibitor of the Sec61 translocon, KZR-508445, potently overcomes IL7-induced GC resistance in a cell line model and in primary patient T-ALL samples, concomitant with a reduction in cell surface IL7R expression. This study establishes the feasibility of targeting the Sec61 translocon as a means of augmenting responses to GC therapy in pediatric T-ALL and provides preclinical evidence supporting further development of KZR-508445 and related compounds for this purpose.

7.3: Results

Sec61 inhibition overcomes IL7-induced DEX resistance in patient T-ALL samples

The Sec61 translocon is an attractive therapeutic target for overcoming IL7-induced DEX resistance due to the dynamic regulation of IL7R expression in response to DEX. Specifically, we analyzed published RNA-seq data generated from clonal cell populations derived from the human T-ALL cell line CCRF-CEM that were treated with DEX for 4 hours (254). Using a false discovery rate cutoff of ≤0.05, we generated a list of 136 genes that were upregulated by at least two-fold following DEX exposure. We then compared this list to a list of over 6,500 predicted Sec61 client proteins, and identified only 25 DEX targets that interact with the Sec61 translocon, one of which is IL7R (Supplemental Figure 7-1).

CT8 is a tool compound belonging to a class of cyclic heptadepsipeptides known as cotransins, which function to inhibit cotranslational translocation via the Sec61 translocon (Figure 7-1A). As an initial evaluation of the efficacy of this therapeutic strategy for overcoming IL7-induced DEX resistance, we utilized cells from 28 fresh diagnostic T-ALL samples that

demonstrate IL7-induced DEX resistance. We exposed these cells to DEX in the presence of

IL7 either alone or in combination with the JAK1/2 inhibitor ruxolitinib (RUX) or CT8, and found

that RUX and CT8 equivalently overcame IL7-induced DEX resistance (Figure 7-1B),

suggesting that Sec61 inhibition may be equally as effective as JAK/STAT pathway inhibition for

augmenting DEX sensitivity.

KZR-508445 is an optimized cotransin that potently modulates IL7R expression and overcomes IL7-induced DEX resistance

Based on these promising initial findings with CT8, we pursued further evaluation of this

therapeutic strategy utilizing KZR-508445, a novel derivative of CT8 with improved potency and

in vivo stability (Figure 7-2A). The CCRF-CEM cell line demonstrates significant upregulation of

cell surface IL7R protein in response to DEX exposure, which was effectively reduced by

nanomolar concentrations of KZR-508445 (Figure 7-2B). Interestingly, while all common γ-chain

cytokine receptors are Sec61 clients, the relative potency of KZR-508445 for reducing cell

surface expression of these receptor chains was significantly greater for IL7R relative to all

other common γ-chain cytokine receptors, with only 36% of the basal level of IL7R remaining at

the cell surface in response 15.6nM KZR-508445, versus greater than 75% for all other

common γ-chain cytokine receptors (Supplemental Figure 7-2A).

We next evaluated the effect of combining KZR-508445 with DEX on cell viability in

CCRF-CEM cells, which demonstrate IL7-induced DEX resistance (254). In the presence of IL7,

KZR-508445 effectively enhanced DEX sensitivity (Figure 7-2C) in a manner that was highly

synergistic with DEX (Figure 7-2D). Importantly, at concentrations at which synergy was

observed, KZR-508445 demonstrated minimal single agent effects on cell viability

(Supplemental Figure 7-2B) or cell proliferation (Supplemental Figure 7-2C), suggesting that the

observed effects on cell viability in the presence of DEX are not due to an overall reduction in

secretory and membrane protein biogenesis. Finally, we evaluated the effect of KZR-508445 on expression of the STAT5 target BCL-2, which is significantly upregulated upon exposure to DEX and IL7. Consistent with its ability to overcome IL7-induced DEX resistance, KZR-508445 inhibited the increase in BCL-2 protein expression in a dose-dependent manner (Figure 7-2E).

The efficacy of KZR-508445 in T-ALL is due to the interaction between Sec61, the IL7R signal peptide, and KZR-508445

To assess the mechanism by which KZR-508445 inhibits the DEX-induced upregulation of cell surface IL7R, we evaluated transcript and protein expression of IL7R in CCRF-CEM cells treated with vehicle control or DEX in the presence or absence of KZR-508445. As previously shown (254), DEX induced a significant increase in *IL7RA* transcript expression and in cell surface IL7R protein. This increase in transcript levels was sustained with the addition of KZR-508445, despite restoration of cell surface IL7R protein to basal levels (Figure 7-3A), consistent with KZR-508445 acting post-transcriptionally to attenuate IL7R expression.

Next, to confirm that this modulation of IL7R expression is due specifically to an interaction between the Sec61 translocon, IL7R peptide, and KZR-508445, we generated expression constructs containing wild-type IL7R and performed site-directed mutagenesis to engineer two leucine substitutions into the IL7R signal sequence (Figure 7-3B). These mutations increase the hydrophobicity of the signal sequence, which is predicted to confer resistance to KZR-508445 by impairing its interaction with IL7R. We then transiently transfected HEK-293T cells with the wild-type and mutant constructs and assessed cell surface IL7R expression. The introduction of these leucine substitutions did not affect basal expression of IL7R at the cell surface (Supplemental Figure 7-3A). However, upon exposure to increasing concentrations of KZR-508445, cells expressing the mutant IL7R showed impaired downregulation of cell surface IL7R (Figure 7-3C), confirming that KZR-508445-mediated

modulation of IL7R expression is due specifically to the interaction between this compound, the IL7R signal sequence, and the Sec61 translocon.

We next asked whether modulation of IL7R expression is necessary for KZR-508445 to enhance DEX sensitivity in CCRF-CEM cells. As previously described (254), we used CRISPR/Cas9 genome editing to generate clonal populations of IL7R knockout CCRF-CEM cells (Supplemental Figure 7-3B). We then treated these cells with DEX with or without KZR-5088445, and found that KZR-508445 had minimal effects to modulate DEX sensitivity in the absence of IL7R expression (Figure 7-3D), suggesting that downregulation of IL7R expression underlies the sensitization to DEX. Further supporting this idea, we also did not observe any effect of KZR-508445 to enhance sensitivity to other chemotherapeutic agents used in the treatment of T-ALL, none of which demonstrate IL7-induced resistance (Supplemental Figure 7-3C). These data suggest that KZR-508445 is not a general chemosensitizer, but instead acts specifically on IL7R to overcome a mechanism of resistance that is unique to DEX.

KZR-508445 is effective in primary patient samples and in an in vivo model system

Following the observed efficacy of KZR-508445 in CCRF-CEM cells, we next sought to determine whether this compound effectively overcomes IL7-induced DEX resistance in primary patient T-ALL samples. We utilized 16 human T-ALLs that demonstrate IL7-induced DEX resistance, and found that *ex vivo* exposure to KZR-508445 effectively inhibited the DEX-induced increase in cell surface IL7R expression (Figure 7-4A). As observed with CT8, KZR-508445 also overcame IL7-induced DEX resistance, restoring DEX sensitivity to that observed in the absence of IL7 (Figure 7-4B). This improved DEX sensitivity was further associated with inhibition of the BCL-2 upregulation observed with the combination of DEX and IL7 (Figure 7-4C).

Finally, we asked whether KZR-508445 is effective *in vivo*. First, we established tolerability by treating non-tumor-bearing NSG mice with three different doses of KZR-508445

administered by weekly intravenous injection. At even the highest dose of KZR-508445, we observed no loss of bodyweight (Supplemental Figure 7-4A) or significant modulation of any measured hematologic parameters (Supplemental Figure 7-4B-D). We then generated an *in vivo* model of T-ALL by transplanting CCRF-CEM cells into NSG mice. To assess the pharmacodynamics of a 22.5mg/kg dose of KZR-508445, we treated mice and measured cell surface expression of CD62L, a Sec61 client, on the cell surface of CCRF-CEM cells in peripheral blood after 24 hours. This revealed significant downregulation of CD62L (Supplemental Figure 7-4C), suggesting that this dose of KZR-508445 is sufficient to modulate expression of Sec61 clients *in vivo*. We then conducted a four-arm trial by treating xenografts with vehicle control, 15mg/kg/day DEX, 22.5mg/kg KZR-508445 twice weekly, or the combination of DEX and KZR-508445. Upon analysis of the percentage of CCRF-CEM cells in the peripheral blood of vehicle- and drug-treated mice, we found that both DEX and KZR-508445 effectively attenuated peripheral disease burden, with a trend towards further attenuation with the combination of DEX and KZR-508445 (Figure 7-4D).

7.4: Discussion

The IL7R signal transduction pathway plays a well-established role in leukemogenesis (289,290), with its importance underscored by the prevalence of mutations in IL7R or components of the downstream signal transduction machinery (182,291), indicating a selective pressure for activation of this pathway in T-ALL. We previously demonstrated that cytokine-mediated activation of this pathway is a prevalent mediator of resistance to GCs, a central component of therapy for T-ALL. In particular, we showed that a key feature of this resistance mechanism is the GC-induced upregulation of IL7R, which potentiates downstream signal transduction leading to the upregulation of pro-survival factors that antagonize DEX-induced

apoptosis (254). Here, we demonstrate that targeting the localization of newly synthesized IL7R to the cell surface is an effective means of overcoming IL7-induced DEX resistance.

Specifically, this study demonstrates the efficacy of KZR-508445, a novel inhibitor of the Sec61 translocon, in a T-ALL cell line and in primary patient T-ALL samples. We demonstrate that KZR-508445 potently inhibits the DEX-induced increase in cell surface IL7R with relative sparing of other cytokine receptors that mediate important T-cell biological functions, suggesting that there may be a range of drug doses that are sufficient for targeting IL7R in T-ALL without significant modulation of common γ-chain cytokine receptors in other T-cell populations. Using a genetic approach, we show that this relative selectivity and potency is conferred by the specific amino acid sequence of the IL7R signal sequence. Furthermore, we find that the reduction in IL7R expression is associated with increased sensitivity to DEX in the presence of IL7, concomitant with a reduction in expression of BCL-2, a downstream transcriptional target of IL7R/JAK/STAT5 pathway signaling. Finally, we provide tolerability data demonstrating that KZR-508445 is well-tolerated *in vivo*, and show that KZR-508445 effectively attenuates disease burden in a xenograft model of T-ALL.

Taken together, these data establish the potential for enhancing GC sensitivity in T-ALL through inhibition of the Sec61 translocon. Despite the vast number of proteins that require trafficking through the cellular secretory pathway prior to secretion from the cell or localization to the plasma membrane, we observed minimal single-agent effects of KZR-508445 in CCRF-CEM cells or in patient T-ALL samples, suggesting that the relative selectivity for IL7R is sufficient to establish a therapeutic window for use in T-ALL. While the relationship between the structure of cotransin derivatives and their selectivity for different Sec61 clients remains poorly understood, it is well-established that this selectivity differs on the basis of the side chains associated with these derivatives (335). This suggests the potential for further development of KZR-508445 and related compounds for clinical use in T-ALL and for other diseases with

unique pathophysiologic or therapeutic dependencies on secreted or membrane-associated proteins.

7.5: Methods

Flow cytometry

Flow cytometry was performed using a BD FACSVerse and data were analyzed using FlowJo software.

Patient T-ALL samples

Diagnostic blood samples were obtained from patients enrolled on the COG trial AALL1231. Written informed consent for the use of diagnostic specimens for research was obtained from patients or their guardians at the time of sample collection, according to the Declaration of Helsinki, the National Cancer Institute, and institutional review boards of participating sites. Fresh T-ALL cells were used in the analysis in Figure 7-1. For the analysis in Figure 7-4, cells were obtained following passaging through NOD/SCID/*Il2rgtm1wjl/*Szj (NSG) mice as patient-derived xenografts (PDXs). These NSG mice were obtained from Jackson Laboratories and T-ALL engraftment was monitored using flow cytometric analysis of peripheral blood with antibodies against human CD45 (BD Biosciences) and CD7 (BioLegend). All PDX experiments were conducted following protocols that were approved by the Institutional Animal Care and Use Committee of Children's Hospital of Philadelphia.

CCRF-CEM cells

CCRF-CEM cells were purchased from the UCSF Cell Culture Facility (ATCC CCL-119). Cells were maintained in RPMI (Mediatech) supplemented with 10% fetal bovine serum (VWR) and antibiotics. Cells were authenticated via short tandem repeat DNA profiling and were routinely tested for mycoplasma contamination using the PlasmoTest detection kit (InvivoGen).

In vitro *viability assays*

In vitro viability assays were performed by exposing CCRF-CEM cells and patient-derived T-ALL cells to vehicle control or to the following drugs at the concentrations indicated in the associated figure legends: DEX (Sigma), RUX (Selleckchem), CT8 (Kezar Life Sciences), KZR-508445 (Kezar Life Sciences), cytarabine (Sigma), methotrexate (Sigma), etoposide (Sigma), and vincristine (Sigma). Viability assays were performed in the absence or presence of recombinant human IL7 (Peprotech) as indicated in the figure legends. Cells were treated for 72 hours (CCRF-CEM cells) or 48 hours (patient-derived T-ALL cells), and were then stained with Hoechst 33258 (Molecular Probes) and analyzed by flow cytometry. Data are presented as the percentage of viable (Hoechst-negative) cells in the drug-treated condition relative to the corresponding vehicle-treated condition.

Measurement of cell surface cytokine receptor expression

The effect of KZR-508445 on common γ-chain cytokine receptors was assessed in human CD8 T-cells isolated from TRIMA residuals enriched for peripheral blood mononuclear cells (PBMCs) and obtained from the Vitalant blood bank. PBMCs were isolated using a Ficoll (GE Healthcare) density gradient in a SepMate PBMC Isolation Tube (STEMCELL Technologies). 5 x 10^7 cells were labeled with biotinylated antibodies against CD4 (clone A161A1; BioLegend), CD19 (clone HIB19; BioLegend), CD11b (clone ICRF44; BioLegend), CD24 (clone ML5; BioLegend), and B220 (clone RA3-6B2; Biolegend). Negative selection was performed by depleting biotin-labeled cells with Biotin Binder Dynabeads (Life Technologies). The remaining cells were cultured in RPMI (Mediatech) supplemented with 10% fetal bovine serum (VWR), glutamine, antibiotics, and 20ng/mL recombinant human IL-2 (Peprotech). Cells were activated by the addition of Human T-Activator CD3/CD28 Dynabeads (Life Technologies).

For analysis of cell surface cytokine receptor expression, CCRF-CEM cells, patient-derived T-ALL cells, or human CD8 T-cells were treated with or without 1μM DEX and/or the

indicated concentrations of KZR-508445 for 24 hours. Cells were then stained with antibodies against the following proteins: IL2Rα (clone M-A251; BioLegend), IL2Rβ (clone TU27; BioLegend), IL2Rγ (clone TUGh4; BioLegend), IL4R (clone G077F6; BioLegend), IL7R (clone A019D5; BioLegend), IL9R (clone AH9R7; BioLegend), IL15R (clone JM7A4; BioLegend), and IL21R (clone 17A12; BioLegend). Cells were also stained with Hoechst 33258 to facilitate gating on the live cell population. Data were recorded as the median fluorescent intensity (MFI) of IL7R in the Hoechst-negative gate.

Proliferation assay

To assess the effects of KZR-508445 on cell proliferation, CCRF-CEM cells were treated with increasing concentrations of KZR-508445 for 72 hours and analyzed using Cell Titer Glo reagent (Promega) according to the manufacturer's instructions.

Measurement of BCL-2 protein expression

CCRF-CEM cells and patient-derived T-ALL cells were treated under the indicated drug conditions for 24 hours. Cells were then fixed with 2% paraformaldehyde and permeabilized with methanol. Cells were stained with an anti-cleaved caspase 3 antibody (clone C92-605; BD Biosciences) and an anti-BCL-2 antibody (clone Bcl2/100; Life Technologies) and analyzed by flow cytometry. Data were recorded as the MFI of BCL-2 in the cleaved caspase 3-negative gate.

IL7R cloning and site-directed mutagenesis

RNA was isolated from CCRF-CEM cells using the RNeasy Mini kit (Qiagen) and cDNA was generated using the Superscript III kit (ThermoFisher). IL7R cDNA was amplified using the following primers: forward – 5'-GAGCTAGAGCTAGCGGCCACCATGACAATTCTAG-3'; reverse

– 5'- CCCTCAGCGGCCGCGAACTGGTTTTGGTAGAAGCTG-3'. IL7R cDNA was cloned into the pCDH Expression Lentivector system (System Biosciences) using the EcoRI and BamHI restriction enzyme sites. The IL7R signal sequence mutant was generated by site-directed mutagenesis performed with the QuickChange II XL Site-Directed Mutagenesis Kit (Agilent Technologies) and the following oligonucleotide: 5'-GGTACAACTTTTTTAATGGTTTTTTTATTACTTCAAGTCGTTTCTGG-3'.

Transfection of HEK-293T cells

Wild-type and mutant IL7R constructs were transfected into HEK-293T cells using Lipofectamine 3000 (Life Technologies) according to the manufacturer's instructions. Sixteen hours after transfection, cells were treated with the indicated concentrations of KZR-508445 for 24 hours prior to analysis of cell surface IL7R expression by flow cytometry, as described above.

Quantitative PCR (qPCR)

For analysis of *IL7RA* transcript expression, CCRF-CEM cells were treated with or without 1µM DEX and/or 200nM KZR-508445 for 16 hours. RNA was isolated using the RNeasy Mini kit and cDNA was generated using the Superscript III kit. Taqman quantitative PCR probes (Applied Biosystems) were used in conjunction with Taqman Master Mix (Applied Biosystems) to assess transcript levels of the following genes: *GAPDH* (Hs02786624_g1; VIC-MGB) and *IL7RA* (Hs00902334_m1; FAM-MGB). Experiments were performed in technical triplicate and were run on a QuantStudio 5 Real-Time PCR Instrument (Applied Biosystems). The fold change in transcript expression was calculated relative to vehicle-treated cells using the delta-delta Ct method, with the use of *GAPDH* transcript for normalization.

CRISPR/Cas9 genome editing of CCRF-CEM cells

IL7R knockout CCRF-CEM cells were generated as previously described (254).

In vivo drug treatment and analysis

All *in vivo* experiments were conducted following protocols that were approved by the Institutional Animal Care and Use Committee of the University of California, San Francisco. To assess *in vivo* drug tolerability, non-tumor-bearing female NSG mice were treated with vehicle control (10% ethanol and 10% Kolliphor) or KZR-508445 via weekly intravenous injection of the indicated doses. Bodyweight was assessed weekly. Hematologic parameters were assessed using the Hemavet System (Drew Scientific). To assess the effects of KZR-508445 on leukemic cell burden, female NSG mice were transplanted with 2×10^6 CCRF-CEM cells via tail vein injection. Beginning on day 4 post-injection, mice were treated with vehicle (PBS) or DEX at 15mg/kg/day and/or vehicle (10% ethanol and 10% Kolliphor) or KZR-508445 at 22.5mg/kg twice weekly. Peripheral blood leukemia burden was assessed by subjecting blood to RBC lysis followed by staining with an anti-human CD45 antibody (clone 2D1; BioLegend) and an anti-human CD62L antibody (clone DREG-56; BioLegend).

Statistical analysis

Statistical analyses were performed using Prism 8 (GraphPad). All tests were two-sided and the threshold for significance was $p \leq 0.05$. Comparisons between groups were made using t-tests, with one-way ANOVA and Tukey's method for multiple comparisons adjustment for comparisons of three or more groups. Interactions between drugs were assessed using Bliss independence analysis (281). Error bars represent the standard error of the mean.

7.6: Acknowledgements
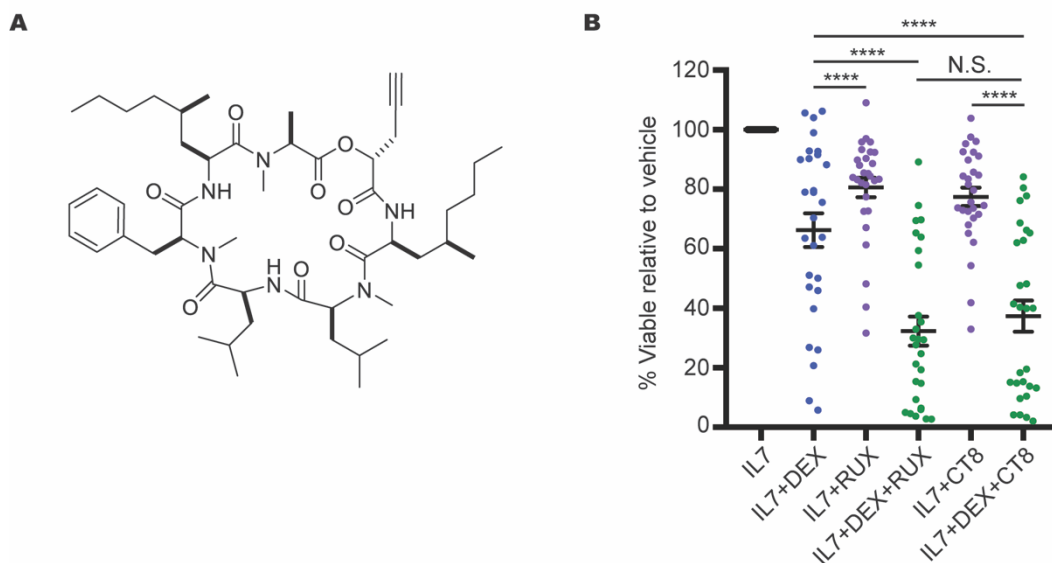
Figure 7-1: CT8 overcomes IL7-induced DEX resistance in patient-derived T-ALL cells. (A) Chemical structure of CT8. **(B)** Viability relative to vehicle control of cells from 28 fresh diagnostic T-ALL samples cultured in the presence of 25ng/mL IL7 with or without 2.5µM DEX and/or 500nM RUX or 2µM CT8 for 48 hours. Statistical significance was assessed using one-way ANOVA with Tukey's method for multiple comparisons adjustment. ****$p<0.0001$, ***$p<0.001$, **$p<0.01$, *$p<0.05$, N.S. – not significant.
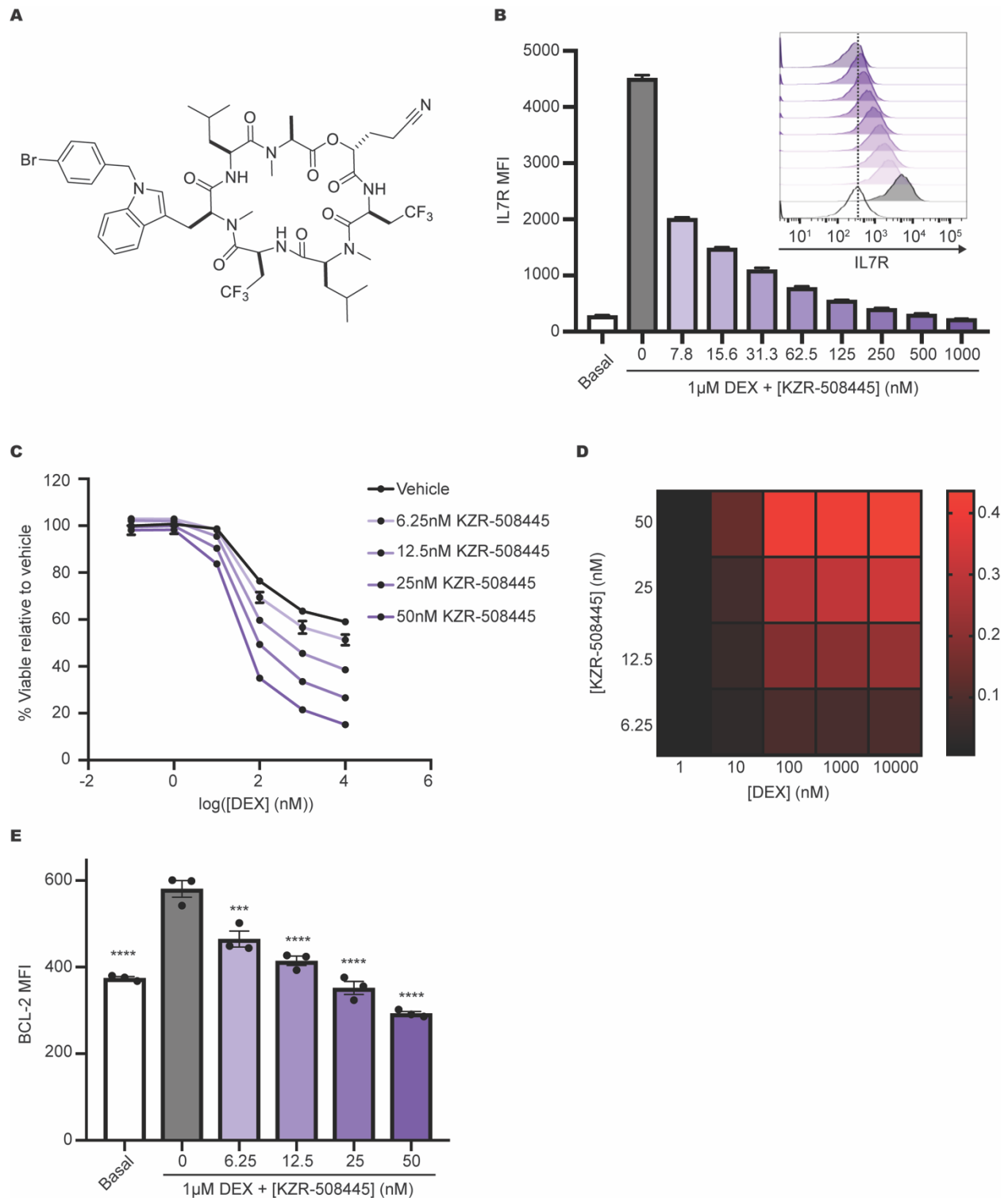
Figure 7-2: KZR-508445 modulates cell surface IL7R expression and overcomes IL7-induced DEX resistance in CCRF-CEM cells. (A) Chemical structure of KZR-508445. **(B)** MFI and representative histograms of cell surface IL7R in CCRF-CEM cells treated with or without 1µM DEX and increasing concentrations of KZR-508445 for 24 hours in technical triplicate. **(C)** Viability relative to vehicle control of CCRF-CEM cells treated with increasing concentrations of

DEX in the presence of 25ng/mL IL7 and/or the indicated concentrations of KZR-508445 for 72 hours in technical triplicate. **(D)** Heatmap of Bliss independence scores calculated as the average of technical triplicates for the combination of DEX and KZR-508445 in CCRF-CEM cells cultured in the presence of 25ng/mL IL7 for 72 hours, in which positive values, indicated in red, are indicative of a synergistic interaction. **(E)** MFI of BCL-2 protein expression in CCRF-CEM cells treated with 100ng/mL IL7 with or without 1μM DEX and/or the indicated concentration of KZR-508445 for 24 hours in technical triplicate. Statistical significance is relative to the DEX-treated condition in the absence of KZR-508445. Statistical significance was assessed using one-way ANOVA with Tukey's method for multiple comparisons adjustment. All data are representative of three independent experiments. ****$p<0.0001$, ***$p<0.001$, **$p<0.01$, *$p<0.05$.
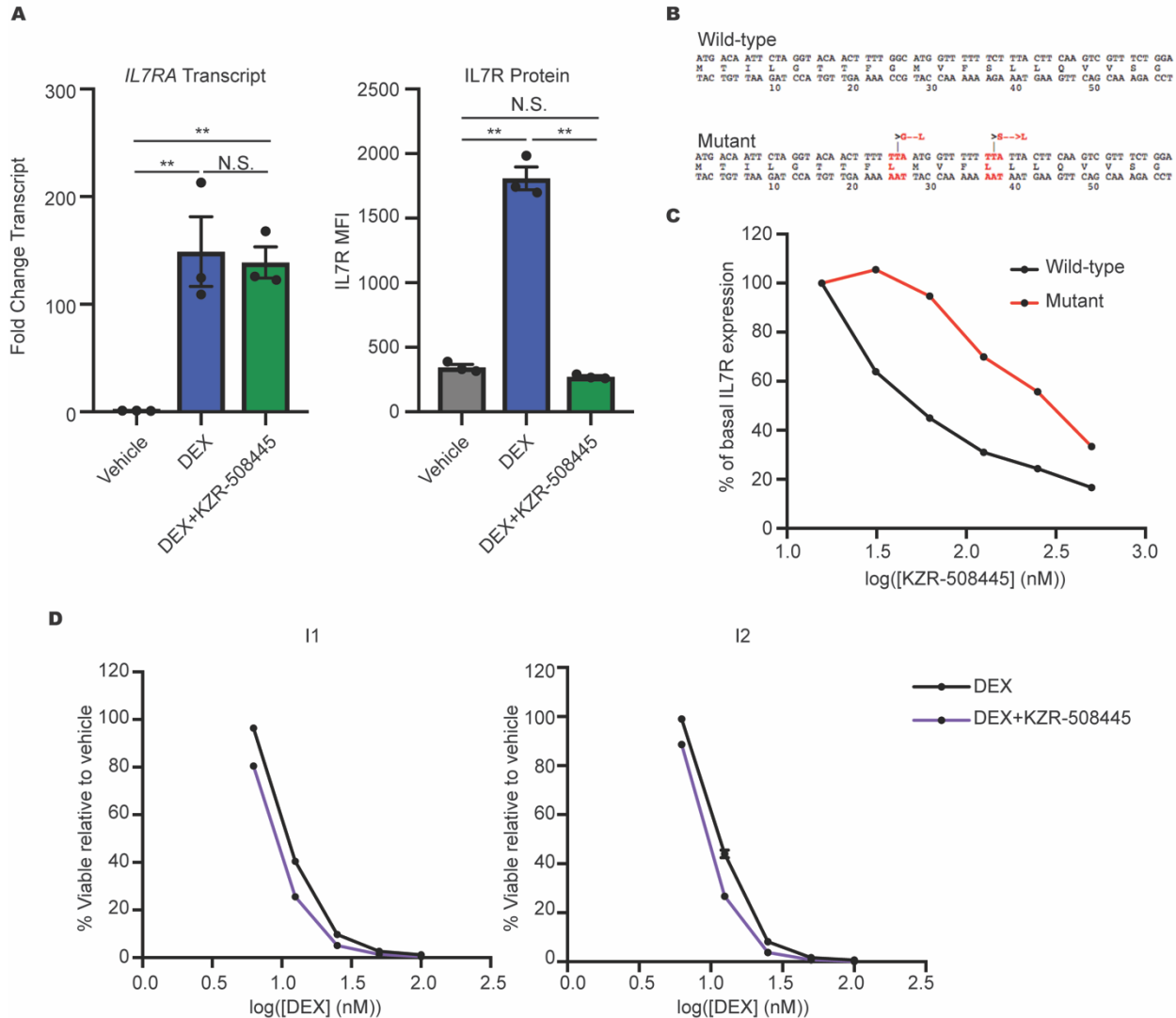
Figure 7-3: KZR-508445 overcomes IL7-induced DEX resistance by interfering with the interaction between nascent IL7R peptide and the Sec61 translocon. (A) Fold change in the transcript expression of *IL7RA* (left) and MFI of IL7R protein (right) in CCRF-CEM cells treated with vehicle or 1μM DEX with or without 200nM KZR-508445 for 16 hours (transcript) or 24 hours (protein) in technical triplicate. Statistical significance was assessed using one-way ANOVA with Tukey's method for multiple comparisons adjustment. **(B)** Sequence of the wild-type IL7R signal sequence and location of the mutations introduced by site-directed mutagenesis. **(C)** MFI of cell surface IL7R in HEK-293T cells transiently transfected with constructs containing wild-type or mutant IL7R and treated with increasing concentrations of KZR-508445 for 24 hours. **(D)** Viability relative to vehicle control in two IL7R knockout CCRF-CEM-derived clones treated with increasing concentrations of DEX with or without 100nM KZR-508445 for 72 hours in technical triplicate. ****$p<0.0001$, ***$p<0.001$, **$p<0.01$, *$p<0.05$, N.S. – not significant. All data are representative of three independent experiments.
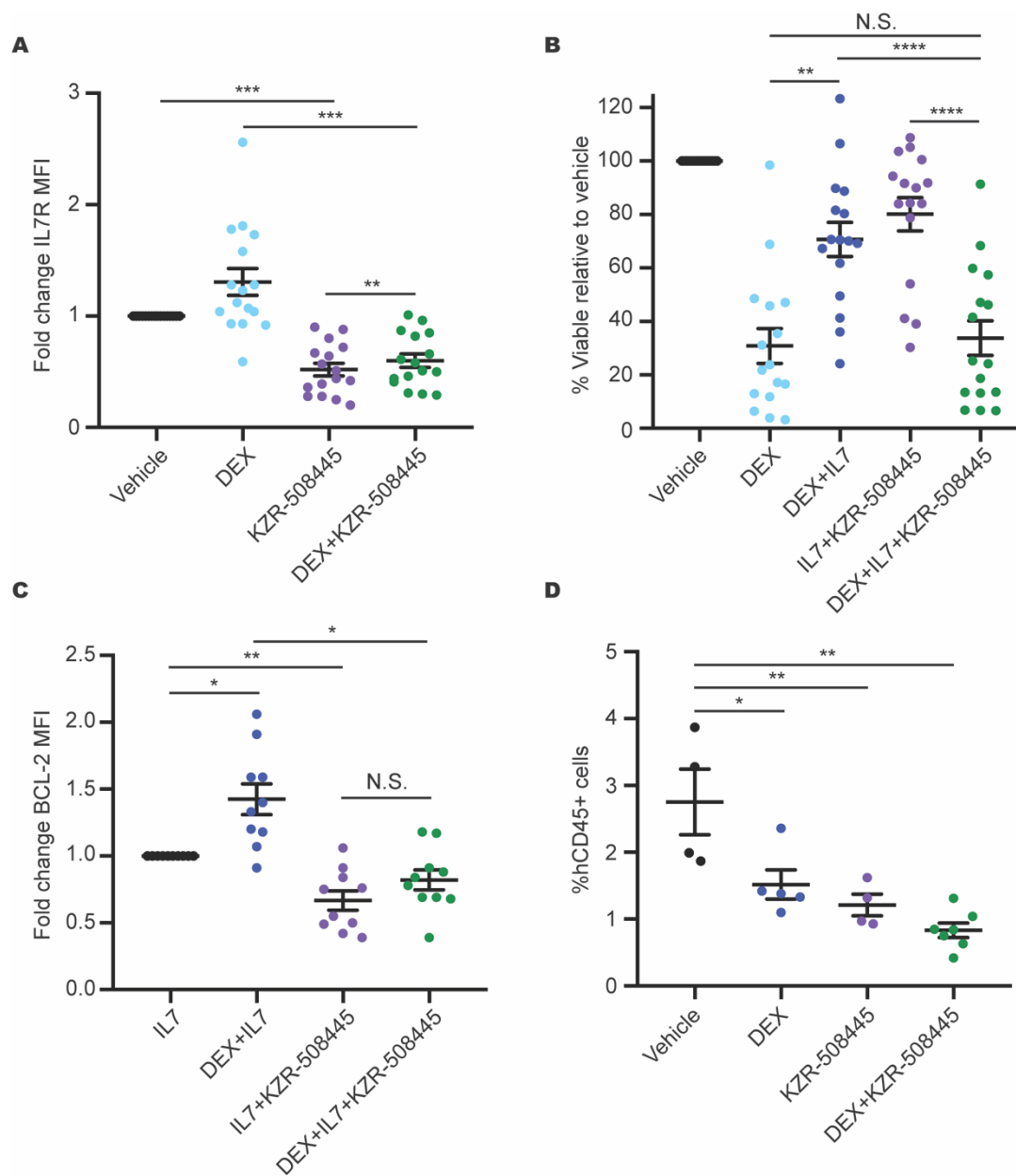
Figure 7-4: KZR-508445 effectively overcomes IL7-induced DEX resistance in patient-derived T-ALL cells and is effective in an *in vivo* model of T-ALL. (A) Fold change in the MFI of IL7R in cells from 16 patient-derived T-ALL samples treated with 1µM DEX with or without 50nM KZR-508445 for 24 hours. **(B)** Viability relative to vehicle control of cells from 16 patient-derived T-ALL samples treated in the presence or absence of 25ng/mL IL7 with or without 1µM DEX and/or 50nM KZR-508445 for 48 hours. **(C)** Fold change in the MFI of BCL-2 in cells from 10 patient-derived T-ALL samples cultured in the presence of 100ng/mL IL7 and treated with or without 1µM DEX and/or 50nM KZR-508445 for 24 hours. **(D)** Percentage of human CD45+ cells in peripheral blood taken on day 11 of treatment from mice transplanted with CCRF-CEM cells. Statistical significance was assessed using one-way ANOVA with Tukey's method for multiple comparisons adjustment. ****$p<0.0001$, ***$p<0.001$, **$p<0.01$, *$p<0.05$, N.S. – not significant.
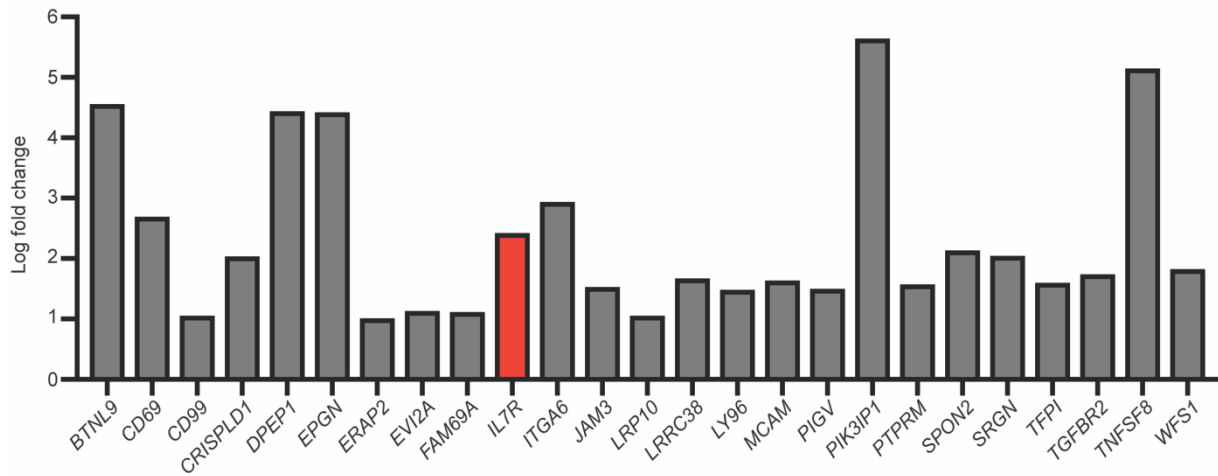
Supplemental Figure 7-1: 25 Sec61 clients are upregulated by DEX. Log fold change in the expression of the DEX target genes corresponding to Sec61 client proteins in clonal populations of CCRF-CEM cells treated with 1μM DEX for four hours.
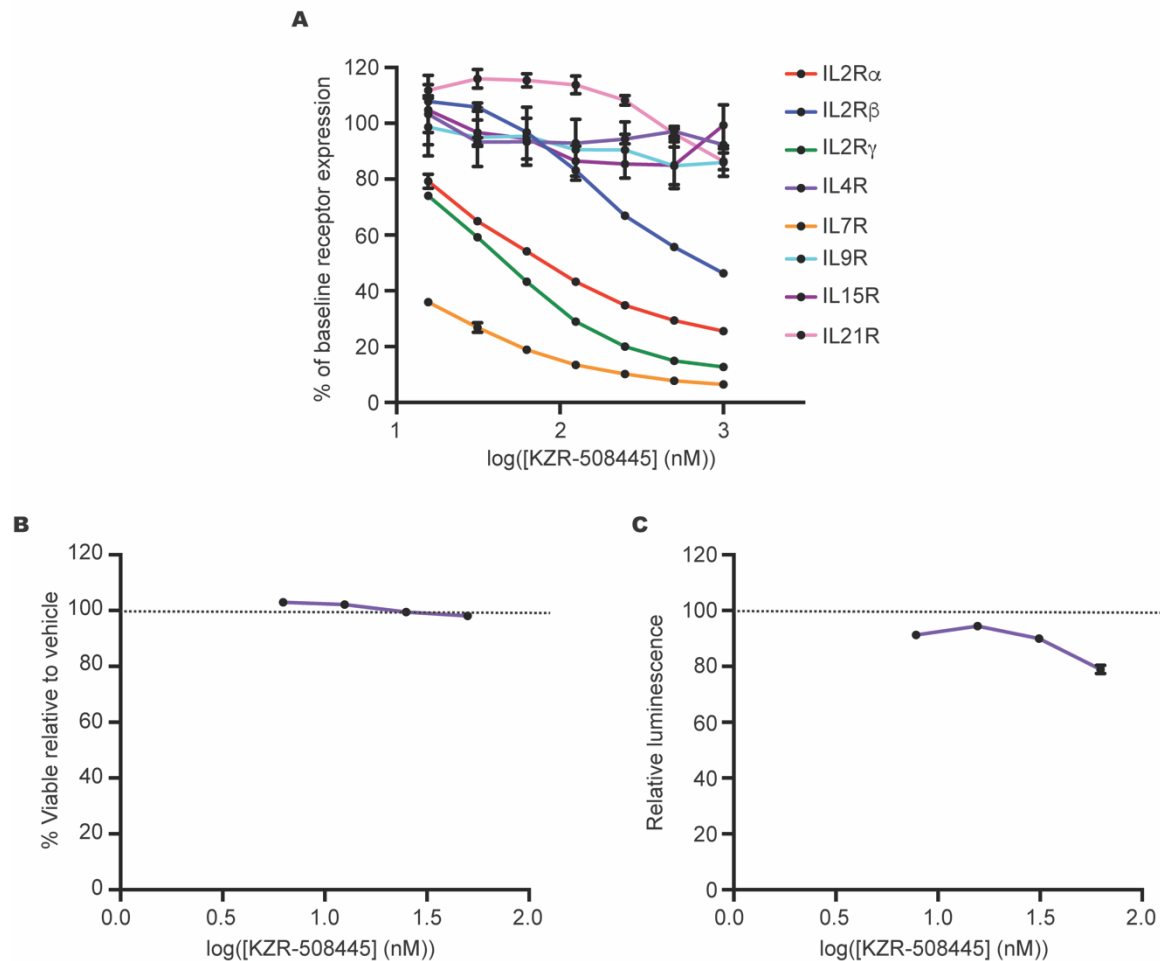
Supplemental Figure 7-2: KZR-508445 shows selective potency for IL7R and has minimal single-agent effects on cell viability and proliferation. (A) MFI relative to baseline values of common γ-chain cytokine receptors in human CD8 T-cells treated with increasing concentrations of KZR-508445 for 24 hours in technical triplicate. **(B)** Viability relative to vehicle control of CCRF-CEM cells treated with increasing concentrations of KZR-508445 for 72 hours in technical triplicate. **(C)** Relative luminescence of CCRF-CEM cells treated with increasing concentrations of KZR-508445 for 72 hours in technical triplicate and analyzed using Cell Titer Glo. All data are representative of three independent experiments.
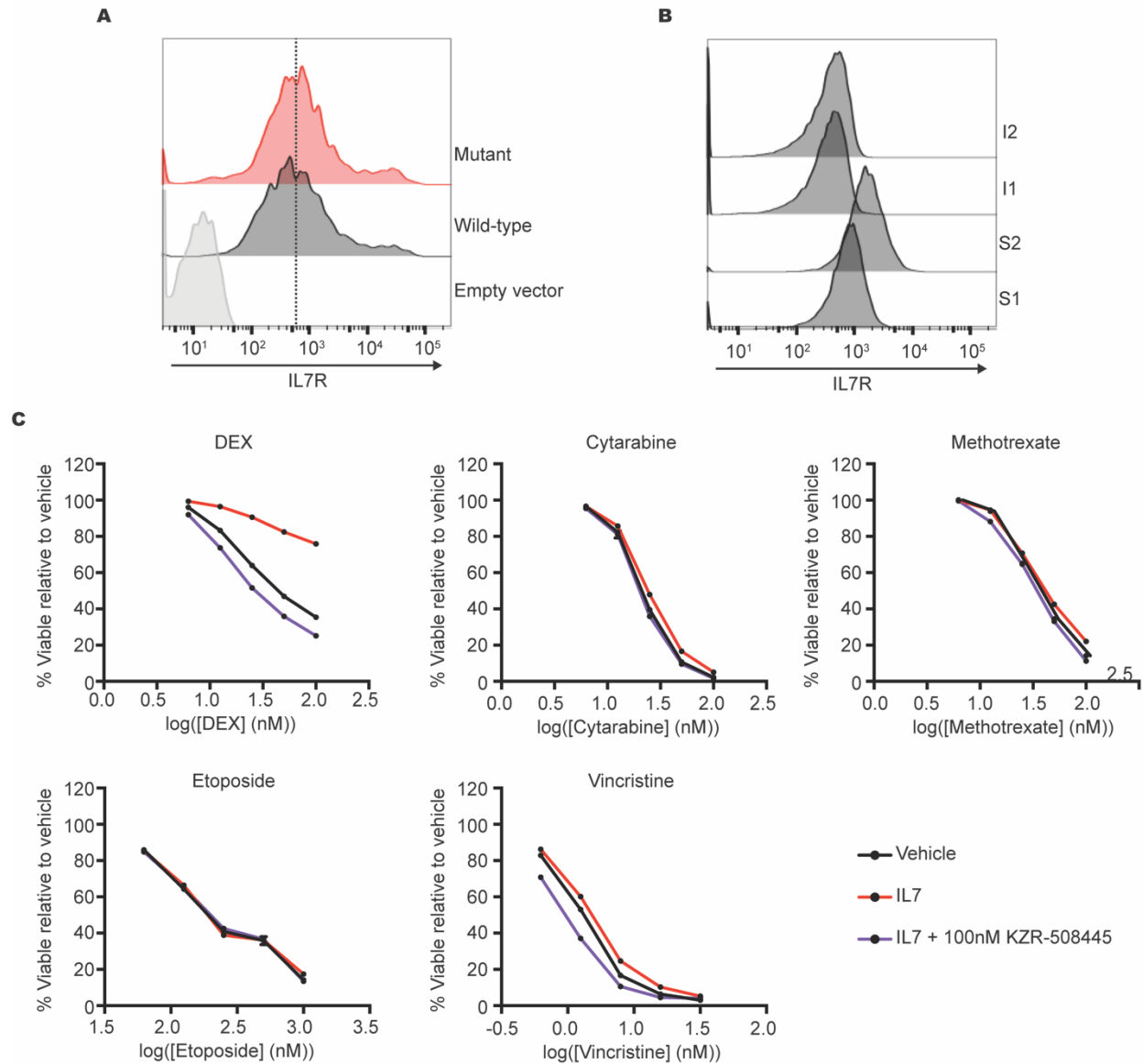
Supplemental Figure 7-3: KZR-508445 sensitizes CCRF-CEM cells to DEX but not to other chemotherapies. (A) Representative histograms of cell surface IL7R in HEK-293T cells transfected with empty vector or wild-type or mutant IL7R constructs. **(B)** Representative histograms of cell surface IL7R in IL7R KO CCRF-CEM cell clones relative to wild-type scramble control clones. **(C)** Viability relative to vehicle control of CCRF-CEM cells treated with increasing concentrations of the indicated chemotherapeutic agent with or without 25ng/mL IL7 and 100nM KZR-508445 for 72 hours in technical triplicate. All data are representative of three independent experiments.
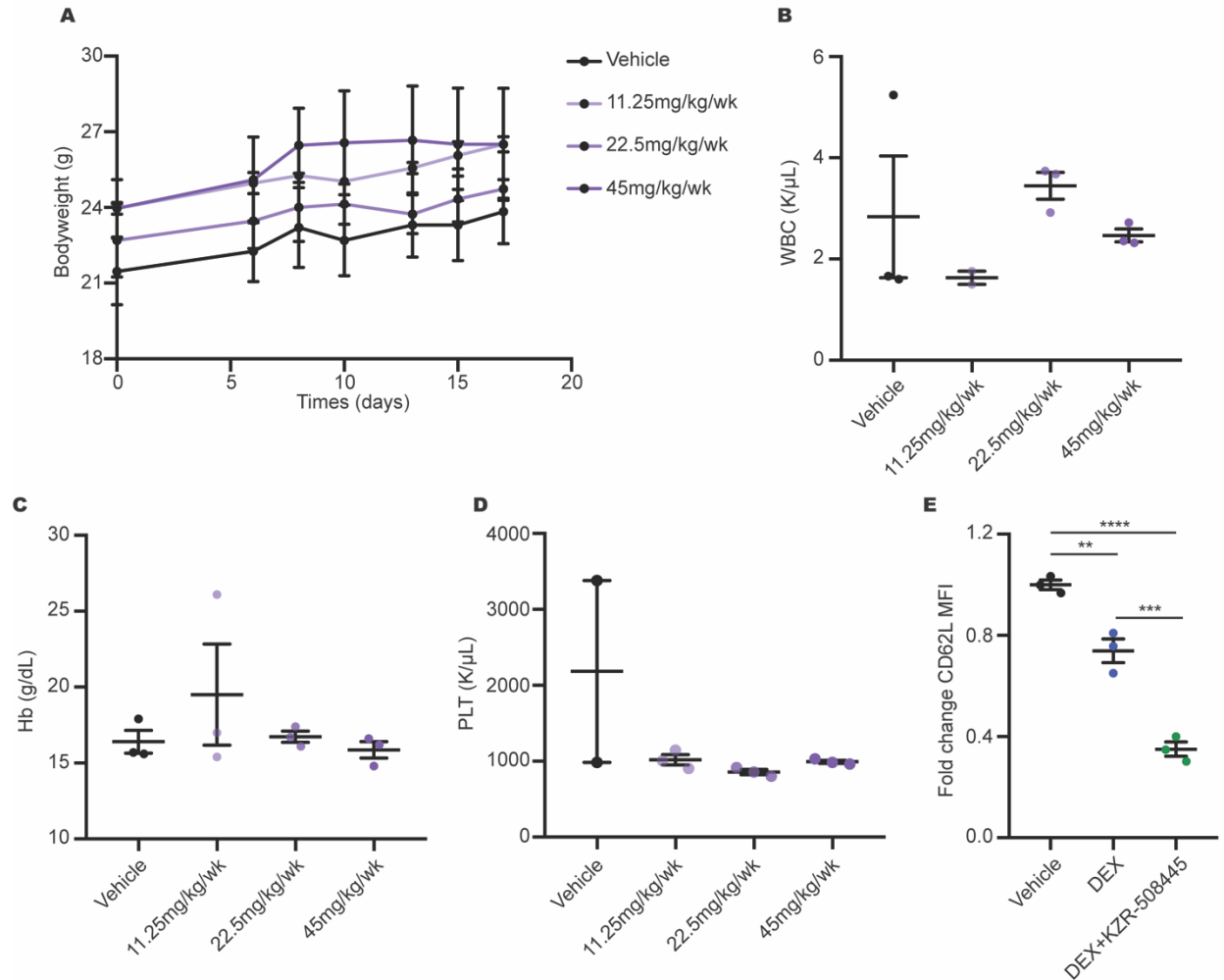
Supplemental Figure 7-4: KZR-508445 is well-tolerated *in vivo*. (A) Change in bodyweight over time of NSG mice treated with vehicle control or the indicated dose of KZR-508445. **(B)** White blood cell count of NSG mice treated with vehicle control or the indicated dose of KZR-508445 for 14 days. **(C)** Hemoglobin levels of NSG mice treated with vehicle control or the indicated dose of KR-508445 for 14 days. **(D)** Platelet count of NSG mice treated with vehicle control or the indicated dose of KZR-508445 for 14 days. **(E)** Fold change in the MFI of CD62L on CD45+ cells in the peripheral blood of NSG mice 24 hours after *in vivo* treatment under the indicated conditions. Statistical significance was assessed using one-way ANOVA with Tukey's method for multiple comparisons adjustment. ****$p<0.0001$, ***$p<0.001$, **$p<0.01$, *$p<0.05$.

# Chapter 8: Ruxolitinib Sensitizes CD8 T-Cells to Dexamethasone-Induced Apoptosis in a Preclinical Model of Hemophagocytic Lymphohistiocytosis

8.1: Abstract

Hemophagocytic lymphohistiocytosis (HLH) is a severe hyperinflammatory syndrome characterized by excessive immune system activation, leading to hypercytokinemia and life-threatening organ damage. Frontline therapy for HLH consists primarily of the glucocorticoid dexamethasone (DEX) and the chemotherapeutic agent etoposide. Many patients, however, are refractory to treatment or relapse after an initial response, resulting in a five-year survival rate of only 61%. Recently, there has been considerable interest in targeting cytokines or their downstream signal transduction effectors as a means of improving clinical outcomes. Many HLH-associated cytokines activate the JAK/STAT pathway, and the JAK1/2 inhibitor ruxolitinib (RUX) has shown efficacy in murine models of HLH and in clinical case reports of refractory HLH. Importantly, JAK/STAT signaling has been shown in other disease contexts to induce DEX resistance in T cells, which are key drivers of HLH. We therefore hypothesized that cytokine-mediated JAK/STAT signaling might contribute to DEX resistance in HLH and that this could be overcome by combination treatment with RUX. Here, we show that plasma from HLH patients confers resistance to DEX in human CD8 T cells. Using lymphocytic choriomeningitis virus to induce an HLH-like disease in perforin-null mice, we further demonstrate that DEX and RUX act cooperatively *in vivo* to attenuate a number of disease parameters. Mechanistically, we establish that the hypercytokinemia of HLH reduces the apoptotic potential of CD8 T cells, leading to relative DEX resistance. Upon concomitant exposure to RUX, this apoptotic potential is restored, thereby sensitizing CD8 T cells to DEX-induced apoptosis.

8.2: Introduction

Hemophagocytic lymphohistiocytosis (HLH) is a hyperinflammatory disease caused by primary or acquired defects in immune function, often in mediators of cellular cytotoxicity. In this setting, stimuli such as infections, malignancies, or autoimmunity appropriately activate the

immune system, but the immune system is unable to control the trigger. The resulting inability to terminate the immune response leads to excessive expansion and activation of innate immune cells and CD8 T cells. These cells in turn secrete large quantities of inflammatory cytokines, producing a cytokine storm that both drives further activation of immune cells and mediates many of the clinical manifestations of HLH, including fever, cytopenias, hyperferritinemia, and multiorgan damage (336).

Most patients who meet the clinical criteria for a diagnosis of HLH are treated according to the HLH-94 or HLH-2004 protocols, which rely primarily on immunosuppression mediated by the glucocorticoid (GC) dexamethasone (DEX) and the chemotherapeutic agent etoposide. If left untreated, HLH is uniformly fatal. Even with treatment, the five-year overall survival rate on the HLH-2004 trial was only 61% (38), reflecting the fact that many patients are refractory to therapy and many more relapse after an initial therapeutic response. As a result, there is significant interest in identifying novel therapeutic agents, including those that may act in conjunction with existing frontline therapies to enhance these clinical outcomes.

The development of these novel therapeutic approaches requires a thorough understanding of the mechanisms of disease pathogenesis. Notably, the hypercytokinemia of HLH is an important mediator of both disease progression and end organ damage (336). One therapeutic strategy, then, involves targeting cytokines themselves or the signal transduction pathways triggered by activation of the corresponding cytokine receptors. One such HLH-associated cytokine is interferon-γ (IFN-γ), and the FDA recently approved emapalumab, a human monoclonal antibody against IFN-γ, for the treatment of pediatric and adult HLH, representing the first approval of a cytokine-directed therapy for HLH (40). IFN-γ, as well as the majority of other cytokines implicated in HLH, exert their cellular effects through activation of the Janus kinases (JAKs), which in turn activate the signal transducer and activator of transcription (STAT) family of transcription factors. Given its central role in cytokine receptor signaling, the

JAK/STAT pathway represents an attractive therapeutic target with the potential to modulate both IFN-γ-mediated effects as well as the effects of a multitude of other cytokines. Indeed, multiple studies in murine models of primary and secondary HLH have revealed that the JAK1/2 inhibitor ruxolitinib (RUX) effectively improves HLH pathology (42,337,338). Similarly, a number of case reports have demonstrated the efficacy of RUX as a salvage therapy for refractory HLH (339,340). However, while RUX has shown efficacy as a single agent in refractory disease, it is currently unknown whether RUX may be effectively used in combination with DEX.

As evidence in favor of a combinatorial approach, we previously demonstrated that cytokine-mediated JAK/STAT signaling confers DEX resistance in T cell acute lymphoblastic leukemia (T-ALL) cells (132,254). GCs, including DEX, act by binding to a cytoplasmic GC receptor (GR) that translocates to the nucleus upon ligand binding (1) where it acts as a transcription factor to activate a gene expression program that induces apoptosis in lymphoid cells (49). We demonstrated in T-ALL cells that the activation of STAT5 in response to the common gamma chain (cγ) cytokine interleukin-7 (IL-7) results in the upregulation of the anti-apoptotic protein BCL-2, which antagonizes this DEX-induced apoptotic program. Importantly, combined treatment with RUX overcame IL-7-induced DEX resistance (254). In the context of HLH, many disease-associated cytokines similarly induce gene expression changes that promote cell survival, thereby creating the potential to interfere with DEX-induced apoptosis. In light of our previous findings in T-ALL, we hypothesized that the rampant hypercytokinemia of HLH and the excessive activation of the JAK/STAT signaling pathway may facilitate a similar mechanism of DEX resistance, which may in turn contribute to poor clinical outcomes in HLH. We therefore evaluated the feasibility and efficacy of combining DEX and RUX as a potential rational therapeutic strategy in the treatment of HLH.

In the current study, we demonstrate that the cytokine composition of plasma from patients with HLH contains elevated levels of cγ cytokines and is indeed sufficient to confer DEX

resistance in CD8 T cells. Using the *Prf1*^{−/−} model of primary HLH, we further show that DEX and RUX cooperatively attenuate many manifestations of disease. Mechanistically, we demonstrate that the hypercytokinemia of HLH increases expression of pro-survival proteins in CD8 T cells, thus reducing the apoptotic potential of these cells to a point where DEX is no longer sufficient to induce apoptosis. We show that concomitant treatment with RUX lowers the apoptotic threshold of CD8 T cells, thereby restoring DEX sensitivity. These findings have important clinical implications, as they demonstrate that a therapeutic strategy combining DEX and RUX has the potential to more effectively control hyperinflammation and immunopathology in HLH and related cytokine storm syndromes.

8.3: Results

The cytokine composition of plasma from patients with HLH confers DEX resistance in CD8 T cells

DEX is a central component of therapy for patients with HLH, but the persistence of poor clinical outcomes on recent trials suggests that DEX resistance may be an important therapeutic obstacle. We previously demonstrated that cytokine-mediated JAK/STAT signaling confers DEX resistance in T-ALL cells (132,254). Given that HLH is characterized by both hypercytokinemia and excessive activation and expansion of CD8 T cells, we hypothesized that a similar mechanism of cytokine-induced DEX resistance might contribute to poor clinical outcomes in these patients. To test this hypothesis, we obtained plasma from patients with HLH and from healthy controls representing a similar distribution of ages and genders and confirmed that a number of disease-associated proteins were significantly elevated in the plasma from the HLH patients (Supplemental Figure 8-1A). We then activated and expanded human CD8 T cells from a single healthy donor and exposed the same T cells to plasma from control or HLH patients

and assessed viability following treatment with DEX. A significant proportion of the plasma samples from HLH patients induced DEX resistance in these CD8 T cells (Figure 8-1A).

Given our previous findings that IL-7-mediated signaling through the JAK/STAT5 axis is sufficient to confer DEX resistance in T-ALL cells (132,254), we asked whether IL-7 and other cγ cytokines were elevated in the plasma from HLH patients. When compared to the plasma from healthy controls, a number of plasma samples from the HLH patients contained high levels of these cytokines, especially IL-7 and IL-15 (Figure 8-1B). Subsequent analyses focused on IL-2, -4, -7, -9, and -15, as these were elevated above the level in the control samples in at least a subset of HLH plasma samples. To determine whether any of these cytokines independently confer DEX resistance, we exposed human CD8 T cells to DEX in the presence or absence of recombinant cytokine and found that all of these cytokines resulted in some degree of resistance (Figure 8-1C). Furthermore, the extent to which each cytokine protected CD8 T cells from DEX-induced cell death was directly proportional to the extent to which each cytokine activated STAT5 (Figure 8-1D), consistent with our previous finding that STAT5 mediates cytokine-induced DEX resistance in T cells (254).

DEX and RUX cooperatively enhance treatment of a murine model of HLH

The finding that cytokine-induced DEX resistance in CD8 T cells correlates with the degree of JAK/STAT5 pathway activation suggests that inhibition of this pathway may enhance DEX sensitivity. Thus, we reasoned that inhibiting JAK1/2 with RUX might augment DEX responses in an *in vivo* model of HLH. To test this, we employed a previously described murine model of primary HLH (338) to ask whether combining DEX with RUX more effectively attenuates disease manifestations relative to treatment with DEX alone. In this model, *Perforin 1* knockout (*Prf1$^{-/-}$*) mice are infected with LCMV-Armstrong, which induces an HLH-like disease that accurately recapitulates many features of human disease (Figures 8-2A-G and Supplemental Figure 8-2A). Levels of the cγ cytokines IL-2 and IL-7 were also markedly

172

increased in the serum of infected animals (Supplemental Figure 8-2B). We first determined that

a DEX dose of 1.5mg/kg/day is sufficient to induce observable modulation of disease

parameters (Supplemental Figures 8-2C-E) and utilized this dose for subsequent combination

experiments. Beginning on day 4 post infection (p.i.), we treated mice with DEX alone or in

combination with RUX-supplemented rodent chow (Incyte), and animals were monitored for

morbidity and mortality. While this dose of DEX did not improve weight loss (Figure 8-2A), it did

significantly extend survival relative to vehicle-treated animals, though all animals in both of

these groups succumbed to disease by day 16 p.i. (Figure 8-2B). In mice treated with RUX

alone or RUX in combination with DEX, there was no observed weight loss or reduction in

survival relative to naïve mice (Figure 8-2A-B).

In a more detailed analysis of disease, naïve and vehicle- and drug-treated LCMV-

infected animals were examined for anemia, thrombocytopenia, and organomegaly. Consistent

with the observed weight loss pattern, RUX treatment, both alone and in combination with DEX,

restored hematocrit and platelet values to those seen in naïve mice, while DEX alone did not

significantly alter these parameters (Figures 8-2C-D). LCMV-infected $Prf1^{-/-}$ mice develop

severe splenomegaly, and while both DEX and RUX demonstrated moderate single agent

effects to reduce spleen size, combination treatment resulted in spleen sizes that were

indistinguishable from naïve mice (Figure 8-2E). We next evaluated innate immune cell

populations in the spleen and found that while neither drug effectively reduced monocyte

numbers (Figure 8-2F), JAK inhibition reduced numbers of neutrophils, and this effect was

significantly enhanced upon combined exposure to DEX (Figure 8-2G). Concordantly, the area

of liver tissue infiltrated by neutrophils in infected mice was also significantly improved with

combination treatment (Supplemental Figure 8-3A).

The combination of DEX and RUX targets activated CD8 T cells

The GC DEX is primarily used in HLH due to its lymphotoxic effects, so we next analyzed vehicle- and drug-treated mice for disease parameters associated with CD8 T cells, which are known to be important drivers of disease (336). Consistent with this, splenic CD4 T cells are not elevated in this model, though numbers were reduced upon drug exposure (Supplemental Figure 8-3B). Overall numbers of splenic CD8 T cells were significantly reduced in treated mice, with the greatest reduction observed in animals treated with the combination of DEX and RUX (Figure 8-3A). Examination of the liver by immunohistochemistry (IHC) also revealed a significant reduction in CD8 T cell infiltration in the mice treated with both DEX and RUX (Figure 8-3B). In order to better understand the activation status of these T cells, we further quantified the numbers of CD8 T cells expressing known activation markers in vehicle- and drug-treated LCMV-infected *Prf1*^{-/-} mice. With respect to effector-like CD8 T cells (CD44hi, CD62Llo), combination treatment reduced cell numbers to nearly half those of vehicle-treated mice, while neither agent alone produced such a dramatic effect (Figure 8-3C). Similarly, numbers of CD8 T cells expressing both the costimulatory molecules CD28 and ICOS were significantly reduced with RUX treatment, and even more so when RUX was combined with DEX (Figure 8-3D). Interestingly, this reduction in the number of activated CD8 T cells was associated with a reduction in the number of these cells expressing the IL-2 receptor CD25 and in the levels of soluble CD25 in the serum (Figures 8-3E-F).

Activation of STAT5 confers DEX resistance in CD8 T cells in vitro

We next sought to understand the mechanistic basis for the cooperative effects of DEX and RUX in this model. Since severe hypercytokinemia is a hallmark feature of HLH, and because it has been previously demonstrated that cytokine receptor signaling via the JAK/STAT5 pathway interferes with DEX-induced apoptosis in primary human T-ALL cells and

in populations of murine thymocytes (254), we hypothesized that the cooperative effect of DEX and RUX on CD8 T cells *in vivo* may be due to enhanced DEX sensitivity as a result of RUX-mediated inhibition of cytokine receptor signaling. To facilitate further mechanistic investigation, we returned to an *ex vivo* system using isolated, activated murine CD8 T cells. We first confirmed that these murine CD8 T cells recapitulate the DEX resistance phenotype that we observed in human CD8 T cells, in which the cγ chain cytokines IL-2, -7, and -15 induce a significant increase in pSTAT5 but not in pSTAT1 or pSTAT3 (Supplemental Figure 8-4A), consistent with reports that STAT5 is the predominant downstream effector of these cytokine receptors (25). Similarly, we confirmed that all three of these cytokines confer resistance to DEX in murine CD8 T cells (Figure 8-4A). Additionally, we established that this resistance phenotype is independent of an underlying genetic defect in cytotoxic function, as we observed equivalent IL-2-induced DEX resistance in CD8 T cells isolated from both wild-type and *Prf1*^{-/-} mice (Supplemental Figure 8-4B). As a result, all subsequent mechanistic analyses were performed using CD8 T cells from wild-type mice.

In addition to the cγ cytokines, cytokines from many other families are elevated in the plasma of patients with HLH (Supplemental Figure 8-1) and in the serum of LCMV-infected *Prf1*^{-/-} mice (Supplemental Figure 8-2A), so we assessed the effect of a number of these other cytokines on DEX sensitivity in CD8 T cells. We observed that, in addition to the cγ cytokine IL-2, only IL-12 conferred any resistance to DEX, while TNF-α, IFN-γ, IL-6, IL-1β, and IL-10 did not (Figure 8-4B). Furthermore, the effects of IL-2 and IL-12 on drug sensitivity were specific to DEX, as we did not detect any IL-2- or IL-12-induced resistance to etoposide, another lymphotoxic agent used in frontline treatment for HLH (Figure 8-4C). Consistent with the pattern of DEX resistance and pSTAT5 activation observed in human CD8 T cells, only IL-2 and IL-12 induced a significant increase in pSTAT5 in murine CD8 T cells, while neither IL-6 nor IFN-γ, two other cytokines that signal through pSTAT5 in other cell types, activated STAT5 under

these conditions (Figure 8-4D and Supplemental Figure 8-4C). Due to the significant DEX resistance observed upon IL-2 exposure, we used IL-2 as a tool in subsequent experiments to evaluate the mechanistic basis for this resistance phenotype. We found that IL-2 induces DEX resistance in a dose-dependent manner, with significant IL-2-induced resistance observed even at very low concentrations of IL-2 (Supplemental Figure 8-4D). To further confirm that this resistance is mediated by JAK/STAT signaling, we asked whether RUX could overcome the IL-2-mediated induction of pSTAT5 and restore DEX sensitivity. CD8 T cells were pre-treated with varying concentrations of RUX for one hour and stimulated with IL-2. RUX abrogated the cytokine-induced increase in pSTAT5 (Figure 8-4E) and completely overcame the associated DEX resistance (Figure 8-4F) in a manner that was both dose-dependent (Figures 8-4E-F) and synergistic with DEX (Figure 8-4G). This was consistent with the RUX-induced reduction in pSTAT5 observed following *in vivo* drug exposure (Supplemental Figure 8-4D). Thus, cytokines that activate STAT5 in CD8 T cells, including those that are known to be pathologically relevant in HLH such as IL-12 and especially cγ cytokines such as IL-2, result in resistance to DEX that is effectively overcome upon concomitant treatment with RUX.

IL-2 inhibits DEX-induced apoptosis of CD8 T cells by altering the balance of BH3 proteins

        To further understand the mechanistic basis for IL-2-induced DEX resistance in CD8 T-cells, we first asked whether IL-2 directly interferes with GR signaling. To determine whether IL-2 receptor (IL-2R) signaling and the resulting activation of pSTAT5 impairs nuclear translocation of ligand-activated GR, we assessed GR nuclear localization in CD8 T cells treated with DEX in the presence or absence of IL-2. We observed that both total and S211 phosphorylated GR, which represents a transcriptionally active modification, effectively co-localized to the nucleus with pSTAT5, suggesting that IL-2R signaling does not impair nuclear translocation of ligand-activated GR (Figure 8-5A). Similarly, IL-2R signaling did not interfere with the capacity for GR to activate gene transcription, as revealed by transcript expression of known direct GR target

genes following treatment with DEX in the presence or absence of IL-2 (Figure 8-5B). Since IL-2 had no effect on GR localization or transcriptional activation, these data suggest that GR signaling remains intact in the presence of IL-2.

DEX has well-established effects on modulation of the intrinsic apoptotic pathway in lymphocytes (18,49), and STAT5 has been shown to directly regulate anti-apoptotic components of this pathway in T-cells (299). We therefore hypothesized that IL-2R signaling may alter the apoptotic potential of CD8 T-cells, making them refractory to the pro-apoptotic effects of DEX. To test this, we first measured expression of anti-apoptotic BCL-2 family members, all of which are STAT5 target genes (299), following exposure to IL-2. CD8 T cells exposed to IL-2 upregulated protein expression of BCL-2, BCL-xL, and MCL-1. Importantly, RUX treatment restored expression of all three anti-apoptotic proteins to basal levels, confirming that these proteins are induced downstream of the IL-2R/JAK/STAT pathway (Figure 8-5C).

In order to determine the functional significance of these changes in protein expression, we utilized BH3 profiling to assess the apoptotic potential of CD8 T-cells treated under these various conditions. In an analysis of CD8 T cells cultured *ex vivo* with DEX with or without IL-2, DEX alone induced a significant increase in priming with respect to BCL-2, BCL-XL, and MCL-1 activity. Consistent with the finding that IL-2 confers DEX resistance, we found that the apoptotic potential of CD8 T cells was significantly reduced in the presence of IL-2, such that DEX was no longer able to increase apoptotic priming. Exposing the cells to RUX, however, blocked IL-2R signaling and was sufficient to restore the basal apoptotic potential of CD8 T-cells. Furthermore, with the addition of RUX, DEX was again capable of increasing apoptotic priming, consistent with the finding that RUX synergizes with DEX in the presence of IL-2 (Figure 8-6A). Finally, to test the relevance of these findings *in vivo*, we performed BH3 profiling on CD8 T cells harvested from naïve and vehicle- and drug-treated LCMV-infected *Prf1*$^{-/-}$ mice. As with the *ex vivo* findings, cells from vehicle-treated LCMV-infected mice showed a reduction in apoptotic potential relative to naïve mice, and this reduction was effectively overcome upon exposure to

DEX and RUX (Figure 8-6B). Taken together, these results support a model in which the hypercytokinemia of HLH, and in particular the elevated levels of cγ cytokines, signal through STAT5 to upregulate anti-apoptotic proteins that protect CD8 T cells from DEX-induced cell death. This effect is inhibited by the JAK1/2 inhibitor RUX, which re-sensitizes cytokine-exposed CD8 T cells to apoptosis and synergizes with DEX to effect cell death.

8.4: Discussion

Survival rates for patients diagnosed with HLH remain at 61% (38), owing to the fact that many patients are refractory to current frontline therapy and many more who experience an initial therapeutic response ultimately relapse. Therefore, there is a considerable need for the development of novel therapeutic strategies to enhance the efficacy of frontline therapy. Hypercytokinemia is a hallmark feature of HLH, and many disease-associated cytokines signal via the JAK/STAT pathway. CD8 T cells both secrete and respond to these cytokines, making them an important cellular target of HLH therapy (336). DEX is therefore a central component of frontline therapy for HLH due to its potent lymphotoxic effects. However, cytokine receptor signaling has been shown to mediate DEX resistance in a number of disease contexts, including asthma (341–344) and T cell leukemia (132,254). We therefore hypothesized that the cytokines associated with HLH may induce relative DEX resistance in CD8 T cells, thereby contributing to these poor clinical outcomes.

In the current study, we found that cytokines from nearly all cytokine classes were elevated in the plasma from HLH patients. In particular, this analysis revealed a previously under-appreciated elevation in the cγ cytokines IL-7 and IL-15, which exert a multitude of critical, well-described effects on T-cell biology (43). Importantly, we showed that plasma from these patients uniformly attenuated DEX sensitivity in CD8 T cells. Using recombinant cytokines to test the sufficiency of cytokine receptor activation for DEX resistance, we found that only those

cytokines that significantly activate STAT5 in CD8 T cells impaired DEX sensitivity. We went on to demonstrate the feasibility and efficacy of a combined therapeutic strategy involving DEX and the JAK1/2 inhibitor RUX in an *in vivo* model of HLH. Here, we found that DEX and RUX cooperatively attenuated many disease manifestations, and in particular showed strong cooperativity with respect to reducing both the absolute numbers of CD8 T cells as well as the numbers of activated CD8 T cells. Mechanistically, we demonstrated that cytokine exposure results in a significant reduction in the apoptotic potential of CD8 T cells, rendering them refractory to the pro-apoptotic effects of DEX. Both *in vivo* and *ex vivo*, we showed that RUX-mediated restoration of this apoptotic potential underlies the synergistic interaction between DEX and RUX.

While we observed improvement in many disease parameters upon combined treatment with DEX and RUX *in vivo*, our mechanistic findings suggest that this combination may be particularly effective due in large part to combinatorial effects on CD8 T cells. Importantly, compelling data demonstrate the necessity of CD8 T cells to the pathogenesis of HLH. In healthy immune responses, immune homeostasis is restored upon clearance of the initiating trigger and subsequent termination of the immune response. CD8 T cells are critical effectors of this process, as they function to target infected or malignant cells directly and to inhibit both the antigen presenting cells (APCs) that promote further T cell activation as well as other T cells themselves through a process known as fratricide (345). Consistent with this critical homeostatic function, mice engineered to produce T cells with impaired perforin- or Fas-dependent killing of APCs have exacerbated HLH-like disease, and depletion of CD8 T cells in this model is protective against HLH (36,346). Mechanistically, this protective effect can be attributed to continued expansion and activation of immune cells in the absence of CD8 T cell cytolytic activity, a process that both requires and results in the production of cytokines, particularly cγ cytokines (347). This central role for CD8 T cells in disease pathogenesis underlies the utility of DEX as a lymphotoxic agent in the treatment of this disease. However, as demonstrated in the

current study, the cγ cytokines IL-2, -7, and -15 potently antagonize DEX-induced apoptosis. Our findings, in conjunction with the established role for CD8 T cells and cγ cytokines in the pathogenesis of HLH, therefore suggest that a therapeutic strategy combining DEX and RUX has the potential to both enhance CD8 T cell killing and attenuate cytokine-mediated contributions to disease progression.

In addition to HLH, DEX is widely used for its immunosuppressive properties in a multitude of other clinical contexts. While our study centered on a model of primary HLH, this paradigm of cytokine-induced DEX resistance has been observed in many other DEX-treated diseases, suggesting that our mechanistic findings have relevance and implications beyond the treatment of HLH. The mechanisms by which T cells become resistant to DEX are not fully elucidated, but it is clear that cytokine signaling plays an important role. Treatment of mouse thymocytes with IL-2 induces expression of pro-survival transcription factors such as c-Fos, AP-1, and c-Myc, and increases NFκB activity (348). Additionally, many cytokines induce expression of the pro-survival protein BCL-2, which directly antagonizes the pro-apoptotic molecule BIM. Consistent with these findings, treatment of human leukemic T cells with cytokines such as IL-2, IL-4, and IL-7 induces resistance to DEX-induced cell death, with IL-7 increasing expression of BCL-2 (132,248,249). Altogether, cytokine-induced DEX resistance is often mediated by the modulation of the levels of the BH3 proteins BCL-2 and BIM, effectors of apoptosis (18,349). Here, we see that cγ cytokines and other cytokines that activate STAT5 in CD8 T cells, such as IL-12, confer DEX resistance in a manner proportional to their degree of STAT5 activation. This likely depends on the induction of expression of a variety of anti-apoptotic molecules downstream of pSTAT5 activity. While we observe increases in the expression of and functional relevance of BCL-2, BCL-xL, and MCL-1, the most relevant survival protein for DEX resistance may be cell and disease context-dependent. Because of this variability and redundancy in pro-survival protein function, our findings indicate that targeting the

upstream JAK/STAT signaling is more therapeutically attractive than targeting these proteins themselves.

While our findings provide compelling evidence for a therapeutic strategy combining DEX and RUX for the treatment of HLH, there are also several important limitations of this work. First, as demonstrated in our own patient cohort, cytokine profiles in the plasma from patients with HLH are highly variable, including with respect to the cγ cytokines. This heterogeneity likely reflects the considerable diversity in the underlying etiology of disease amongst patients meeting the diagnostic criteria for HLH (37). Importantly, our study relies upon a genetic model of primary HLH, a disease entity known to be driven in large part by excessive CD8 T cell activity. Other related hyperinflammatory diseases, such as macrophage activation syndrome (MAS), are known to be significantly less T cell-dependent and may therefore have a distinct plasma cytokine composition (350). Our findings suggest that synergistic effects on T cells underlie the efficacy of this combined strategy, and further studies are needed to elucidate the clinical potential for combining DEX and RUX in other hyperinflammatory conditions. However, as RUX inhibits signaling downstream of all JAK1/2-activating cytokine receptors regardless of the initiating ligand and cytokine receptor, the use of RUX in combination with DEX likely has broader applicability to these other conditions.

Importantly, a therapeutic strategy combining DEX and RUX has the potential for imminent clinical translation. DEX is already a component of frontline therapy for HLH (38). Due to relatively poor clinical outcomes on currently established treatment protocols, the ethical introduction of novel therapeutic agents into future protocols will require combination with existing standard of care. The safety and efficacy of RUX has already been established, including in pediatric populations (351), suggesting the feasibility of adding RUX to existing treatment protocols for HLH. Furthermore, although HLH is a rare immunological disorder, hyperinflammation is a shared feature of many diseases for which DEX is a critical component of therapy. We believe that the findings presented here support a role for combining DEX and

RUX as a means of more effectively controlling inflammation and reducing the associated immunopathology in HLH and related cytokine storm syndromes.

8.5: Methods

Study Design

For the preclinical trial experiments in this study, sample sizes were selected based on previous experience with this model (42), which demonstrated that the chosen sample sizes were sufficient to identify differences between treatment groups. Sample sizes were not altered during the course of the study. *In vivo* treatment was terminated on day 8, which was defined prior to the initiation of the experiment and was consistent with previous applications of this model (42). For all experiments, endpoints were prospectively selected and were based on the peak of the CD8 T cell response to LCMV or humanely defined in protocols approved by the Institutional Animal Care and Use Committees of St. Jude Children's Research Hospital. Outliers were removed using one-way ANOVA with Grubb's test. All experiments presented in this study were performed on a minimum of four biological replicates, and when indicated in the corresponding figure legends, data are presented as the combined analysis from two independent experiments.

The objective of this study was to assess the utility of combining the JAK inhibitor RUX with the GC DEX, as we hypothesized that the hypercytokinemia associated with HLH may impair DEX sensitivity. This study utilized plasma samples from patients with HLH, an *in vivo* genetic model of primary HLH, and *ex vivo* analysis of human and murine CD8 T cells. The preclinical trial constituted a controlled laboratory experiment in which mice were randomized to receive vehicle control, DEX alone, RUX alone, or the combination of DEX and RUX. Due to the nature of drug administration, researchers were not blinded to treatment groups.

Patient Samples

Pre-treatment plasma samples were obtained from 15 pediatric patients with confirmed primary or secondary HLH who were treated at Texas Children's Hospital. Control plasma was obtained from pediatric patients of a similar age and gender distribution who were treated at Texas Children's Hospital for non-inflammatory conditions. Studies were performed according to protocols approved by the Institutional Review Board of Baylor College of Medicine.

Mice

Perforin-deficient (C57BL/6 *Prf1*tm1Sdz/J) and WT (C57BL/6-J) mice were purchased from the Jackson Laboratory and subsequently bred and maintained in specific pathogen-free facilities at St. Jude Children's Research Hospital or the University of California, San Francisco. Experimental animals were age- and sex-matched and were used at 6 to 12 weeks of age. All animal experiments were conducted following protocols that were approved by the Institutional Animal Care and Use Committees of St. Jude Children's Research Hospital or the University of California, San Francisco.

Primary HLH model and in vivo *treatment*

LCMV-Armstrong was originally provided by John Wherry (University of Pennsylvania) and propagated in BHK (CL-13) cells as previously described (ref). *Prf1*$^{-/-}$ mice were infected with 2×10^5 plaque forming units (pfu) of LCMV via intraperitoneal injection. Beginning on day 4 post-injection, mice were treated with vehicle control, DEX alone, RUX alone, or the combination of DEX and RUX. DEX was administered at 1.5mg/kg/day by intraperitoneal injection, with the exception of the survival study (Supplemental Figure 8-2B), where DEX was administered ad lib in drinking water containing 7.5μg/mL of DEX. RUX was administered ad lib in modified rodent chow (Incyte) containing 2g RUX per 1kg of chow, resulting in a dose of approximately 60mg/kg/day. For most experiments, treatment continued through day 8 post-

infection, and animals were sacrificed for analysis the following morning. For the survival study, treatment extended from day 7 to 17, and mice were sacrificed when moribund or at the termination of the study on day 17. For analysis of pSTAT5 in CD8 T cells following *in vivo* drug treatment, mice received one dose of 1.5 mg/kg DEX, 60mg/kg RUX, or both via intraperitoneal injection on day 4 p.i., and animals were sacrificed 12 hours later.

T cell activation and expansion

For isolation of human CD8 T cells, TRIMA residuals enriched for peripheral blood mononuclear cells (PBMCs) were obtained from the Vitalant blood bank. PBMCs were isolated using a Ficoll (GE Healthcare) density gradient in a SepMate PBMC Isolation Tube (STEMCELL Technologies). 5×10^7 cells were labeled with biotinylated antibodies against CD4 (clone A161A1; BioLegend), CD19 (clone HIB19; BioLegend), CD11b (clone ICRF44; BioLegend), CD24 (clone ML5; BioLegend), and B220 (clone RA3-6B2; Biolegend). Negative selection was performed by depleting biotin-labeled cells with Biotin Binder Dynabeads (Life Technologies). The remaining cells were cultured in RPMI (Mediatech) supplemented with 10% fetal bovine serum (VWR), glutamine, antibiotics, and 20ng/mL recombinant human IL-2 (Peprotech). Cells were activated by the addition of Human T-Activator CD3/CD28 Dynabeads (Life Technologies).

Murine CD8 T cells were isolated from the spleens of WT or *Prf1*^{-/-} C57BL/6 mice. Red blood cell lysis was performed and CD8 T cells were isolated using negative selection with Biotin Binder Dynabeads following staining of 5×10^7 cells with biotinylated antibodies against CD4 (clone GK1.5; Biolegend), CD19 (clone 6D5; BioLegend), CD11b (clone M1/70; BioLegend), CD24 (M1/69; BioLegend), and B220 (RA3-6B2; BioLegend). The remaining cells were cultured in DMEM (Mediatech) supplemented with 20% fetal bovine serum, glutamine, non-essential amino acids, sodium pyruvate, HEPES, antibiotics, 2-mercaptoethanol, and 20ng/mL recombinant murine IL-2 (Peprotech). Cells were activated by the addition of Mouse T-Activator CD3/CD28 Dynabeads (Life Technologies).

Flow Cytometry

For the analysis of murine cell populations from the spleens of vehicle- and drug-treated mice, splenocytes were stained with the following fluorescently-labeled antibodies: TCRβ (clone H57-597), F4/80 (clone BM8.1), NK1.1 (clone PK136), Ly6C (clone HK1.4), CD11c (clone N418), CD11b (clone M1/70), CD8 (clone 53-6.7), CD19 (clone 1D3), Ly6G- (clone 1A8), CD4 (clone GK1.5), CD44 (clone IM7), CD62L (clone MEL-14), and CD25 (PC61.5.3) (eBioscience, Biolegend, Tonbo Biosciences, and R&D Systems). For the analysis of pSTAT5, intracellular IL-2, and for BH3 profiling, CD8 T cells were identified by gating on the TCRβ/CD8 double positive population. All flow cytometry data were acquired with a BD LSRII Fortessa or a BD FACSVerse and analyzed using FlowJo software.

Phosphoflow cytometry for measurement of STAT proteins following cytokine stimulation was performed as previously described (132). Briefly, human or murine CD8 T cells were allowed to rest for one hour in serum free media and were stimulated with recombinant murine or human cytokines (Peprotech) at a concentration of 100ng/mL for 15 minutes unless otherwise indicated. Cells were subsequently fixed with 2% paraformaldehyde and permeabilized with methanol. For analysis of pSTAT5 in CD8 T cells from vehicle- and drug-treated mice, cells were immediately fixed and permeabilized following harvesting from mice. STAT protein staining was performed with antibodies against pSTAT1 pY701 (BD Biosciences), pSTAT3 pY705 (BD Biosciences), and pSTAT5 pY694 (BD Biosciences) and data were recorded as the median fluorescent intensity (MFI).

For the analysis of BCL-2, BCL-XL, and MCL-1 protein expression, murine CD8 T cells were fixed and permeabilized as described above. They were then stained with an anti-cleaved caspase 3 antibody (clone C92-605; BD Biosciences) and with antibodies against BCL-2 (clone BCL/10C4; BioLegend), BCL-XL (clone 54H6; Cell Signaling Technology) or MCL-1 (clone

D2W9E; Cell Signaling Technology) and data were recorded as the MFI in the cleaved caspase 3-negative gate.

T cell viability assays

Human T cell viability assays were performed by culturing human CD8 T cells in plasma obtained from the Vitalant blood bank or from control or HLH patients treated at Texas Children's Hospital. Plasma was supplemented with RPMI 1640 Amino Acids Solution (Sigma-Aldrich), RPMI 1640 Vitamins Solution (Sigma-Aldrich), and D-(+)-Glucose Solution (Sigma-Aldrich). Murine CD8 T cells were cultured in supplemented DMEM, as described above. Cells were aliquoted into a round bottom 96-well plate at 10^5 cells per well and treated with vehicle control (DMSO), DEX (Sigma-Aldrich), and/or RUX (Selleck Chemicals) with or without supplementation with recombinant cytokine for 48 hours for human T cells and 24 hours for murine T cells. To assess viability, cells were stained with Hoechst 33258 (Molecular Probes) and analyzed by flow cytometry. Data were recorded as the percentage of Hoechst-negative cells and all viability data were normalized to the viability of the relevant vehicle control condition.

Complete Blood Counts (CBCs), Histology, and Plasma Protein Quantification

All CBCs and histologic analyses were performed by the veterinary pathology core facilities at St. Jude Children's Research Hospital. For CBCs, heparinized blood samples were analyzed on a Forecyte multi-species hematology system (Oxford Science). For histology and immunohistochemistry (IHC), tissues were fixed in 10% neutral buffered formalin and embedded in paraffin. De-paraffinized sections were stained with hematoxylin and eosin (Richard-Allan Scientific) and labeled with biotinylated antibodies against CD3 (M20, Santa Cruz) or Ly6B.2 (Neut 7/4, Novus Biologicals), which were detected with HRP-labeled streptavidin (Thermo Fisher) and counterstained with hematoxylin. Images were acquired on a ScanScope XT

scanner and digitized to scalable images up to a 20X objective (Leica Biosystems). The area encompassed by inflammatory foci was determined using FIJI image analysis in a blinded fashion.

Plasma protein quantification from human plasma samples was performed using the Milliplex MAP Human Cytokine Panel I (Millipore) for the MagPix instrument. For quantification of proteins from mouse serum, a Milliplex mouse cytokine/chemokine magnetic bead panel (EMD Millipore) was used according to the manufacturer's instructions, and results were collected and analyzed with BIO-Plex 200 System (Bio-Rad) and xPONENT software. Ferritin and sCD25 were measured with ELISA kits (ALPCO and R&D Systems, respectively).

Western blotting

To assess cytoplasmic and nuclear localization of STAT5 and GR, murine CD8 T cells were pre-treated with vehicle control or 10ng/mL IL-2 for one hour prior to treatment with vehicle control or 1µM DEX for 30 minutes. Cytoplasmic and nuclear protein lysates were generated using the NE-PER kit (ThermoFisher). Immunoblotting was performed with the following antibodies: pSTAT5 pY694 (Cell Signaling Technology), total STAT5 (clone D2O6Y; Cell Signaling Technology), GR pS211 (Cell Signaling Technology), total GR (clone D6H2L; Cell Signaling Technology), β-actin (clone 8H10D10; Cell Signaling Technology), and p84 (Genetex). Donkey anti-rabbit IRDye800 and donkey anti-mouse IRDye680 secondary antibodies (LI-COR Biosciences) were used for detection and imaging was performed using the Odyssey Imaging System (LI-COR Biosciences).

Quantitative PCR (qPCR)

For analysis of GR target gene expression, murine CD8 T cells were pre-treated with vehicle control or 10ng/mL IL-2 for one hour prior to treatment with vehicle control or 1µM DEX for four hours. RNA was isolated using the RNeasy Mini Kit (Qiagen) and cDNA was generated

using the Superscript III kit (ThermoFisher). Taqman quantitative PCR probes (Applied

Biosystems) were used in conjunction with Taqman Master Mix (Applied Biosystems) to assess

transcript levels of the following genes: *Gapdh* (Mm99999915_g1; VIC-MGB), *Bcl2l11*

(Mm00437796_m1; FAM-MGB), *Gilz* (Mm00726417_s1; FAM-MGB), and *Fkbp5*

(Mm00487406_m1; FAM-MGB). Experiments were performed in technical triplicate and were

run on a QuantStudio 5 Real-Time PCR Instrument (Applied Biosystems).The fold change in

transcript expression was calculated relative to cells cultured without DEX using the delta-delta

Ct method, with the use of *Gapdh* transcript for normalization.

BH3 Profiling

BH3 profiling was performed according to established methods (13). Briefly, *ex vivo*

activated and expanded murine CD8 T cells were cultured in the presence or absence of

10ng/mL IL-2, 1µM DEX, and 500nM RUX for 16 hours prior to analysis and were subsequently

stained with LIVE/DEAD Fixable Violet Dead Cell Stain (Life Technologies) to facilitate gating on

the live cell population. For analysis of apoptotic potential in CD8 T cells following *in vivo*

treatment, analysis was performed immediately after harvesting cells from mice. Cells were

permeabilized with digitonin (Sigma-Aldrich) and exposed to ABT-199 (ApexBio), WEHI-539

(ApexBio), S63845 (Selleck Chemicals), or NOXA peptide (New England Peptide) at the

indicated concentrations for 90 minutes prior to fixation with paraformaldehyde. Cells were then

stained with an anti-cytochrome c antibody (clone 6H2.B4; BioLegend) and analyzed by flow

cytometry. Cells exposed to alamethicin (Alfa Aesar) or DMSO were used as positive and

negative controls and percent priming was calculated based on the relative cytochrome c

release in cells exposed to BH3 mimetics or NOXA peptide relative to these controls.

Statistical Analyses

Statistical analyses were performed using Prism 8 (GraphPad). All tests were two-sided and the threshold for significance was p≤0.05. Comparisons between groups were made using t-tests, with one-way ANOVA and Tukey's method for multiple comparisons adjustment used for comparisons of three or more groups. For *in vivo* survival analysis, the log-rank test was used to perform pairwise comparisons between survival curves. Interactions between drugs were assessed using Bliss independence analysis (281). Error bars represent the standard error of the mean. Outliers were removed using one-way ANOVA with Grubb's test.

8.6: Acknowledgements

Figure 8-1: The cytokine composition of plasma from patients with HLH confers DEX resistance in CD8 T cells. (A) Viability relative to vehicle control in human CD8 T cells cultured in plasma from control patients or patients with HLH and treated with 1μM DEX for 48 hours. **(B)** Levels of common gamma chain cytokines in plasma from control patients versus patients with HLH. **(C)** Viability relative to vehicle control of human CD8 T cells following exposure to 1μM DEX for 48 hours in the presence or absence of 10ng/mL of the indicated cytokine in technical triplicate. Statistical significance is relative to the no cytokine condition. **(D)** MFI and representative histograms of pSTAT5 in human CD8 T cells following stimulation with 100ng/mL of the indicated cytokine for 15 minutes in technical triplicate. Statistical significance is relative to the basal condition. Statistical significance was assessed using two-sample t-tests (A and B) or one-way ANOVA with Tukey's method for multiple comparisons adjustment (C and D). The data in panels C and D are representative of three independent experiments. ****$p<0.0001$, ***$p<0.001$, **$p<0.01$, *$p<0.05$.
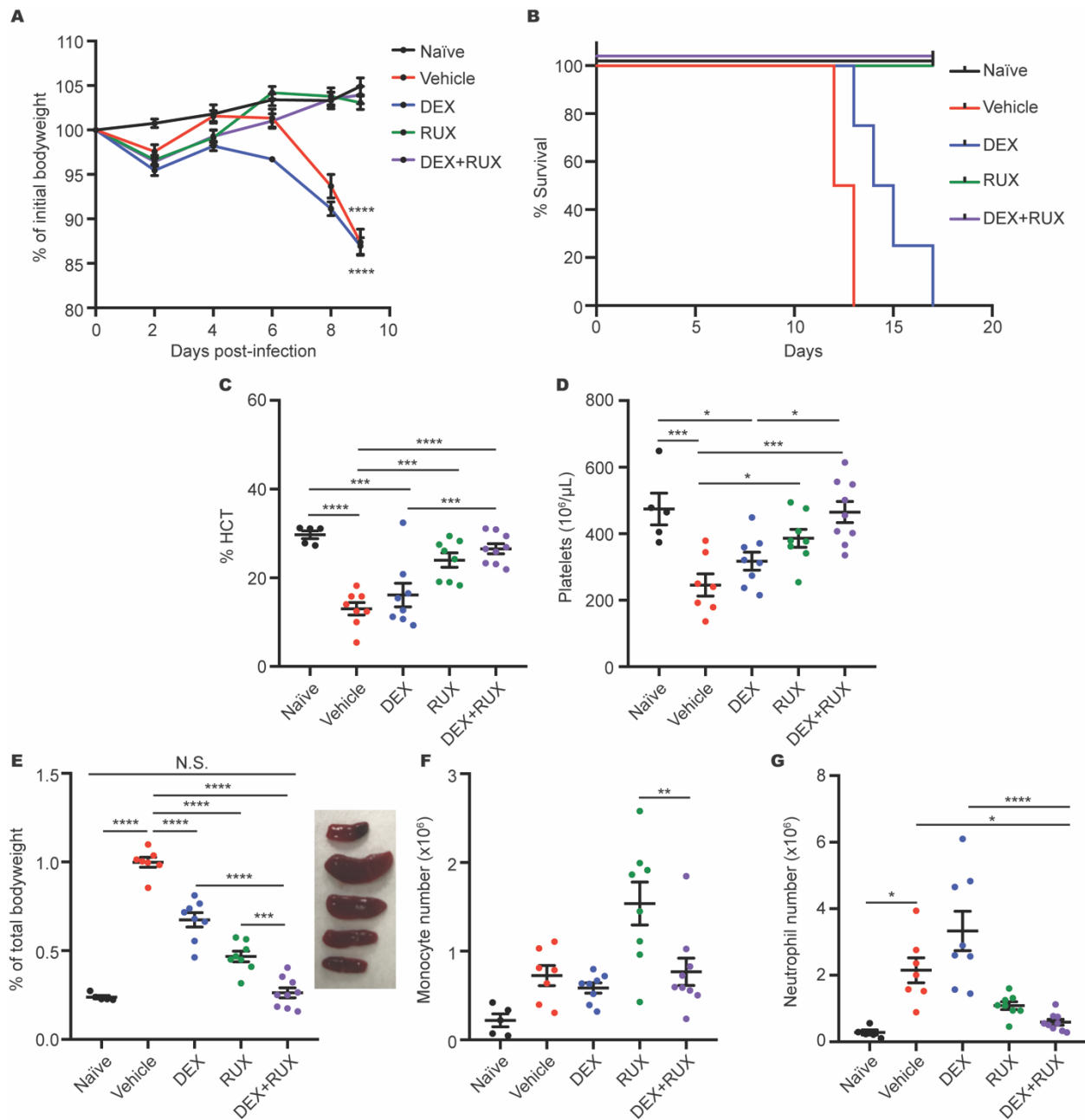
Figure 8-2: The combination of DEX and RUX cooperatively attenuates disease manifestations in an *in vivo* model of HLH. (A) Bodyweight over time relative to baseline bodyweight of naïve mice and vehicle- and drug-treated LCMV-infected mice. Statistical significance is relative to the naïve condition. **(B)** Survival of naïve mice and vehicle- and drug-treated LCMV-infected mice. **(C)** Hematocrit values in naïve mice and vehicle- and drug-treated LCMV-infected mice on day 9 post-infection. **(D)** Platelet count in naïve mice and vehicle- and drug-treated LCMV-infected mice on day 9 post-infection. **(E)** Spleen weight as percentage of initial bodyweight and representative spleen images from naïve and vehicle- and drug-treated LCMV-injected mice on day 9 post-infection. **(F)** Number of monocytes in spleens from naïve and vehicle- and drug-treated LCMV-infected mice on day 9 post-infection. **(G)** Number of neutrophils in spleens from naïve and vehicle- and drug-treated LCMV-infected mice on day 9 post-infection. Statistical significance was assessed using one-way ANOVA with Tukey's

method for multiple comparisons adjustment (A, C-H). With the exception of panel B, all data represent a combined analysis of two independent experiments. ****p<0.0001, ***p<0.001, **p<0.01, *p<0.05, N.S. – not significant.

A

B

Naïve

Vehicle

DEX

RUX

DEX+RUX

C

D

E

F
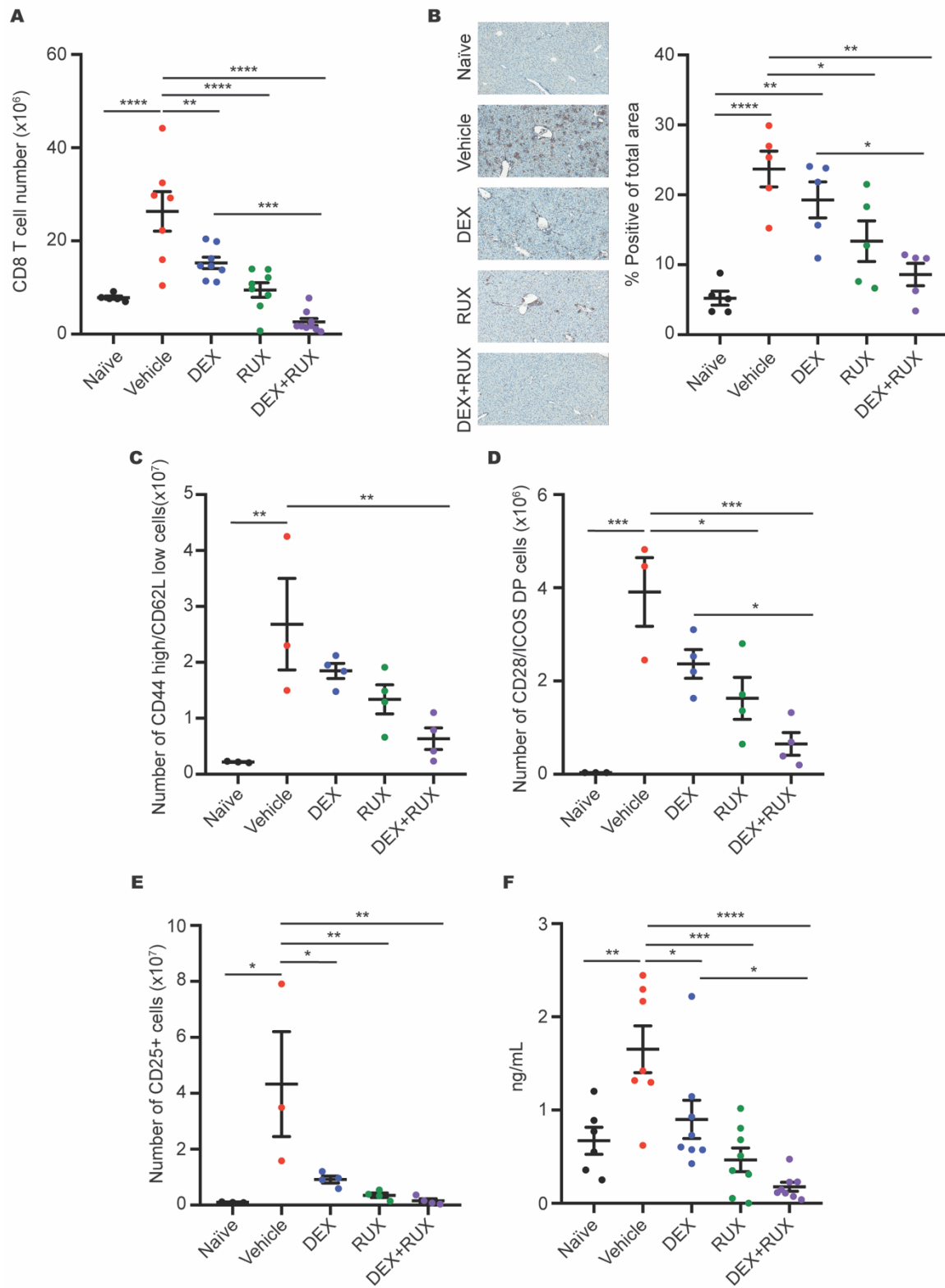
Figure 8-3: The combination of DEX and RUX cooperatively attenuates CD8 T cell number and markers of CD8 T cell activation in an *in vivo* model of HLH. (A) Number of splenic CD8 T cells in naïve and vehicle- and drug-treated LCMV-infected mice on day 9 post-infection. **(B)** Representative histologic images and number of CD3+ cells in livers from naïve and vehicle- and drug-treated LCMV-infected mice on day 9 post-infection. **(C)** Number CD44 high/CD62L low cells in spleens from naïve and vehicle- and drug-treated LCMV-infected mice on day 9 post-infection. **(D)** Number of CD28 and ICOS double positive cells in spleens from naïve and vehicle- and drug-treated LCMV-infected mice on day 9 post-infection. **(E)** Number of CD25 positive CD8 T cells in spleens from naïve and vehicle- and drug-treated LCMV-infected mice on day 9 post-infection. **(F)** Levels of soluble CD25 in plasma from naïve and vehicle- and drug-treated LCMV-infected mice on day 9 post-infection. Statistical significance was assessed using one-way ANOVA with Tukey's method for multiple comparisons adjustment (A-F). The data in panels A and F represent a combined analysis of two independent experiments. ****$p<0.0001$, ***$p<0.001$, **$p<0.01$, *$p<0.05$, N.S. – not significant.
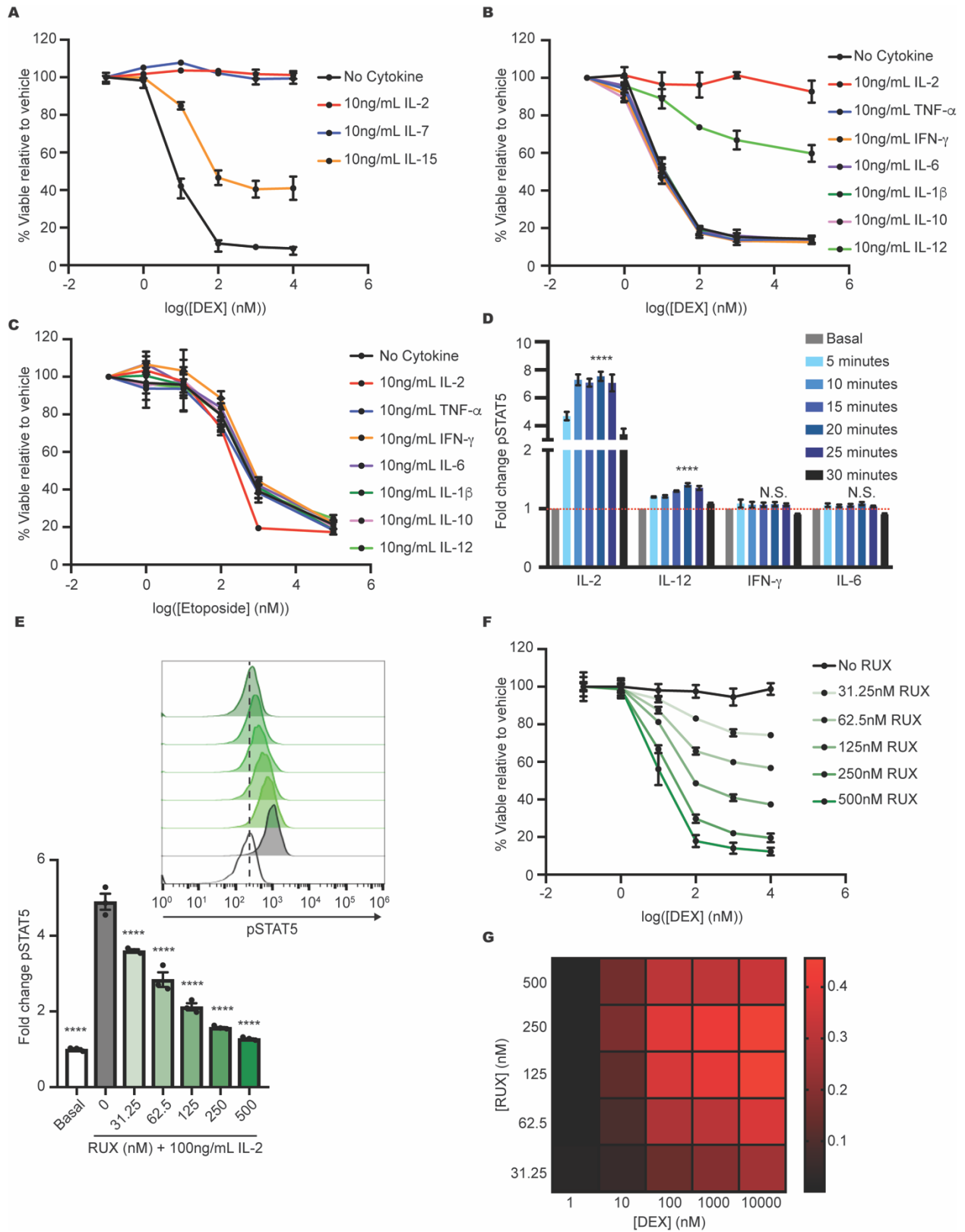
Figure 8-4: Common gamma chain cytokines activate STAT5 and confer DEX resistance in murine CD8 T cells. (A) Viability relative to vehicle control of murine CD8 T cells treated with increasing concentrations of DEX in the absence or presence of 10ng/mL of the indicated common gamma chain cytokine for 24 hours in technical triplicate. **(B)** Viability relative to vehicle control of murine CD8 T cells treated with increasing concentrations of DEX in the absence or presence of 10ng/mL of the indicated cytokine for 24 hours in technical triplicate. **(C)** Viability relative to vehicle control of murine CD8 T cells treated with increasing concentrations of etoposide in the absence or presence of 10ng/mL of the indicated cytokine for 24 hours in technical triplicate. **(D)** Fold change in the MFI of pSTAT5 in murine CD8 T cells stimulated with 100ng/mL of the indicated cytokine for the indicated period of time in technical triplicate. Statistical significance is indicated for the difference between the basal condition and the peak pSTAT5 value for each cytokine. **(E)** Fold change and representative histograms of pSTAT5 in murine CD8 T cells in the basal condition or after one-hour pre-treatment with the indicated concentration of RUX followed by a 15-minute stimulation with 100ng/mL IL-2 in technical triplicate. Statistical significance is relative to the vehicle-treated IL-2-stimulated condition. **(F)** Viability relative to vehicle control of murine CD8 T cells treated with increasing concentrations of DEX in the presence of 10ng/mL IL-2 and the indicated concentration of RUX for 24 hours in technical triplicate. **(G)** Heatmap of Bliss independence scores calculated as the average of technical triplicates of cell viability in murine CD8 T cells treated with the indicated concentrations of DEX and RUX in the presence of 10ng/mL IL2 for 24 hours. Positive values, indicated in red, are indicative of a synergistic interaction. Statistical significance was assessed using two-sample t-tests (D) or one-way ANOVA with Tukey's method for multiple comparisons adjustment (E). All data are representative of three independent experiments. ****$p<0.0001$, ***$p<0.001$, **$p<0.01$, *$p<0.05$, N.S. – not significant.
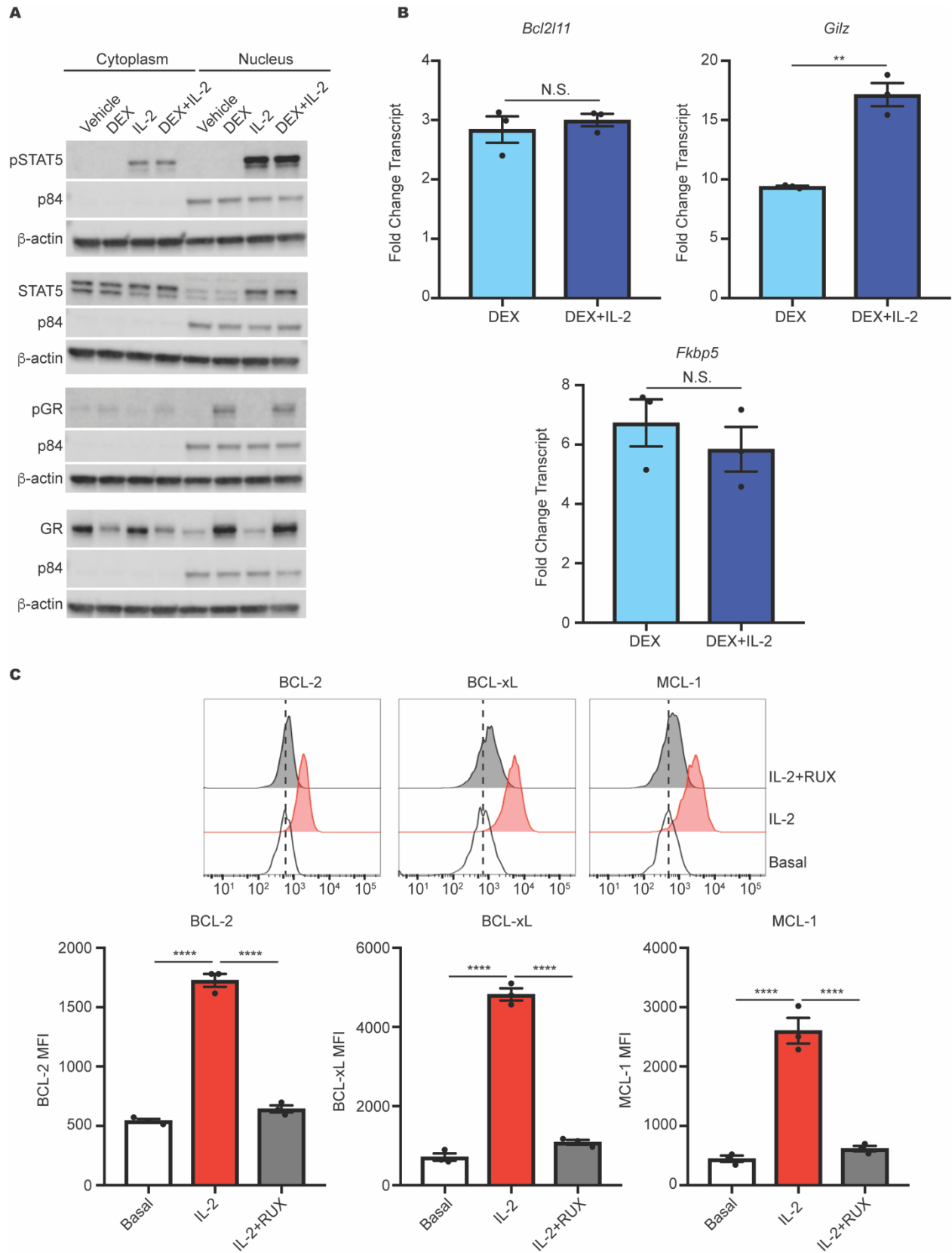
Figure 8-5: IL-2 upregulates anti-apoptotic proteins. (A) Western blot of cytoplasmic and nuclear total and phosphorylated STAT5 and GR in murine CD8 T cells pre-treated or not with

10ng/mL IL-2 followed by treatment with vehicle control or 1μM DEX for 30 minutes. β-actin is used as a cytoplasmic loading control and p84 is used as a nuclear loading control. **(B)** Fold change in transcript expression of the direct GR target genes *Bcl2l11, Gilz,* and *Fkbp5* in murine CD8 T cells pre-treated or not with 10ng/mL IL-2 for one hour followed by treatment with vehicle control or 1μM DEX for four hours in technical triplicate. Fold change values are relative to untreated or IL-2 treated cells, respectively. **(C)** MFIs and representative histograms of BCL-2, BCL-XL, and MCL-1 protein expression in murine CD8 T cells in the basal state or following exposure to 10ng/mL IL-2 with or without 500nM RUX for 24 hours in technical triplicate. Statistical significance was assessed using two-sample t-tests (B) or one-way ANOVA with Tukey's method for multiple comparisons adjustment (C). All data are representative of three independent experiments. ****$p<0.0001$, ***$p<0.001$, **$p<0.01$, *$p<0.05$, N.S. – not significant.

A

BCL-2 Activity

BCL-xL Activity

MCL-1 Activity

B

BCL-2 Activity

BCL-xL Activity

MCL-1 Activity
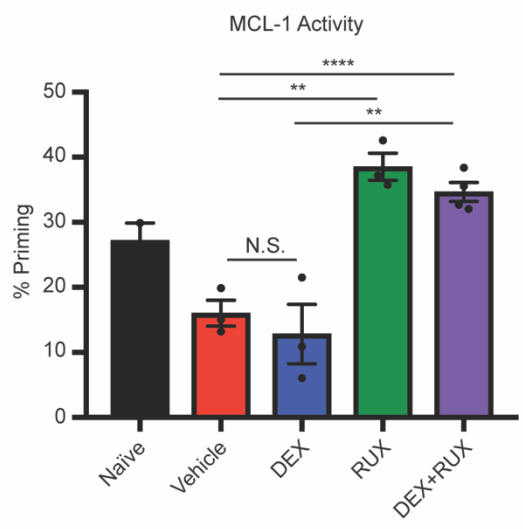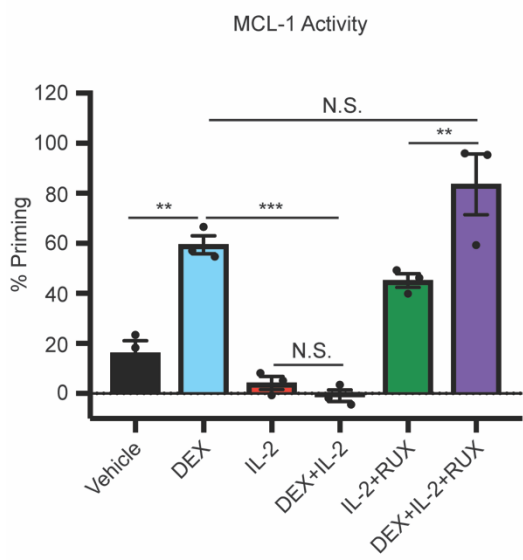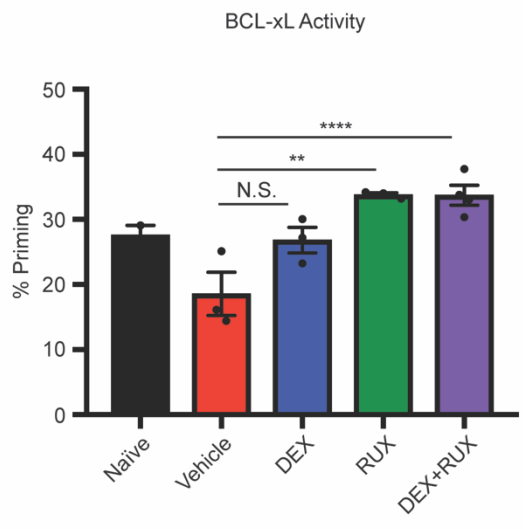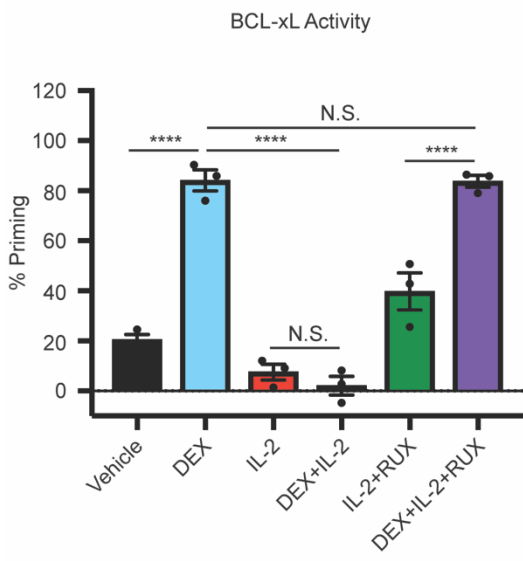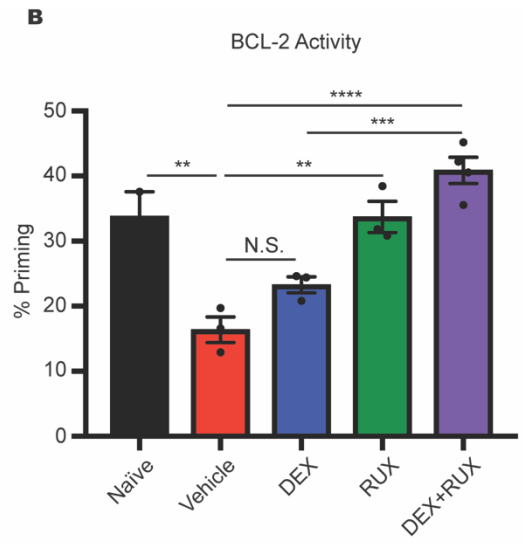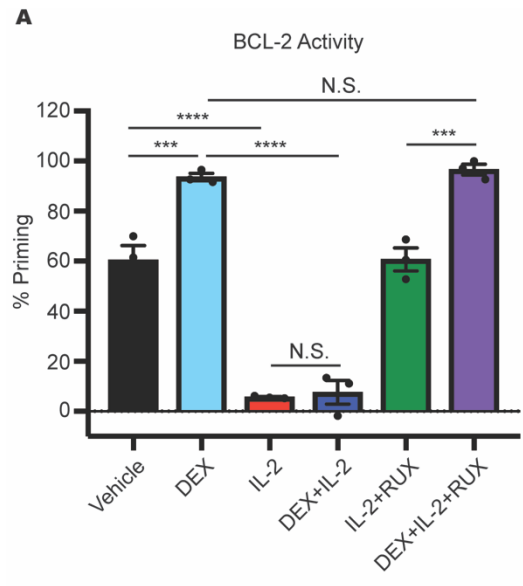
Figure 8-6: Cytokine exposure decreases the apoptotic potential of CD8 T cells and this apoptotic potential is restored upon RUX exposure. (A) Percent priming values generated from BH3 profiling of murine CD8 T cells treated *ex vivo* with or without 10ng/mL IL-2, 1µM DEX, and/or 500nM RUX for 16 hours in technical triplicate prior to BH3 profiling with 1µM ABT-199 to measure BCL-2 activity, 10µM WEHI-539 to measure BCL-XL activity, or 10µM synthetic NOXA peptide to measure MCL-1 activity. (B) Percent priming values generated from BH3 profiling of murine CD8 T cells harvested on day 9 post-infection from naïve or vehicle- or drug-treated LCMV-infected mice prior to BH3 profiling with 10µM ABT-199 to measure BCL-2 activity, 10µM WEHI-539 to measure BCL-XL activity, or 10µM S63845 to measure MCL-1 activity. Statistical significance was assessed using one-way ANOVA with Tukey's method for multiple comparisons adjustment. The data in panel A are representative of three independent experiments. ****$p<0.0001$, ***$p<0.001$, **$p<0.01$, *$p<0.05$, N.S. – not significant.
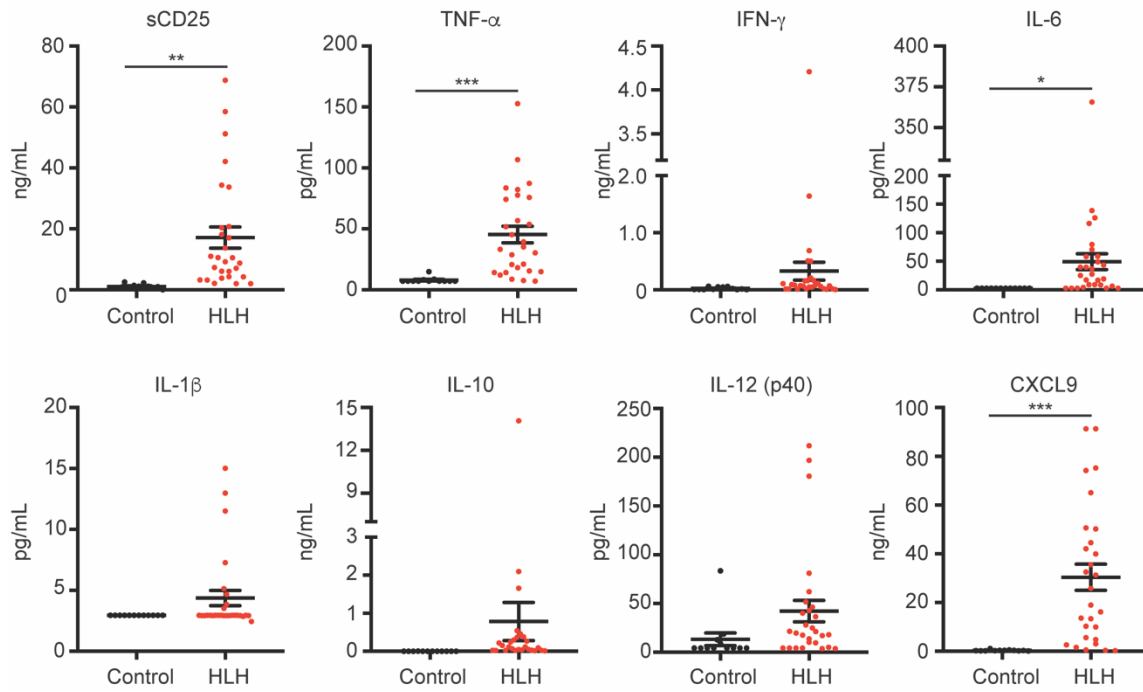
Supplemental Figure 8-1: Disease-associated proteins are elevated in the plasma from patients with HLH. Levels of HLH-associated plasma proteins in plasma from control patients versus patients with HLH. Statistical significance was assessed using two-sample t-tests. ****p<0.0001, ***p<0.001, **p<0.01, *p<0.05.
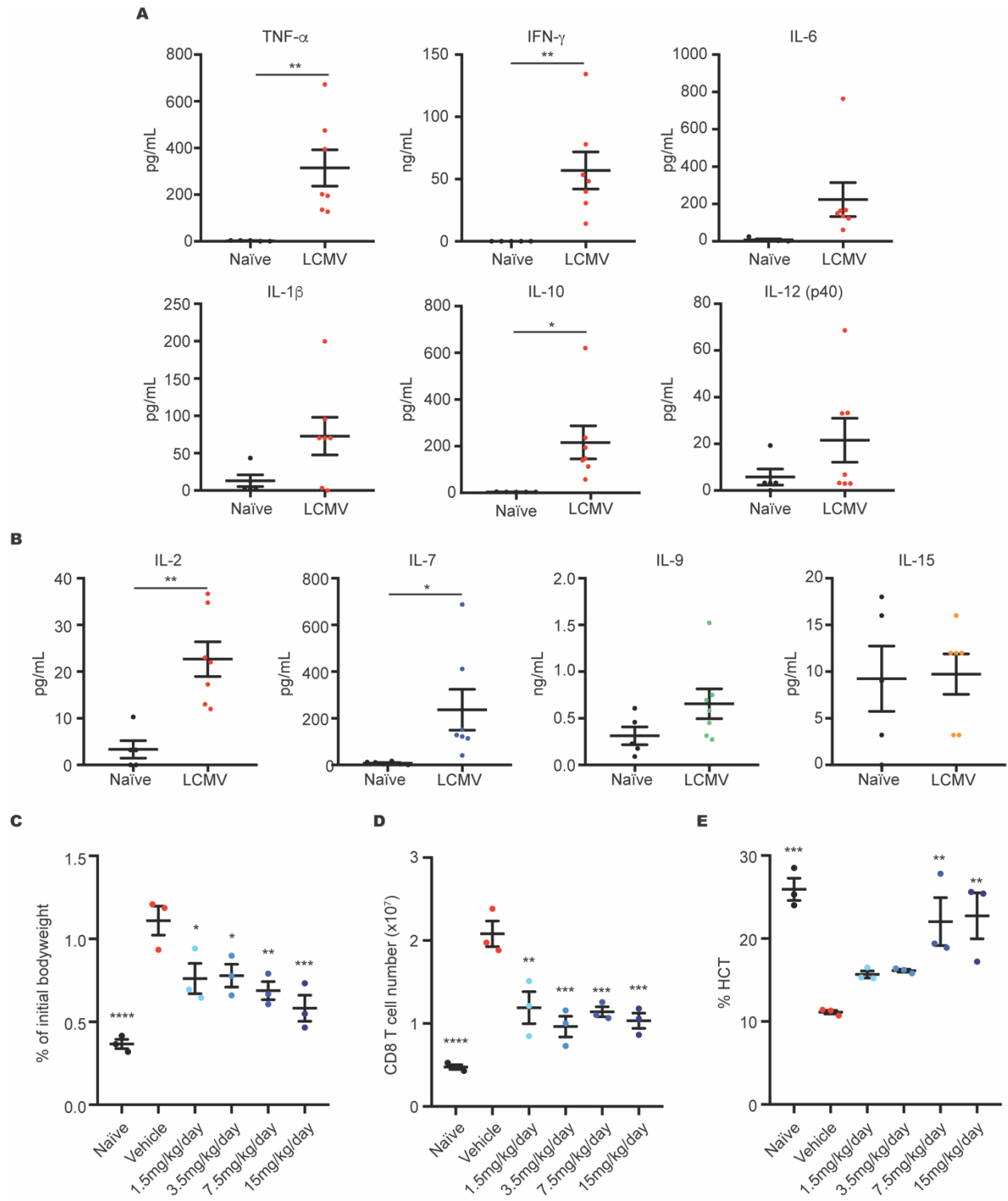
Supplemental Figure 8-2: HLH-like disease in *Prf1⁻/⁻* mice recapitulates key features of human disease. (A) Levels of HLH-associated plasma proteins in plasma from naïve mice or LCMV-infected vehicle-treated mice on day 9 post-infection. **(B)** Levels of common gamma chain cytokines in plasma from naïve mice or LCMV-infected vehicle-treated mice on day 9 post-infection. **(C)** Bodyweight on day 9 post-infection relative to baseline bodyweight in naïve

and vehicle- or DEX-treated mice. Statistical significance is relative to the vehicle-treated condition. **(D)** Number of CD8 T cells in spleens from naïve and vehicle- and drug-treated LCMV-infected mice on day 9 post-infection. Statistical significance is relative to the vehicle-treated condition. **(E)** Hematocrit values in naïve mice and vehicle- and drug-treated LCMV-infected mice on day 9 post-infection. Statistical significance is relative to the vehicle-treated condition. Statistical significance was assessed using two-sample t-tests (A and B) or one-way ANOVA with Tukey's method for multiple comparisons adjustment (C-E). ****$p<0.0001$, ***$p<0.001$, **$p<0.01$, *$p<0.05$.
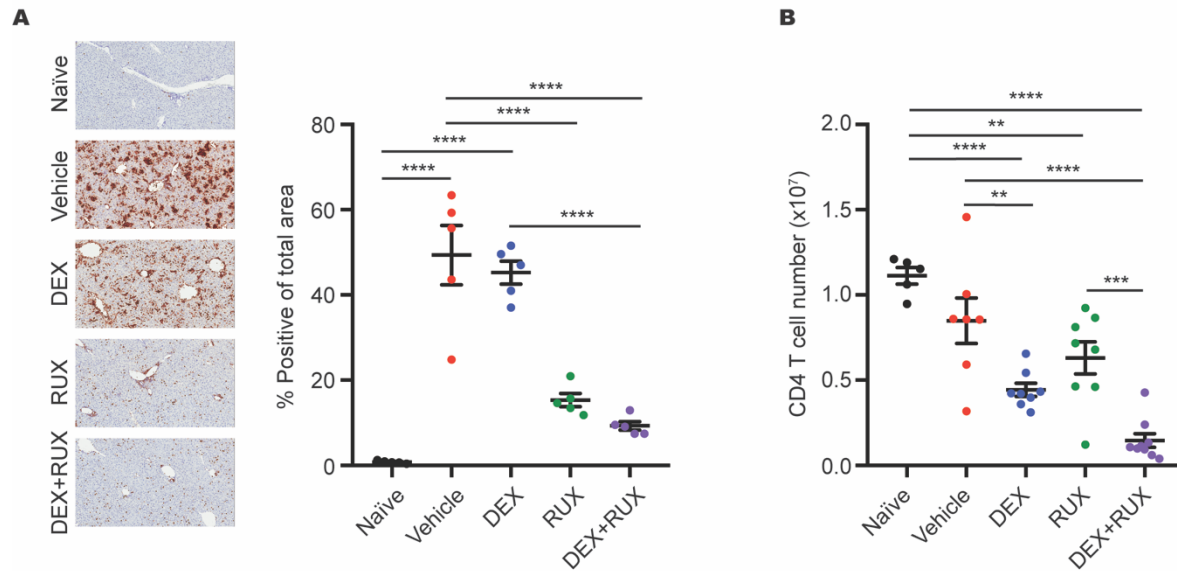
Supplemental Figure 8-3: Neutrophils and CD4 T cells are affected by drug exposure *in vivo*. (A) Representative histologic images and number of Ly5B.2+ cells in livers from naïve and vehicle- and drug-treated LCMV-infected mice on day 9 post-infection. **(B)** Number of CD4 T cells in spleens from naïve and vehicle- and drug-treated LCMV-infected mice on day 9 post-infection. Statistical significance was assessed using one-way ANOVA with Tukey's method for multiple comparisons adjustment. The data in panel B represent a combined analysis of two independent experiments. ****p<0.0001, ***p<0.001, **p<0.01, *p<0.05.
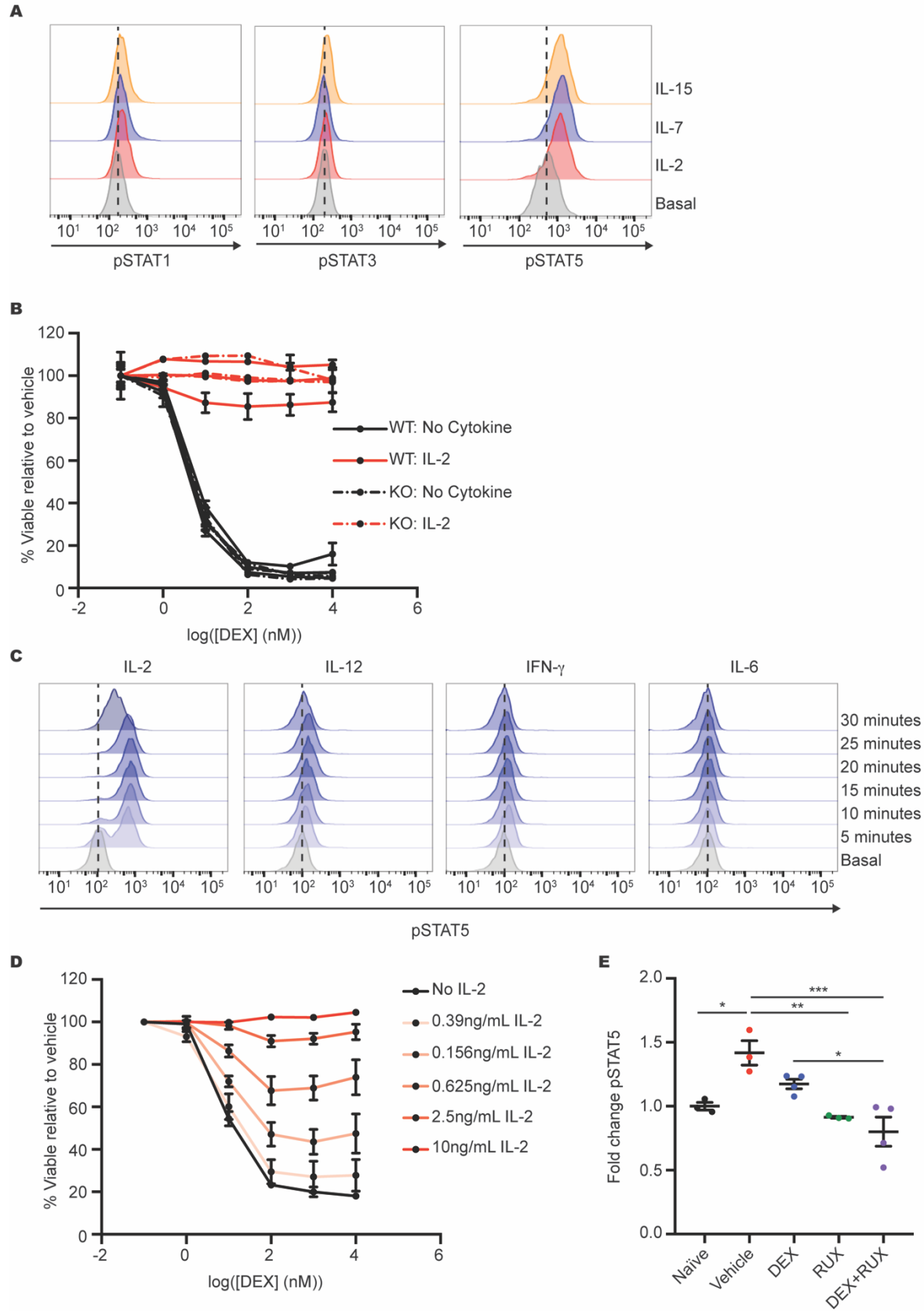
Supplemental Figure 8-4: STAT5-activating cytokines confer DEX resistance in murine CD8 T-cells. (A) Representative histograms of pSTAT1, pSTAT3, and pSTAT5 in murine CD8 T cells in the basal state or following stimulation with 10ng/mL of the indicated cytokine for 15 minutes. **(B)** Viability relative to vehicle control of WT or *Prf1*-/- murine CD8 T cells treated with increasing concentrations of DEX in the absence or presence of 10ng/mL IL-2 for 24 hours in technical triplicate. **(C)** Representative histograms of pSTAT5 in murine CD8 T cells following stimulation with 10ng/mL of the indicated cytokine for the indicated period of time. **(D)** Viability relative to vehicle control of murine CD8 T cells treated with increasing concentrations of DEX in the presence or absence of the indicated concentration of IL-2 for 24 hours in technical triplicate. **(E)** Fold change in pSTAT5 MFI from murine CD8 T cells harvested from naïve and vehicle- and drug-treated LCMV-infected mice on day four post-injection 12 hours after a single dose of 1.5mg/kg DEX and/or 60mg/kg RUX. Statistical significance was assessed using one-way ANOVA with Tukey's method for multiple comparisons adjustment (E). The data in panels A-D are representative of three independent experiments. ****$p<0.0001$, ***$p<0.001$, **$p<0.01$, *$p<0.05$.

Chapter 9: Conclusions and Future Directions

Glucocorticoid (GC) resistance is an important barrier to successful therapy in lymphoid-driven diseases. The overarching objective of this work was to identify novel concepts and to contribute mechanistic insights into existing concepts regarding the ways in which lymphoid cells resist the pro-apoptotic effects of GCs. In contrast to many studies in the field of cancer biology that focus on understanding mechanisms of drug resistance that are acquired during exposure to therapy, the studies presented here focus instead on elucidating intrinsic drivers of GC resistance that pose therapeutic challenges beginning at the time of disease diagnosis. Specifically, these studies utilized a developmental lens to consider the unique fact that, in addition to their pharmacologic use, GCs are endogenous hormones that engage in extensive interactions with the immune system. The physiologic co-existence of GCs and immune cells necessitates intrinsic resistance mechanisms to protect lymphoid cell populations from GC-induced cell death at distinct stages of development and under certain environmental conditions. Through the use of multiple disease models, this work highlights a number of unifying themes that contribute to our understanding of this unique and complex interplay between GCs and the immune system and the ways in which intrinsic GC resistance mechanisms may be co-opted to interfere with GC therapy in lymphoid-driven diseases.

Beginning with Philadelphia chromosome-like acute lymphoblastic leukemia (ALL), we established the relationship between aberrant cytokine receptor activity and GC resistance. In Ph-like ALL, cytokine receptor signaling is dysregulated due to frequent chromosomal translocations involving the cytokine receptor gene *CRLF2*, which are often accompanied by activating mutations in downstream signal transduction effectors such as *JAK2.* Using a cohort of primary patient Ph-like ALL samples, we demonstrated that the presence of these genomic lesions was uniformly associated with GC resistance. In the context of these genomic alterations, signal transduction inhibitors effectively induced GC sensitivity.

We then turned our attention to T-cell ALL (T-ALL), a disease complicated by a lack of clinically relevant biomarkers, impeding efforts to risk stratify patients and implement precision

medicine-based approaches to treatment. This work expanded upon our previous findings that the cytokine interleukin-7 (IL7) mediates GC resistance in a subset of T-ALLs. In contrast to Ph-like ALL, where our findings supported the idea that genotype is an important driver of phenotype, we found that IL7-induced GC resistance most commonly occurred in the absence of activating mutations in the IL7 receptor (IL7R) signaling pathway. We therefore sought to understand both *how* IL7 confers GC resistance and *why* this occurs only in a subset of T-ALLs. Mechanistically, we encountered an intriguing paradox in which GCs induce their own resistance by augmenting IL7 receptor (IL7R) pathway signaling, contributing to an anti-apoptotic state that is refractory to the pro-apoptotic effects of GCs. We demonstrated that this mechanism also conferred GC resistance in early populations of developing thymocytes but not in later populations, suggesting that it plays a role in protecting those early populations from apoptosis in the presence of endogenous GCs. Using RNA-seq to analyze primary patient T-ALLs, we showed that T-ALLs arising from those same stages of thymocyte development tended to retain this pattern of resistance. When considered in light of the processes that occur during normal thymopoiesis, these data were consistent with the idea that GC-induced apoptosis of thymocytes prior to T-cell receptor (TCR) selection would be maladaptive, as it would dramatically reduce the pool of thymocytes generating potentially productive TCR rearrangements. Similarly, our data supported previous findings that the later double positive thymocytes are highly sensitive to GCs, which act endogenously to induce apoptosis in thymocytes lacking functional TCRs. Taken together, these data highlight the utility of considering drug sensitivity in the context of developmental processes, as we have shown that these are tightly linked with respect to GC sensitivity.

To expand upon key elements of these findings, we pursued two additional studies in T-ALL, one focused on the identification of a gene expression-based biomarker for therapeutic response and another on evaluating the efficacy of a novel therapeutic strategy for overcoming IL7-induced GC resistance. In the first study, we analyzed RNA-seq data from two cohorts of T-

ALL patients enrolled on Children's Oncology Group trials to discover that diagnostic samples

from patients who went on to have detectable residual disease at the end of induction therapy

had gene expression patterns that differed significantly from those of patients without detectable

disease at the end of induction. In addition to providing the first steps towards a clinically

tractable assay for predicting responses to induction therapy, this study identified further

insights into the relationship between T-cell development and therapeutic response, particularly

given the fact that induction therapy relies heavily on the use of GCs. Specifically, this analysis

demonstrated that T-ALLs with immunophenotypic features characteristic of a later stage of

development but with positive minimal residual disease (MRD) at the end of induction had a

gene expression signature that looked identical to that of T-ALLs arising earlier in T-cell

development. Though identified through entirely independent methods, these data accurately

recapitulate the findings discussed above regarding the relationship between developmental

stage and GC sensitivity, and suggest that assessing the developmental stage of a T-ALL

through gene expression profiling may have prognostic and therapeutic relevance.

Drawing on the precedent for the incorporation of the LDA card into the clinical

management of patients with Ph-like ALL, ongoing efforts are focused on generating an

analogous targeted gene expression assay for the prediction of MRD in newly-diagnosed T-ALL

patients, with the intention of validating the prognostic significance of such an assay in

independent patient cohorts. In addition to its potential clinical utility, future applications of these

gene expression data may also include establishing the feasibility of a precision medicine-based

approach to the treatment of T-ALL. Specifically, our preliminary data regarding the association

between gene expression signatures and BCL-2 expression suggest that a subset of T-ALL

patients may benefit from targeted inhibition of BCL-2 as a therapeutic strategy. Further analysis

of these data for other potential therapeutic targets, in conjunction with preclinical trials

conducted in clinically-relevant PDX model systems, is likely to be a powerful approach to

identifying rational therapeutic strategies for the treatment of this highly heterogeneous disease.

Finally, one important caveat of this work is that, while MRD status remains an important prognostic indicator, the primary goal in the treatment of T-ALL is the prevention of relapse. Despite the clinical significance of this endpoint, the patient cohorts utilized in this study were too small to provide sufficient power for addressing this important question. Future studies in larger datasets may be more adequately powered to assess the relationship between gene expression patterns and risk of relapse, potentially facilitating the development of a similar sample score metric for prediction of these outcomes.

As an alternative to JAK/STAT pathway inhibition, we also took advantage of our mechanistic understanding of IL7-induced GC resistance to hypothesize that preventing localization of IL7R to the cell surface would effectively restore GC sensitivity in the presence of IL7. Using KZR-508445, an inhibitor of the Sec61 translocon, we demonstrated the utility of inhibiting the cellular secretory pathway to enhance GC sensitivity in T-ALL. Furthermore, we demonstrated that this compound is well-tolerated in mice, and showed preliminary data to suggest that it may act effectively in conjunction with GCs in an *in vivo* model of T-ALL. Future studies are needed to further establish the *in vivo* utility of this compound in a patient-derived xenograft model established from T-ALLs that demonstrate IL7-induced GC resistance.

Finally, we extended our analysis of the interaction between cytokines and GCs to a model of hemophagocytic lymphohistiocytosis (HLH), a rare and complicated hyperinflammatory condition in which CD8 T-cells are a well-established driver of disease. As with T-ALL, GCs are a central component of therapy for HLH, and we hypothesized that the rampant hypercytokinemia that classically occurs in this disease may confound the use of GCs in this context and contribute to poor clinical outcomes. Consistent with our hypothesis, we found that the cytokine composition of patient plasma was sufficient to confer GC resistance in CD8 T-cells. Using an *in vivo* model of HLH, we demonstrated that inhibiting cytokine receptor signaling with ruxolitinib profoundly attenuated many disease parameters, but was particularly effective for augmenting GC sensitivity in CD8 T-cells, both with respect to reducing their abundance and

their activation status. We went on to show in a series of *ex vivo* mechanistic studies using murine T-cells that, just as was observed in T-ALL, cytokine-induced GC resistance occurs due to the altered apoptotic potential of T-cells in the presence of cytokine, which is effectively reduced with ruxolitinib, thereby facilitating GC-induced apoptosis.

While these mechanistic studies focused on the effects of combining dexamethasone and ruxolitinib on CD8 T-cells, it is important to note that our evaluation of disease parameters in the *in vivo* model demonstrated profound effects of ruxolitinib, both alone and in combination with dexamethasone, on other cell lineages, including monocytes and neutrophils. While CD8 T-cells are a well-established driver of disease in primary HLH, these other lineages likely play a more central role in related hyperinflammatory conditions, including macrophage activation syndrome (MAS). Further studies focused on elucidating the mechanistic basis for the efficacy of this therapeutic strategy in those other lineages therefore have the potential to increase the clinical utility of this drug combination for the treatment of a wider spectrum of hyperinflammatory conditions.

In conclusion, the extension of our work from T-ALL to HLH serves to increase the generalizability of our findings and contribute to our conceptual understanding of intrinsic mechanisms of GC resistance. Specifically, this work suggests that cytokines are ubiquitous drivers of GC resistance across the spectrum of T-cell development, and that local and systemic regulation of cytokine production as well as developmentally-regulated patterns of cytokine receptor expression likely underlie the differential sensitivity of healthy T-cell populations to endogenous GCs. Our findings suggest that these patterns of sensitivity can be extrapolated to a number of disease contexts, where they in turn contribute to poor therapeutic efficacy. Taken together, our work highlights the importance of considering GCs not just as therapeutic agents, but as endogenous hormones that have complex physiologic interactions with immune cells, which in turn have important therapeutic implications that are amenable to the inclusion of signal transduction inhibitors as a means of enhancing the efficacy of GC therapy.

References

1. Yamamoto KR. Steroid receptor regulated transcription of specific genes and gene networks. Annu Rev Genet. 1985;19:209–52.

2. Schmidt S, Rainer J, Ploner C, Presul E, Riml S, Kofler R. Glucocorticoid-induced apoptosis and glucocorticoid resistance: molecular mechanisms and clinical relevance. Cell Death Differ. 2004 Jul;11 Suppl 1:S45-55.

3. Ramamoorthy S, Cidlowski JA. Corticosteroids: Mechanisms of Action in Health and Disease. Rheum Dis Clin North Am. 2016 Feb;42(1):15–31, vii.

4. Spits H. Development of alphabeta T cells in the human thymus. Nat Rev Immunol. 2002 Oct;2(10):760–72.

5. Jaffe HL. THE INFLUENCE OF THE SUPRARENAL GLAND ON THE THYMUS : III. STIMULATION OF THE GROWTH OF THE THYMUS GLAND FOLLOWING DOUBLE SUPRARENALECTOMY IN YOUNG RATS. J Exp Med. 1924 Nov 30;40(6):753–9.

6. Inomata T, Nakamura T. Influence of adrenalectomy on the development of the neonatal thymus in the rat. Biol Neonate. 1989;55(4–5):238–43.

7. Zacharchuk CM, Merćep M, Chakraborti PK, Simons SS, Ashwell JD. Programmed T lymphocyte death. Cell activation- and steroid-induced pathways are mutually antagonistic. J Immunol Baltim Md 1950. 1990 Dec 15;145(12):4037–45.

8. Ashwell JD, King LB, Vacchio MS. Cross-talk between the T cell antigen receptor and the glucocorticoid receptor regulates thymocyte development. Stem Cells Dayt Ohio. 1996 Sep;14(5):490–500.

9. D'Arcy MS. Cell death: a review of the major forms of apoptosis, necrosis and autophagy. Cell Biol Int. 2019 Jun;43(6):582–92.

10. Brunelle JK, Letai A. Control of mitochondrial apoptosis by the Bcl-2 family. J Cell Sci. 2009 Feb 15;122(Pt 4):437–41.

11. Kutuk O, Letai A. Regulation of Bcl-2 family proteins by posttranslational modifications. Curr Mol Med. 2008 Mar;8(2):102–18.

12. Montero J, Letai A. Dynamic BH3 profiling-poking cancer cells with a stick. Mol Cell Oncol. 2016 May;3(3):e1040144.

13. Ryan J, Montero J, Rocco J, Letai A. iBH3: simple, fixable BH3 profiling to determine apoptotic priming in primary tissue by flow cytometry. Biol Chem. 2016 Feb 23;

14. Chonghaile TN, Roderick JE, Glenfield C, Ryan J, Sallan SE, Silverman LB, et al. Maturation stage of T-cell acute lymphoblastic leukemia determines BCL-2 versus BCL-XL dependence and sensitivity to ABT-199. Cancer Discov. 2014 Sep;4(9):1074–87.

15. Delbridge ARD, Strasser A. The BCL-2 protein family, BH3-mimetics and cancer therapy. Cell Death Differ. 2015 Jul;22(7):1071–80.

16. Abrams MT, Robertson NM, Yoon K, Wickstrom E. Inhibition of glucocorticoid-induced apoptosis by targeting the major splice variants of BIM mRNA with small interfering RNA and short hairpin RNA. J Biol Chem. 2004 Dec 31;279(53):55809–17.

17. Erlacher M, Michalak EM, Kelly PN, Labi V, Niederegger H, Coultas L, et al. BH3-only proteins Puma and Bim are rate-limiting for gamma-radiation- and glucocorticoid-induced apoptosis of lymphoid cells in vivo. Blood. 2005 Dec 15;106(13):4131–8.

18. Jing D, Bhadri VA, Beck D, Thoms JAI, Yakob NA, Wong JWH, et al. Opposing regulation of BIM and BCL2 controls glucocorticoid-induced apoptosis of pediatric acute lymphoblastic leukemia cells. Blood. 2015 Jan 8;125(2):273–83.

19. Dinarello CA. Historical insights into cytokines. Eur J Immunol. 2007 Nov;37 Suppl 1:S34-45.

20. Cirillo E, Giardino G, Gallo V, D'Assante R, Grasso F, Romano R, et al. Severe combined immunodeficiency--an update. Ann N Y Acad Sci. 2015 Nov;1356:90–106.

21. Leonard WJ, O'Shea JJ. Jaks and STATs: biological implications. Annu Rev Immunol. 1998;16:293–322.

22. Morris R, Kershaw NJ, Babon JJ. The molecular details of cytokine signaling via the JAK/STAT pathway. Protein Sci Publ Protein Soc. 2018;27(12):1984–2009.

23. Villarino AV, Kanno Y, Ferdinand JR, O'Shea JJ. Mechanisms of Jak/STAT signaling in immunity and disease. J Immunol Baltim Md 1950. 2015 Jan 1;194(1):21–7.

24. O'Shea JJ, Murray PJ. Cytokine signaling modules in inflammatory responses. Immunity. 2008 Apr;28(4):477–87.

25. Lin JX, Migone TS, Tsang M, Friedmann M, Weatherbee JA, Zhou L, et al. The role of shared receptor motifs and common Stat proteins in the generation of cytokine pleiotropy and redundancy by IL-2, IL-4, IL-7, IL-13, and IL-15. Immunity. 1995 Apr;2(4):331–9.

26. Linabery AM, Ross JA. Trends in childhood cancer incidence in the U.S. (1992-2004). Cancer. 2008 Jan 15;112(2):416–32.

27. Hunger SP, Lu X, Devidas M, Camitta BM, Gaynon PS, Winick NJ, et al. Improved survival for children and adolescents with acute lymphoblastic leukemia between 1990 and 2005: a report from the children's oncology group. J Clin Oncol Off J Am Soc Clin Oncol. 2012 May 10;30(14):1663–9.

28. Tasian SK, Loh ML, Hunger SP. Childhood acute lymphoblastic leukemia: Integrating genomics into therapy. Cancer. 2015 Oct 15;121(20):3577–90.

29. Pearson OH, Eliel LP. Use of pituitary adrenocorticotropic hormone (ACTH) and cortisone in lymphomas and leukemias. J Am Med Assoc. 1950 Dec 16;144(16):1349–53.

30. Lauten M, Möricke A, Beier R, Zimmermann M, Stanulla M, Meissner B, et al. Prediction of outcome by early bone marrow response in childhood acute lymphoblastic leukemia treated in the ALL-BFM 95 trial: differential effects in precursor B-cell and T-cell leukemia. Haematologica. 2012 Jul;97(7):1048–56.

31. Schmiegelow K, Nyvold C, Seyfarth J, Pieters R, Rottier MM, Knabe N, et al. Post-induction residual leukemia in childhood acute lymphoblastic leukemia quantified by PCR correlates with in vitro prednisolone resistance. Leukemia. 2001 Jul;15(7):1066–71.

32. Teachey DT, Hunger SP. Predicting relapse risk in childhood acute lymphoblastic leukaemia. Br J Haematol. 2013 Sep;162(5):606–20.

33. Caplan A, Fett N, Rosenbach M, Werth VP, Micheletti RG. Prevention and management of glucocorticoid-induced side effects: A comprehensive review: Ocular, cardiovascular, muscular, and psychiatric side effects and issues unique to pediatric patients. J Am Acad Dermatol. 2017 Feb;76(2):201–7.

34. Brisse E, Wouters CH, Matthys P. Hemophagocytic lymphohistiocytosis (HLH): A heterogeneous spectrum of cytokine-driven immune disorders. Cytokine Growth Factor Rev. 2015 Jun;26(3):263–80.

35. Kägi D, Ledermann B, Bürki K, Seiler P, Odermatt B, Olsen KJ, et al. Cytotoxicity mediated by T cells and natural killer cells is greatly impaired in perforin-deficient mice. Nature. 1994 May 5;369(6475):31–7.

36. Jordan MB, Hildeman D, Kappler J, Marrack P. An animal model of hemophagocytic lymphohistiocytosis (HLH): CD8+ T cells and interferon gamma are essential for the disorder. Blood. 2004 Aug 1;104(3):735–43.

37. Chinn IK, Eckstein OS, Peckham-Gregory EC, Goldberg BR, Forbes LR, Nicholas SK, et al. Genetic and mechanistic diversity in pediatric hemophagocytic lymphohistiocytosis. Blood. 2018 05;132(1):89–100.

38. Bergsten E, Horne A, Aricó M, Astigarraga I, Egeler RM, Filipovich AH, et al. Confirmed efficacy of etoposide and dexamethasone in HLH treatment: long-term results of the cooperative HLH-2004 study. Blood. 2017 21;130(25):2728–38.

39. Zinter MS, Hermiston ML. Calming the storm in HLH. Blood. 2019 Jul 11;134(2):103–4.

40. Al-Salama ZT. Emapalumab: First Global Approval. Drugs. 2019 Jan;79(1):99–103.

41. Locatelli F, Jordan MB, Allen CE, Cesaro S, Rizzari C, Rao A, et al. Safety and Efficacy of Emapalumab in Pediatric Patients with Primary Hemophagocytic Lymphohistiocytosis. In 2018.

42. Albeituni S, Verbist KC, Tedrick PE, Tillman H, Picarsic J, Bassett R, et al. Mechanisms of action of ruxolitinib in murine models of hemophagocytic lymphohistiocytosis. Blood. 2019 Jul 11;134(2):147–59.

43. Lin J-X, Leonard WJ. The Common Cytokine Receptor γ Chain Family of Cytokines. Cold Spring Harb Perspect Biol. 2018 04;10(9).

44. Schrappe M, Reiter A, Zimmermann M, Harbott J, Ludwig WD, Henze G, et al. Long-term results of four consecutive trials in childhood ALL performed by the ALL-BFM study group from 1981 to 1995. Berlin-Frankfurt-Münster. Leukemia. 2000 Dec;14(12):2205–22.

45. Fisher RI, Gaynor ER, Dahlberg S, Oken MM, Grogan TM, Mize EM, et al. Comparison of a standard regimen (CHOP) with three intensive chemotherapy regimens for advanced non-Hodgkin's lymphoma. N Engl J Med. 1993 Apr 8;328(14):1002–6.

46. Dördelmann M, Reiter A, Borkhardt A, Ludwig WD, Götz N, Viehmann S, et al. Prednisone response is the strongest predictor of treatment outcome in infant acute lymphoblastic leukemia. Blood. 1999 Aug 15;94(4):1209–17.

47. Mathew BS, Carson KA, Grossman SA. Initial response to glucocorticoids. Cancer. 2006 Jan 15;106(2):383–7.

48. Oakley RH, Cidlowski JA. The biology of the glucocorticoid receptor: new signaling mechanisms in health and disease. J Allergy Clin Immunol. 2013 Nov;132(5):1033–44.

49. Schmidt S, Rainer J, Ploner C, Presul E, Riml S, Kofler R. Glucocorticoid-induced apoptosis and glucocorticoid resistance: molecular mechanisms and clinical relevance. Cell Death Differ. 2004 Jul;11 Suppl 1:S45-55.

50. Ploner C, Rainer J, Niederegger H, Eduardoff M, Villunger A, Geley S, et al. The BCL2 rheostat in glucocorticoid-induced apoptosis of acute lymphoblastic leukemia. Leukemia. 2008 Feb;22(2):370–7.

51. Charmandari E, Kino T, Chrousos GP. Primary generalized familial and sporadic glucocorticoid resistance (Chrousos syndrome) and hypersensitivity. Endocr Dev. 2013;24:67–85.

52. Bray PJ, Cotton RGH. Variations of the human glucocorticoid receptor gene (NR3C1): pathological and in vitro mutations and polymorphisms. Hum Mutat. 2003 Jun;21(6):557–68.

53. Harmon JM, Thompson EB. Isolation and characterization of dexamethasone-resistant mutants from human lymphoid cell line CEM-C7. Mol Cell Biol. 1981 Jun;1(6):512–21.

54. Ashraf J, Thompson EB. Identification of the activation-labile gene: a single point mutation in the human glucocorticoid receptor presents as two distinct receptor phenotypes. Mol Endocrinol Baltim Md. 1993 May;7(5):631–42.

55. Powers JH, Hillmann AG, Tang DC, Harmon JM. Cloning and expression of mutant glucocorticoid receptors from glucocorticoid-sensitive and -resistant human leukemic cells. Cancer Res. 1993 Sep 1;53(17):4059–65.

56. Hala M, Hartmann BL, Böck G, Geley S, Kofler R. Glucocorticoid-receptor-gene defects and resistance to glucocorticoid-induced apoptosis in human leukemic cell lines. Int J Cancer. 1996 Nov 27;68(5):663–8.

57. Strasser-Wozak EM, Hattmannstorfer R, Hála M, Hartmann BL, Fiegl M, Geley S, et al. Splice site mutation in the glucocorticoid receptor gene causes resistance to

glucocorticoid-induced apoptosis in a human acute leukemic cell line. Cancer Res. 1995 Jan 15;55(2):348–53.

58. Hillmann AG, Ramdas J, Multanen K, Norman MR, Harmon JM. Glucocorticoid receptor gene mutations in leukemic cells acquired in vitro and in vivo. Cancer Res. 2000 Apr 1;60(7):2056–62.

59. Riml S, Schmidt S, Ausserlechner MJ, Geley S, Kofler R. Glucocorticoid receptor heterozygosity combined with lack of receptor auto-induction causes glucocorticoid resistance in Jurkat acute lymphoblastic leukemia cells. Cell Death Differ. 2004 Jul;11 Suppl 1:S65-72.

60. Beesley AH, Weller RE, Senanayake S, Welch M, Kees UR. Receptor mutation is not a common mechanism of naturally occurring glucocorticoid resistance in leukaemia cell lines. Leuk Res. 2009 Feb;33(2):321–5.

61. Tissing WJE, Meijerink JPP, den Boer ML, Brinkhof B, van Rossum EFC, van Wering ER, et al. Genetic variations in the glucocorticoid receptor gene are not related to glucocorticoid resistance in childhood acute lymphoblastic leukemia. Clin Cancer Res Off J Am Assoc Cancer Res. 2005 Aug 15;11(16):6050–6.

62. Irving JAE, Minto L, Bailey S, Hall AG. Loss of heterozygosity and somatic mutations of the glucocorticoid receptor gene are rarely found at relapse in pediatric acute lymphoblastic leukemia but may occur in a subpopulation early in the disease course. Cancer Res. 2005 Nov 1;65(21):9712–8.

63. Mullighan CG, Phillips LA, Su X, Ma J, Miller CB, Shurtleff SA, et al. Genomic analysis of the clonal origins of relapsed acute lymphoblastic leukemia. Science. 2008 Nov 28;322(5906):1377–80.

64. Oshima K, Khiabanian H, da Silva-Almeida AC, Tzoneva G, Abate F, Ambesi-Impiombato A, et al. Mutational landscape, clonal evolution patterns, and role of RAS mutations in relapsed acute lymphoblastic leukemia. Proc Natl Acad Sci U S A. 2016 04;113(40):11306–11.

65. Pui CH, Dahl GV, Rivera G, Murphy SB, Costlow ME. The relationship of blast cell glucocorticoid receptor levels to response to single-agent steroid trial and remission response in children with acute lymphoblastic leukemia. Leuk Res. 1984;8(4):579–85.

66. Quddus FF, Leventhal BG, Boyett JM, Pullen DJ, Crist WM, Borowitz MJ. Glucocorticoid receptors in immunological subtypes of childhood acute lymphocytic leukemia cells: a Pediatric Oncology Group Study. Cancer Res. 1985 Dec;45(12 Pt 1):6482–6.

67. Kato GJ, Quddus FF, Shuster JJ, Boyett J, Pullen JD, Borowitz MJ, et al. High glucocorticoid receptor content of leukemic blasts is a favorable prognostic factor in childhood acute lymphoblastic leukemia. Blood. 1993 Oct 15;82(8):2304–9.

68. Grausenburger R, Bastelberger S, Eckert C, Kauer M, Stanulla M, Frech C, et al. Genetic alterations in glucocorticoid signaling pathway components are associated with adverse prognosis in children with relapsed ETV6/RUNX1-positive acute lymphoblastic leukemia. Leuk Lymphoma. 2016 May;57(5):1163–73.

69. Lauten M, Cario G, Asgedom G, Welte K, Schrappe M. Protein expression of the glucocorticoid receptor in childhood acute lymphoblastic leukemia. Haematologica. 2003 Nov;88(11):1253–8.

70. Denton RR, Eisen LP, Elsasser MS, Harmon JM. Differential autoregulation of glucocorticoid receptor expression in human T- and B-cell lines. Endocrinology. 1993 Jul;133(1):248–56.

71. Ramdas J, Liu W, Harmon JM. Glucocorticoid-induced cell death requires autoinduction of glucocorticoid receptor expression in human leukemic T cells. Cancer Res. 1999 Mar 15;59(6):1378–85.

72. Gomi M, Moriwaki K, Katagiri S, Kurata Y, Thompson EB. Glucocorticoid effects on myeloma cells in culture: correlation of growth inhibition with induction of glucocorticoid receptor messenger RNA. Cancer Res. 1990 Mar 15;50(6):1873–8.

73. Asnafi V, Buzyn A, Le Noir S, Baleydier F, Simon A, Beldjord K, et al. NOTCH1/FBXW7 mutation identifies a large subgroup with favorable outcome in adult T-cell acute lymphoblastic leukemia (T-ALL): a Group for Research on Adult Acute Lymphoblastic Leukemia (GRAALL) study. Blood. 2009 Apr 23;113(17):3918–24.

74. Clappier E, Collette S, Grardel N, Girard S, Suarez L, Brunie G, et al. NOTCH1 and FBXW7 mutations have a favorable impact on early response to treatment, but not on outcome, in children with T-cell acute lymphoblastic leukemia (T-ALL) treated on EORTC trials 58881 and 58951. Leukemia. 2010 Dec;24(12):2023–31.

75. Malyukova A, Brown S, Papa R, O'Brien R, Giles J, Trahair TN, et al. FBXW7 regulates glucocorticoid response in T-cell acute lymphoblastic leukaemia by targeting the glucocorticoid receptor for degradation. Leukemia. 2013 Apr;27(5):1053–62.

76. Paugh SW, Bonten EJ, Savic D, Ramsey LB, Thierfelder WE, Gurung P, et al. NALP3 inflammasome upregulation and CASP1 cleavage of the glucocorticoid receptor cause glucocorticoid resistance in leukemia cells. Nat Genet. 2015 Jun;47(6):607–14.

77. Oakley RH, Sar M, Cidlowski JA. The human glucocorticoid receptor beta isoform. Expression, biochemical properties, and putative function. J Biol Chem. 1996 Apr 19;271(16):9550–9.

78. Shahidi H, Vottero A, Stratakis CA, Taymans SE, Karl M, Longui CA, et al. Imbalanced expression of the glucocorticoid receptor isoforms in cultured lymphocytes from a patient with systemic glucocorticoid resistance and chronic lymphocytic leukemia. Biochem Biophys Res Commun. 1999 Jan 27;254(3):559–65.

79. Koga Y, Matsuzaki A, Suminoe A, Hattori H, Kanemitsu S, Hara T. Differential mRNA expression of glucocorticoid receptor alpha and beta is associated with glucocorticoid sensitivity of acute lymphoblastic leukemia in children. Pediatr Blood Cancer. 2005 Aug;45(2):121–7.

80. Haarman EG, Kaspers GJL, Pieters R, Rottier MMA, Veerman AJP. Glucocorticoid receptor alpha, beta and gamma expression vs in vitro glucocorticod resistance in childhood leukemia. Leukemia. 2004 Mar;18(3):530–7.

81. Beger C, Gerdes K, Lauten M, Tissing WJE, Fernandez-Munoz I, Schrappe M, et al. Expression and structural analysis of glucocorticoid receptor isoform gamma in human leukaemia cells using an isoform-specific real-time polymerase chain reaction approach. Br J Haematol. 2003 Jul;122(2):245–52.

82. Grad I, Picard D. The glucocorticoid responses are shaped by molecular chaperones. Mol Cell Endocrinol. 2007 Sep 15;275(1–2):2–12.

83. Lauten M, Beger C, Gerdes K, Asgedom G, Kardinal C, Welte K, et al. Expression of heat-shock protein 90 in glucocorticoid-sensitive and -resistant childhood acute lymphoblastic leukaemia. Leukemia. 2003 Aug;17(8):1551–6.

84. Tissing WJE, Meijerink JPP, den Boer ML, Brinkhof B, Pieters R. mRNA expression levels of (co)chaperone molecules of the glucocorticoid receptor are not involved in glucocorticoid resistance in pediatric ALL. Leukemia. 2005 May;19(5):727–33.

85. John S, Sabo PJ, Johnson TA, Sung M-H, Biddie SC, Lightman SL, et al. Interaction of the glucocorticoid receptor with the chromatin landscape. Mol Cell. 2008 Mar 14;29(5):611–24.

86. Pottier N, Yang W, Assem M, Panetta JC, Pei D, Paugh SW, et al. The SWI/SNF chromatin-remodeling complex and glucocorticoid resistance in acute lymphoblastic leukemia. J Natl Cancer Inst. 2008 Dec 17;100(24):1792–803.

87. Hogan LE, Meyer JA, Yang J, Wang J, Wong N, Yang W, et al. Integrated genomic analysis of relapsed childhood acute lymphoblastic leukemia reveals therapeutic strategies. Blood. 2011 Nov 10;118(19):5218–26.

88. Bhatla T, Wang J, Morrison DJ, Raetz EA, Burke MJ, Brown P, et al. Epigenetic reprogramming reverses the relapse-specific gene expression signature and restores chemosensitivity in childhood B-lymphoblastic leukemia. Blood. 2012 May 31;119(22):5201–10.

89. Gruhn B, Naumann T, Gruner D, Walther M, Wittig S, Becker S, et al. The expression of histone deacetylase 4 is associated with prednisone poor-response in childhood acute lymphoblastic leukemia. Leuk Res. 2013 Oct;37(10):1200–7.

90. Jones CL, Bhatla T, Blum R, Wang J, Paugh SW, Wen X, et al. Loss of TBL1XR1 disrupts glucocorticoid receptor recruitment to chromatin and results in glucocorticoid resistance in a B-lymphoblastic leukemia model. J Biol Chem. 2014 Jul 25;289(30):20502–15.

91. Liu Y, Easton J, Shao Y, Maciaszek J, Wang Z, Wilkinson MR, et al. The genomic landscape of pediatric and young adult T-lineage acute lymphoblastic leukemia. Nat Genet. 2017 Aug;49(8):1211–8.

92. Zhang J, Mullighan CG, Harvey RC, Wu G, Chen X, Edmonson M, et al. Key pathways are frequently mutated in high-risk childhood acute lymphoblastic leukemia: a report from the Children's Oncology Group. Blood. 2011 Sep 15;118(11):3080–7.

93. Moffitt AB, Dave SS. Clinical Applications of the Genomic Landscape of Aggressive Non-Hodgkin Lymphoma. J Clin Oncol Off J Am Soc Clin Oncol. 2017 Mar 20;35(9):955–62.

94. Revollo JR, Cidlowski JA. Mechanisms generating diversity in glucocorticoid receptor signaling. Ann N Y Acad Sci. 2009 Oct;1179:167–78.

95. Raker VK, Becker C, Steinbrink K. The cAMP Pathway as Therapeutic Target in Autoimmune and Inflammatory Diseases. Front Immunol. 2016;7:123.

96. Gruol DJ, Campbell NF, Bourgeois S. Cyclic AMP-dependent protein kinase promotes glucocorticoid receptor function. J Biol Chem. 1986 Apr 15;261(11):4909–14.

97. Medh RD, Saeed MF, Johnson BH, Thompson EB. Resistance of human leukemic CEM-C1 cells is overcome by synergism between glucocorticoid and protein kinase A pathways: correlation with c-Myc suppression. Cancer Res. 1998 Aug 15;58(16):3684–93.

98. Zhang L, Insel PA. The pro-apoptotic protein Bim is a convergence point for cAMP/protein kinase A- and glucocorticoid-promoted apoptosis of lymphoid cells. J Biol Chem. 2004 May 14;279(20):20858–65.

99. Dong H, Carlton ME, Lerner A, Epstein PM. Effect of cAMP signaling on expression of glucocorticoid receptor, Bim and Bad in glucocorticoid-sensitive and resistant leukemic and multiple myeloma cells. Front Pharmacol. 2015;6:230.

100. Lerner A, Epstein PM. Cyclic nucleotide phosphodiesterases as targets for treatment of haematological malignancies. Biochem J. 2006 Jan 1;393(Pt 1):21–41.

101. Ogawa R, Streiff MB, Bugayenko A, Kato GJ. Inhibition of PDE4 phosphodiesterase activity induces growth suppression, apoptosis, glucocorticoid sensitivity, p53, and p21(WAF1/CIP1) proteins in human acute lymphoblastic leukemia cells. Blood. 2002 May 1;99(9):3390–7.

102. Tiwari S, Dong H, Kim EJ, Weintraub L, Epstein PM, Lerner A. Type 4 cAMP phosphodiesterase (PDE4) inhibitors augment glucocorticoid-mediated apoptosis in B cell chronic lymphocytic leukemia (B-CLL) in the absence of exogenous adenylyl cyclase stimulation. Biochem Pharmacol. 2005 Feb 1;69(3):473–83.

103. Meyers JA, Taverna J, Chaves J, Makkinje A, Lerner A. Phosphodiesterase 4 inhibitors augment levels of glucocorticoid receptor in B cell chronic lymphocytic leukemia but not in normal circulating hematopoietic cells. Clin Cancer Res Off J Am Assoc Cancer Res. 2007 Aug 15;13(16):4920–7.

104. Kim S-W, Rai D, Aguiar RCT. Gene set enrichment analysis unveils the mechanism for the phosphodiesterase 4B control of glucocorticoid response in B-cell lymphoma. Clin Cancer Res Off J Am Assoc Cancer Res. 2011 Nov 1;17(21):6723–32.

105. Shipp MA, Ross KN, Tamayo P, Weng AP, Kutok JL, Aguiar RCT, et al. Diffuse large B-cell lymphoma outcome prediction by gene-expression profiling and supervised machine learning. Nat Med. 2002 Jan;8(1):68–74.

106. Pearson G, Robinson F, Beers Gibson T, Xu BE, Karandikar M, Berman K, et al. Mitogen-activated protein (MAP) kinase pathways: regulation and physiological functions. Endocr Rev. 2001 Apr;22(2):153–83.

107. Tanaka T, Okabe T, Gondo S, Fukuda M, Yamamoto M, Umemura T, et al. Modification of glucocorticoid sensitivity by MAP kinase signaling pathways in glucocorticoid-induced T-cell apoptosis. Exp Hematol. 2006 Nov;34(11):1542–52.

108. Miller AL, Webb MS, Copik AJ, Wang Y, Johnson BH, Kumar R, et al. p38 Mitogen-activated protein kinase (MAPK) is a key mediator in glucocorticoid-induced apoptosis of lymphoid cells: correlation between p38 MAPK activation and site-specific phosphorylation of the human glucocorticoid receptor at serine 211. Mol Endocrinol Baltim Md. 2005 Jun;19(6):1569–83.

109. Lu J, Quearry B, Harada H. p38-MAP kinase activation followed by BIM induction is essential for glucocorticoid-induced apoptosis in lymphoblastic leukemia cells. FEBS Lett. 2006 Jun 12;580(14):3539–44.

110. Harada H, Quearry B, Ruiz-Vela A, Korsmeyer SJ. Survival factor-induced extracellular signal-regulated kinase phosphorylates BIM, inhibiting its association with BAX and proapoptotic activity. Proc Natl Acad Sci U S A. 2004 Oct 26;101(43):15313–7.

111. Rambal AA, Panaguiton ZLG, Kramer L, Grant S, Harada H. MEK inhibitors potentiate dexamethasone lethality in acute lymphoblastic leukemia cells through the pro-apoptotic molecule BIM. Leukemia. 2009 Oct;23(10):1744–54.

112. Rogatsky I, Logan SK, Garabedian MJ. Antagonism of glucocorticoid receptor transcriptional activation by the c-Jun N-terminal kinase. Proc Natl Acad Sci U S A. 1998 Mar 3;95(5):2050–5.

113. Jones CL, Gearheart CM, Fosmire S, Delgado-Martin C, Evensen NA, Bride K, et al. MAPK signaling cascades mediate distinct glucocorticoid resistance mechanisms in pediatric leukemia. Blood. 2015 Nov 5;126(19):2202–12.

114. Burotto M, Chiou VL, Lee J-M, Kohn EC. The MAPK pathway across different malignancies: a new perspective. Cancer. 2014 Nov 15;120(22):3446–56.

115. Morishita N, Tsukahara H, Chayama K, Ishida T, Washio K, Miyamura T, et al. Activation of Akt is associated with poor prognosis and chemotherapeutic resistance in pediatric B-precursor acute lymphoblastic leukemia. Pediatr Blood Cancer. 2012 Jul 15;59(1):83–9.

116. Piovan E, Yu J, Tosello V, Herranz D, Ambesi-Impiombato A, Da Silva AC, et al. Direct reversal of glucocorticoid resistance by AKT inhibition in acute lymphoblastic leukemia. Cancer Cell. 2013 Dec 9;24(6):766–76.

117. Kino T, Souvatzoglou E, De Martino MU, Tsopanomihalu M, Wan Y, Chrousos GP. Protein 14-3-3sigma interacts with and favors cytoplasmic subcellular localization of the glucocorticoid receptor, acting as a negative regulator of the glucocorticoid signaling pathway. J Biol Chem. 2003 Jul 11;278(28):25651–6.

118. Habib T, Sadoun A, Nader N, Suzuki S, Liu W, Jithesh PV, et al. AKT1 has dual actions on the glucocorticoid receptor by cooperating with 14-3-3. Mol Cell Endocrinol. 2017 Jan 5;439:431–43.

119. Silveira AB, Laranjeira ABA, Rodrigues GOL, Leal PC, Cardoso BA, Barata JT, et al. PI3K inhibition synergizes with glucocorticoids but antagonizes with methotrexate in T-cell acute lymphoblastic leukemia. Oncotarget. 2015 May 30;6(15):13105–18.

120. Evangelisti C, Cappellini A, Oliveira M, Fragoso R, Barata JT, Bertaina A, et al. Phosphatidylinositol 3-kinase inhibition potentiates glucocorticoid response in B-cell acute lymphoblastic leukemia. J Cell Physiol. 2018 Mar;233(3):1796–811.

121. Hay N, Sonenberg N. Upstream and downstream of mTOR. Genes Dev. 2004 Aug 15;18(16):1926–45.

122. Wei G, Twomey D, Lamb J, Schlis K, Agarwal J, Stam RW, et al. Gene expression-based chemical genomics identifies rapamycin as a modulator of MCL1 and glucocorticoid resistance. Cancer Cell. 2006 Oct;10(4):331–42.

123. Gu L, Zhou C, Liu H, Gao J, Li Q, Mu D, et al. Rapamycin sensitizes T-ALL cells to dexamethasone-induced apoptosis. J Exp Clin Cancer Res CR. 2010 Nov 18;29:150.

124. Batista A, Barata JT, Raderschall E, Sallan SE, Carlesso N, Nadler LM, et al. Targeting of active mTOR inhibits primary leukemia T cells and synergizes with cytotoxic drugs and signaling inhibitors. Exp Hematol. 2011 Apr;39(4):457-472.e3.

125. Zhang C, Ryu Y-K, Chen TZ, Hall CP, Webster DR, Kang MH. Synergistic activity of rapamycin and dexamethasone in vitro and in vivo in acute lymphoblastic leukemia via cell-cycle arrest and apoptosis. Leuk Res. 2012 Mar;36(3):342–9.

126. Schult C, Dahlhaus M, Glass A, Fischer K, Lange S, Freund M, et al. The dual kinase inhibitor NVP-BEZ235 in combination with cytotoxic drugs exerts anti-proliferative activity towards acute lymphoblastic leukemia cells. Anticancer Res. 2012 Feb;32(2):463–74.

127. Hall CP, Reynolds CP, Kang MH. Modulation of Glucocorticoid Resistance in Pediatric T-cell Acute Lymphoblastic Leukemia by Increasing BIM Expression with the PI3K/mTOR Inhibitor BEZ235. Clin Cancer Res Off J Am Assoc Cancer Res. 2016 Feb 1;22(3):621–32.

128. Murray PJ. The JAK-STAT signaling pathway: input and output integration. J Immunol Baltim Md 1950. 2007 Mar 1;178(5):2623–9.

129. Roberts KG, Morin RD, Zhang J, Hirst M, Zhao Y, Su X, et al. Genetic alterations activating kinase and cytokine receptor signaling in high-risk acute lymphoblastic leukemia. Cancer Cell. 2012 Aug 14;22(2):153–66.

130. Stöcklin E, Wissler M, Gouilleux F, Groner B. Functional interactions between Stat5 and the glucocorticoid receptor. Nature. 1996 Oct 24;383(6602):726–8.

131. Wu S-C, Li LS, Kopp N, Montero J, Chapuy B, Yoda A, et al. Activity of the Type II JAK2 Inhibitor CHZ868 in B Cell Acute Lymphoblastic Leukemia. Cancer Cell. 2015 Jul 13;28(1):29–41.

132. Delgado-Martin C, Meyer LK, Huang BJ, Shimano KA, Zinter MS, Nguyen JV, et al. JAK/STAT pathway inhibition overcomes IL7-induced glucocorticoid resistance in a subset of human T-cell acute lymphoblastic leukemias. Leukemia. 2017 May 9;

133. Oppermann S, Lam AJ, Tung S, Shi Y, McCaw L, Wang G, et al. Janus and PI3-kinases mediate glucocorticoid resistance in activated chronic leukemia cells. Oncotarget. 2016 Nov 8;7(45):72608–21.

134. Tzoneva G, Ferrando AA. Recent advances on NOTCH signaling in T-ALL. Curr Top Microbiol Immunol. 2012;360:163–82.

135. De Keersmaecker K, Lahortiga I, Mentens N, Folens C, Van Neste L, Bekaert S, et al. In vitro validation of gamma-secretase inhibitors alone or in combination with other anti-cancer drugs for the treatment of T-cell acute lymphoblastic leukemia. Haematologica. 2008 Apr;93(4):533–42.

136. Real PJ, Tosello V, Palomero T, Castillo M, Hernando E, de Stanchina E, et al. Gamma-secretase inhibitors reverse glucocorticoid resistance in T cell acute lymphoblastic leukemia. Nat Med. 2009 Jan;15(1):50–8.

137. Samon JB, Castillo-Martin M, Hadler M, Ambesi-Impiobato A, Paietta E, Racevskis J, et al. Preclinical analysis of the γ-secretase inhibitor PF-03084014 in combination with glucocorticoids in T-cell acute lymphoblastic leukemia. Mol Cancer Ther. 2012 Jul;11(7):1565–75.

138. Milano J, McKay J, Dagenais C, Foster-Brown L, Pognan F, Gadient R, et al. Modulation of notch processing by gamma-secretase inhibitors causes intestinal goblet cell metaplasia and induction of genes known to specify gut secretory lineage differentiation. Toxicol Sci Off J Soc Toxicol. 2004 Nov;82(1):341–58.

139. Agnusdei V, Minuzzo S, Frasson C, Grassi A, Axelrod F, Satyal S, et al. Therapeutic antibody targeting of Notch1 in T-acute lymphoblastic leukemia xenografts. Leukemia. 2014 Feb;28(2):278–88.

140. Palacios EH, Weiss A. Function of the Src-family kinases, Lck and Fyn, in T-cell development and activation. Oncogene. 2004 Oct 18;23(48):7990–8000.

141. Serafin V, Capuzzo G, Milani G, Minuzzo SA, Pinazza M, Bortolozzi R, et al. Glucocorticoid resistance is reverted by LCK inhibition in pediatric T-cell acute lymphoblastic leukemia. Blood. 2017 21;130(25):2750–61.

142. Harr MW, Caimi PF, McColl KS, Zhong F, Patel SN, Barr PM, et al. Inhibition of Lck enhances glucocorticoid sensitivity and apoptosis in lymphoid cell lines and in chronic lymphocytic leukemia. Cell Death Differ. 2010 Sep;17(9):1381–91.

143. Seckl JR. 11beta-hydroxysteroid dehydrogenases: changing glucocorticoid action. Curr Opin Pharmacol. 2004 Dec;4(6):597–602.

144. Sai S, Nakagawa Y, Sakaguchi K, Okada S, Takahashi H, Hongo T, et al. Differential regulation of 11beta-hydroxysteroid dehydrogenase-1 by dexamethasone in glucocorticoid-sensitive and -resistant childhood lymphoblastic leukemia. Leuk Res. 2009 Dec;33(12):1696–8.

145. Sai S, Nakagawa Y, Yamaguchi R, Suzuki M, Sakaguchi K, Okada S, et al. Expression of 11beta-hydroxysteroid dehydrogenase 2 contributes to glucocorticoid resistance in lymphoblastic leukemia cells. Leuk Res. 2011 Dec;35(12):1644–8.

146. Tao Y, Gao L, Wu X, Wang H, Yang G, Zhan F, et al. Down-regulation of 11β-hydroxysteroid dehydrogenase type 2 by bortezomib sensitizes Jurkat leukemia T cells against glucocorticoid-induced apoptosis. PloS One. 2013;8(6):e67067.

147. Garbrecht MR, Schmidt TJ. Expression and Regulation of 11- β Hydroxysteroid Dehydrogenase Type 2 Enzyme Activity in the Glucocorticoid-Sensitive CEM-C7 Human Leukemic Cell Line. ISRN Oncol. 2013;2013:245246.

148. Homma H, Maruyama H, Niitsu Y, Listowsky I. A subclass of glutathione S-transferases as intracellular high-capacity and high-affinity steroid-binding proteins. Biochem J. 1986 May 1;235(3):763–8.

149. Anderer G, Schrappe M, Brechlin AM, Lauten M, Muti P, Welte K, et al. Polymorphisms within glutathione S-transferase genes and initial response to glucocorticoids in childhood acute lymphoblastic leukaemia. Pharmacogenetics. 2000 Nov;10(8):715–26.

150. Beesley AH, Firth MJ, Ford J, Weller RE, Freitas JR, Perera KU, et al. Glucocorticoid resistance in T-lineage acute lymphoblastic leukaemia is associated with a proliferative metabolism. Br J Cancer. 2009 Jun 16;100(12):1926–36.

151. Samuels AL, Heng JY, Beesley AH, Kees UR. Bioenergetic modulation overcomes glucocorticoid resistance in T-lineage acute lymphoblastic leukaemia. Br J Haematol. 2014 Apr;165(1):57–66.

152. Holleman A, Cheok MH, den Boer ML, Yang W, Veerman AJP, Kazemier KM, et al. Gene-expression patterns in drug-resistant acute lymphoblastic leukemia cells and response to treatment. N Engl J Med. 2004 Aug 5;351(6):533–42.

153. Hulleman E, Kazemier KM, Holleman A, VanderWeele DJ, Rudin CM, Broekhuis MJC, et al. Inhibition of glycolysis modulates prednisolone resistance in acute lymphoblastic leukemia cells. Blood. 2009 Feb 26;113(9):2014–21.

154. Buentke E, Nordström A, Lin H, Björklund A-C, Laane E, Harada M, et al. Glucocorticoid-induced cell death is mediated through reduced glucose metabolism in lymphoid leukemia cells. Blood Cancer J. 2011 Jul;1(7):e31.

155. Ariës IM, Hansen BR, Koch T, van den Dungen R, Evans WE, Pieters R, et al. The synergism of MCL1 and glycolysis on pediatric acute lymphoblastic leukemia cell survival and prednisolone resistance. Haematologica. 2013 Dec;98(12):1905–11.

156. Pang Y-Y, Wang T, Chen F-Y, Wu Y-L, Shao X, Xiao F, et al. Glycolytic inhibitor 2-deoxy-d-glucose suppresses cell proliferation and enhances methylprednisolone sensitivity in non-Hodgkin lymphoma cells through down-regulation of HIF-1α and c-MYC. Leuk Lymphoma. 2015 Jun;56(6):1821–30.

157. Chan LN, Chen Z, Braas D, Lee J-W, Xiao G, Geng H, et al. Metabolic gatekeeper function of B-lymphoid transcription factors. Nature. 2017 23;542(7642):479–83.

158. Madden EA, Bishop EJ, Fiskin AM, Melnykovych G. Possible role of cholesterol in the susceptibility of a human acute lymphoblastic leukemia cell line to dexamethasone. Cancer Res. 1986 Feb;46(2):617–22.

159. Samuels AL, Beesley AH, Yadav BD, Papa RA, Sutton R, Anderson D, et al. A pre-clinical model of resistance to induction therapy in pediatric acute lymphoblastic leukemia. Blood Cancer J. 2014 Aug 1;4:e232.

160. Lawrie CH. MicroRNAs in hematological malignancies. Blood Rev. 2013 May;27(3):143–54.

161. Han B-W, Feng D-D, Li Z-G, Luo X-Q, Zhang H, Li X-J, et al. A set of miRNAs that involve in the pathways of drug resistance and leukemic stem-cell differentiation is associated with the risk of relapse and glucocorticoid response in childhood ALL. Hum Mol Genet. 2011 Dec 15;20(24):4903–15.

162. Hezaveh K, Kloetgen A, Bernhart SH, Mahapatra KD, Lenze D, Richter J, et al. Alterations of microRNA and microRNA-regulated messenger RNA expression in germinal center B-cell lymphomas determined by integrative sequencing analysis. Haematologica. 2016;101(11):1380–9.

163. Harada M, Pokrovskaja-Tamm K, Söderhäll S, Heyman M, Grander D, Corcoran M. Involvement of miR17 pathway in glucocorticoid-induced cell death in pediatric acute lymphoblastic leukemia. Leuk Lymphoma. 2012 Oct;53(10):2041–50.

164. Li X-J, Luo X-Q, Han B-W, Duan F-T, Wei P-P, Chen Y-Q. MicroRNA-100/99a, deregulated in acute lymphoblastic leukaemia, suppress proliferation and promote apoptosis by regulating the FKBP51 and IGF1R/mTOR signalling pathways. Br J Cancer. 2013 Oct 15;109(8):2189–98.

165. Ledderose C, Möhnle P, Limbeck E, Schütz S, Weis F, Rink J, et al. Corticosteroid resistance in sepsis is influenced by microRNA-124--induced downregulation of glucocorticoid receptor-α. Crit Care Med. 2012 Oct;40(10):2745–53.

166. Liang Y-N, Tang Y-L, Ke Z-Y, Chen Y-Q, Luo X-Q, Zhang H, et al. MiR-124 contributes to glucocorticoid resistance in acute lymphoblastic leukemia by promoting proliferation, inhibiting apoptosis and targeting the glucocorticoid receptor. J Steroid Biochem Mol Biol. 2017;172:62–8.

167. Kim J, Jeong D, Nam J, Aung TN, Gim J-A, Park KU, et al. MicroRNA-124 regulates glucocorticoid sensitivity by targeting phosphodiesterase 4B in diffuse large B cell lymphoma. Gene. 2015 Mar 1;558(1):173–80.

168. Kotani A, Ha D, Hsieh J, Rao PK, Schotte D, den Boer ML, et al. miR-128b is a potent glucocorticoid sensitizer in MLL-AF4 acute lymphocytic leukemia cells and exerts cooperative effects with miR-221. Blood. 2009 Nov 5;114(19):4169–78.

169. Kotani A, Ha D, Schotte D, den Boer ML, Armstrong SA, Lodish HF. A novel mutation in the miR-128b gene reduces miRNA processing and leads to glucocorticoid resistance of MLL-AF4 acute lymphocytic leukemia cells. Cell Cycle Georget Tex. 2010 Mar 15;9(6):1037–42.

170. Huang B, Zhao J, Lei Z, Shen S, Li D, Shen G-X, et al. miR-142-3p restricts cAMP production in CD4+CD25- T cells and CD4+CD25+ TREG cells by targeting AC9 mRNA. EMBO Rep. 2009 Feb;10(2):180–5.

171. Lv M, Zhang X, Jia H, Li D, Zhang B, Zhang H, et al. An oncogenic role of miR-142-3p in human T-cell acute lymphoblastic leukemia (T-ALL) by targeting glucocorticoid receptor-α and cAMP/PKA pathways. Leukemia. 2012 Apr;26(4):769–77.

172. Yang A, Ma J, Wu M, Qin W, Zhao B, Shi Y, et al. Aberrant microRNA-182 expression is associated with glucocorticoid resistance in lymphoblastic malignancies. Leuk Lymphoma. 2012 Dec;53(12):2465–73.

173. Chen P, Shen T, Wang H, Ke Z, Liang Y, Ouyang J, et al. MicroRNA-185-5p restores glucocorticoid sensitivity by suppressing the mammalian target of rapamycin complex (mTORC) signaling pathway to enhance glucocorticoid receptor autoregulation. Leuk Lymphoma. 2017 Feb 28;1–11.

174. Pui C-H, Mullighan CG, Evans WE, Relling MV. Pediatric acute lymphoblastic leukemia: where are we going and how do we get there? Blood. 2012 Aug 9;120(6):1165–74.

175. Ronson A, Tvito A, Rowe JM. Treatment of Relapsed/Refractory Acute Lymphoblastic Leukemia in Adults. Curr Oncol Rep. 2016;18(6):39.

176. Liu Y-F, Wang B-Y, Zhang W-N, Huang J-Y, Li B-S, Zhang M, et al. Genomic Profiling of Adult and Pediatric B-cell Acute Lymphoblastic Leukemia. EBioMedicine. 2016 Jun;8:173–83.

177. Liu Y, Easton J, Shao Y, Maciaszek J, Wang Z, Wilkinson MR, et al. The genomic landscape of pediatric and young adult T-lineage acute lymphoblastic leukemia. Nat Genet. 2017 Aug;49(8):1211–8.

178. De Keersmaecker K, Atak ZK, Li N, Vicente C, Patchett S, Girardi T, et al. Exome sequencing identifies mutation in CNOT3 and ribosomal genes RPL5 and RPL10 in T-cell acute lymphoblastic leukemia. Nat Genet. 2013 Feb;45(2):186–90.

179. Lugthart S, Cheok MH, den Boer ML, Yang W, Holleman A, Cheng C, et al. Identification of genes associated with chemotherapy crossresistance and treatment response in childhood acute lymphoblastic leukemia. Cancer Cell. 2005 Apr;7(4):375–86.

180. Holleman A, Cheok MH, den Boer ML, Yang W, Veerman AJP, Kazemier KM, et al. Gene-expression patterns in drug-resistant acute lymphoblastic leukemia cells and response to treatment. N Engl J Med. 2004 Aug 5;351(6):533–42.

181. Stam RW, Den Boer ML, Schneider P, de Boer J, Hagelstein J, Valsecchi MG, et al. Association of high-level MCL-1 expression with in vitro and in vivo prednisone resistance in MLL-rearranged infant acute lymphoblastic leukemia. Blood. 2010 Feb 4;115(5):1018–25.

182. Li Y, Buijs-Gladdines JGCAM, Canté-Barrett K, Stubbs AP, Vroegindeweij EM, Smits WK, et al. IL-7 Receptor Mutations and Steroid Resistance in Pediatric T cell Acute Lymphoblastic Leukemia: A Genome Sequencing Study. PLoS Med. 2016 Dec;13(12):e1002200.

183. Bakker E, Qattan M, Mutti L, Demonacos C, Krstic-Demonacos M. The role of microenvironment and immunity in drug response in leukemia. Biochim Biophys Acta. 2016 Mar;1863(3):414–26.

184. Konopleva M, Tabe Y, Zeng Z, Andreeff M. Therapeutic targeting of microenvironmental interactions in leukemia: mechanisms and approaches. Drug Resist Updat Rev Comment Antimicrob Anticancer Chemother. 2009 Oct;12(4–5):103–13.

185. Tavor S, Petit I. Can inhibition of the SDF-1/CXCR4 axis eradicate acute leukemia? Semin Cancer Biol. 2010 Jun;20(3):178–85.

186. Konopleva MY, Jordan CT. Leukemia stem cells and microenvironment: biology and therapeutic targeting. J Clin Oncol Off J Am Soc Clin Oncol. 2011 Feb 10;29(5):591–9.

187. Manabe A, Coustan-Smith E, Behm FG, Raimondi SC, Campana D. Bone marrow-derived stromal cells prevent apoptotic cell death in B-lineage acute lymphoblastic leukemia. Blood. 1992 May 1;79(9):2370–7.

188. Manabe A, Murti KG, Coustan-Smith E, Kumagai M, Behm FG, Raimondi SC, et al. Adhesion-dependent survival of normal and leukemic human B lymphoblasts on bone marrow stromal cells. Blood. 1994 Feb 1;83(3):758–66.

189. Takada Y, Ye X, Simon S. The integrins. Genome Biol. 2007;8(5):215.

190. Hsieh Y-T, Gang EJ, Geng H, Park E, Huantes S, Chudziak D, et al. Integrin alpha4 blockade sensitizes drug resistant pre-B acute lymphoblastic leukemia to chemotherapy. Blood. 2013 Mar 7;121(10):1814–8.

191. Shalapour S, Hof J, Kirschner-Schwabe R, Bastian L, Eckert C, Prada J, et al. High VLA-4 expression is associated with adverse outcome and distinct gene expression changes in childhood B-cell precursor acute lymphoblastic leukemia at first relapse. Haematologica. 2011 Nov;96(11):1627–35.

192. Shishido S, Bönig H, Kim Y-M. Role of integrin alpha4 in drug resistance of leukemia. Front Oncol. 2014;4:99.

193. Bradstock K, Makrynikola V, Bianchi A, Byth K. Analysis of the mechanism of adhesion of precursor-B acute lymphoblastic leukemia cells to bone marrow fibroblasts. Blood. 1993 Dec 1;82(11):3437–44.

194. Papayannopoulou T, Craddock C, Nakamoto B, Priestley GV, Wolf NS. The VLA4/VCAM-1 adhesion pathway defines contrasting mechanisms of lodgement of transplanted murine hemopoietic progenitors between bone marrow and spleen. Proc Natl Acad Sci U S A. 1995 Oct 10;92(21):9647–51.

195. Craddock CF, Nakamoto B, Elices M, Papayannopoulou T h. The role of CS1 moiety of fibronectin in VLA mediated haemopoietic progenitor trafficking. Br J Haematol. 1997 Apr;97(1):15–21.

196. Mudry RE, Fortney JE, York T, Hall BM, Gibson LF. Stromal cells regulate survival of B-lineage leukemic cells during chemotherapy. Blood. 2000 Sep 1;96(5):1926–32.

197. Sarkar S, Svoboda M, de Beaumont R, Freedman AS. The role of Aktand RAFTK in beta1 integrin mediated survival of precursor B-acute lymphoblastic leukemia cells. Leuk Lymphoma. 2002 Aug;43(8):1663–71.

198. Astier AL, Xu R, Svoboda M, Hinds E, Munoz O, de Beaumont R, et al. Temporal gene expression profile of human precursor B leukemia cells induced by adhesion receptor: identification of pathways regulating B-cell survival. Blood. 2003 Feb 1;101(3):1118–27.

199. Jacamo R, Chen Y, Wang Z, Ma W, Zhang M, Spaeth EL, et al. Reciprocal leukemia-stroma VCAM-1/VLA-4-dependent activation of NF-κB mediates chemoresistance. Blood. 2014 Apr 24;123(17):2691–702.

200. Arcangeli A, Pillozzi S, Becchetti A. Targeting ion channels in leukemias: a new challenge for treatment. Curr Med Chem. 2012;19(5):683–96.

201. Pillozzi S, Masselli M, De Lorenzo E, Accordi B, Cilia E, Crociani O, et al. Chemotherapy resistance in acute lymphoblastic leukemia requires hERG1 channels and is overcome by hERG1 blockers. Blood. 2011 Jan 20;117(3):902–14.

202. Kapp TG, Rechenmacher F, Sobahi TR, Kessler H. Integrin modulators: a patent review. Expert Opin Ther Pat. 2013 Oct;23(10):1273–95.

203. Hsieh YT, Gang EJ, Shishido SN, Kim HN, Pham J, Khazal S, et al. Effects of the small-molecule inhibitor of integrin α4, TBC3486, on pre-B-ALL cells. Leukemia. 2014 Oct;28(10):2101–4.

204. Fagerholm SC, Varis M, Stefanidakis M, Hilden TJ, Gahmberg CG. alpha-Chain phosphorylation of the human leukocyte CD11b/CD18 (Mac-1) integrin is pivotal for integrin activation to bind ICAMs and leukocyte extravasation. Blood. 2006 Nov 15;108(10):3379–86.

205. Rhein P, Mitlohner R, Basso G, Gaipa G, Dworzak MN, Kirschner-Schwabe R, et al. CD11b is a therapy resistance- and minimal residual disease-specific marker in precursor B-cell acute lymphoblastic leukemia. Blood. 2010 May 6;115(18):3763–71.

206. Naci D, El Azreq M-A, Chetoui N, Lauden L, Sigaux F, Charron D, et al. α2β1 integrin promotes chemoresistance against doxorubicin in cancer cells through extracellular signal-regulated kinase (ERK). J Biol Chem. 2012 May 18;287(21):17065–76.

207. Angst BD, Marcozzi C, Magee AI. The cadherin superfamily: diversity in form and function. J Cell Sci. 2001 Feb;114(Pt 4):629–41.

208. Heuberger J, Birchmeier W. Interplay of cadherin-mediated cell adhesion and canonical Wnt signaling. Cold Spring Harb Perspect Biol. 2010 Feb;2(2):a002915.

209. Chae W-J, Bothwell ALM. Canonical and Non-Canonical Wnt Signaling in Immune Cells. Trends Immunol. 2018;39(10):830–47.

210. Neumann M, Seehawer M, Schlee C, Vosberg S, Heesch S, von der Heide EK, et al. FAT1 expression and mutations in adult acute lymphoblastic leukemia. Blood Cancer J. 2014 Jun 27;4:e224.

211. Morris LGT, Kaufman AM, Gong Y, Ramaswami D, Walsh LA, Turcan Ş, et al. Recurrent somatic mutation of FAT1 in multiple human cancers leads to aberrant Wnt activation. Nat Genet. 2013 Mar;45(3):253–61.

212. Yang Y, Mallampati S, Sun B, Zhang J, Kim S-B, Lee J-S, et al. Wnt pathway contributes to the protection by bone marrow stromal cells of acute lymphoblastic leukemia cells and is a potential therapeutic target. Cancer Lett. 2013 Jun 1;333(1):9–17.

213. Hogan LE, Meyer JA, Yang J, Wang J, Wong N, Yang W, et al. Integrated genomic analysis of relapsed childhood acute lymphoblastic leukemia reveals therapeutic strategies. Blood. 2011 Nov 10;118(19):5218–26.

214. Dandekar S, Romanos-Sirakis E, Pais F, Bhatla T, Jones C, Bourgeois W, et al. Wnt inhibition leads to improved chemosensitivity in paediatric acute lymphoblastic leukaemia. Br J Haematol. 2014 Oct;167(1):87–99.

215. de Bock CE, Ardjmand A, Molloy TJ, Bone SM, Johnstone D, Campbell DM, et al. The Fat1 cadherin is overexpressed and an independent prognostic factor for survival in paired diagnosis-relapse samples of precursor B-cell acute lymphoblastic leukemia. Leukemia. 2012 May;26(5):918–26.

216. de Bock CE, Down M, Baidya K, Sweron B, Boyd AW, Fiers M, et al. T-cell acute lymphoblastic leukemias express a unique truncated FAT1 isoform that cooperates with NOTCH1 in leukemia development. Haematologica. 2019 May;104(5):e204–7.

217. Yau T, Dan X, Ng CCW, Ng TB. Lectins with potential for anti-cancer therapy. Mol Basel Switz. 2015 Feb 26;20(3):3791–810.

218. Thijssen VL, Heusschen R, Caers J, Griffioen AW. Galectin expression in cancer diagnosis and prognosis: A systematic review. Biochim Biophys Acta. 2015 Apr;1855(2):235–47.

219. Nabi IR, Shankar J, Dennis JW. The galectin lattice at a glance. J Cell Sci. 2015 Jul 1;128(13):2213–9.

220. Yamamoto-Sugitani M, Kuroda J, Ashihara E, Nagoshi H, Kobayashi T, Matsumoto Y, et al. Galectin-3 (Gal-3) induced by leukemia microenvironment promotes drug resistance and bone marrow lodgment in chronic myelogenous leukemia. Proc Natl Acad Sci U S A. 2011 Oct 18;108(42):17468–73.

221. Fei F, Abdel-Azim H, Lim M, Arutyunyan A, von Itzstein M, Groffen J, et al. Galectin-3 in pre-B acute lymphoblastic leukemia. Leukemia. 2013 Dec;27(12):2385–8.

222. Fei F, Joo EJ, Tarighat SS, Schiffer I, Paz H, Fabbri M, et al. B-cell precursor acute lymphoblastic leukemia and stromal cells communicate through Galectin-3. Oncotarget. 2015 May 10;6(13):11378–94.

223. Hu K, Gu Y, Lou L, Liu L, Hu Y, Wang B, et al. Galectin-3 mediates bone marrow microenvironment-induced drug resistance in acute leukemia cells via Wnt/β-catenin signaling pathway. J Hematol OncolJ Hematol Oncol. 2015 Jan 27;8:1.

224. Ruvolo PP, Ruvolo VR, Benton CB, AlRawi A, Burks JK, Schober W, et al. Combination of galectin inhibitor GCS-100 and BH3 mimetics eliminates both p53 wild type and p53 null AML cells. Biochim Biophys Acta. 2016 Apr;1863(4):562–71.

225. Clark MC, Pang M, Hsu DK, Liu F-T, de Vos S, Gascoyne RD, et al. Galectin-3 binds to CD45 on diffuse large B-cell lymphoma cells to regulate susceptibility to cell death. Blood. 2012 Nov 29;120(23):4635–44.

226. Streetly MJ, Maharaj L, Joel S, Schey SA, Gribben JG, Cotter FE. GCS-100, a novel galectin-3 antagonist, modulates MCL-1, NOXA, and cell cycle to induce myeloma cell death. Blood. 2010 May 13;115(19):3939–48.

227. Chauhan D, Li G, Podar K, Hideshima T, Neri P, He D, et al. A novel carbohydrate-based therapeutic GCS-100 overcomes bortezomib resistance and enhances dexamethasone-induced apoptosis in multiple myeloma cells. Cancer Res. 2005 Sep 15;65(18):8350–8.

228. Nwabo Kamdje AH, Krampera M. Notch signaling in acute lymphoblastic leukemia: any role for stromal microenvironment? Blood. 2011 Dec 15;118(25):6506–14.

229. Li X, von Boehmer H. Notch Signaling in T-Cell Development and T-ALL. ISRN Hematol. 2011;2011:921706.

230. Schmitt TM, Zúñiga-Pflücker JC. Induction of T cell development from hematopoietic progenitor cells by delta-like-1 in vitro. Immunity. 2002 Dec;17(6):749–56.

231. Siebel C, Lendahl U. Notch Signaling in Development, Tissue Homeostasis, and Disease. Physiol Rev. 2017 01;97(4):1235–94.

232. Harrison JS, Rameshwar P, Chang V, Bandari P. Oxygen saturation in the bone marrow of healthy volunteers. Blood. 2002 Jan 1;99(1):394.

233. Ke Q, Costa M. Hypoxia-inducible factor-1 (HIF-1). Mol Pharmacol. 2006 Nov;70(5):1469–80.

234. Sahlgren C, Gustafsson MV, Jin S, Poellinger L, Lendahl U. Notch signaling mediates hypoxia-induced tumor cell migration and invasion. Proc Natl Acad Sci U S A. 2008 Apr 29;105(17):6392–7.

235. Zou J, Li P, Lu F, Liu N, Dai J, Ye J, et al. Notch1 is required for hypoxia-induced proliferation, invasion and chemoresistance of T-cell acute lymphoblastic leukemia cells. J Hematol OncolJ Hematol Oncol. 2013 Jan 5;6:3.

236. Takebe N, Nguyen D, Yang SX. Targeting notch signaling pathway in cancer: clinical development advances and challenges. Pharmacol Ther. 2014 Feb;141(2):140–9.

237. Takam Kamga P, Dal Collo G, Midolo M, Adamo A, Delfino P, Mercuri A, et al. Inhibition of Notch Signaling Enhances Chemosensitivity in B-cell Precursor Acute Lymphoblastic Leukemia. Cancer Res. 2019 Feb 1;79(3):639–49.

238. Nwabo Kamdje AH, Mosna F, Bifari F, Lisi V, Bassi G, Malpeli G, et al. Notch-3 and Notch-4 signaling rescue from apoptosis human B-ALL cells in contact with human bone marrow-derived mesenchymal stromal cells. Blood. 2011 Jul 14;118(2):380–9.

239. Meng X, Matlawska-Wasowska K, Girodon F, Mazel T, Willman CL, Atlas S, et al. GSI-I (Z-LLNle-CHO) inhibits γ-secretase and the proteosome to trigger cell death in precursor-B acute lymphoblastic leukemia. Leukemia. 2011 Jul;25(7):1135–46.

240. DeAngelo DJ, Stone RM, Silverman LB, Stock W, attar EC, Fearen I, et al. A phase I clinical trial of the notch inhibitor MK-0752 in patients with T-cell acute lymphoblastic leukemia/lymphoma (T-ALL) and other leukemias.

241. Real PJ, Tosello V, Palomero T, Castillo M, Hernando E, de Stanchina E, et al. Gamma-secretase inhibitors reverse glucocorticoid resistance in T cell acute lymphoblastic leukemia. Nat Med. 2009 Jan;15(1):50–8.

242. Balkwill F. TNF-alpha in promotion and progression of cancer. Cancer Metastasis Rev. 2006 Sep;25(3):409–16.

243. Riether C, Schürch CM, Ochsenbein AF. Regulation of hematopoietic and leukemic stem cells by the immune system. Cell Death Differ. 2015 Feb;22(2):187–98.

244. Warzocha K, Bienvenu J, Ribeiro P, Moullet I, Dumontet C, Neidhardt-Berard EM, et al. Plasma levels of tumour necrosis factor and its soluble receptors correlate with clinical features and outcome of Hodgkin's disease patients. Br J Cancer. 1998 Jun;77(12):2357–62.

245. Warzocha K, Ribeiro P, Bienvenu J, Roy P, Charlot C, Rigal D, et al. Genetic polymorphisms in the tumor necrosis factor locus influence non-Hodgkin's lymphoma outcome. Blood. 1998 May 15;91(10):3574–81.

246. Lauten M, Matthias T, Stanulla M, Beger C, Welte K, Schrappe M. Association of initial response to prednisone treatment in childhood acute lymphoblastic leukaemia and polymorphisms within the tumour necrosis factor and the interleukin-10 genes. Leukemia. 2002 Aug;16(8):1437–42.

247. Gu L, Findley HW, Zhu N, Zhou M. Endogenous TNFalpha mediates cell survival and chemotherapy resistance by activating the PI3K/Akt pathway in acute lymphoblastic leukemia cells. Leukemia. 2006 May;20(5):900–4.

248. Zubiaga AM, Munoz E, Huber BT. IL-4 and IL-2 selectively rescue Th cell subsets from glucocorticoid-induced apoptosis. J Immunol Baltim Md 1950. 1992 Jul 1;149(1):107–12.

249. Kam JC, Szefler SJ, Surs W, Sher ER, Leung DY. Combination IL-2 and IL-4 reduces glucocorticoid receptor-binding affinity and T cell response to glucocorticoids. J Immunol Baltim Md 1950. 1993 Oct 1;151(7):3460–6.

250. Serafin V, Capuzzo G, Milani G, Minuzzo SA, Pinazza M, Bortolozzi R, et al. Glucocorticoid resistance is reverted by LCK inhibition in pediatric T-cell acute lymphoblastic leukemia. Blood. 2017 21;130(25):2750–61.

251. McCarty JM, Yee EK, Deisher TA, Harlan JM, Kaushansky K. Interleukin-4 induces endothelial vascular cell adhesion molecule-1 (VCAM-1) by an NF-kappa b-independent mechanism. FEBS Lett. 1995 Sep 25;372(2–3):194–8.

252. Juneja HS, Schmalsteig FC, Lee S, Chen J. Vascular cell adhesion molecule-1 and VLA-4 are obligatory adhesion proteins in the heterotypic adherence between human leukemia/lymphoma cells and marrow stromal cells. Exp Hematol. 1993 Mar;21(3):444–50.

253. Mazzucchelli R, Durum SK. Interleukin-7 receptor expression: intelligent design. Nat Rev Immunol. 2007 Feb;7(2):144–54.

254. Meyer LK, Huang B, Roy R, Hechmer A, Anica M. Wandler, Delgado-Martin C, et al. Glucocorticoids Paradoxically Induce Intrinsic Steroid Resistance through a STAT5-Mediated Survival Mechanism in T-Cell Acute Lymphoblastic Leukemia. Blood. 2018;

255. Ray RJ, Furlonger C, Williams DE, Paige CJ. Characterization of thymic stromal-derived lymphopoietin (TSLP) in murine B cell development in vitro. Eur J Immunol. 1996 Jan;26(1):10–6.

256. Harvey RC, Mullighan CG, Chen I-M, Wharton W, Mikhail FM, Carroll AJ, et al. Rearrangement of CRLF2 is associated with mutation of JAK kinases, alteration of IKZF1, Hispanic/Latino ethnicity, and a poor outcome in pediatric B-progenitor acute lymphoblastic leukemia. Blood. 2010 Jul 1;115(26):5312–21.

257. Meyer LK, Delgado-Martin C, Maude SL, Teachey DT, Hermiston ML. CRLF2 Rearrangement Status in Ph-like ALL Predicts Intrinsic Glucocorticoid Resistance In Vitro that is Reversible with Targeted MAPK and PI3K Pathway Inhibition. Blood. 2016;128.

258. Cramer SD, Aplan PD, Durum SK. Therapeutic targeting of IL-7Rα signaling pathways in ALL treatment. Blood. 2016 28;128(4):473–8.

259. Maude SL, Dolai S, Delgado-Martin C, Vincent T, Robbins A, Selvanathan A, et al. Efficacy of JAK/STAT pathway inhibition in murine xenograft models of early T-cell precursor (ETP) acute lymphoblastic leukemia. Blood. 2015 Mar 12;125(11):1759–67.

260. Maude SL, Tasian SK, Vincent T, Hall JW, Sheen C, Roberts KG, et al. Targeting JAK1/2 and mTOR in murine xenograft models of Ph-like acute lymphoblastic leukemia. Blood. 2012 Oct 25;120(17):3510–8.

261. Sokol CL, Luster AD. The chemokine system in innate immunity. Cold Spring Harb Perspect Biol. 2015 Jan 29;7(5).

262. Pozzobon T, Goldoni G, Viola A, Molon B. CXCR4 signaling in health and disease. Immunol Lett. 2016;177:6–15.

263. Gachet S, Genescà E, Passaro D, Irigoyen M, Alcalde H, Clémenson C, et al. Leukemia-initiating cell activity requires calcineurin in T-cell acute lymphoblastic leukemia. Leukemia. 2013 Dec;27(12):2289–300.

264. Passaro D, Irigoyen M, Catherinet C, Gachet S, Da Costa De Jesus C, Lasgi C, et al. CXCR4 Is Required for Leukemia-Initiating Cell Activity in T Cell Acute Lymphoblastic Leukemia. Cancer Cell. 2015 Jun 8;27(6):769–79.

265. van den Berk LCJ, van der Veer A, Willemse ME, Theeuwes MJGA, Luijendijk MW, Tong WH, et al. Disturbed CXCR4/CXCL12 axis in paediatric precursor B-cell acute lymphoblastic leukaemia. Br J Haematol. 2014 Jul;166(2):240–9.

266. Konoplev S, Jorgensen JL, Thomas DA, Lin E, Burger J, Kantarjian HM, et al. Phosphorylated CXCR4 is associated with poor survival in adults with B-acute lymphoblastic leukemia. Cancer. 2011 Oct 15;117(20):4689–95.

267. Sison EAR, Rau RE, McIntyre E, Li L, Small D, Brown P. MLL-rearranged acute lymphoblastic leukaemia stem cell interactions with bone marrow stroma promote survival and therapeutic resistance that can be overcome with CXCR4 antagonism. Br J Haematol. 2013 Mar;160(6):785–97.

268. Sison EAR, Magoon D, Li L, Annesley CE, Rau RE, Small D, et al. Plerixafor as a chemosensitizing agent in pediatric acute lymphoblastic leukemia: efficacy and potential mechanisms of resistance to CXCR4 inhibition. Oncotarget. 2014 Oct 15;5(19):8947–58.

269. Cooper TM, Sison EAR, Baker SD, Li L, Ahmed A, Trippett T, et al. A phase 1 study of the CXCR4 antagonist plerixafor in combination with high-dose cytarabine and etoposide in children with relapsed or refractory acute leukemias or myelodysplastic syndrome: A Pediatric Oncology Experimental Therapeutics Investigators' Consortium study (POE 10-03). Pediatr Blood Cancer. 2017 Aug;64(8).

270. Pieters R, Hunger SP, Boos J, Rizzari C, Silverman L, Baruchel A, et al. L-asparaginase treatment in acute lymphoblastic leukemia: a focus on Erwinia asparaginase. Cancer. 2011 Jan 15;117(2):238–49.

271. Kumar K, Kaur J, Walia S, Pathak T, Aggarwal D. L-asparaginase: an effective agent in the treatment of acute lymphoblastic leukemia. Leuk Lymphoma. 2014 Feb;55(2):256–62.

272. Iwamoto S, Mihara K, Downing JR, Pui C-H, Campana D. Mesenchymal cells regulate the response of acute lymphoblastic leukemia cells to asparaginase. J Clin Invest. 2007 Apr;117(4):1049–57.

273. Roberts KG, Li Y, Payne-Turner D, Harvey RC, Yang Y-L, Pei D, et al. Targetable kinase-activating lesions in Ph-like acute lymphoblastic leukemia. N Engl J Med. 2014 Sep 11;371(11):1005–15.

274. Tasian SK, Doral MY, Borowitz MJ, Wood BL, Chen I-M, Harvey RC, et al. Aberrant STAT5 and PI3K/mTOR pathway signaling occurs in human CRLF2-rearranged B-precursor acute lymphoblastic leukemia. Blood. 2012 Jul 26;120(4):833–42.

275. Cario G, Zimmermann M, Romey R, Gesk S, Vater I, Harbott J, et al. Presence of the P2RY8-CRLF2 rearrangement is associated with a poor prognosis in non-high-risk precursor B-cell acute lymphoblastic leukemia in children treated according to the ALL-BFM 2000 protocol. Blood. 2010 Jul 1;115(26):5393–7.

276. Goleva E, Kisich KO, Leung DYM. A role for STAT5 in the pathogenesis of IL-2-induced glucocorticoid resistance. J Immunol Baltim Md 1950. 2002 Nov 15;169(10):5934–40.

277. Brode S, Farahi N, Cowburn AS, Juss JK, Condliffe AM, Chilvers ER. Interleukin-5 inhibits glucocorticoid-mediated apoptosis in human eosinophils. Thorax. 2010 Dec;65(12):1116–7.

278. Mullighan CG. The genomic landscape of acute lymphoblastic leukemia in children and young adults. Hematol Educ Program Am Soc Hematol Am Soc Hematol Educ Program. 2014 Dec 5;2014(1):174–80.

279. Russell LJ, Capasso M, Vater I, Akasaka T, Bernard OA, Calasanz MJ, et al. Deregulated expression of cytokine receptor gene, CRLF2, is involved in lymphoid transformation in B-cell precursor acute lymphoblastic leukemia. Blood. 2009 Sep 24;114(13):2688–98.

280. Schultz KR, Carroll A, Heerema NA, Bowman WP, Aledo A, Slayton WB, et al. Long-term follow-up of imatinib in pediatric Philadelphia chromosome-positive acute lymphoblastic leukemia: Children's Oncology Group study AALL0031. Leukemia. 2014 Jul;28(7):1467–71.

281. Zhao W, Sachsenmeier K, Zhang L, Sult E, Hollingsworth RE, Yang H. A New Bliss
      Independence Model to Analyze Drug Combination Data. J Biomol Screen. 2014
      Jun;19(5):817–21.

282. Liu Y, Easton J, Shao Y, Maciaszek J, Wang Z, Wilkinson MR, et al. The genomic
      landscape of pediatric and young adult T-lineage acute lymphoblastic leukemia. Nat
      Genet [Internet]. 2017 Jul 3;advance online publication. Available from:
      http://dx.doi.org/10.1038/ng.3909

283. Pui C-H, Carroll WL, Meshinchi S, Arceci RJ. Biology, risk stratification, and therapy of
      pediatric acute leukemias: an update. J Clin Oncol Off J Am Soc Clin Oncol. 2011 Feb
      10;29(5):551–65.

284. Bhojwani D, Pui C-H. Relapsed childhood acute lymphoblastic leukaemia. Lancet Oncol.
      2013 May;14(6):e205-217.

285. Gao J, Liu W-J. Prognostic value of the response to prednisone for children with acute
      lymphoblastic leukemia: a meta-analysis. Eur Rev Med Pharmacol Sci. 2018
      Nov;22(22):7858–66.

286. Erlacher M, Knoflach M, Stec IEM, Böck G, Wick G, Wiegers GJ. TCR signaling inhibits
      glucocorticoid-induced apoptosis in murine thymocytes depending on the stage of
      development. Eur J Immunol. 2005 Nov;35(11):3287–96.

287. Jamieson CA, Yamamoto KR. Crosstalk pathway for inhibition of glucocorticoid-induced
      apoptosis by T cell receptor signaling. Proc Natl Acad Sci U S A. 2000 Jun
      20;97(13):7319–24.

288. Tsitoura DC, Rothman PB. Enhancement of MEK/ERK signaling promotes glucocorticoid resistance in CD4+ T cells. J Clin Invest. 2004 Feb;113(4):619–27.

289. Ribeiro D, Melão A, van Boxtel R, Santos CI, Silva A, Silva MC, et al. STAT5 is essential for IL-7-mediated viability, growth, and proliferation of T-cell acute lymphoblastic leukemia cells. Blood Adv. 2018 Sep 11;2(17):2199–213.

290. Silva A, Laranjeira ABA, Martins LR, Cardoso BA, Demengeot J, Yunes JA, et al. IL-7 contributes to the progression of human T-cell acute lymphoblastic leukemias. Cancer Res. 2011 Jul 15;71(14):4780–9.

291. Treanor LM, Zhou S, Janke L, Churchman ML, Ma Z, Lu T, et al. Interleukin-7 receptor mutants initiate early T cell precursor leukemia in murine thymocyte progenitors with multipotent potential. J Exp Med. 2014 Apr 7;211(4):701–13.

292. Chen W, Dang T, Blind RD, Wang Z, Cavasotto CN, Hittelman AB, et al. Glucocorticoid receptor phosphorylation differentially affects target gene expression. Mol Endocrinol Baltim Md. 2008 Aug;22(8):1754–66.

293. Abe A, Tani-ichi S, Shitara S, Cui G, Yamada H, Miyachi H, et al. An Enhancer of the IL-7 Receptor α-Chain Locus Controls IL-7 Receptor Expression and Maintenance of Peripheral T Cells. J Immunol Baltim Md 1950. 2015 Oct 1;195(7):3129–38.

294. Franchimont D, Galon J, Vacchio MS, Fan S, Visconti R, Frucht DM, et al. Positive effects of glucocorticoids on T cell function by up-regulation of IL-7 receptor alpha. J Immunol Baltim Md 1950. 2002 Mar 1;168(5):2212–8.

295. Kakal JA, Ghazawi FM, Faller EM, Sugden SM, Parmar P, MacPherson PA. Transcriptional regulation of the IL-7Rα gene by dexamethasone and IL-7 in primary human CD8 T cells. Immunogenetics. 2017 Jan;69(1):13–27.

296. Shimba A, Cui G, Tani-Ichi S, Ogawa M, Abe S, Okazaki F, et al. Glucocorticoids Drive Diurnal Oscillations in T Cell Distribution and Responses by Inducing Interleukin-7 Receptor and CXCR4. Immunity. 2018 20;48(2):286-298.e6.

297. Lee H-C, Shibata H, Ogawa S, Maki K, Ikuta K. Transcriptional regulation of the mouse IL-7 receptor alpha promoter by glucocorticoid receptor. J Immunol Baltim Md 1950. 2005 Jun 15;174(12):7800–6.

298. Kruth KA, Fang M, Shelton DN, Abu-Halawa O, Mahling R, Yang H, et al. Suppression of B-cell development genes is key to glucocorticoid efficacy in treatment of acute lymphoblastic leukemia. Blood. 2017 01;129(22):3000–8.

299. Kanai T, Seki S, Jenks JA, Kohli A, Kawli T, Martin DP, et al. Identification of STAT5A and STAT5B target genes in human T cells. PloS One. 2014;9(1):e86790.

300. Berki T, Pálinkás L, Boldizsár F, Németh P. Glucocorticoid (GC) sensitivity and GC receptor expression differ in thymocyte subpopulations. Int Immunol. 2002 May;14(5):463–9.

301. Boldizsár F, Pálinkás L, Czömpöly T, Bartis D, Németh P, Berki T. Low glucocorticoid receptor (GR), high Dig2 and low Bcl-2 expression in double positive thymocytes of BALB/c mice indicates their endogenous glucocorticoid hormone exposure. Immunobiology. 2006;211(10):785–96.

302. Gruber J, Sgonc R, Hu YH, Beug H, Wick G. Thymocyte apoptosis induced by elevated endogenous corticosterone levels. Eur J Immunol. 1994 May;24(5):1115–21.

303. Lee MS, Hanspers K, Barker CS, Korn AP, McCune JM. Gene expression profiles during human CD4+ T cell differentiation. Int Immunol. 2004 Aug;16(8):1109–24.

304. Foo J, Michor F. Evolution of acquired resistance to anti-cancer therapy. J Theor Biol. 2014 Aug 21;355:10–20.

305. Pieters R, Huismans DR, Loonen AH, Hählen K, van der Does-van den Berg A, van Wering ER, et al. Relation of cellular drug resistance to long-term clinical outcome in childhood acute lymphoblastic leukaemia. Lancet Lond Engl. 1991 Aug 17;338(8764):399–403.

306. Inaba H, Pui C-H. Glucocorticoid use in acute lymphoblastic leukaemia. Lancet Oncol. 2010 Nov;11(11):1096–106.

307. Doench JG, Fusi N, Sullender M, Hegde M, Vaimberg EW, Donovan KF, et al. Optimized sgRNA design to maximize activity and minimize off-target effects of CRISPR-Cas9. Nat Biotechnol. 2016 Feb;34(2):184–91.

308. Schumann K, Lin S, Boyer E, Simeonov DR, Subramaniam M, Gate RE, et al. Generation of knock-in primary human T cells using Cas9 ribonucleoproteins. Proc Natl Acad Sci U S A. 2015 Aug 18;112(33):10437–42.

309. Brinkman EK, Chen T, Amendola M, van Steensel B. Easy quantitative assessment of genome editing by sequence trace decomposition. Nucleic Acids Res. 2014 Dec 16;42(22):e168.

310. Robinson MD, McCarthy DJ, Smyth GK. edgeR: a Bioconductor package for differential expression analysis of digital gene expression data. Bioinforma Oxf Engl. 2010 Jan 1;26(1):139–40.

311. Subramanian A, Tamayo P, Mootha VK, Mukherjee S, Ebert BL, Gillette MA, et al. Gene set enrichment analysis: a knowledge-based approach for interpreting genome-wide expression profiles. Proc Natl Acad Sci U S A. 2005 Oct 25;102(43):15545–50.

312. Iyer G, Hanrahan AJ, Milowsky MI, Al-Ahmadie H, Scott SN, Janakiraman M, et al. Genome sequencing identifies a basis for everolimus sensitivity. Science. 2012 Oct 12;338(6104):221.

313. Al-Ahmadie H, Iyer G, Hohl M, Asthana S, Inagaki A, Schultz N, et al. Synthetic lethality in ATM-deficient RAD50-mutant tumors underlies outlier response to cancer therapy. Cancer Discov. 2014 Sep;4(9):1014–21.

314. Li H, Durbin R. Fast and accurate short read alignment with Burrows-Wheeler transform. Bioinforma Oxf Engl. 2009 Jul 15;25(14):1754–60.

315. DePristo MA, Banks E, Poplin R, Garimella KV, Maguire JR, Hartl C, et al. A framework for variation discovery and genotyping using next-generation DNA sequencing data. Nat Genet. 2011 May;43(5):491–8.

316. Cibulskis K, Lawrence MS, Carter SL, Sivachenko A, Jaffe D, Sougnez C, et al. Sensitive detection of somatic point mutations in impure and heterogeneous cancer samples. Nat Biotechnol. 2013 Mar;31(3):213–9.

317. Clarke L, Fairley S, Zheng-Bradley X, Streeter I, Perry E, Lowy E, et al. The international Genome sample resource (IGSR): A worldwide collection of genome variation

incorporating the 1000 Genomes Project data. Nucleic Acids Res. 2017 04;45(D1):D854–9.

318. Lek M, Karczewski KJ, Minikel EV, Samocha KE, Banks E, Fennell T, et al. Analysis of protein-coding genetic variation in 60,706 humans. Nature. 2016 18;536(7616):285–91.

319. Tate JG, Bamford S, Jubb HC, Sondka Z, Beare DM, Bindal N, et al. COSMIC: the Catalogue Of Somatic Mutations In Cancer. Nucleic Acids Res. 2019 Jan 8;47(D1):D941–7.

320. Robinson JT, Thorvaldsdóttir H, Winckler W, Guttman M, Lander ES, Getz G, et al. Integrative genomics viewer. Nat Biotechnol. 2011 Jan;29(1):24–6.

321. Ryan J, Letai A. BH3 profiling in whole cells by fluorimeter or FACS. Methods San Diego Calif. 2013 Jun 1;61(2):156–64.

322. Fellmann C, Hoffmann T, Sridhar V, Hopfgartner B, Muhar M, Roth M, et al. An optimized microRNA backbone for effective single-copy RNAi. Cell Rep. 2013 Dec 26;5(6):1704–13.

323. Winter SS, Dunsmore KP, Devidas M, Wood BL, Esiashvili N, Chen Z, et al. Improved Survival for Children and Young Adults With T-Lineage Acute Lymphoblastic Leukemia: Results From the Children's Oncology Group AALL0434 Methotrexate Randomization. J Clin Oncol Off J Am Soc Clin Oncol. 2018 10;36(29):2926–34.

324. Schrappe M, Valsecchi MG, Bartram CR, Schrauder A, Panzer-Grümayer R, Möricke A, et al. Late MRD response determines relapse risk overall and in subsets of childhood T-cell ALL: results of the AIEOP-BFM-ALL 2000 study. Blood. 2011 Aug 25;118(8):2077–84.

325. Coustan-Smith E, Mullighan CG, Onciu M, Behm FG, Raimondi SC, Pei D, et al. Early T-cell precursor leukaemia: a subtype of very high-risk acute lymphoblastic leukaemia. Lancet Oncol. 2009 Feb;10(2):147–56.

326. Coustan-Smith E, Mullighan CG, Onciu M, Behm FG, Raimondi SC, Pei D, et al. Early T-cell precursor leukaemia: a subtype of very high-risk acute lymphoblastic leukaemia. Lancet Oncol. 2009 Feb;10(2):147–56.

327. Moore NC, Anderson G, Williams GT, Owen JJ, Jenkinson EJ. Developmental regulation of bcl-2 expression in the thymus. Immunology. 1994 Jan;81(1):115–9.

328. Maese L, Tasian SK, Raetz EA. How is the Ph-like signature being incorporated into ALL therapy? Best Pract Res Clin Haematol. 2017;30(3):222–8.

329. Barata JT, Cardoso AA, Nadler LM, Boussiotis VA. Interleukin-7 promotes survival and cell cycle progression of T-cell acute lymphoblastic leukemia cells by down-regulating the cyclin-dependent kinase inhibitor p27(kip1). Blood. 2001 Sep 1;98(5):1524–31.

330. Barata JT, Cardoso AA, Boussiotis VA. Interleukin-7 in T-cell acute lymphoblastic leukemia: an extrinsic factor supporting leukemogenesis? Leuk Lymphoma. 2005 Apr;46(4):483–95.

331. Johnson AE, van Waes MA. The translocon: a dynamic gateway at the ER membrane. Annu Rev Cell Dev Biol. 1999;15:799–842.

332. Garrison JL, Kunkel EJ, Hegde RS, Taunton J. A substrate-specific inhibitor of protein translocation into the endoplasmic reticulum. Nature. 2005 Jul 14;436(7048):285–9.

333. Van Puyenbroeck V, Vermeire K. Inhibitors of protein translocation across membranes of the secretory pathway: novel antimicrobial and anticancer agents. Cell Mol Life Sci CMLS. 2018 May;75(9):1541–58.

334. Ruiz-Saenz A, Sandhu M, Carrasco Y, Maglathlin RL, Taunton J, Moasser MM. Targeting HER3 by interfering with its Sec61-mediated cotranslational insertion into the endoplasmic reticulum. Oncogene. 2015 Oct 8;34(41):5288–94.

335. Maifeld SV, MacKinnon AL, Garrison JL, Sharma A, Kunkel EJ, Hegde RS, et al. Secretory protein profiling reveals TNF-α inactivation by selective and promiscuous Sec61 modulators. Chem Biol. 2011 Sep 23;18(9):1082–8.

336. Janka GE. Familial and acquired hemophagocytic lymphohistiocytosis. Annu Rev Med. 2012;63:233–46.

337. Maschalidi S, Sepulveda FE, Garrigue A, Fischer A, de Saint Basile G. Therapeutic effect of JAK1/2 blockade on the manifestations of hemophagocytic lymphohistiocytosis in mice. Blood. 2016 07;128(1):60–71.

338. Das R, Guan P, Sprague L, Verbist K, Tedrick P, An QA, et al. Janus kinase inhibition lessens inflammation and ameliorates disease in murine models of hemophagocytic lymphohistiocytosis. Blood. 2016 Mar 31;127(13):1666–75.

339. Broglie L, Pommert L, Rao S, Thakar M, Phelan R, Margolis D, et al. Ruxolitinib for treatment of refractory hemophagocytic lymphohistiocytosis. Blood Adv. 2017 Aug 22;1(19):1533–6.

340. Sin JH, Zangardi ML. Ruxolitinib for secondary hemophagocytic lymphohistiocytosis: First case report. Hematol Oncol Stem Cell Ther. 2017 Aug 16;

341. Tliba O, Damera G, Banerjee A, Gu S, Baidouri H, Keslacy S, et al. Cytokines induce an early steroid resistance in airway smooth muscle cells: novel role of interferon regulatory factor-1. Am J Respir Cell Mol Biol. 2008 Apr;38(4):463–72.

342. Bouazza B, Krytska K, Debba-Pavard M, Amrani Y, Honkanen RE, Tran J, et al. Cytokines alter glucocorticoid receptor phosphorylation in airway cells: role of phosphatases. Am J Respir Cell Mol Biol. 2012 Oct;47(4):464–73.

343. Pazdrak K, Straub C, Maroto R, Stafford S, White WI, Calhoun WJ, et al. Cytokine-Induced Glucocorticoid Resistance from Eosinophil Activation: Protein Phosphatase 5 Modulation of Glucocorticoid Receptor Phosphorylation and Signaling. J Immunol Baltim Md 1950. 2016 Nov 15;197(10):3782–91.

344. Britt RD, Thompson MA, Sasse S, Pabelick CM, Gerber AN, Prakash YS. Th1 cytokines TNF-α and IFN-γ promote corticosteroid resistance in developing human airway smooth muscle. Am J Physiol Lung Cell Mol Physiol. 2019 01;316(1):L71–81.

345. Huang JF, Yang Y, Sepulveda H, Shi W, Hwang I, Peterson PA, et al. TCR-Mediated internalization of peptide-MHC complexes acquired by T cells. Science. 1999 Oct 29;286(5441):952–4.

346. Chen M, Felix K, Wang J. Critical role for perforin and Fas-dependent killing of dendritic cells in the control of inflammation. Blood. 2012 Jan 5;119(1):127–36.

347. Leonard WJ, Lin J-X, O'Shea JJ. The γc Family of Cytokines: Basic Biology to Therapeutic Ramifications. Immunity. 2019 16;50(4):832–50.

348. Distelhorst CW. Recent insights into the mechanism of glucocorticosteroid-induced apoptosis. Cell Death Differ. 2002 Jan;9(1):6–19.

349. Webb MS, Miller AL, Johnson BH, Fofanov Y, Li T, Wood TG, et al. Gene networks in glucocorticoid-evoked apoptosis of leukemic cells. J Steroid Biochem Mol Biol. 2003 Jun;85(2–5):183–93.

350. Crayne CB, Albeituni S, Nichols KE, Cron RQ. The Immunology of Macrophage Activation Syndrome. Front Immunol. 2019;10:119.

351. Loh ML, Tasian SK, Rabin KR, Brown P, Magoon D, Reid JM, et al. A phase 1 dosing study of ruxolitinib in children with relapsed or refractory solid tumors, leukemias, or myeloproliferative neoplasms: A Children's Oncology Group phase 1 consortium study (ADVL1011). Pediatr Blood Cancer. 2015 Oct;62(10):1717–24.

Publishing Agreement

It is the policy of the University to encourage the distribution of all theses, dissertations, and manuscripts. Copies of all UCSF theses, dissertations, and manuscripts will be routed to the library via the Graduate Division. The library will make all theses, dissertations, and manuscripts accessible to the public and will preserve these to the best of their abilities, in perpetuity.

Please sign the following statement:

I hereby grant permission to the Graduate Division of the University of California, San Francisco to release copies of my thesis, dissertation, or manuscript to the Campus Library to provide access and preservation, in whole or in part, in perpetuity.

DocuSigned by:

Lauren Meyer

C4C857FDC2A0402...

Author Signature

12/17/2019

Date